City Research Online

City, University of London Institutional Repository

Citation: Wang, W. (1993). Self-mixing interference in semiconductor lasers: Experimental and theoretical studies. (Unpublished Doctoral thesis, City, University of London)

This is the accepted version of the paper.

This version of the publication may differ from the final published version.

City Research Online: http://openaccess.city.ac.uk/   publications@city.ac.uk

Self-mixing Interference
in Semiconductor Lasers:
Experimental and Theoretical Studies

By

WEN-MING WANG

To my beloved parents......

Self-mixing Interference in Semiconductor Lasers: Experimental and Theoretical Studies

Table of Contents

Chapter 1 Introduction

Chapter 2 Introduction to optical interferometry

Appendix: List of publications

[1] "**Laser Doppler velocimetry by direct amplitude modulation on a multi-mode laser diode**" <u>Conf. on Sensors and Their Applications,</u> 22-25 Sept., 1991, Edinburgh, UK, published on <u>Sensors: Technology. System and Their Application,</u> pp.347-352, Adam Hilger Pub., 1991.

[2] "**A systematic classification and identification of optical fibre sensors**" <u>Sensors and Actuators,</u> A, **29**, pp.21-36, 1991.

[3] "**A review and classification of optical fibre sensors**" <u>ACTA. IMEKO,</u> Sept., 1991, Beijing, China.

[4] "**An interferometer incorporating active optical feedbback from a diode laser with applications to coherent ranging and vibbrational measurement**" <u>Proc. in 8th Optical Fiber Sensors Conf.,</u> IEEE Catalog #92CH3107-0, pp.358-361, 1992.

[5] "**Fiber-optic Doppler velocimeter that incorporates active optical feedback from a diode laser**" <u>Optics Letter,</u> **17**, pp.819-821, 1992.

[6] "**Characteristics of a dual diode laser-based feedback interferometer with applications for extended ranging and directional discrimination**" <u>Techn. Dig. of XVIII International Quantum Electron. Conf.,</u> June 14-19, Vienna, Austria, pp.66-68, 1992.

[7] "**Characteristics of a diode laser-based self-mixing interferometer**" <u>Proc. of Conf. on Appl. Opt. and Opto-electron.</u> 14-19, Sept., 1992, Leeds, pp.207-210.

[8] "**Self-mixing interference in a diode laser: Experimental observations and theoretical analysis**" <u>Appl. Opt.,</u> **32**, pp.1551-1558, 1993.

[9] "**Active optical feedback in a dual diode laser configuration applied to displacement measurement with wide dynamic range**" <u>Appl. Opt.</u>(accepted), 1993.

[10] "**Theory of self-mixing interference in a diode laser**" Submitted to <u>J. of Lightwave Technology,</u> 1993.

ABSTRACT

Experimental observations linked to a theoretical analysis of the so-called "self-mixing interference" in semiconductor lasers are presented, and several schemes using the self-mixing technique applied to the measurement of various physical parameters are proposed in this thesis.

A theory of self-mixing interference inside a single-longitudinal-mode diode laser is developed, based on steady-state equations of the lasing condition in a Fabry-Perot type laser cavity. The resulting theoretical models are first presented, and through them the necessary theory for an analysis of the self-mixing interference in a single-mode diode laser is given. It was shown that the optical intensity modulation produced by an external optical feedback was due to the variations in the threshold gain and the laser spectral distribution of the device used. The gain variation results in an optical intensity modulation, and the spectral variation determines both the modulation waveform shapes and the coherence properties of the interference. The theoretical analysis of the self-mixing interference yielded a simulation of the laser power modulation which was then investigated experimentally.

The semiconductor laser used in the experiment functions not only as a conventional light source but also as a self-aligned interferometer and a detector. The laser sends light, either in free space or through an optical fibre, to a changing target from which the optical backscatter is fed back into the laser and detected by the internal photodetector. This self-mixing effect inside the laser cavity results in the laser power variation which is related to the changes of the external physical parameters. The monitoring of the laser power thus provides a simple method for optical sensing.

In the experiments performed, three significant conclusions are drawn: (i) the occurance of the self-mixing interference is not dependent on the initial coherence length of

the diode laser in the absence of external optical feedback, (ii) the interference is not dependent on the use of a single-mode or a multi-mode laser as the source and (iii) the interference is independent of the type of fibre employed, i.e. whether it is single-mode or multi-mode. Comparison of this kind of interference with that in a conventional interferometer shows that (i) self-mixing interference has the same phase sensitivity as that of the conventional arrangement; (ii) the modulation depth of the interference is comparable to that of a conventional interferometer and (iii) the directional information of the phase movement and that of a moving object scattering the light can be obtained from the sawtooth-like interference signal. The above factors have significant implications for optical sensing of a wide range of physical parameters.

Finally, several application schemes of the self-mixing interference technique are investigated, and the preliminary experimental results achieved highlight its significant advantages of simplicity, compactness and robustness, and the self-aligning, self-detecting abilities of self-mixing interferometry, when compared to the use of conventional interference methods.

ACKNOWLEGEMENTS

DECLARATION

I grant powers of discretion to the City University Librarian to allow this thesis to be copied in whole or in part without further reference to me. This permission covers only single copies made for study purposes, subject to normal conditions of acknowlegement.

LIST OF FIGURES AND TABLES

Chapter 4

Chapter 5

Chapter 6

Tables

List of Symbols Used

α—linewidth enhancement factor in semiconductor lasers;

β—proportionality coefficient;

χ—inverse spontaneous lifetime of the exited carriers;

φ_i—phases of electric fields(i=0, 1, 2, 3,......);

ϕ—phase;

Φ—phase;

γ—optical loss per unit length;

Γ—optical cavity loss;

κ_g—proportionality coefficient;

λ—wavelength;

$\delta\lambda$—wavelength spread;

μ—micro;

ν—optical frequency;

ν_{th}—optical frequency at threshold;

$\Delta\nu$—frequency spacing;

$\delta\nu$—spectral linewidth;

ω—angular frequency;

$\delta\varphi$—phase difference;

$\Delta\varphi$—phase difference;

ρ—degree of coherence;

θ—phase difference;

τ_c—coherence time;

τ_e—effective roundtrip time delay;

τ_i—roundtrip time delay(i=1, 2);

ξ—feedback coupling coefficient;

A_i—amplitudes of electric fields,(i= 0, 1, 2, 3,......);

c—the speed of light;

C—feedback coefficient;

d—distance;

D—grating spacing;

Δd—distance difference;

e—electric charge;

E_i—electric fields (i=0, 1, 2, 3,......);

f—proportionality factor;

g—optical gain per unit length;

g_{th}—optical gain per unit length at threshold;

G_i—gain transfer functions(i=0, 1, 2, 3,......);

G—optical cavity gain;

ΔG—optical gain variation;

h—slit separation, or the Planck's constant;

I_i—optical intensity(i=0, 1, 2, 3,......);

J—injection current;

J_{th}—threshold current;

$\overline{k_i}$—propagation vectors of electric fields(i=0, 1, 2, 3,......);

k—wavenumber, or Boltzmann constant;

l_c—coherence length;

Δl—optical path difference inside the laser cavity;

L—length;

ΔL—optical path difference;

m—modulation coefficient, or integer;

n—refractive index;

Δn—refractive index variation;

N—carrier density;

N_c—elctron numbers of conduction band;

N_v—electron numbers of valence band;

$p(\nu)$—power spectrum;

p_o—proportionality coefficient;

P—optical power;

q—integer;

r—reflection coefficient;

$\bar{r}$—position vector;

R—power reflection coefficient, or spontaneous emission rate;

$R(\nu)$—roundtrip gain transfer function;

t—time, or transmission coefficient;

Δt—time difference;

T—power transmission coefficient, or temperature;

V—visibility function;

Vg—effective group velocity;

x—distance;

y—distance;

z—z axis.

Chapter 1

Introduction

§1.1 Historical background

The effects of external optical feedback on the output of a laser have been observed to have a profound influence on the behaviour of the laser output intensity[Fujiwara et al 1981, Agrawal et al 1984], its threshold gain[Osmundsen & Grade 1983] and output spectrum[Miles et al 1980, Fleming & Mooradian 1981, and Yasaka et al 1991], and the physics underlying this behaviour is complicated and has been extensively discussed in the literature by various authors[Lang and Kobayashi 1980, Favre et al 1982, Acket et al 1984, Lenstra et al 1985, Henry and Kazarinov 1986, Petermann 1991b].

The effects of the feedback may cause a serious problem in the achievement of a satisfactory laser output in such applications as optical communications, fibre optical sensors, as well as optical recording. External optical feedback often arises in practice because of unintentional reflections from various optical components back into the laser cavity[Hirota & Suematsu 1979]. For example, reflections at fibre ends or from various surfaces, back into laser diodes can increase the intensity noise of a laser system[Lang & Kobayashi 1980, Petermann & Weidel 1981], modify the coherence properties of the laser source used in an interferometer[Goldberg et al 1982 and Woodward & Thompson 1992] or degrade the modulation response characteristics of an optical communication system[Cho & Umeda 1986, Temkin et al 1986]. A dramatic effect of this nature has been described by Lenstra et al[1985] who termed it "coherence collapse"[Dente et al 1988, Cohen & Lenstra 1989]. He showed

that the feedback may increase the spectral linewidth of the laser to many times that of the solitary laser linewidth with a consequential "collapse" in the coherent length of the laser from several meters to a few millimetres.

External optical feedback is commonly used to alter the characteristics of a semiconductor laser, such as reducing spectral linewidth[Agrawal et al 1984], selecting longitudinal-mode[Fleming & Mooradian 1981, and Barwood et al 1992] and wavelength tuning[Chuang et al 1990]. In these cases, it is often beneficial to operate diode lasers with optical feedback. For example, the commercially available diode laser(Sharp LT035) has incorporated an external cavity to improve the wavelength stability[Sharp 1992]. Economic production of these external cavity devices, fabricated in an "integrated form", is potentially possible for wide applications.

External feedback effects have been also studied for interferometric applications. In such studies, a portion of light emitted from a laser source is usually reflected by a distant external target back into the laser cavity. The reflecting light mixes "actively" with the light inside the cavity and as a result modulates the laser output power. This modulated laser output power may be monitored by an external photodetector(in the case of a gas laser)[Ashby & Jephcott 1963], by an internal photodetector(with a diode laser package)[Dandridge et al 1980], or alternatively by measuring the junction voltage variation[Shinohara et al 1986] in the laser device caused by this external feedback. Measurements of the amplitude and/or the phase information of the laser power modulation have been widely used to sense physical parameters such as the index of refraction[Gerardo & Verdeyen 1963 and Ashby et al 1965], and velocity[Rudd 1968], and for ranging[Beheim & Fritsch 1986 and de Groot et al 1988] or displacement monitoring [Dandridge et al 1980 and Yoshino et al 1987]. In these schemes the laser is used not only as a light source but also as an interferometer, also acting as an amplifier to the measurement signal, which presents some significant advantages, in practice, in terms of simplicity, compactness and robustness[Jentink et al 1988]. It is this approach with which

this thesis is concerned and the intensity variations produced by the feedback is termed the **"self-mixing interference"** to distinguish it from the phenomenon of conventional interference[Wang et al 1992].

In the early 1960s, King and Steward[1963] observed that the intensity of a helium-neon(He-Ne) laser beam could be influenced by feeding some of the output radiation back into the laser cavity. Their experiments showed that the change of resulting intensity was dependent on the phase of the feedback and that these intensity variations, induced by the external feedback, could be detected easily, even using an insensitive photodetector. They also found that the intensity modulation was similar to that produced by a conventional interferometer, such as the "fringe" shift corresponding to an optical displacement of $\lambda/2$, λ being the oscillation wavelength of the laser. The term "laser interferometer" was then used by Ashby and Jephcott[1963] to describe a laser system subject to this type of feedback. In such an arrangement changes in the optical path length of the external cavity, produced by the longitudinal motion of the external reflecting target[King & Steward 1963] or by refractive index changes within the external cavity[Gerardo & Verdeyen 1963], caused a modulation of the laser intensity which could be monitored and then utilized for optical sensing, for example for displacement, for velocity measurement or for ranging, as with other optical techniques [Mitsuhashi et al 1976, and Yoshino et al 1987]. This approach was later developed by Rudd[1968], Lawrence et al[1972], Abshire[1974] and Churnside et al[1982] for atmospheric laser Doppler measurements.

With the progress in semiconductor laser technology in the 1980s, the phenomenon of backscattered modulation or self-mixing interference from diffuse-targets has been investigated by a number of researchers. A diode laser sensor was first reported by Dandridge et al[1980] for displacement measurement. Later a small laser Doppler velocimeter was reported by Shinohara et al[1986] using the self-mixing effect in a semiconductor laser. Based on the Shinohara's experimental results, Shimizu[1987] found that the direction of the

Doppler velocity could be determined from the shape of sawtooth-like waveforms observed in the self-mixing signal. These shapes reverse when the direction of movement of the target is reversed. A theoretical model was developed by Jentink et al[1988] and the self-mixing effect was explained simply in term of the interference between light inside the laser cavity and light re-entering the laser cavity. This assumption led to an obviously incorrect conclusion, in that the spectral linewidth of the laser mode of the multi-mode laser diode used in their experiments was less than 2×10^{-3} nm, which corresponds to an unusually long coherence length(160 mm) for a multi-mode laser, which conflicted with their own measurements using conventional interferometry for the linewidth of 4.6 nm.

It has been known that the main features of the self-mixing interference are similar to those produced by conventional interference, but some characteristics observed in the self-mixing interference have been found to be dramatically **different** from those of a conventional interferometer. In order to interpret the phenomena observed in self-mixing interference, a number of theories have been developed. The early theories, presented by Gerado and Verdeyen[1964], Hooper and Bekefi[1966], Uchida[1967] and Potter[1969], were modelled on a laser cavity subject to a variable loss. A simple feedback amplifier model was also used by Rudd[1968] to describe the intensity modulation in a He-Ne laser which was employed not only as a light source, but also as a mixer-oscillator for velocity measurement. Churnside et al[1984] again studied laser Doppler velocimetry operating with external feedback. They used diffusely reflecting targets and observed the self-mixing effect with a CO_2 laser, and termed this effect "backscatter modulation" as an alternative to self-mixing interference. Jentink et al[1986] used semiconductor lasers for velocity measurement and explained, as stated earlier, the intensity modulation in terms of the conventional interference between light inside the laser cavity and light reentering the cavity. De Groot et al[1988] disagreed with their assumption and developed their own theoretical model based on the mode structure of a three-mirror Fabry-Perot cavity, to explain the self-mixing signal

generation as applied to velocimetry and ranging. The intensity modulation was explained as being due to the change of the carrier density inside the laser cavity. A further theoretical analysis for a multi-mode self-mixing laser was carried out by de Groot[1990], in which the intensity modulation was explained as a spectral mode modulation. Very recently, Koelink et al[1992a] presented a short outline of a theoretical model to explain the power fluctuations in their fibre optical self-mixing laser Doppler velocimeter, and later presented a computer simulation model to explain the sawtooth-like signals obtained[Koelink et al 1992b]. A simple theoretical analysis for self-mixing interference has also been presented by the author of this thesis[Wang et al 1993a]. In this analysis the power modulation due to the self-mixing is shown to be affected by the reflectivity variations of the laser facets, and this is discussed further in this thesis. However the spectral variations and other effects were not considered in the analysis.

The physics of external optical feedback in diode lasers has been extensively studied in the context of external cavity locking mechanisms[Lang & Kobayashi 1980, Mark et al 1988] and optical noise[Hirota & Suematsu 1979, Spano et al 1984, and Henry & Kazarinov 1986]. The various theories developed for the modulation effect due to external optical feedback upon the laser output concentrate on the explanation of the experimentally-related observations, and often results in confusing interpretations of the self-mixing effects. It is obvious, as stated previously, that some phenomena observed with external optical feedback are dramatically **different** from those of conventional interferometry, and they cannot be simply explained using existing coherent interference theory[Olessen et al 1986, Jentink et al 1988]. Examples of these phenomena, that are not adequately explained, include the direction-dependent sawtooth-like output signals produced[Shimizu 1987], the waveform sign inversion between the two emission facets[de Groot et al 1988] and the dependence of the output on the initial coherence length of the laser used[Wang et al 1992a], particularly when self-mixing interference occurs in a multi-mode laser.

It has been well-known that optical feedback has a profound effect on the optical spectrum and the threshold gain of a diode laser[Olssen and Tang 1981, Goldberg et al 1982, Osmundsen et al 1983]. The physics of a diode laser with external optical feedback could be understood from the analysis of the external cavity locking mechanisms and optical noise. With very weak feedback the spectral linewidth may be narrowed or broadened, depending on the phase of the feedback relative to the optical field within the active laser, and this has been used for laser linewidth reduction[Patzak et al 1983] and frequency tuning[Chuang et al 1990]. When the distance of an external reflector is smaller than the coherence length of the solitary laser used, a compound cavity model has been used by Lang and Kobayashi[1980] to interpret the observed phenomena. However, similar results to coherent feedback have been observed when the feedback field is incoherent with that inside the laser cavity. Some of these phenomena are linewidth reduction[Yasaka et al 1991], coherence collapse[Cohen et al 1990], and even with the reflector distance as long as 7 km, using optical fibres, the laser spectrum is affected[Agrawal et al 1984]. It is clear, from the existing coherent theory, that the coherent characteristics should not be observed if the fields superimposed are incoherent.

Therefore, it is evident from the above investigations that the output characteristics of a semiconductor laser are significantly altered by external optical feedback, no matter whether the feedback is fully coherent or incoherent with the cavity radiation of the solitary laser. The spectral linewidth of the diode laser may be broadened to many times that of the solitary laser linewidth, resulting in "coherence collapse"[Lenstra 1985]. However it has been observed, under certain conditions, when self-mixing occurs beyond the coherence length of the solitary laser used, the coherence is enhanced by the feedback and again this is obviously due to the change of the spectral distribution. For example in the studies reported by Mark et al[1985] the normal spectral linewidth of 17 MHz of a single mode diode laser was reduced to a value as low as 1 Hz with Rayleigh backscatter light from a long fibre, which represents a coherence length of $\sim 3 \times 10^5$ km. It also shown that the spectral linewidth was inversely

proportional to the fibre length. Both these phenomena will be discussed by the author of this thesis and a theoretical explanation to both "coherence enhancement" and "coherence collapse" will be presented in Chapter 4.

A significant **difference** of self-mixing interference to conventional interference results from the spectral change of the light source in the presence of external optical feedback. According to the Heisenberg's uncertainty principle, the product of the spectral linewidth of the light source and the coherence time is close to unity. The coherence length is thus completely determined by the spectral linewidth, in another words, the conventional temporal coherence is based on the stablized spectral output of the laser used. Conventional interference patterns could not be observed if the OPD of the interfering beams were beyond the coherence length of the laser. However, with the case of optical feedback, the spectral distribution changes and thus the coherence of the laser device is now not dependent on the coherence length of the solitary laser but on the actual lasing spectrum in the presence of the feedback. In addition, from the viewpoint of a laser oscillation, the laser oscillation may be considered as a **frequency selecting process**, in which only those lights satisfying the oscillation conditions are able to produce laser output, and the rest is filtered out from the laser cavity and has no influence on the laser output power. This means that the self-mixing interference is subject to a non-linear superposition process due to the laser oscillation, which is significantly different from the conventional interference effect. A detailed theoretical and experimental study of the external optical feedback effect for optical sensing applications constitute the main contents of this thesis, as discussed later in detail.

§1.2 Aims and objectives of the thesis

The purpose of this thesis, is not simply to perform an experimental and theoretical investigation of the optical noise properties of the semiconductor laser subjected to external feedback, but to study the intensity modulation characteristics of the self-mixing effects,

induced by the optical feedback field. The thesis is also concerned with the applications of external optical feedback effects for optical sensing techniques, i.e. the self-mixing interferometry in semiconductor lasers, and their theoretical investigations. As the self-mixing process is not a linear superposition of electrical fields as is the case in conventional interference processes, the theories developed based on the existing coherence theory are inadequate for explaining such self-mixing effects observed. Also the external feedback actually constitutes a part of the laser source, its presence thus changes the oscillation condition and the lasing spectrum of the laser, and therefore changes the coherence properties of the laser used in the presence of external feedback. All of these make the self-mixing process complicated and not easy to understand, and a new analytical method is therefore needed for further understanding some of the phenomena observed and for better implementing of the self-mixing techniques in optical sensing applications.

The main **aims** of this thesis are

(i) to present a clear theoretical description of the self-mixing interference phenomenon in semiconductor lasers;

(ii) to give a reasonable explanation to "coherence", sawtooth-like waveform signal as well as waveform sign inversion, resulting from the self-mixing process;

(iii) to compare theoretically and experimentally the self-mixing interference, occurring in semiconductor lasers, with the conventional optical interference;

(iv) to verify the results from the theoretical analysis with experiments performed;

(v) to demonstrate the use of the self-mixing techniques for practical applications in optical sensor systems.

Following this introductory chapter, dealing with the background to the phenomena to be discussed and the presentations of the aims and objectives of the thesis, Chapter 2 and 3 give brief descriptions of relevant optical interferometry and semiconductor laser physics. The purpose of these two chapters is to review the basic characteristics of optical interference and semiconductor lasers. They are presented as the necessary background information, to understand the external optical feedback effect. Chapter 4 presents a theoretical analysis of self-mixing interference in a single-longitudinal-mode semiconductor laser. This theory is based on the field analysis approach, which is used to describe the steady-state laser field. Since the self-mixing interference process is a relatively-slow, the transit time properties of the laser oscillation may be neglected, and the theoretical analysis is essentially based on the three mirror Fabry-Perot laser structure. Chapter 5 records the results of a series of detailed experimental studies of the self-mixing interference. The experimental observations are compared with those obtained from a conventional interferometer. In Chapter 6 several applications of self-mixing interferometry have been investigated and results are reported, which highlight the simplicity, compactness and robustness of the self-mixing method. Finally Chapter 7 presents an overall summary of the work done and some suggestions for further studies.

Chapter 2

Introduction to optical interferometry

§2.1 Introduction

Optical interferometry is an elegant branch of optics, which has been playing an increasingly important role in a wide variety of physical measurements, by offering high resolving power and increased sensitivity[Smith 1971, Born & Wolf 1975, and Jackson 1987]. The technique of interferometry is derived from interference which occurs when radiation follows more than one path from its source to the point of detection and results in optical intensity variations as the point of detection is moved. The recent important studies of optical interferometry date from the work of Michelson, who invented the best known and most versatile interferometric device, called the Michelson interferometer, and was awarded, in 1907, the Nobel prize in physics for his contributions to the spectroscopic and metrological investigations with this device[Fowles 1968].

The principle of optical interferometry is based on the linear superposition of two or more coherent optical beams and the well-known experiment of such a two beam interference was Young's experiment as presented in the next section. The superposition of optical beams always gives rise to interference and yields an observable interference pattern on the screen of detection if the beams superimposed are strictly monochromatic light, and such an interference phenomenon is said to be coherent. On the other hand, if the superposition produces no interference pattern, it is because the light beams were incoherent. In this Chapter, the interference phenomenon is first described, the basic principles of the Michelson

and the Fabry-Perot interferometers are then presented, and the concept of coherence is finally introduced to give a simple description of the coherence theory.

§2.2 Interference phenomena

The principle of linear superposition, two-beam interference and the interference of multiple-beams are briefly described in this section.

§2.2.1 The principle of linear superposition

Interference phenomenon results from the interaction of two or more wave trains with an increase in intensity at some points and a decrease at others. If these wave trains are of strictly monochromatic light, their interaction at a given point in space will always give rise to interference and result in the display of an observable interference pattern on a screen. It is known that the theory of optical interference is based essentially on the **principle of linear superposition** of electrical fields. According to this principle, the electrical field E produced at a given point in space is equal to the vector sum of the different electrical fields

$$E = E_1 + E_2 + E_3 + \cdots \tag{2-1}$$

where $\overline{E}_1, \overline{E}_2, \overline{E}_3, \cdots$ are the electrical field vectors from different sources respectively, at the point in question.

For simplicity, let us consider two plane harmonic linearly polarised waves of the same frequency ω. The electrical fields, $\overline{E}_1$ and $\overline{E}_2$, are then

$$E_1 = \overline{A}_1 \, exp[-j(\overline{k_1} \cdot \overline{r} - \omega t + \varphi_1)] \tag{2-2}$$

and

$$\overline{E}_2 = \overline{A}_2 \, exp[-j(\overline{k_2} \cdot \overline{r} - \omega t + \varphi_2)] \tag{2-3}$$

where φ_1, φ_2 represent any initial phases of the two electrical field sources; $\overline{A}_1$ and $\overline{A}_2$ are constant real vectors of the two waves respectively; $\overline{k_1}$, $\overline{k_2}$, represent the field propagation vectors respectively; $\overline{r}$ is the position vector of the two electrical fields; t is the time and ω is the optical frequency.

In this case, a characteristic field is created in which bright and dark "fringes" appear where the waves reinforce and cancel each other, respectively. Thus, the superposition of the two plane waves results in an intensity distribution, I, which is proportional to the square of the amplitude of the electrical field at the point in question, and is given by

$$I = \mid \overline{E} \mid^2 = \overline{E} \cdot \overline{E}^* = (\overline{A}_1 + \overline{A}_2) \cdot (\overline{A}_1 + \overline{A}_2)^* = \mid \overline{A}_1 \mid^2 + \mid \overline{A}_2 \mid^2 + 2 \overline{A}_1 \cdot \overline{A}_2 \cos \theta$$

$$= I_1 + I_2 + 2 \overline{A}_1 \cdot \overline{A}_2 \cos \theta \qquad (2\text{-}4)$$

where $\mid \overline{E} \mid$ represents the amplitude of electrical field vector $\overline{E}$, $\overline{E}^*$ denotes the complex conjugate of the field $\overline{E}$, and $I_1 = \mid \overline{A}_1 \mid^2$, $I_2 = \mid \overline{A}_2 \mid^2$, representing the intensities of two plane waves respectively, $\overline{A}_1 = \mid \overline{E}_1 \mid$, $\overline{A}_2 = \mid \overline{E}_2 \mid$, being the field amplitudes of the two waves respectively and

$$\theta = \overline{k_1} \cdot \overline{r} - \overline{k_2} \cdot \overline{r} + \varphi_1 - \varphi_2 \qquad (2\text{-}5)$$

The term $2 \overline{A}_1 \cdot \overline{A}_2 \cos \theta$ is called the interference term. This term indicates that the intensity, I, can be greater or less than the individual intensity sum $I_1 + I_2$, depending on the value of θ. Since θ is dependent on $\overline{r}$, periodic spatial variations in the intensity occur, and these are termed **interference fringes** or an **interference pattern**.

§2.2.2 Two-beam interference

Two-beam interference is the simplest and most often studied interference phenomenon. The first experimental demonstration of such interference was performed by Thomas Young

in 1802, as shown in Figure 2.1, where light, from a light source, S, is passed through a pinhole S_1 to illuminate an aperture consisting of two narrow slits or pinholes, S_2 and S_3. If a white screen is placed in the region beyond the slits, a pattern of bright and dark interference
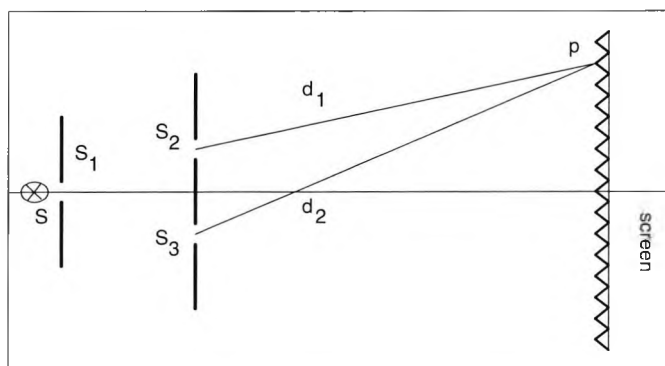
Figure 2.1 Young's experiment of two beam interference

S—the light source, S_1, S_2, S_3—pinholes, p—the observing point on the screen,

d_1, d_2—the distances between the point p and the pinholes S_1, S_2

bands can be seen.

To analyse the results of Young's experiment, the important factor is to find the interference term which is determined by the phase difference between the two waves arriving at a given point p over the distance d_1 and d_2. Assuming that the distance, x, from the apertures to the screen is large enough, as shown in Figure 2.2, the fields produced by S_2 and S_3 may be considered approximately to be the plane harmonic waves, given by Equation (2-2) and (2-3). Here $\overline{k_1}$ and $\overline{k_2}$ are the propagation vectors of the two component waves arriving from S_2 an S_3, respectively, and $\overline{r}$ is the position vector of a point in the region of space near the screen. If the distance, x, from the screen centre to the double slits is large compared to both distance, y, and slit separation, h, the phase difference, θ, can thus be obtained as

$$\theta = (\overline{k_1} - \overline{k_2}) \cdot \overline{r} + \varphi_1 - \varphi_2 = \frac{kyh}{x} - \Delta\varphi \qquad (2\text{-}6)$$
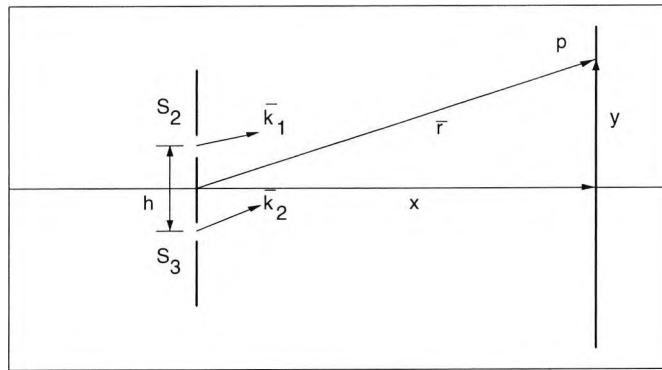
Figure 2.2 Geometry for analyzing two beam interference

h—the slit separation, y—the distance between the point p and the screen centre,

x—the distance from the screen to the double slits, $\bar{r}$—the position vector from the centre

of the double slits to the point p, $\bar{k}_1$, $\bar{k}_2$—the propagation vectors from the slits S_1, S_2.

where k is the wavenumber and $\Delta\varphi = \varphi_1 - \varphi_2$ is the initial phase difference. Thus, the intensity distribution, I, from Equation(2-4), is given by

$$I = |\bar{E}|^2 = |\bar{A}_1|^2 + |\bar{A}_2|^2 + 2\bar{A}_1 \cdot \bar{A}_2 \cos\left(\frac{khy}{x} - \Delta\varphi\right) \tag{2-7}$$

Now if the slits are identical and $\Delta\varphi$ is zero, the above formula reduces to

$$I = 2I_0\left[1 + \cos\left(\frac{khy}{x}\right)\right] \tag{2-8}$$

where $I_o = |\bar{A}_1|^2 = |\bar{A}_2|^2$. The intensity distribution, therefore, varies between zero and $4I_o$ depending on the argument of the cosine, and this implies that the intensity variation caused by the phase difference, θ, can be observed, and used for some physical measurements, which results in a corresponding change of phase. Examples are displacement, refractive index or distance and the measurement method based on the use of such interference phenomena is known as **optical interferometry**.

§2.2.3 Interference of multiple-beams

Interference with multiple-beams instead of simply with two-beams has led to very important advances. The principle of multiple-beam interference is to employ a succession of coherent beams, all specifically related in phase and intensity, and combine them to produce interference fringes. The simplest structure for obtaining multiple-beam interference is shown in Figure 2.3, in which two parallel, partially reflecting plane surfaces, are used to form the multiple reflection between them. The surfaces may be semitransparent mirrors, or merely two facets of a solid-state laser crystal. The primary beam, E_o, is partially reflected and partially transmitted at the first surface. The transmitted part is subsequently partially reflected back and forth between the two mirror surfaces. To analyze this, let r be the coefficient of reflection and t the coefficient of transmission of the mirrors. Then the amplitudes of the successive internally reflected rays are given by $E_o t$, $E_o t r$, $E_o t r^2$, $\cdots$, where E_o is the amplitude of the primary beam. It follows that the amplitudes of the successive transmitted rays are $E_o t^2$, $E_o t^2 r^2$, $E_o t^2 r^4$, $\cdots$, and the amplitudes of the
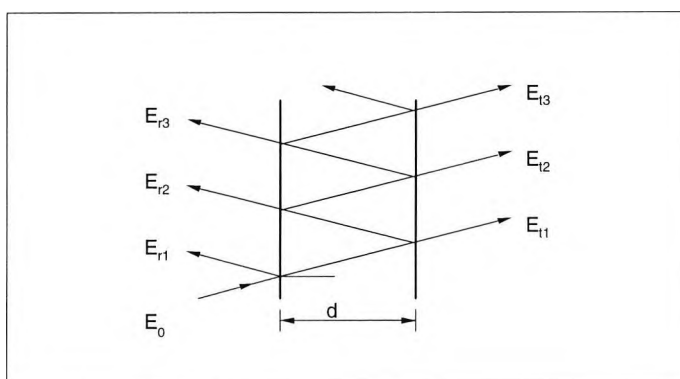
Figure 2.3 Multiple reflection between two parallel mirrors

separated by a distance d

E_0—the incident light beam, E_{r1}, E_{r2}, ...—the partly reflected light beams from the mirrors, E_{t1}, E_{t2}, ...—the partly transmitted light beams from the mirrors.

successive reflected rays are $E_o r$, $E_o t^2 r$, $E_o t^2 r^3$, $\cdots$, as indicated in Figure 2.3 as E_{t1}, E_{t2}, E_{t3}, $\cdots$, and E_{r1}, E_{r2}, E_{r3}, $\cdots$, respectively. The geometric path difference between any two successive transmitted rays is *2dcos*θ where *d* is the separation between the reflecting surfaces, and θ is the angle either ray makes with the surface normal. The corresponding phase difference δφ between two successive rays is then given by

$$\delta\varphi = 2k\,d\cos\theta = 4\pi\frac{d}{\lambda}\cos\theta \qquad (2\text{-}9)$$

Adding the amplitudes of all of the transmitted rays, the transmitted electrical field, E_t, is obtained as

$$E_t = E_o\,t^2 + E_o\,t^2\,r^2\,e^{j\delta\varphi} + E_o\,t^2\,r^4\,e^{j2\delta\varphi} + \cdots$$

$$= \frac{E_o\,t^2}{1-r^2 e^{j\delta\varphi}} \qquad (2\text{-}10)$$

The intensity $I_t = |E_t|^2$ of the transmitted light is thus given by

$$I_t = \frac{I_o\,|t|^4}{|1-r^2 e^{j\delta\varphi}|^2} \qquad (2\text{-}11)$$

where $I_t = |E_t|^2$ is the intensity of the incident beam.

Furthermore, if *R* denotes the power reflection and *T* the power transmission of the one surface, then in terms of *r* and *t*, we have

$$R = |r|^2, \; T = |t|^2 \qquad (2\text{-}12)$$

Equation (2-11) can be then rewritten in the following alternative form:

$$I_t = \frac{I_o T^2}{(1-R)^2}\frac{1}{1 + f\sin^2(\frac{\delta\varphi}{2})} \qquad (2\text{-}13)$$

where $f = \dfrac{4R}{(1-R)^2}$ is a measure of the sharpness of the interference fringes.
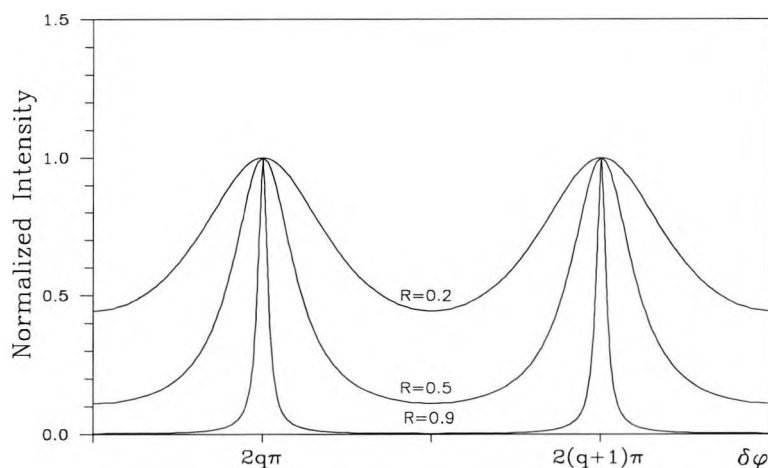
Figure 2.4 Intensity distribution of multi-beam interference

The intensity distribution variation with $\delta\varphi$ is shown in Figure 2.4 corresponding to different values of f. When R is small, for example, $R=0.2$, $f=1.25$ is also small the interference fringes are broad and indistinct, whereas $R=0.9$ is very large, leading to $f=360$, which is also very large, the fringes become very sharp and distinct.

§2.3 Basic interferometers

Two of the most important interferometers used in modern optics are introduced in this section. They are: (i) the Michelson interferometer, based on two-beam interference; and (ii) the Fabry-Perot interferometer, employing multiple-beam interference.

§2.3.1 Michelson interferometer

The optical interference of two light waves may be achieved physically by various means, for example, by making use of reflection, refraction or polarisation. One of the best known and most investigated interferometers is the Michelson interferometer. The basic configuration is illustrated in Figure 2.5, where light from a monochromatic source(S) is made parallel by the lens(L_1). The light then falls on a beam splitter(BS) so that part of the
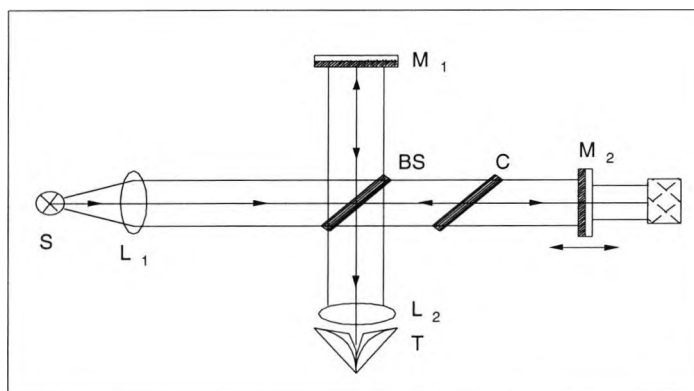
Figure 2.5 The Michelson interferometer

S—the light source for the interferometer, L1, L2—the lenses, M1, M2—

the mirrors, BS—the beam splitter, C—the compensator plate, T—telescope.

light passes through BS and is reflected first by a mirror(M_2) and then by BS so as to enter the

telescope(T). The rest of the light is reflected at the rear face of BS, then by a mirror(M_1)

from where it passes through BS to the telescope. The two beams of light entering the

telescope are coherent if the path difference is less than the coherence length of the source and

interference fringes can then be seen through the telescope. The compensator plate(C), which

is a plate of glass of identical thickness to BS, is often included to ensure that the two arms of

the interferometer can be made equal in terms of the optical path length reviewed.

The interference pattern is observed at T. Here the light appears to come from two

virtual point sources S' and S'', and the phase difference, θ, between them results from the

separation of the two mirrors, M_1 and M_2, and may be expressed as:

$$\theta = 2k(d_1 - d_2) = 4\pi\frac{\Delta d}{\lambda} \tag{2-14}$$

where d_1, d_2 represent respectively the optical length between the mirror and the beam

splitter, BS, and $\Delta d = (d_1 - d_2)$ is the length difference between them, λ is the wavelength of

the light source. If one of the mirrors, say M_2, is free to move, then the optical path difference $2\Delta d$ (and thus the phase, θ) of the light reflected from it will change relative to that reflected from M_1 and the interference pattern will cross the field of view. If Δd changes by $\lambda/2$, the resulting phase change of 2π will lead to a fringe shift. The distance moved by M_2 can therefore be measured in terms of fringe shift, although such measurements are usually limited by the coherence length of the light source used. For absolute distance measurement, the measurement range is usually limited to be within $\lambda/4$, which is only about 2×10^{-7} m for a typical solid-state laser source, operating at a wavelength of ~800 nm[Jackson 1987].

§ 2.3.2 Fabry-Perot interferometer

The Fabry-Perot interferometer, devised by C. Fabry and A. Perot in 1899 has been widely used to measure wavelengths with high precision and to study the fine structure of spectral lines, and the Fabry-Perot cavity structure constitutes the simplest laser resonator configuration. It is well-known that the Fabry-Perot interferometer is based on the principle of multiple-beam interference effect, as presented in the proceeding section. A generalised FP interferometer, as illustrated in Figure 2.6, consists of two plane and parallel mirrors with
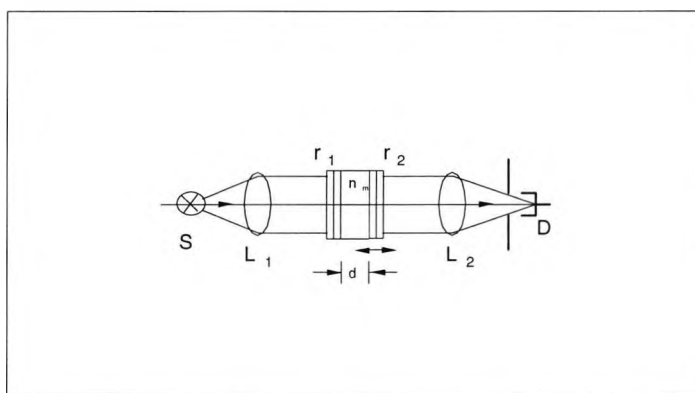
Figure 2.6 The Fabry-Perot interferometer

S—the light source, L_1, L_2—the lenses, r_1, r_2—the reflection coefficients of the FP mirrors, d—the separation between the FP mirrors, n—the refractive index, D—an optical detector.

amplitude coefficients of reflection r_1 and r_2 separated by a distance d containing a medium of refractive index n, the light from a point source(S) is collimated by lens, L_1, and propagates into the FP cavity. The output light from the cavity is then focused by a further lens, L_2, onto a detector, D, through a pinhole. When one of the cavity mirrors is displaced along the optical axis, a periodic intensity variation may be detected by the detector, D, i.e. the fringes produced by the multiple-beam interference inside the FP cavity. For a passive FP interferometer, there is no amplification inside the cavity, but for an active FP cavity structure, for example a laser, there is an amplification produced by stimulated radiation
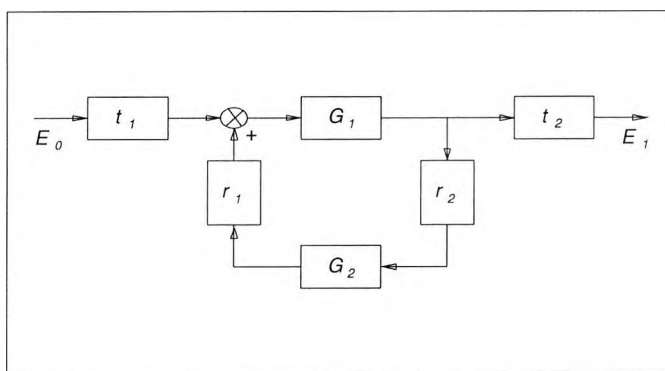
Figure 2.7 Block diagram of the FP feedback system

E0, E1—the incident light beam and the transmitted light beam, t1, t2—the amplitude coefficients of transmission, r1, r2—the amplitude coefficents of reflection, G1, G2—the gain transfer functions of the light waves inside the FP cavity.

inside the laser cavity. The general case of the FP feedback system may be depicted as is shown schematically in Figure 2.7, where t_1 and t_2 represent the amplitude coefficients of transmission; $G_1(v)$ and $G_2(v)$ represent respectively the gain transfer functions of the light waves in the forward and backward directions inside the FP cavity; and v is the optical frequency. The transfer function, $H(v)$, of the above system may be given by

$$H(v) = \frac{t_1 t_2 G_1(v)}{1 - r_1 r_2 G_1(v) G_2(v)} \qquad (2\text{-}15)$$

The transfer functions G_1 and G_2 are considered generally to be identical in both directions, and they may be expressed as

$$G_1(v) = G_2(v) = exp[-j2\pi v\frac{nd'}{c} + (g-\gamma)\frac{d'}{2}] \qquad (2\text{-}16)$$

where $d' = d \cos \theta$, and θ represents the angle between the ray and the mirror normal; g and γ are the optical gain and loss of the cavity per unit length respectively. In the case of a passive FP cavity structure, it may be considered that there is no absorption and no amplification inside the cavity, and the transfer function $H(v)$ may thus be reduced to

$$H(v) = \frac{t_1 t_2 exp[-j\varphi]}{1 - r_1 r_2 exp[-j2\varphi]} \qquad (2\text{-}17)$$

where $\varphi = 2\pi v\frac{nd'}{c}$

The power transmission T_p of this FP system is simply given by

$$T_p = |H(v)|^2 = H(v)H^*(v)$$

$$= \frac{(t_1 t_2)^2}{1 + (r_1 r_2)^2 - 2r_1 r_2 \cos (2\varphi)} \qquad (2\text{-}18)$$

Now $R_1 = r_1^2$, and $R_2 = r_2^2$. For a lossless mirror, then, $T_1 = t_1^2 = 1 - r_1^2 = 1 - R_1$, $T_2 = t_2^2 = 1 - r_2^2 = 1 - R_2$, the above expression (2-18) thus becomes

$$T_p = \frac{(1 - R_1)(1 - R_2)}{[1 - (R_1 R_2)^{1/2}]^2 + 4(R_1 R_2)^{1/2} \sin^2\varphi} \qquad (2\text{-}19)$$

It can be seen that if $R_1=R_2=R$, the above expression is identical with the expression(2-13). To illustrate the characteristics of the FP interferometer, the intensity transmission, T_p, versus the frequency, v, of the incident wave is depicted in Figure 2.8. The curve consists of a series of equally spaced maxima with the phase, φ, corresponding to an integral multiple of π radians, i.e. $\varphi=q\pi$, where q is a positive integer and the frequencies v_q of these maxima are given by
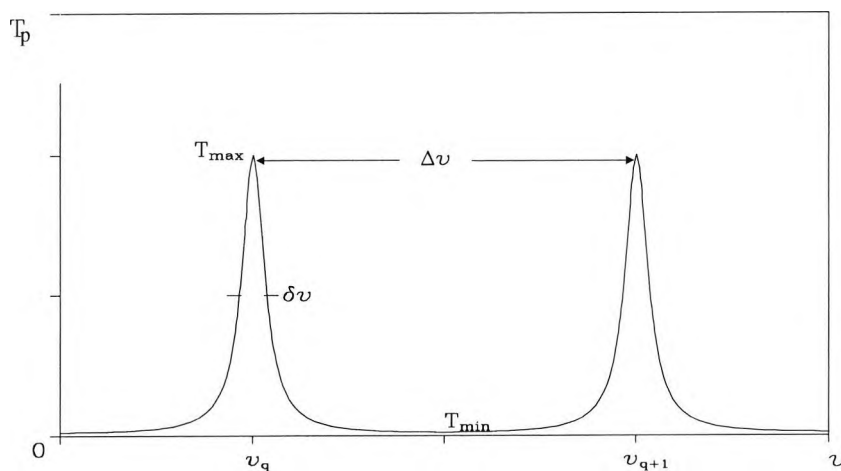
Figure 2.8 Intensity transmission vs. incident frequency

$$\nu_q = q\frac{c}{2nd'} \tag{2-20}$$

The frequency difference between two consecutive maxima, $\Delta\nu$ is termed the free spectral range of the interferometer and is given by

$$\Delta\nu = \frac{c}{2nd'} \tag{2-21}$$

From Figure 2.8 it is easy to see that the FP interferometer is like an optical filter in which only those specified frequencies of incident light may pass the interferometer. The maximum and minimum values of the transmission T_p are respectively

$$T_{max} = \frac{(1 - R_1)(1 - R_2)}{[1 - (R_1 R_2)^{1/2}]^2} \tag{2-22}$$

and

$$T_{min} = \frac{(1 - R_1)(1 - R_2)}{[1 + (R_1 R_2)^{1/2}]^2} \tag{2-23}$$

To express the spectral half-width $\delta\nu$ of a transmission peak, the following condition arises

$$\frac{T_{max}}{2} = \frac{(1 - R_1)(1 - R_2)}{[1 - (R_1 R_2)^{1/2}]^2 + 4(R_1 R_2)^{1/2} \sin^2(q\pi + \delta\varphi)} \tag{2-24}$$

where $\delta\varphi$ is the phase deviation from the central peak($\varphi = q\pi$), it may be assumed that this phase deviation $\delta\varphi$ is very small, with $\delta\varphi \ll \pi/2$, and thus $\sin(\delta\varphi) \approx \delta\varphi = 2\pi(\delta v/2)\dfrac{nd'}{c}$. Substituting Equation(2-22) into (2-24) gives

$$(\delta\varphi)^2 = \frac{(1 - \sqrt{R_1 R_2})^2}{4\sqrt{R_1 R_2}} \tag{2-25}$$

and thus the half-width, δv, may be expressed by

$$\delta v = \frac{c}{2nd'} \frac{1 - (R_1 R_2)^{1/2}}{\pi(R_1 R_2)^{1/4}} \tag{2-26}$$

To provide a measure of the filter properties of the FP cavity, it is more convenient to define that the "finesse" F of the interferometer as[Svelto 1989]

$$F = \frac{free\ spectral\ range}{full\ width\ at\ half{-}maximum}$$

$$= \frac{\Delta v}{\delta v} = \frac{\pi(R_1 R_2)^{1/4}}{1 - (R_1 R_2)^{1/2}} \tag{2-27}$$

which indicates how narrow the transmission peak is in comparison to the free spectral range.

§2.4 Coherence

In the proceeding sections, it has been assumed that the optical fields were completely coherent, monochromatic, and constant in amplitude. However, light produced by a real physical source is never strictly monochromatic[Dandridge et al 1981]. The amplitude and phase undergo irregular fluctuations with the result that the visibility is less than that of the interference pattern which would be formed by a truly monochromatic light source. The properties of a light source that are relevant to the interference phenomenon can be conveniently expressed in terms of the concept of optical coherence. In this section, the

concepts of temporal and spatial coherence, fringe visibility, coherence length and spectral linewidth are introduced[Born & Wolf 1975, Fowles 1968, and Perina 1985].

§2.4.1 Temporal and spatial coherence

Light waves at two points or more in space or time that are capable, in principle, of being superimposed to produce interference effects are said to be **coherent**. The coherence is a measure of the extent to which a phase relationship is maintained both across the beam(spatial coherence) and along the beam(temporal coherence). For our studies in semiconductor lasers, the laser used is considered to be a point source because of the small emitting area of the semiconductor laser, the spatial coherence may thus be neglected in the theoretical analysis and the term coherence hereafter therefore refers to the temporal coherence, which plays a very important role in the self-mixing interference.

Temporal coherence may be defined in terms of the time for which the radiation emitted by a source remains predictable in phase. Assuming that the two interfering beams in the Michelson interferometer are of equal amplitude A, and the two beams originate from the same spatial source, the total field, $\overline{E}_{total}$, at the point of detection, D, is

$$\overline{E}_{total} = \overline{E}_1(t) + \overline{E}_2(t - \Delta t) \qquad (2\text{-}28)$$

where Δt represents the time delay between two interfering beams, which is linked to the optical path difference(ΔL) by $\Delta t = \Delta L/c$, c being the speed of light. In the actual case of interference, the amplitudes and phases vary with time in a random fashion. The intensity at D is usually defined as the time average of the instantaneous light intensity, which can be expressed accordingly, as

$$I = \; < \overline{E}_{total} \cdot \overline{E}_{total} > \; = \; <(\overline{E}_1 + \overline{E}_2) \cdot (\overline{E}_1^{\;*} + \overline{E}_2^{\;*})>$$

If the elctric fields are assumed to be stationary, i.e. the time average is independent of the origin of time, and that they have the same polarization so that their vectorial nature can be ignored. Then the above expression can be written as

$$I = I_1^2 + I_2^2 + 2Re<A_1A_2^*> \qquad (2\text{-}29)$$

where $I_1 = <|A_1|^2>$, $I_2 = <|A_2|^2>$, and A_1, A_2 are the amplitudes of the electric fields respectively. The last term in the above expression represents the interference between the two beams. If the optical field is perfectly sinusoidal, i.e. the light source is perfectly monochromatic, then this expression reduces to the standard interference formulation

$$I = I_o(1 + \cos \theta) \qquad (2\text{-}30)$$

where I_o is the average intensity; $\theta = 2\pi v \dfrac{\Delta L}{c}$ is the optical phase difference between the two beams, which determines completely the intensity variations around I_o. However, if the source is not monochromatic but has a spectral composition given by its power spectrum function, $p(v)$, the two beam interference may then be related directly to the power spectrum of the source. If the source is considered to be spatially coherent (a point source) , but temporally incoherent, the intensity, I, at D for such a non-monochromatic light source is given by a summation over the complete spectrum $p(v)$, namely,

$$I = \int_0^\infty p(v)[1 + \cos (2\pi v \Delta t)] \, dv \qquad (2\text{-}31)$$

where $p(v)$ is the power spectrum function of light source.

To illustrate the relationship between the interference and the power spectrum, the intensity distribution, I, for a number of different optical sources is shown in Figure 2.9. Fig. 2.9(a) shows the normal cosinusoidal fringes observed for a perfectly monochromatic source. Fig. 2.9(b) illustrates the effect of a finite linewidth spectrum on the fringes observed from a
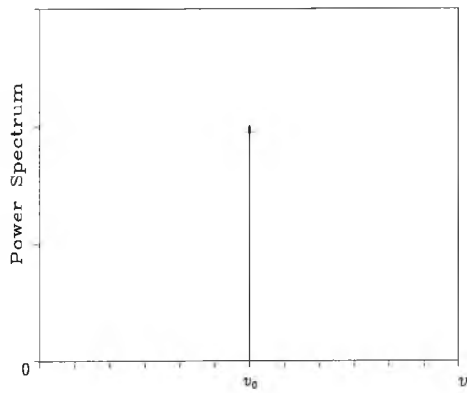
(a1) Spectrum of monochromatic light
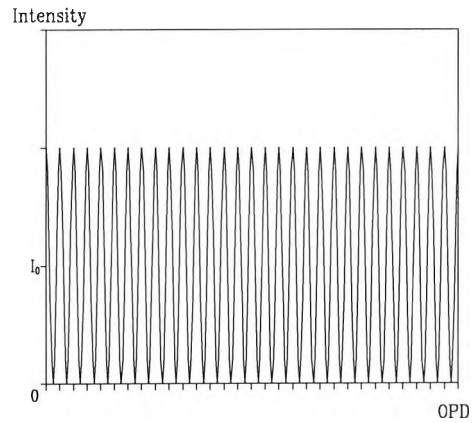
(a2) The corresponding fringe patterns
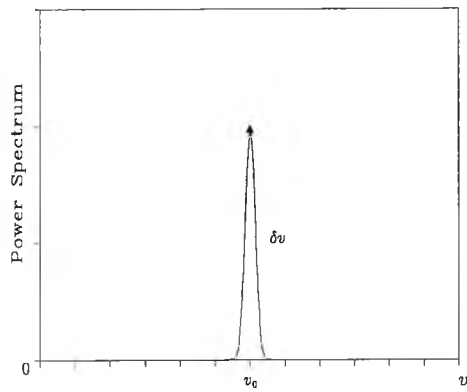
(b1) A finite width spectrum
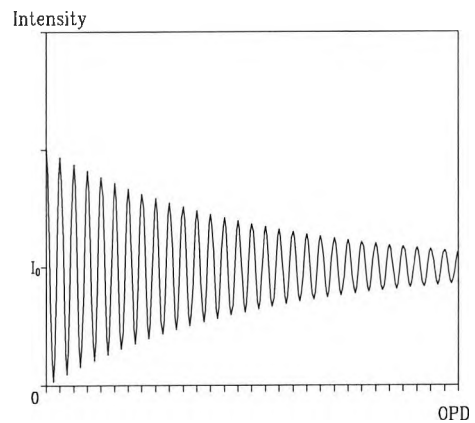
(b2) The corresponding fringe patterns
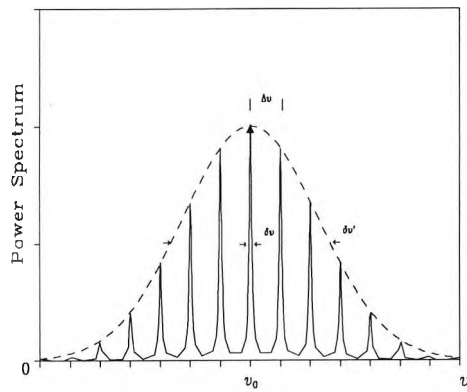
(c1) A multi-mode spectrum
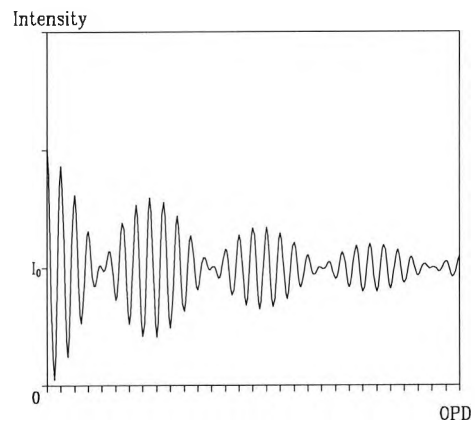
(c2) The corresponding fringe patterns

Figure 2.9 The source spectra and their correponding fringe patterns

single frequency source. Fig.2.9(c) shows the intensity distribution of interference when the source used has a multi-mode spectral distribution.

§2.4.2 Degree of coherence

Light cannot be simply considered as either being coherent or incoherent; it has different degrees of coherence. Considering two wavetrains of light, each of finite length Δs, overlaping to their full extent in space or time, such complete overlap will result in distinct maxima and minima of the highest degree of contrast. Even if the wavetrains overlap only in part, interference is possible, although the degree of contrast of the fringes is less, depending on the degree of overlap[Fowles 1968].

In general, a normalized correlation function, ρ, is defined to describe the degree of coherence, which has a value between zero and one. In terms of $|\rho|$, the following types of coherence may be defined and are illustrated schematically in Fig. 2.9

$$|\rho| = 1 \qquad \text{complete coherence[Figure 2.9(a)]}$$
$$0 < |\rho| < 1 \qquad \text{partial coherence[Figure 2.9(b), and (c)]}$$
$$|\rho| = 0 \qquad \text{complete incoherence}$$

For two beam interference, ρ is also termed the fringe visibility function, V, and may be expressed as:

$$V = \rho = \frac{I_{\max} - I_{\min}}{I_{\max} + I_{\min}} \qquad (2\text{-}32)$$

where I_{max} and I_{min} are the two limits of intensity variations. In this case, the visibility or degree of coherence, V, represents the fringe contrast. For a perfectly monochromatic light source, it is easy to calculate that the visibility function, V is 1, by using equ.(2.31), which means that the two beam interference is completely coherent no matter how large the optical path difference between the two beams. In practice, the light source has always finite spectral

width. For example, the power spectrum of a single mode laser may be considered to be a Lorentzian distribution, as shown in Fig.2.9(b), and it can be expressed as:

$$p(\nu) = \frac{p_o}{(\nu - \nu_o)^2 + (\delta\nu/2)^2} \tag{2-33}$$

where p_o is proportionality constant, ν_o is the central optical frequency, and $\delta\nu$ is the full-width at half-maximum of the power spectrum.

From Equations(2-31) and (2-33), the intensity, I, for two beam interference may thus be expressed as:

$$I = I_o\{1 + exp[-\frac{\delta\nu}{2}|\frac{\Delta L}{c}|] \cos(2\pi\nu_o\frac{\Delta L}{c})\} \tag{2-34}$$

where ΔL represents the optical path difference(OPD). Figure 2.9(b) shows the intensity variation with ΔL. Substituting Equation(2-34) into Equation(2-32), the visibility function, V can be calculated to be

$$V = exp[-\frac{\delta\nu}{2}|\frac{\Delta L}{c}|] \tag{2-35}$$

This function represents an exponential decay of the interference fringes along ΔL. The maximum visibility occurs when the two arms of interferometer is balanced, i.e. ΔL=0. The visibility function is illustrated in Fig. 2.10.

§2.4.3 Coherence length and spectral linewidth

A useful indicator of the temporal coherence is the coherence time or coherence length(related by the velocity of light in the medium under consideration) within which the optical interference phenomenon could be observed. There is no standard definition of coherence length or coherence time, but an often used definition is that the coherence length
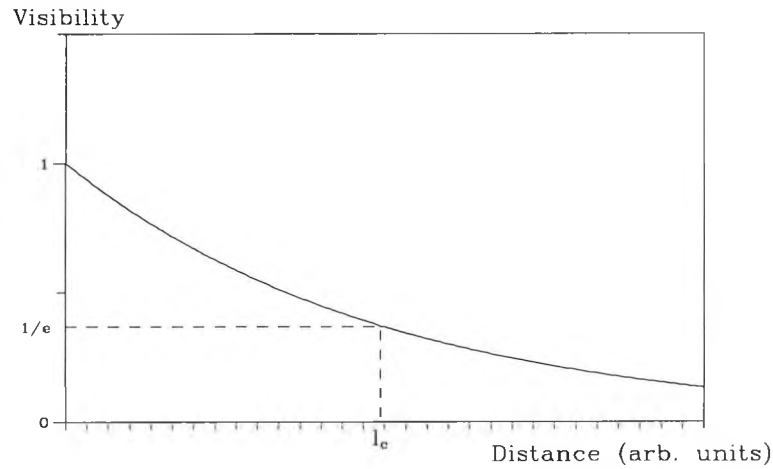
Figure 2.10 Visibility function of a finite width spectrum
illustrating the definition of l_c, the coherence length.

represents the distance, l_c, between two interfering beams, where the visibility function drops to $\frac{1}{e}$, as shown in Figure 2.10.

According to this definition, the value of the coherence length, l_c, may be obtained from Equation(2-35), which gives the following condition

$$\frac{\delta v}{2}\frac{2\,l_c}{c} = 1 \tag{2-36}$$

where δv is the full-width at half-maximum(FWHM) of the spectral distribution and c is the speed of light. Obviously, the coherence length, l_c, and coherence time, τ_c, may be calculated from the above equation, they are:

$$l_c = \frac{c}{\delta v} \quad or \quad \tau_c = \frac{l_c}{c} = \frac{1}{\delta v} \tag{2-37}$$

This equation can be converted to calculate the coherence length, l_c , in terms of the central wavelength of light, λ_o, and the spread of wavelengths emitted, $\delta\lambda$, as

$$l_c = \frac{\lambda_o^2}{\delta\lambda} \tag{2-38}$$

It is clear that the expression(2-37) represents the well-known Heisenberg Uncertainty relation. Obviously the coherence length or time is therefore determined completely by the source spectral spread, and this implies that the temporal coherence is only a reflection of the source spectral distribution. If the spectrum is changed, the coherence properties will be changed. This important property will be studied in detail later in terms of the the self-mixing effect.

§2.6 Summary

The optical interference phenomenon forms the basis of modern optical interferometry. The principle of linear superposition of the fields, two-beam interference and the interference of multiple optical beams have been briefly discussed. Based on the principle of two-beam interference, the Michelson interferometer is the best representive and the most investigated, whilst the Fabry-Perot device is the most well-known interferometer for multiple beam interference and is widely used as the laser cavity structure for most types of lasers. The basic principles of these two type of interferometers have been described in this Chapter.

Coherence is an important concept in optical interferometry and is of particular concern in the later studies of self-mixing interference in diode lasers. It has been shown, in this Chapter, that the coherence property of a light source is completely determined by its spectral distribution. The narrower the spectral linewidth of the source, the longer its coherence length, and the optical interference is closely related to the coherence. If the light source for an interferometer is incoherent, no interference phenomena will be observed.

Chapter 3

Principles of semiconductor lasers

§3.1 Introduction

This thesis deals with the so-called "self-mixing interference" in semiconductor lasers, which essentially relates two important phenomena: the optical interference effect produced by the external optical feedback field and the mechanism of semiconductor laser sources. In the self-mixing configuration the semiconductor laser is viewed not only as a conventional light source, but also as an interferometer; the combination of both functions makes the self-mixing interferometric system simple, compact and easy to align.

It is obvious that the semiconductor laser itself plays an extremely important role in the self-mixing interference effect to be discussed. In order to study the self-mixing effect inside a semiconductor laser in detail, it is essential to understand the basic principle of semiconductor laser oscillation, its lasing characteristics, and the spectral properties and the coherence properties associated with the self-mixing interference. In this Chapter, the basic properties of semiconductor lasers are presented, with a simple description of the laser structure. A simplified theory, which is based on the rate equations and the field approach, is also presented[Verdeyen 1981, Loudon 1983, and Petermann 1991a].

§3.2 Properties of semiconductor lasers

Semiconductor lasers are widely used for many applications, ranging from playing music on compact discs to sending signals through optical fibres, because of their

compactness, high output power and compatability with semiconductor electronic components. The process of light emission in semiconductor materials is due to the presence of recombination radiation of electrons and holes where the recombination energy is released as light. This process is also called current injection, so semiconductor lasers have been termed **injection lasers** or **diode lasers**[Rieck 1970, Thompson 1980, Hecht 1988, and Sevlto 1989].

§3.2.1 Semiconductors

A semiconductor is a material with electrical properties intermediate between those of a conductor and an insulator. The electrons in a conductor(e. g. a metal) are free to move in the material and carry an electrical current. The electrons in an insulator are tightly bonded to atoms, and thus cannot move. In a semiconductor, some electrons are loosely bonded to atoms, so some movement is possible.

The movement of electrons in the conduction band and holes in the valence band results in the conduction of electrical current in the semiconductor material. The related energy-level diagram is illustrated in Figure 3.1. The **valence band** is almost full of electrons, while the **conduction band** is almost empty and the gap in between is termed the **energy gap**.
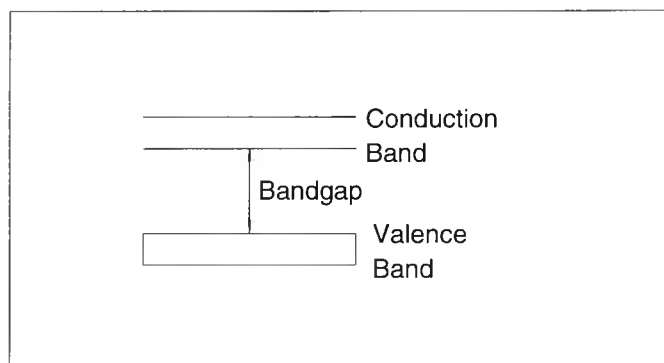
Figure 3.1 Energy-level diagram in a pure semiconductor

In a pure semiconductor material(or intrinsic material) the number of electrons and holes must be always equal and this number can be changed by either changing the temperature or changing the electron and hole populations through other means. If the temperature of a semiconductor is raised, then it becomes possible for electrons in the valence band to be thermally excited into the conduction band, where they can move about freely. The number of electrons depends on the size of the gap and the temperature, and according to the Boltzmann law

$$\frac{N_c}{N_v} = exp[-\frac{1}{kT}(E_c - E_v)] \tag{3-1}$$

where N_c and N_v are the numbers of electrons in the conduction band and valence band, respectively, E_c-E_v is the energy difference between the two states, k is the Boltzmann constant and T is the temperature(in Kelvin).

Another way of changing the electron and hole population is by doping the semiconductor with atoms whose valences differ from that of the host material(i. e. by adding impurities). For example, suppose that silicon(tetravalent) is dopped with phosphorous which is pentavalent. Each phosphorus atom replaces one of the silicon atoms and four of its five valence electrons are used to satisfy the bonding requirements of its four neighbours[Figure 3.2(a)], and the fifth is left free to conduct electricity in the crystal. A semiconductor doped
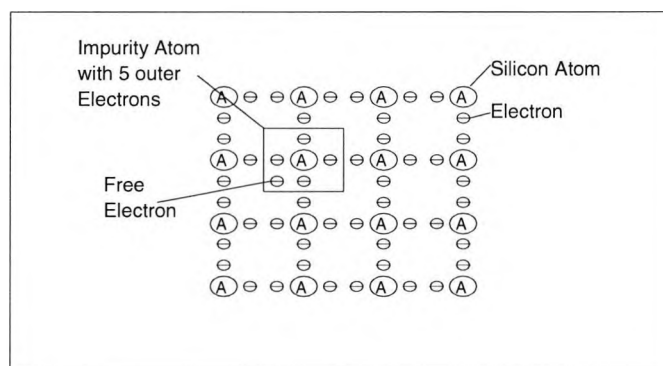
Figure 3.2(a) Bonding in doped n-type silicon
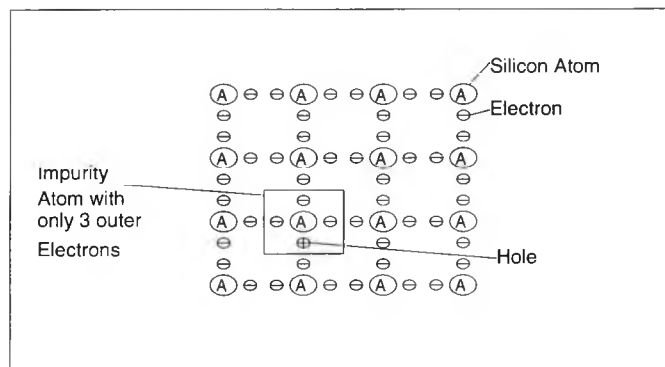
Figure 3.2(b) Bonding in doped p-type silicon

with such electron donors is called an n-type semiconductor, because the doping produces negative current carriers.

In another case, the impurity atom may have only three electrons. All three electrons form bonds with surrounding atoms, but a "hole" remains in the crystal where the forth electron should be, as shown in Figure 3.2(b). An electron from elsewhere in the crystal can move in to fill the hole, which in effect causes the hole to move to the place where the electron used to be. Thus, the hole can "move" or carry current in the semiconductor. The material doped with such electron acceptors are called p-type semiconductors.

§3.2.2 Light emission from the semiconductor junction

The semiconductor laser is basically a p-n junction which is formed between two parts of a semiconductor crystal with different doping. In practice, the semiconductor begins as a substrate(e.g. a modest level of p-doping). Then additional dopants(e.g. a n-doping) are diffused into the material from one side of the crystal, forming in the top layer of the semiconductor an n-type material, while the bottom remains p-type material, as shown in Figure 3.3. Such a device acts as a diode, i. e. a device that will pass current in one direction but not in the other. The junction between the n- and p-type materials is thin(about 0.1 to 1
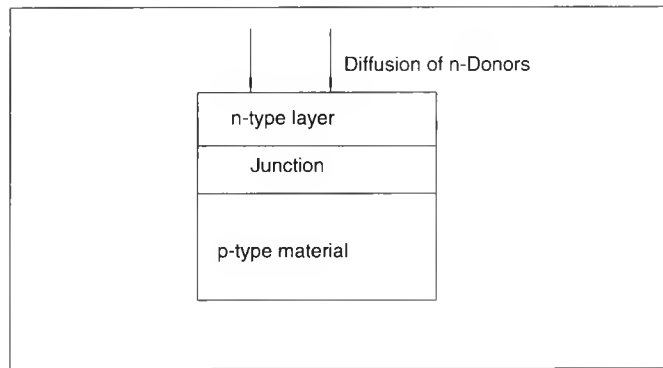
Figure 3.3 A p-n junction by doping of semiconductor crystal

μm) and represents many atomic layers. The hole concentration is roughly that of the p-type impurities, the electron concentration is roughly that of the n-type impurities.

Suppose that a semiconductor diode is forwarded-biased(i.e. a positive voltage is applied to the p-side and a negative voltage to the n-side), as shown in Figure 3.4, the **p** carriers in the **p** region are attracted to the negative electrode, while the **n** carriers in the **n** region are attracted to the positive electrode. This pulls all the current carriers across the junction. The result is that the current starts flowing in an electronic diode, but in an optical device, the electrons from the n-type material recombine with holes from the p-type material,
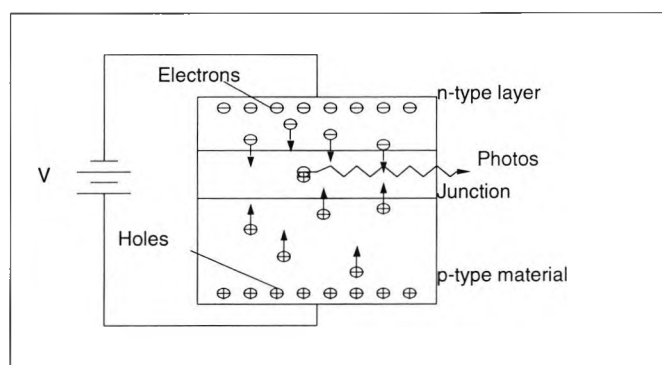
Figure 3.4 Forward-biasing p-n junction in a semiconductor

releasing energy at the junction and much of this recombination energy is released as light. Light emission from the recombining electrons and holes serves as the basics of light-emitting diodes(LEDs) and diode lasers(LDs).

§3.2.3 Semiconductor lasers

In a light-emitting diode(LED), the light is produced by spontaneous emission and radiates in every direction. The upper limit of the wavelength of light emitted is determined by the band gap *Eg* and is given by

$$E_g = E_c - E_v = \frac{hc}{\lambda} \ or \ \lambda = \frac{hc}{E_g} \tag{3-2}$$

where λ is the wavelength of emitting light, *h* is the Planck's constant(4.135×10^{-15} eV/Hz) and *c* is the speed of light in vacuum($2.988 \times 10^{+8}$ m/s)

Unlike LEDs, semiconductor lasers are obtained by cleaving the ends of the semiconductor crystal to form two parallel reflective crystal surfaces(illustrated by Figure 3.5) so that part of the generated light can be reflected back into the semiconductor material. Because of the high refractive index of the semiconductor crystal, the end-facets give a high reflectivity and form a Fabry-Perot resonator, which has a considerable finesse. This resonator
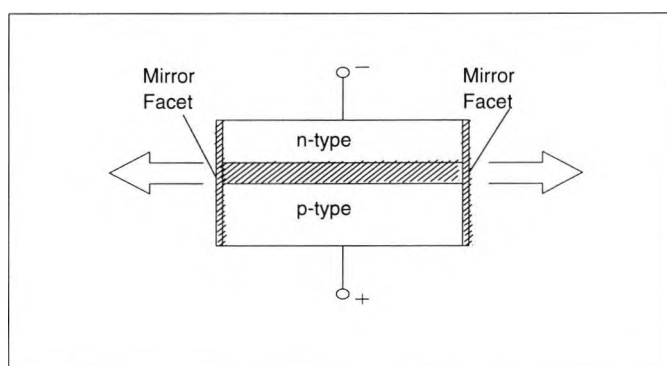
Figure 3.5 A semiconductor laser by cleaving crystal facets

may be excited into laser oscillation, approximately over the thickness of the region where the injected carriers recombine, when the injection current is raised above a certain value known as the "**threshold**". In this process of laser oscillation, the electrons participate in three types of interaction with the photons, namely **spontaneous emission**. **absorption**, and **stimulated emission**. The first transition process, named **spontaneous emission**, occurs when an electron in the conduction band falls into the valence band during the recombination, it emits much of the energy in the form of a photon with energy roughly equivalent to that of the **band gap**.

The second transition process, **absorption**, occurs when a photon of light strikes an electron in the valence band. The photon is absorbed, and the electron concerned is raised to an empty state in the conduction band. This phenomenon is called induced absorption.

The third transition process, **stimulated emission**, occurs when a photon strikes an electron in the conduction band and emits a second photon. The emitted photon has essentially the same frequency, the same phase and travels in the same direction as the incident photon. This phenomenon is called stimulated emission.

The stimulated emission process is unlikely to occur when the semiconductor is in a state of thermal equilibrium because of the small number of electrons in the conduction band. However, above threshold the number of electrons in the bottom of the conduction band is made to exceed the number of the holes in the top of the valence band. This condition is well-known in other type of lasers as **population inversion,** and it is achieved in a semiconductor laser by applying an injection current to a p-n junction. In the population inversion state, stimulated emission predominates over induced absorption, resulting in the amplification of light.

When the semiconductor material forming the resonator is brought to a state of population inversion, light generated by spontaneous emission is amplified and repeatly reflected by the front and rear reflective facets. Light emitted in any direction not parallel to
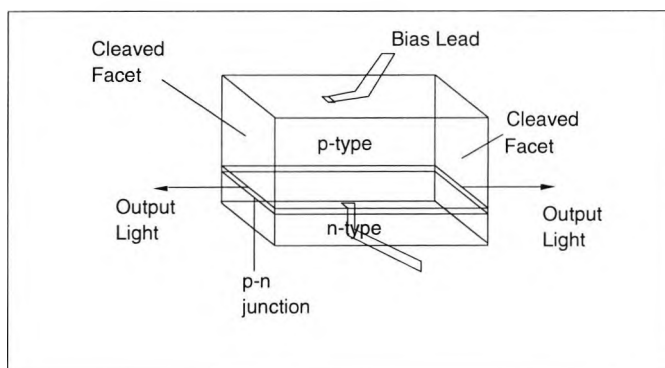
Figure 3.6 Typical broad-area p-n homojunction GaAs Laser

the optical axis of the resonator will pass through the sides of the resonator and not be amplified further. The component of the spontaneously emitted light which travels parallel to the optical axis, will be repeatedly reflected by the mirror facets. As the light travels through the semiconductor material, it is amplified by stimulated emission. At each reflection, the beam is partially transmitted through the reflective facets. Laser oscillation begins when the amount of amplified light becomes equal to the total amount lost through the sides of the resonator, through the mirror facets, and through absorption by the semiconductor material etc. Figure 3.6 shows a schematic of a broad-area p-n homojunction GaAs semiconductor laser.

§3.3 Structures of semiconductor lasers

There are a variety of semiconductor laser structures which have been developed and used[Sharma 1974, and Hecht 1989]. In this thesis, the detailed structures will not be investigated but the focus will be on broad categories that cover the most important types and concentrate on the variations which have the most significant effects on the performance of the **self-mixing interference**.

§3.3.1 Homojunction semiconductor laser

Homojunction semiconductor lasers are made entirely of a single semiconductor compound, typically gallium arsenide, with different portions of the device having different dopings. The junction layer is the interface between n- and p-doped regions of the same material. This structure was used in the first diode lasers but has since been replaced by other structures which can provide better laser characteristics.

In a homojunction laser, the semiconductor has essentially a uniform reflective index throughout , so light building up in the active layer can diffuse into surrounding layers. The schematics of the structure, the refractive index profile and the beam confinement is shown as in Figure 3.7(a).

§3.3.2 Single-heterojunction lasers

Single-heterojunction lasers are those in which the active layer has one boundary with a material having a different bandgap. In practice, this means that it is sandwiched between two layers of different chemical compositions(typically GaAs and GaAlAs), as shown in Figure 3.7(b), which have different bandgaps. Most often the active layer is GaAs, and the laser
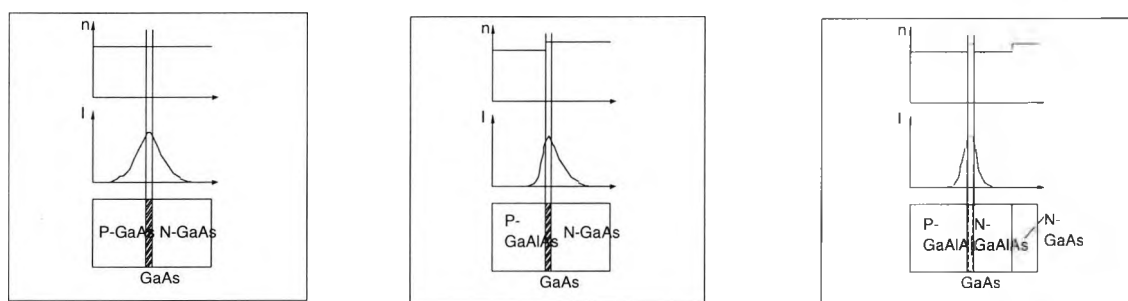
(a) Homostructure laser   (b) Single-heterostructure laser   (c) Double-heterostructure

Figure 3.7 Different types of semiconductor lasers corresponding to refractive index profiles, intensity distributions and structures. n-refractive index, I-intensity

emission wavelength is ~904 nm. Single-heterojunction lasers have more useful laser characteristics than homojunction lasers and are widely used to produce high peak powers in pulsed operation. They are offered as single devices or as "arrays" assembled from separate chips. However, single-heterojunction lasers are relatively inefficient and have high threshold currents that make them unsuitable for continuous or high-duty-cycle operation, such as in fibre-optic communications systems.

§3.3.3 Double-heterojunction lasers

Double-heterjunction lasers have an active(light-emitting) layer bounded by two layers of different materials, for example GaAs sandwiched between two GaAlAs layers, as shown in Figure 3.7(c). These lasers have proved the most suitable for continuous operation and have found widespread use in fibre optics. They cannot produce pulses with high peak power, but can operate continuously or with high-duty-cycle at powers of up to tens of milliwatts at room temperature. Their active layers are thinner than those of single-heterojunction lasers, so they can have threshold current densities low enough to operate continuously at room temperature.

§3.3.4 Stripe-geometry lasers

Stripe-geometry lasers are a sub-category of double-heterjunction lasers in which the emission is confined to a narrow stripe along the length of the laser, as shown in Figure 3.8. Typically the stripe is 1 to 10 μm wide, compared with widths of 50 μm or more for earlier double-heterojunction diode lasers. The stripe-geometry laser has a number of attractive features. Because the drive current is concentrated in a smaller stripe area, the threshold current for laser action is lower than that in wider-stripe lasers. The narrower stripe also improves beam quality by limiting the number of spatial modes in which the laser can oscillate, often to a single mode. The small emitting area corresponding to the stripe width is important for fibre optic applications, because it aids in coupling to single-mode fibres.
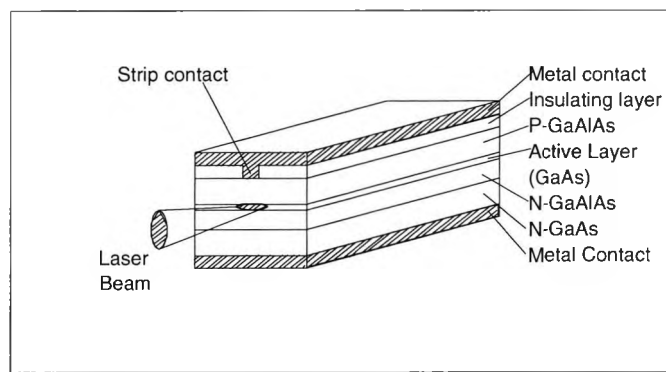
Figure 3.8 A schematic of a stripe-geometry double heterostructure semiconductor laser

The active-region width can be limited by two basic techniques. One is called **gain guiding** and relies on variations in the injection-carrier density and optical gain across the active region. The other is **index guiding**, in which the active region is defined by changes in the composition of the semiconductor that establish refractive index boundaries in the plane of the active region. Index-guided lasers tend to have better-quality beams, sharper turn on, and more linear output-current characteristics, and have found increasing uses in applications that require small spot size. However, they are vulnerable to some noise and feedback effects, for applications in communication and conventional interferometric optical sensors.

Gain in semiconductor lasers is very high, so the resonator cavities are short, typically a few hundred micrometers long. The resonator cavities are unusual in shape because of the nature of the active layer, which typically is a tenth of a micrometer to a couple of micrometers thick, and between a few and about 100 µm wide.

§3.3.5 Distributed feedback lasers

Conventional semiconductor lasers have a gain bandwidth broad enough to span several longitudinal modes. Above threshold, one mode usually dominates the laser output spectrum,

but changes in temperature and other operating conditions can cause a semiconductor laser to "hop" from one dominant mode to an adjacent one. To obtain a stable single longitudinal mode spectrum, a typical approach is use of the distributed feedback(DFB) laser, as shown in Figure 3.9. It contains a diffraction grating that scatters light back into the active layer. The grating can be along the length of the part of the active layer where there is gain(Figure 3.9(a)), or it can extend beyond the ends of the region where there is also gain(Figure 3.9(b)). The feedback leads to interference effects which allow oscillation only at wavelengths which are reinforced by the scattering effects.

The grating spacing(D) needed to select a particular wavelength(λ) in a distributed-feedback laser depends on the refractive index in the laser medum(n) and the value of a positive integer m in that gives the order of distributed-feedback coupling

$$D = m\frac{\lambda}{2n}$$
(3-3)

Typical values of m are 1 or 2. For a 1.55 mm DFB laser made of InGaAsP(n=3.4) with m=2, the value of D is found to be 456 nm. Thus the DFB limits laser oscillation to a single
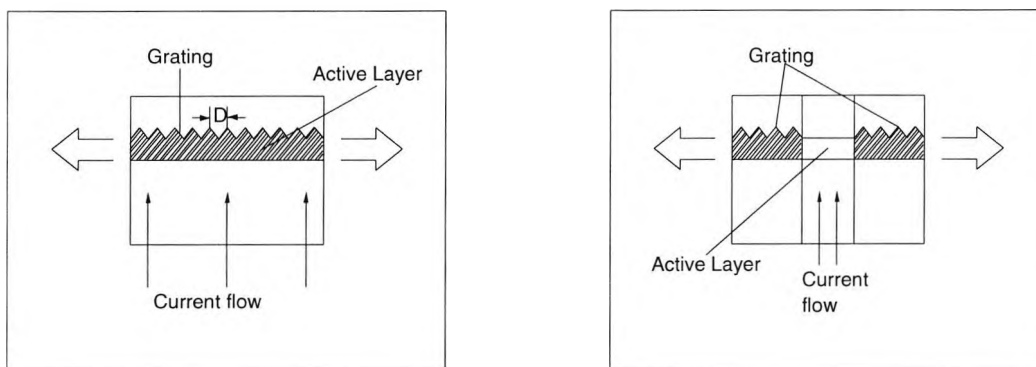
(a) Distributed feedback along active layer   (b) Distributed feedback outside active layer

Figure 3.9 Distributed feedback semiconductor lasers

longitudinal mode, giving the laser a very narrow bandwidth. The oscillation wavelength does shift slightly with temperature because the refractive index, *n*, is a function of temperature, but this change is much smaller than the wavelength shifts in conventional semiconductor lasers. DFB lasers are quite expensive and difficult to fabricate because of the complexity of their structure.

§3.4 Light/current characteristics

Semiconductor lasers are compact sources of high power near-infrared radiation. They are driven by low power electrical injection and are compatible with semiconductor circuitry, which results in an all-solid state, rugged, reliable device. Modulation of the laser output is extremely simple to accomplish. Light/current characteristics represent the basic properties of semiconductor lasers and this is the most important factor describing the quantum efficiency[Petermann 1991a].

At low current levels, the semiconductor lasers generate some spontaneous emission as do LEDs. However, as the current level increases, the lasers pass a threshold where the population becomes inverted and laser action begins. A graph of output optical power(P) versus the injection current(J) is illustrated as in Figure 3.10. Below threshold, light is emitted
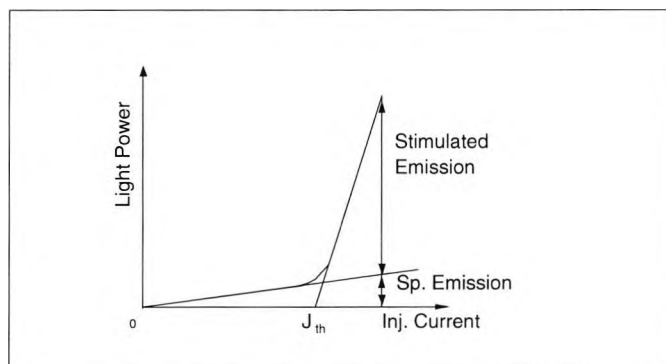
Figure 3.10 Laser light power vs. injection current

with very low efficiency. Once the current has passed the threshold level, the light output rises steeply, indicating the presence of stimulated emission. The spontaneous emission has a low quantum efficiency so that considerable optical power is emitted only above threshold, where the carrier density is considered to be clamped because any further current increase does not yield a further increase of the carrier density. Therefore any injected electron in excess of the threshold current must contribute to the stimulated emission and the emitted stimulated power becomes proportional to (J-J_{th}), where J_{th} is the threshold current.

§3.5 Simple theory of a single-mode semiconductor laser

Laser radiation can be generally described by a complex electric field as a classical self-sustained oscillation[Lax 1967]. The lasing characteristics may thus be either described by using the rate equations[Adams 1973] or by the field equations approach[Verdeyen 1981]. Under ideal conditions, laser radiation will oscillate at a discrete frequency dictated by the laser cavity mode that has the highest gain-to-loss ratio, however, the presence of various noise sources in the lasing process makes the laser field unable to oscillate at a pure frequency(i.e. a single frequency sinusoidal wave) but with a limited spectral linewidth. A formula for the linewidth of gas lasers was first derived by Schawlow and Towns[1958], the lineshape for such a gas laser was found to be Lorentzian and the linewidth to be narrowed inversely with the laser output power.

The first linewidth measurement for AlGaAs semiconductor lasers were made by Fleming and Moordian[1981a]. They confirmed that the lineshape was Lorentzian and the linewidth was narrowed inversely with power as expected, but the width was much greater than that predicted by the previous formula. Later the lineshape of a single-mode semiconductor laser was found by Daino et al[1982] to be not a perfect Lorentzian, but having adjacent satellite peaks, as shown in Figure 3.11. These satellite peaks have a magnitude of
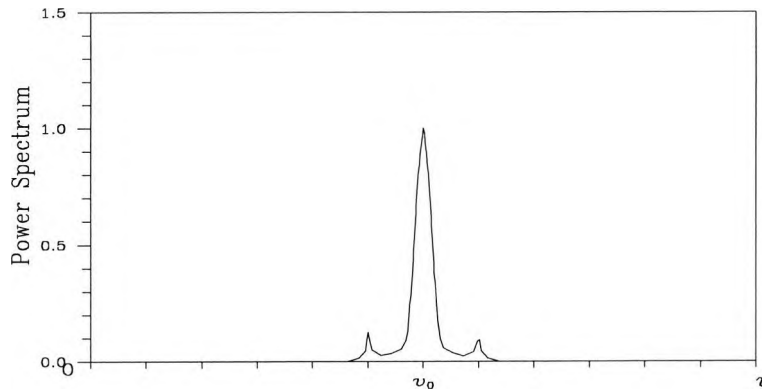
Figure 3.11 The laser spectrum with satellite side peaks

X-axis—the laser optical frequency,

Y- axis —the normalized laser power spectrum.

about 1% of the main peak[Vahala et al 1983]. The deviations of semiconductor laser characteristics from the well accepted theory for the operation of gas lasers have been extensively studied by a number of researchers, such as Hang and Haken[1967], Henry[1982, 1986], Vahala and Yariv[1983]. In this section, the steady-state conditions for laser oscillation are analysed and then the well-known standard laser equations are introduced, and finally the lasing spectral linewidth and the coherence concerned for optical interferometry are considered .

§3.5.1 Lasing conditions

In the following analysis, the simplest laser cavity structure is considered, which is represented by a Fabry-Perot type cavity, as shown in Figure 3.12, where a stripe waveguide along the active layer is formed and the optical wave may propagate along this waveguide until it is reflected after a length, d, at the cleaved rear endface of the laser device. The high degree reflection occurs because of the mismatch between the refractive index of the semiconductor($n=3.6$) and the surrounding air($n=1.0$), and the corresponding power reflection coefficient may be calculated to be about 0.32.
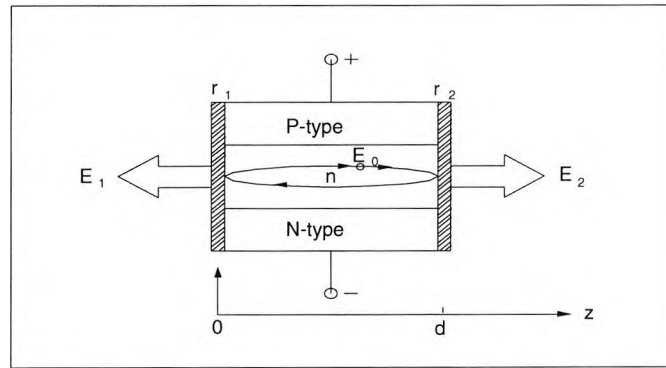
Figure 3.12 Fabry-Perot cavity structure of a diode laser

E_0—an initial electric field vector inside the laser cavity, E_1, E_2—

electric field vectors of laser output in its two directions, r_1, r_2—

amplitude reflection coefficients of the laser facets, n—refractive

index of the laser cavity material, d—laser cavity length

The electric field travelling to the right is designated the positive direction(z direction) and the facet r_1 is given the initial position($z=0$) of the z axis. E_1 and E_2 represent the electric vectors of the light waves emitted through the two facet mirrors of the laser cavity respectively. An initial electric field, E_o, inside the cavity will be amplified due to stimulated emission both in the forward direction and in the backward direction. The gain transfer function $G(v)$, according to Equation(2.16), may be expressed as

$$G(v) = exp[-j2\pi v\frac{nz}{c} + (g - \gamma)\frac{z}{2}]$$ (3-4)

where v is the optical emission frequency, g is the optical gain due to the stimulated emission(per unit length cm^{-1}) and γ accounts for the optical loss within the laser cavity per unit length(cm^{-1}). After a complete roundtrip via the laser facets r_1 and r_2, the transfer function $R(v)$ may be expressed as

$$R(v) = r_1\ r_2\ G_1(v)G_2(v)$$
$$= r_1\ r_2\ exp[-j4\pi v\frac{nd}{c} + (g - \gamma)d]$$ (3-5)

where $G_1(\nu)$, $G_2(\nu)$ represent the gain transfer functions in the forward and backward directions repectively. For a stationary laser oscillation, the amount of amplified light becomes equal to the total light lost through the sides of the cavity, the laser facets and by absorption in the semiconductor material. This requirement leads to

$$R(\nu) = r_1\, r_2\, exp[-j4\pi\nu\frac{nd}{c} + (g - \gamma)d] = 1 \qquad (3\text{-}6)$$

It implies that the occurance of laser oscillation requires the roundtrip gain to be equal to unity. It is easy to see that this condition cannot be realised in a passive FP cavity because there is no stimulated radiation and the maximum transmission through the cavity is always less than 1. However, in an active cavity, this condition can be realised because the light inside the cavity is repeatedly amplified through the stimulated emission process. The amplified light will cause a lasing state after undergoing several transits of the cavity. It is known that the amplitude of the amplified light cannot be increased without limit, it will be clamped finally by the gain saturation of the laser material. Thus once a stablized optical flux is established inside the cavity, the laser oscillation will be formed and light waves with the same phase, and the same direction, will be emitted from the cavity. The modulus of Equation(3-6) yields the amplitude condition for the required gain g, while the roundtrip phase condition, by equating the phase to an integral multiple of 2π radians, results in the expected lasing frequency, ν_o.

If the required laser gain and the possible oscillation frequencies at threshold are denoted respectively as g_{th} and ν_{th}, the following two conditions from Equ.(3-6) may be obtained

(i) $\qquad\qquad r_1 r_2 exp[(g_{th} - \gamma)d] = 1$

and

(ii) $\qquad\qquad \Phi = 4\pi\nu_{th}\frac{nd}{c} = 2q\pi, \quad q = 1, 2, 3, ...$

The amplitude condition (i) results in the following gain expression for laser oscillation

$$g_{th} = \gamma + \frac{1}{d}\, ln\frac{1}{r_1\, r_2} \qquad (3\text{-}7)$$

and the phase condition (ii) leads to the oscillation frequencies being given by

$$\nu_{th} = q\frac{c}{2nd}$$ (3-8)

where g_{th} accounts for the minimum gain for the laser oscillation, which is termed the **threshold gain** and ν_{th} represents a series of the possible oscillating frequencies inside the laser cavity, with the modal spacing $\Delta\nu = \dfrac{c}{2nd}$. However, the actual lasing frequencies (or modes) are determined by the gain spectral distribution of the laser cavity material, typically the spectral width being around 5 nm, which permits several longitudinal modes of the laser cavity to be excited[Lang & Kobayashi 1980]. In a single mode laser there is only one stable lasing frequency that oscillates, but in a multi-mode semiconductor laser there are a number of stable lasing frequencies oscillating at any one time. For simplicity of the theoretical analysis, the case of a single-longitudinal mode laser only is considered in the theory.

Equation (3-8) represents a laser oscillating at a series of discrete frequencies, each frequency determined by the value of q. In the single mode case(for a given value of q) this particular lasing frequency ν_{th} is dependent on the cavity length, d, and the refractive index, n, of the laser crystal, it is known that the value of this refractive index is strongly dependent on both the excited carrier density, N, and the temperature of the semiconductor material. The fluctuations of the carrier numbers, the quantum nature of the laser oscillation, the environmental temperature drift as well as other factors will contribute to a finite spectral width to this lasing frequency, and the laser cannot oscillate simply at one discrete frequency but with a non-zero spectral distribuation around the central lasing frequency ν_o.

To take into account the dispersion effect (i.e. the variation of the refractive index with frequency), an effective group refractive index n_g of the lasing mode is defined as:

$$n_g = n_o + \nu\frac{dn}{d\nu} = n_o + \Delta n$$ (3-9)

where n_o is the effective refractive index for the lasing mode and Δn accounts for the changes of the refractive index due to dispersion. Substituting Equation(3-9) into (3-8), the lasing frequency ν_{th} in Equation(3-8) may be expressed as

$$
\begin{aligned}
\nu_{th} &= q\,\frac{c}{2(n_o + \Delta n)d} \\
&\approx q\,\frac{c}{2n_o d} - q\,\frac{\Delta n c}{2n_o^2 d} = \nu_o - \nu_o\frac{\Delta n}{n_o}
\end{aligned}
\tag{3-10}
$$

where ν_o represents the central lasing frequency and the second term in the above expression accounts for the deviation of the lasing frequency from the central frequency ν_o due to the variation of the refractive index Δn.

§3.5.2 Standard laser equations

The field approach described in the previous section is useful in analyzing the steady state behaviour of the laser oscillation. To describe the dynamic characteristics of the laser oscillation, the standard laser equations are often used[Lang & Kobayashi 1980, Streifer et al 1982, Marcuse 1983, Schunk & Petermann 1988]. Under lasing conditions, the semiconductor laser cavity is filled with a gain medium which amplifies the lasing light by stimulated emission and compensates for the cavity losses. The following laser equations have been widely adopted for describing the semiconductor lasing process

$$
\frac{dE}{dt} = [-j2\pi\nu(N) + \frac{1}{2}(G(N) - \Gamma)]E(t)
\tag{3-11}
$$

$$
\frac{dN}{dt} = \frac{J}{e} - \chi N - G(N)|E(t)|^2
\tag{3-12}
$$

where $E(t)$ is the electric field, normalised to represent the photon numbers inside the lasing mode; $\nu(N)$ is the cavity resonance frequency; $G(N)$ and Γ are the cavity gain and loss per second respectively, and N is the carrier density inside the laser cavity. They are linked to the optical gain g and loss γ by

$$
G(N) = V_g\, g(N)
\tag{3-13}
$$

$$
\Gamma = V_g\, \gamma
\tag{3-14}
$$

with $V_g = \dfrac{c}{n_g}$ is the effective group velocity of light inside the laser cavity, and χ is the inverse spontaneous lifetime of the excited carriers; J is the injection current; and e is the electronic charge.

§3.5.3 Steady-state conditions

To achieve laser oscillation, it is known that the electric field is amplified repeatedly inside the cavity, yet the amplitude of the oscillation will be not amplified infinitely, but will be limited by the gain saturation and other nonlinear effects in the lasing process. The electrical field $E(t)$ will approach a steady-state value and form a stablized oscillation field, this electrical field can be determined from Equation(3-11) by setting $E(t)$ to be

$$E(t) = A \, \exp[-j2\pi v_{th} t] \tag{3-15}$$

where A is a constant representing the stablized oscillation amplitude of the electrical field and v_{th} represents the output frequency of the laser oscillation in the steady-state.

By substituting Equation(3-15) into Equation(3-11) and separating the real and imaginary parts of the equation, the following results are obtained

$$G(N) - \Gamma = 0 \tag{3-16}$$

and

$$v(N) - v_{th} = 0 \tag{3-17}$$

Thus the required threshold gain and the lasing frequency may be obtained from the above equations, and they are respectively

$$G_{th} = G(N_{th}) = V_g \, \gamma + \frac{c}{n_o d} \ln \frac{1}{r_1 r_2} \tag{3-18}$$

and

$$v_{th} = v(N_{th}) = q \, \frac{c}{2 n_o d} \tag{3-19}$$

where N_{th} is the carrier density at threshold. In such an ideal lasing condition, the laser is spectrally quite pure, that is to say the output of the laser would possess a δ-function spectrum(a single frequency) so that the oscillating output wave is an ideal sinusoidal function with variation in time. However, any lasing system will be affected by some kind of noise. For example, the effect of amplitude fluctuations of the electrical field will add a background to the output signal, and the phase fluctuations will result in the broadening of the output signal spectrum from the δ-function spectrum into one of finite width. A detailed analysis of the spectral linewidth is discussed in next sub-section.

§3.5.4 Spectral linewidth

As mentioned previously, experimental work was undertaken by Fleming and Moordian[1981] to measure the linewidth of a single mode AlGaAs semiconductor laser. The lineshape of the laser output has been found to be Lorentzian and the linewidth narrowed with increasing power, but the spectral width was found to be much wider than that predicted[Saito & Yamamoto 1983]. To explain this deviation, a linewidth theory for single mode semiconductor lasers was later developed by Henry[1982]. He found that the linewidth enhancement in semiconductor lasers was due to the changes in the real and imaginary parts of the refractive index with the changes in carrier number. A parameter termed the **linewidth enhancement factor**, α,[Osinski & Buus 1987] has then been defined as

$$\alpha = \frac{\Delta n'}{\Delta n''}$$
(3-20)

where $\Delta n'$ and $\Delta n''$ are those changes in the real and imaginary parts of the refractive index n in the laser cavity.

Below threshold, the power spectrum of a single-mode semiconductor laser was calculated by Henry from his theoretical formula to be

$$p(\nu) = \frac{R}{[2\pi(\nu_o - \nu) + \frac{\alpha}{2}\Delta G]^2 + (\frac{\Delta G}{2})^2}$$
(3-21)

where R is the spontaneous emission rate, and ΔG is the change of laser gain, $G(N)$, with the carrier density. It is obvious, from the above expression, that below threshold the laser has a Lorentzian lineshape and that its linewidth may be expressed as

$$\delta v = -\frac{\Delta G}{2\pi} = \frac{R}{2\pi I} \qquad (3\text{-}22)$$

where I is the intensity of the optical output power. The spectral distribution is illustrated in Figure 3.13.
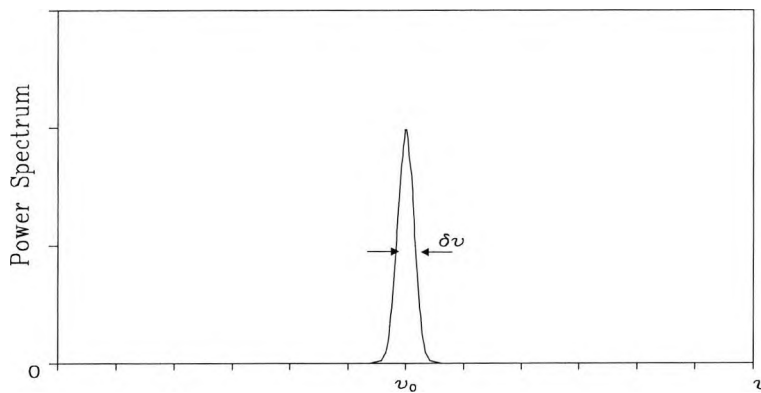
Figure 3.13 The power spectrum of a semiconductor laser

below threshold

X-axis—laser power spectral amplitude,

Y-axis—optical frequency, v , δv—spectral linewidth.

Above threshold, laser intensity fluctuations becomes stabilized but the phase may take any value. If the fluctuations in the laser intensity are neglected, and it is assumed that the phase fluctuations in the laser field are descibed by a Gaussian variable, the laser lineshape can be still considered as Lorentzian, but its linewidth becomes

$$\delta v = (1 + \alpha^2)\frac{R}{4\pi I} \qquad (3\text{-}23)$$

where the factor $\dfrac{(1 + \alpha^2)}{2}$ accounts for the linewidth broadening for lasers operating above threshold[Henry 1986].

However, experimentally, the laser spectrum has been found to consist of the main lasing line surrounding by subsidiary satellite side peaks(Figure 3.11). The side bands are spaced at intervals of the relaxation resonant frequency. This asymmetric linestructure has been considered to be due to the coupling between the intensity fluctuations and the amplitude-phase fluctuations at the relaxation frequency[Henry 1983]. Therefore the lineshape of the laser is not exactly Lorentzian[Vahala et al 1983], but with the side peak amplitudes being roughly 1% of the lasing peak amplitude. It was also found that the side peaks increase with the increasing of laser output power.

§3.6 Summary

The basic principles of semiconductor lasers or diode lasers have been presented in this Chapter. The process of light emission in semiconductor materials is due to the presence of recombination radiation of electrons and holes and the energy of this recombination is released as light. The simplest structure of a semiconductor light emission device is a P-N junction which is formed between two parts of a semiconductor crystal with different doping and where the light is produced by the spontaneous emission if it is forward-biased. When the end surfaces of a semiconductor P-N junction crystal are cleaved and made parallel, the light generated by the spontaneous emission will be amplified backward and forward by the stimulated emission inside the two parallel reflective surfaces and finally form the laser oscillation, when the injection current is raised above the threshold, and thus a semiconductor laser is constructed.

There are a number of semiconductor laser structures, ranging from homojunction to heterojunction, to the distributed feedback(DFB) laser structure. The homojunction laser is formed by a single layer of a P-N junction, while the heterojunction laser has two or more layers bounded with different semiconductor materials, with the special structure, the active layer of laser emission is confined to a very narrow strip which allows the laser to be operated

at a very low current density and be able to work continuously at room temperature. For a DFB laser, there is a diffraction grating inside the laser cavity, which is used to select a specific wavelength and allows the laser oscillation only on a stable single longitudinal mode spectrum.

The output of a semiconductor laser is quite different from a LED as the stimulated emission dominates the light emission process above threshold and the quantum efficiency of the laser is increased sharply after the injection current is raised, in excess of the threshold current. The light radiation of a semiconductor laser has been analysed under its steady-state conditions and also described by using standard laser equations. Under ideal lasing conditions, the output lightwave of the laser oscillation is an ideal sinusoidal time function, but the presence of amplitude and phase flunctuations results in an output spectrum of a finite width, and the linewidth is further enhanced in semiconductor lasers due to the changes in the real and imaginary parts of the refractive index with carrier number. Although the lineshape of semiconductor laser spectrum has been found to be not exactly Lorentzian as expected, the spectrum has been considered generally to follow the Lorentzian distribution for simplicity of theoretical analysis as the amplitudes of the satellite peaks account only for ~1% of the main peak amplitude.

Chapter 4

Theory of self-mixing interference in a single-longitudinal-mode diode laser

§4.1. Introduction

Theories of semiconductor lasers with external optical feedback have been extensively studied for the past decade. Most of them have been used to explain the spectral characteristics of single-longitudinal-mode semiconductor lasers in the presence of external feedback[Lang & Kobayashi 1980, Favre et al 1982, Osmundsen & Grade 1983, Spano et al 1984, Olessen et al 1986, Petermann 1991b, and Hamel et al 1992], while the others concentrate on the interference phenomena of self-mixing effects on the laser output power[Olsson & Tang 1981, de Groot et al 1988, Jentink et al 1988, de Groot 1990, and Koelink et al 1992b]. Since the characteristics of a multi-longitudinal-mode diode laser in the presence of external feedback are particularly complicated and difficult to express analytically, only the case of an original single-mode diode laser is usually considered in the theoritical analysis, yet the results obtained from the single-mode laser may generally be extended to explain those phenomena observed with a multi-mode diode laser as the multi-mode laser may be considered simply to be superimposed by different single-mode lasers without taking account of mode dispersion effect.

As the effects of external optical feedback have profound influences not only on the lasing spectrum but also on the threshold gain, the laser output power variation in the presence of the external optical feedback should reflect all of those changes on the lasing

conditions[Lang & Kobayashi 1980, Favre et al 1982, Acket et al 1984, Agrawal et al 1984, Schunk & petermann 1988, and Cohen & Lenstra 1989].

In this chapter, a self-mixing interference theory, based on the stationary equation of a single-longitudial-mode diode laser, has been developed, with the aim being to analyze the experimental observations. Theoretical models have been presented through the analysis of the laser oscillation conditions. The self-mixing interference is found to be the consequence of the spectral and laser threshold modulations, which is introduced by external optical feedback. For a weak feedback level and a short external cavity length, the lasing spectrum can easily show single-mode operation, and the intensity modulation is similar to conventional two beam interference, and thus the characteristics of the intensity modulation, the frequency shifts, the spectral linewidth variations as well as the visibility function can be expressed analytically, and from this theory the sawtooth-like waveform and the sign inversion observed can be explained satisfactorily. For a large feedback coefficient [i.e. C>1 defined in Equation(4-22)] [Tkach & Chraplyvy 1986], the laser spectrum will eventually be characterised by multiple external cavity modes. In this case, the visibility function will be separated by the external cavity modes, the self-mixing interference is limited by the spectral linewidth of each of the single modes, and the larger the level of feedback, the narrower the spectral linewidth, and therefore the longer the coherence length. In the special case given, the feedback light wave is considered to be coherent with the light wave inside the cavity, no matter how far away the external reflector is. Any further increase of the feedback level may lead to the laser operation running into the "coherence collapse" region, in which no intensity modulation can be observed[Cohen et al 1990]. In this Chapter, the theory of self-mixing interference in a single-mode diode laser is presented in Section 4.2, where the intensity modulation, the frequency shift, the linewidth variation and the power modulation are discussed analytically. Section 4.3 shows the comparison of the theoretical analysis to the experimental results reported. Summaries are presented in Section 4.4

§4.2 Self-mixing interference theory in a single-mode diode laser

In this section, the influences of self-mixing effects due to the feedback on lasing conditions are studied. The resulting changes on the lasing spectrum and threshold gain shift the lasing frequency, cause the variations of spectral linewidth and modulate the laser output power (or intensity).

§4.2.1 Influences of self-mixing effects on lasing conditions

Self-mixing effects on semiconductor lasers have been found to result in the output power variations[Dandridge et al 1980, Shinohara et al 1986]. When this occurs, the level of external optical feedback is usually considered to be weak because the reflection is frequently scattered from a diffuse reflector and the amount of reflection is generally less than 1% of the output light. A schematic for the self-mixing feedback laser is shown in Figure 4.1, where r_1, and r_2 denote the amplitude reflection coefficients of the laser facets r_1 and r_2 respectively, r_3 represents the amplitude reflection coefficient of the external reflector r_3, n_1 and n_2 represent respectively the refractive indexes of the laser cavity and the external cavity, d_1 and d_2 are the
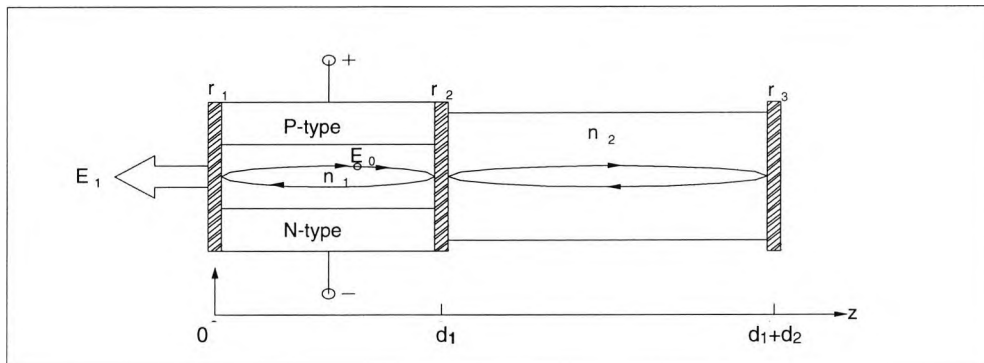
Figure 4.1 Schematic arrangement of a diode laser

with external optical feedback

E_0—initial light wave inside the cavity, E_1—laser output light wave,

r_1, r_2, r_3—amplitude reflection coefficients of the laser facets and the external

reflector, n_1, n_2—refractive indices of the laser cavity and the external

cavity, d_1, d_2—laser cavity length and external cavity length.

laser cavity length and the external cavity length respectively. The corresponding block diagram of the above external cavity laser is illustrated in Figure 4.2, in the forms of the transfer functions G_i ($i = 1, 2, 3, 4$), where G_1 and G_2 have the same form as that of Equ(2-16), whilst G_3 and G_4 may be expressed as

$$G_3 = G_4 = G_{ext}(\nu) = \exp[-j2\pi\nu\frac{n_2 d_2}{c}] \qquad (4\text{-}1)$$
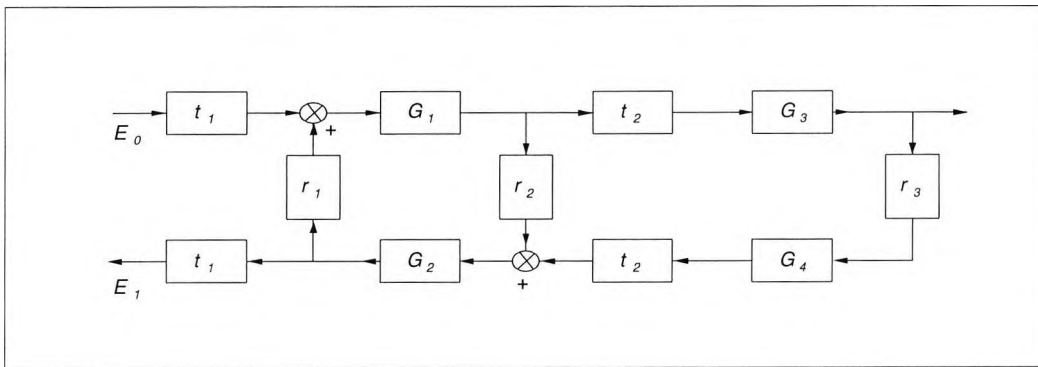
Figure 4.2 Block diagram of self-mixing feedback system

E0—initial light wave inside the cavity, E1—laser output light wave, G1, G2, G3, G4—cavity gain transfer functions in forward and backward directions, t1, t2—transmission coefficients of laser facets, r1, r2, r3—reflection coefficients of individual facets.

where only the phase change of the electric field needs to be represented within the external cavity as the cavity is considered to be a lossless passive FP cavity where no amplification of light exists. The roundtrip transfer function, which represents the light wave inside the laser cavity of undergoing a complete roundtrip within both the cavity **r₁—r₂** and the extended cavity **r₁—r₃**, may thus be expressed as

$$R(\nu) = r_1 r_2 G_1 G_2 (1 + t_2^2 \frac{r_3}{r_2} G_3 G_4)$$

$$= r_1 r_2 \exp[-j4\pi\nu\frac{n_1 d_1}{c} + (g-\gamma)d_1]\{1 + (1-R_2)\frac{r_3}{r_2}\exp[-j4\pi\nu\frac{n_2 d_2}{c}]\} \qquad (4\text{-}2)$$

where v is the optical frequency. The term $(1 - R_2) = t_2^2$ accounts for the light transmission through the laser facet r_2 at $z=d_1$, where $R_2 = |r_2|^2$, c is the speed of light in a vacuum, g is the linear gain per unit length due to the stimulated emission, and γ accounts for any optical loss per unit length within the laser cavity. Equation(4-2) neglects the multiple reflection effect within the external cavity, as it is justified to neglect this multiple reflection effect when the feedback is weak in the self-mixing system($|r_3| \ll |r_2|$) .

For a stationary laser oscillation, the roundtrip transfer function $R(v)$, after a complete roundtrip inside the compound cavity, requires that

$$R(v) = 1 \tag{4-3}$$

which means that the amount of light amplified by the stimulation becomes equal to the total light losses which occur by transmission through the sides of the laser cavity, through the external cavity and the mirror facets, and by absorption in the semiconductor material. Taking account of these effects and applying condition(4-3), Equation(4.2) becomes

$$r_1 r_2 \left\{ 1 + (1-R_2)\frac{r_3}{r_2}\exp[-j4\pi v\frac{n_2 d_2}{c}] \right\} \exp[-j4\pi v\frac{n_1 d_1}{c} + (g -\gamma)d_1] = 1 \tag{4-4}$$

If an effective reflection coefficient r_2' is defined as:

$$r_2'(v) = r_2[1 + (1 - R_2)\frac{r_3}{r_2}\exp[-j2\pi v\frac{\Delta L}{c}] \tag{4-5}$$

where $\Delta L = 2n_2 d_2$ is the optical path difference of the external cavity, then Equation(4-4) may be rewritten as

$$r_1 r_2'(v)\exp[-j2\pi v\frac{\Delta l}{c} + (g - \gamma)d_1] = 1 \tag{4-6}$$

where $\Delta l = 2n_1 d_1$ is the OPD of the solitary laser cavity. This expression is similar to that requirement of a two-mirror Fabry-Perot type laser for steady-state oscillation in Equation(3-6). The new threshold gain, g_{th}', may be written as

$$g_{th}' = \gamma + \frac{1}{2d_1} \ln\frac{1}{R_1 R_2'} = g_{th} + \Delta g \tag{4-7}$$

where $R_1 = |r_1|^2$ and $R_2' = |r_2'|^2$. g_{th} represents the threshold gain of the solitary laser in the absence of feedback and is given by

$$g_{th} = \gamma + \frac{1}{2d_1}\ln\frac{1}{R_1 R_2} \qquad (4\text{-}8)$$

where Δg represents the required gain for the laser operation in the presence of feedback. By substituting Equation(4-5) and (4-8) into Equation(4-7), the deviation, Δg, of the threshold gain may be expressed as

$$\Delta g = -\frac{1}{2d_1}\ln[1 + \xi^2 + 2\xi\cos(2\pi v\frac{\Delta L}{c})] \qquad (4\text{-}9)$$

where

$$\xi = (1 - R_2)\frac{r_3}{r_2} \qquad (4\text{-}10)$$

representing the coupling from the external reflection into the laser cavity.

The phase condition required may thus be expressed as:

$$\Phi(v) = \phi_1(v) + \phi_2(v) = 2q\pi \qquad (4\text{-}11)$$

where q is an integer and

$$\phi_1 = 2\pi v\frac{\Delta l}{c} \qquad (4\text{-}12)$$

accounting for the roundtrip phase in the absence of the feedback and

$$\phi_2(v) = \tan^{-1}\frac{\xi\sin(2\pi v\frac{\Delta L}{c})}{1 + \xi\cos(2\pi v\frac{\Delta L}{c})} \qquad (4\text{-}13)$$

representing the additional phase induced by the feedback.

In the case of no optical feedback($r_3=0$), the gain and the phase conditions reduce to the well-known expressions in Eqns(3-7) and (3-8) as

$$g_{th}' = g_{th} = \gamma + \frac{1}{2d_1}\ln\frac{1}{R_1 R_2} \qquad (4\text{-}14)$$

$$\Phi(\nu) = \phi_1(\nu) = 2\pi\nu\frac{\Delta l}{c} = 2q\pi \qquad (4\text{-}15)$$

where R_1 and R_2 represent the power reflection coefficients of the laser facets respectively.

In general, it is assumed that under the condition of weak feedback level, $\Delta g << g_{th}$ i.e. ($\xi << 1$), and therefore, the excess gain Δg and the additional phase $\phi_2(\nu)$ may be given approximately as:

$$\Delta g \approx -\frac{\xi}{d_1}\cos(2\pi\nu\frac{\Delta L}{c}) \qquad (4\text{-}16)$$

and

$$\phi_2 \approx \xi\sin(2\pi\nu\frac{\Delta L}{c}) \qquad (4\text{-}17)$$

§4.2.2. Lasing frequency shifts under weak optical feedback

For the laser oscillation with a week feeback level, the phase of the roundtrip transfer function, $R(\nu)$, may be reduce to

$$\Phi(\nu) = 2\pi\nu n_1\frac{2d_1}{c} + \xi\sin(2\pi\nu\frac{\Delta L}{c}) \qquad (4\text{-}18)$$

It may further be written as

$$\Phi(\nu) = 2\pi\nu_{th}\tau_1 + 2\pi(\nu - \nu_{th})\tau_1 + 2\pi\nu_{th}\frac{2(\Delta n_1)d_1}{c} + \xi\sin(2\pi\nu\tau_2) \qquad (4\text{-}19)$$

where $\tau_1 = \frac{2\overline{n_1}d_1}{c}$ and $\tau_2 = \frac{2n_2d_2}{c}$ are the roundtrip time delays inside the laser cavity and inside the external cavity respectively, $\overline{n_1}$ is the effective refractive index of the laser cavity, and Δn_1 represents the change of the cavity refractive index with carrier density. Since the first term in Eqn(4-19) has already met the phase condition of the laser oscillation of $2q\pi$, it requires that the sum of the rest items must meet the following condition

$$\Delta\phi(\nu) = 2\pi(\nu - \nu_{th})\tau_1 + 2\pi\nu_{th}\frac{2(\Delta n_1)d_1}{c} + \xi\sin(2\pi\nu\tau_2) = 0 \qquad (4\text{-}20)$$

As the effective refractive index n_1 depends on the optical frequency, ν, and the carrier density, N, the above equation may be expressed further as

$$\Delta\phi(\nu) = 2\pi(\nu - \nu_{th})\tau_1 + \xi\sqrt{1 + \alpha^2}\sin[2\pi\nu\tau_2 + \arctan(\alpha)] = 0 \qquad (4\text{-}21)$$

where α is the spectral linewidth enhancement factor[Equation(3-20)], and ν_{th} is the emission frequency without feedback. In order to classify the different feedback levels clearly, an important parameter C has been defined[Tkach & Chraplyvy 1986] as

$$C = \frac{\tau_2}{\tau_1}\xi\sqrt{1 + \alpha^2} \qquad (4\text{-}22)$$

where the value of τ_2 reflects the length of the external cavity and ξ represents the strength of external feedback light which is coupled back into the laser cavity. This parameter divides the external feedback level into two basic catergories: the first is when the feedback level is weak, the value of C is less than 1, and the second is when *C>1* , accounting for a strong feedback level, and a special case, when the value of C is equal to 1, representing a critical point.

In the case of weak feedback(*C<1*), the phase change $\Delta\phi$ versus the emission frequency, ν, is a monotonic function, as depicted schematically in Figure 4-3, where the *x* axis represents the frequency difference from the lasing frequency in the absence of the feedback, the upper curve represents the variations of the spectral distribution, the middle curve denotes the phase deviation, $\Delta\phi$, and the lower curve is the threshold gain variation due to the feedback. It can be seen that there is only one intersect across the frequency axis for *Δφ=0* and thus there exists only one single emission frequency. In addition, the emission frequency is shifted downward and the linewidth is reduced from 60 MHz in the absence of feedback to 35 MHz in the presence of feedback(*C=0.44*). Under this weak condition, Eqn.(4-20) can be solved using its first order approximation and thus the emission frequency, ν, is given as:

$$\nu = \nu_{th} - \frac{1}{2\pi\tau_2}\frac{C\sin[2\pi\nu_{th}\tau_2 + \arctan(\alpha)]}{\{1 + C\cos[2\pi\nu_{th}\tau_2 + \arctan(\alpha)]\}} \qquad (4\text{-}23)$$

$\delta\nu_0=60\text{MHz}, \quad \delta\nu=35\text{MHz}, \quad L_{ext}\sim 2\text{cm}, \quad C=0.44$
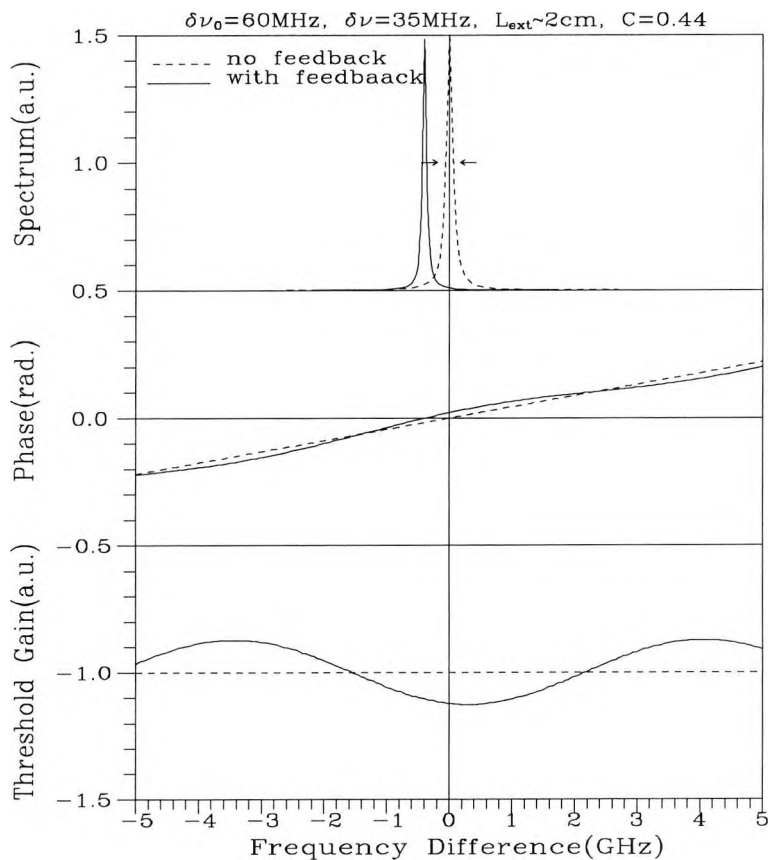
Figure 4.3 Schematics of optical spectrum, phase change and threshold gain versus optical frequency difference

This equation expresses the value of the emission frequency shifts in the presence of the weak feedback and shows that the frequency shift is a periodic function with respect to the external reflection phase $\Delta\phi_2 \ (= 2\pi\nu_{th}\dfrac{\Delta L}{c})$. For small values of C, the variation of the frequency is a sinusoidal waveform, but for larger C the shifts becomes sawtooth-like. The frequency shifts versus the phase variation of external feedback field, $\Delta\phi_2$, is depicted in Figure 4.4, where the central line represents the lasing frequency of the solitary laser($C=0$). The y axis represents the lasing frequency difference between the actual lasing frequency in the presence of the feedback and the threshold frequency in the absence of the feedback. For $C>1$, the phase deviation, $\Delta\phi$, is no longer a monotonic function but has multiple intersects with the frequency axis, ν, which results in multiple solutions for equation (4-20), as
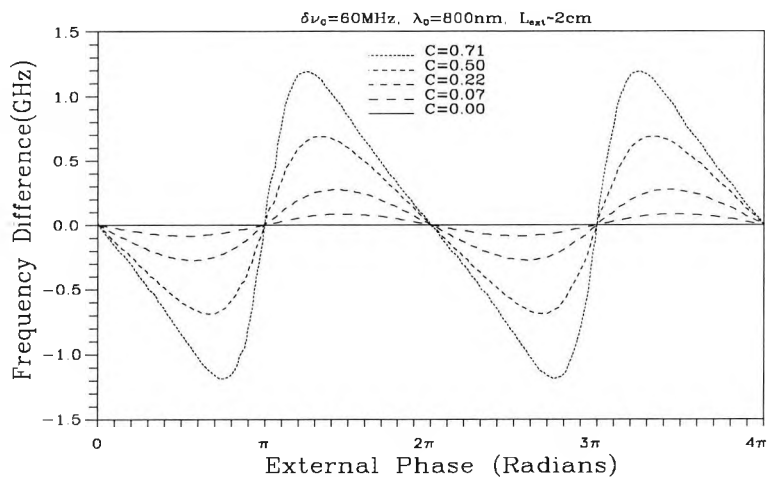
Figure 4.4 Frequency shifts versus external phase change
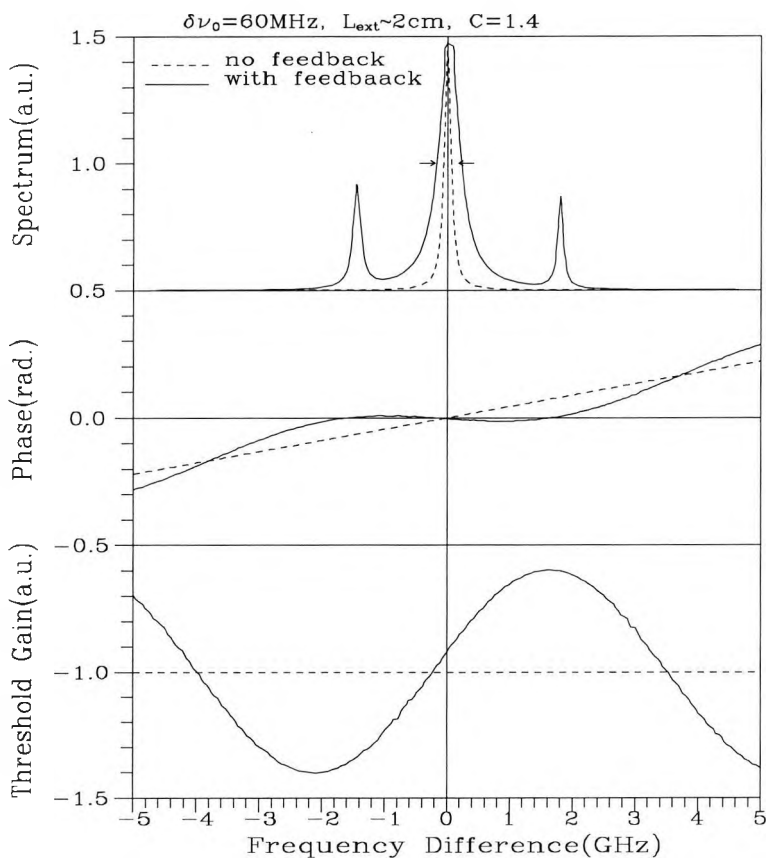
Figure 4.5 A schematic of lasing condition at multiple

solutions for phase change, threshold gain and optical frequency

illustrated schematically in Figure 4.5($C=1.4$), where the actual lasing modes also depend on the lasing gain condition. It was reported[Petermann 1990] that the external cavity mode with the narrowest linewidth is more stable than the external cavity mode with the lowest threshold gain, and eventually several external cavity modes may start to oscillate for a strong feedback level, and the laser thus becomes a multi-mode device.

§4.2.3. Spectral linewidth with weak external feedback

Above threshold, both the spectral linewidth and the coherence time of a semiconductor laser are determined by the phase fluctuations of the laser electric field, which may be described as Brownian motion or phase diffusion[Lax 1967, Henry 1986]. Since the lasing spectrum is strongly dependent on the lasing phase condition, the fluctuations of the phase in the presence of the feedback has a great influence on the laser spectral distribution.

In general, the power spectrum of a single-mode diode laser can be assumed to be Lorentzian in shape[Fleming and Mooradian 1981, Henry 1982, Saito & Yamamoto 1983], although this assumption is not entirely correct due to the relaxation oscillation in a single-mode semiconductor laser [Vahara et al 1983]. For simplicity, the spectral linewidth, δv, may be considered to be inversely proportional to the square of the effective round trip delay, τ_e, i.e.

$$\delta v \propto \frac{1}{\tau_e^2} \tag{4-24}$$

where the effective round trip delay in the presence of the feedback is given by:

$$\tau_e = \frac{1}{2\pi} \frac{d\Delta\phi}{dv} = \tau_1\{1 + C\cos[2\pi v\tau_2 + \arctan(\alpha)]\} \tag{4-25}$$

For weak feedback($C<1$), the lasing spectral linewidth, δv, is obtained simply as:

$$\delta v = \frac{\delta v_o}{\{1 + C\cos[2\pi v\tau_2 + \arctan(\alpha)]\}^2} \tag{4-26}$$
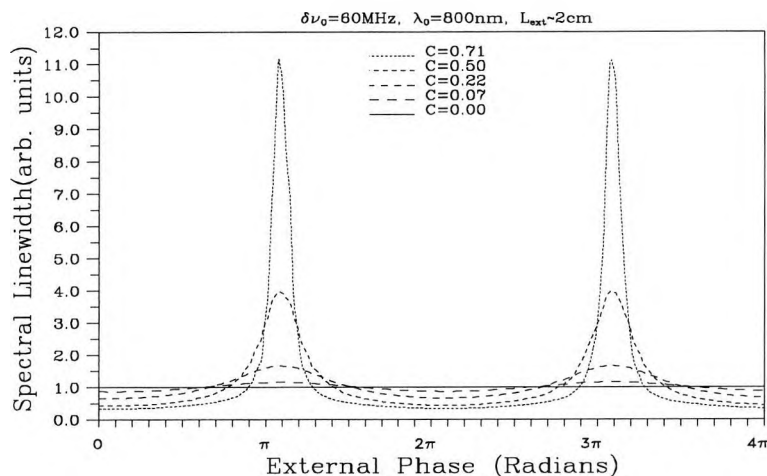
Figure 4.6 Spectral linewidth versus external phase change

where δv_o is the linewidth of the solitary laser in the absence of the feedback. Equation (4-26) remains valid and the lasing spectrum also remains in a single-mode operation only if the feedback level is weak($C<1$). Obviously, the spectral linewidth is determined by the feedback coefficient, C, the linewidth enhancement factor, α, and the external phase, $\Delta\phi_2(= 2\pi v\frac{\Delta L}{c}$), with the emission frequency, v, given by equation (4-23). The linewidth variation is depicted in Figure 4-6. It is easy to see that the linewidth may be narrowed or broadened depending on the strength and the phase of the feedback field. For $C \to 1$, the denominator of equation(4-26) may approach zero, corresponding to an infinite linewidth, but in practice this represents only a **turning point** for the laser oscillation, it means that, after this point, the multiple external modes may start lasing. Figure 4.7 shows the phase condition for $C=1$ with the phase adjusted to a maximum linewidth output, and in this case, Eqn.(4-23) no longer holds due to the derivative of the phase approaching zero, which will give an infinite linewidth, but as the phase variation is not linear, the linewidth is actually determined by the intersects of the phase variation, $\Delta\phi$, against the x axis and will result in a very large value.

$\delta\nu_0$=60MHz, $\delta\nu$=660MHz, L_{ext}~2cm, C=1.0
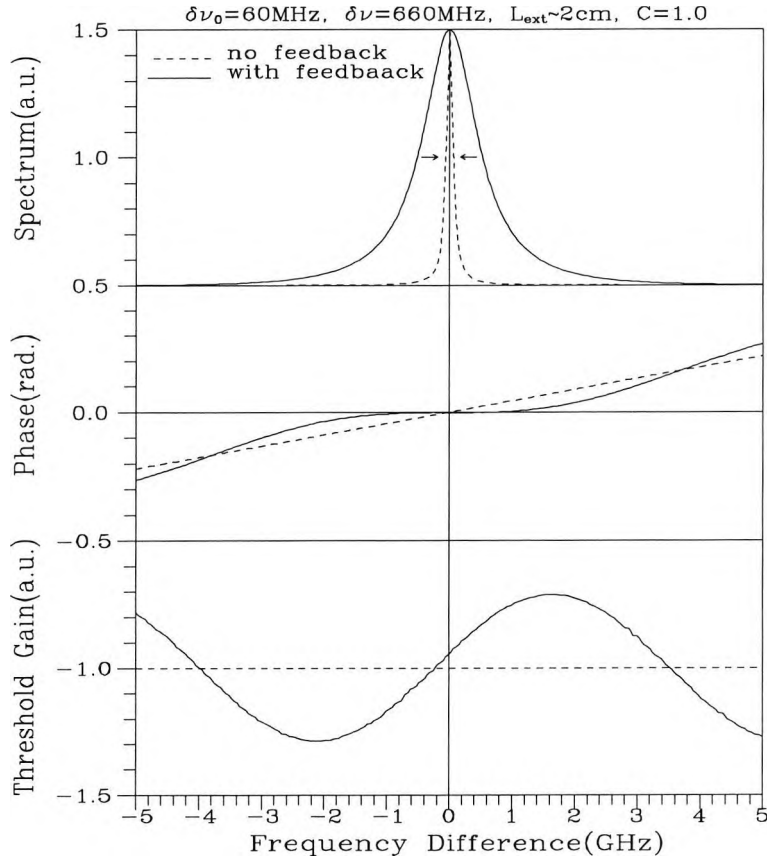
Figure 4.7 A schematic of lasing condition at C=1

§4.2.4. Intensity modulation with weak external feedback

The optical gain, g, due to the stimulated emission inside the laser cavity is determined by the injection carrier density, N, which can be described by the rate equation Equ(3-14) as:

$$\frac{dN}{dt} = \frac{J}{e} - \chi N - G(N)I \qquad (4\text{-}27)$$

where J is the injection current, e is the electric charge, χ is the inverse spontaneous lifetime of the excited carriers and I is the optical intensity in the lasing mode that is normalised to represent the number of the photons, S, in the laser cavity and have the intensity $I = |E(t)|^2$, where E(t) is the electric field vector inside the cavity. $G(N)$ is the modal gain per second due to stimulated emission and may be expressed as:

$$G(N) = \beta(N\text{-}N_c) \qquad (4\text{-}28)$$

where β is a proportionality coefficient and N_c is a constant. The modal gain is related to the linear gain, g, by $G(N) = V_g \, g(N)$, where V_g is the effective group velocity in the active layer.

Assuming that the laser in the absence of feedback and in the presence of feedback, is in a steady state and characterised respectively by the optical intensities I_o and I, and carrier densities, N_o and N. This implies that equation (4-27) meets the conditions

$$\frac{J}{e} = \chi N_o + V_g \, g(N_o) I_o \tag{4-29}$$

and

$$\frac{J}{e} = \chi N + V_g \, g(N) I \tag{4-30}$$

By linearisation of $g(N)$, centred around N_o, the following arises

$$g(N) = g(N_o) + \frac{dg}{dN} \Delta N = g_o + \Delta g \tag{4-31}$$

where $g_o = g(N_o)$ and $\Delta g = \kappa_l \Delta N$ with $\kappa_l = \frac{dg}{dN}$.

By substituting equation (4-29) into (4-30) and assuming that $\Delta g \ll g_o$, then the following first order expression for the intensity, I, is derived as

$$I = I_o(1 - \kappa_g \Delta g) \tag{4-32}$$

where

$$\kappa_g = \frac{1}{g_o}(1 + \frac{\chi}{\kappa_l I_o}) $$

representing a proportionality coefficient related to the gain, g_o, and the intensity I_o in the absence of the feedback . By substituting equation (4-16) into equation (4-31), the intensity, I, is given by

$$I = I_o[1 + m \cos(2\pi v \frac{\Delta L}{c})] \tag{4-33}$$
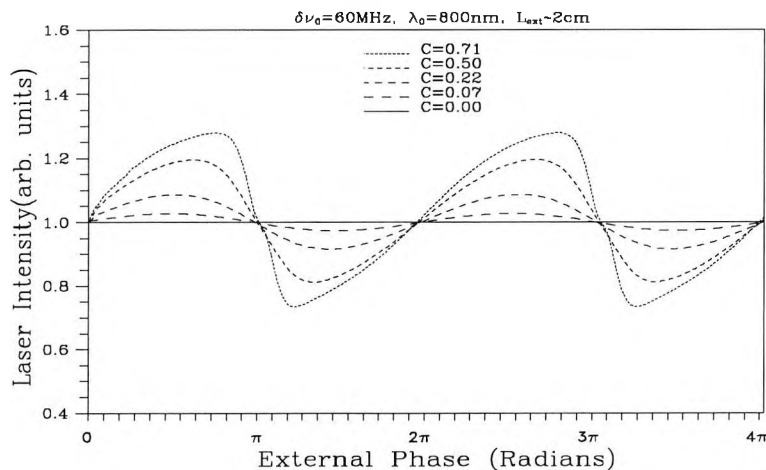
Figure 4.8 Optical intensity versus external phase change

where m $(= \dfrac{\xi \kappa_g}{d_1})$ is termed here the modulation coefficient. This expression describes theoretically the modulation of the laser optical intensity by the feedback, which has the same form as that of two-beam interference[Eqn.(2-29)] but has thus been termed "self-mixing interference" to distinguish it from that produced by conventional interference. Obviously the intensity modulation is a repetitive function with a period of 2π radians. It is worthwhile noting that the modulation coefficient, m, is not a constant as in conventional interference, but varies nearly inversely with the optical intensity, I_o. The intensity variations with the external phase are shown graphically as in Figure 4.8, corresponding to different feedback coefficients.

§4.2.5. Output power and visibility function of self-mixing interference

The visibility function is a measure of the coherence characteristics of a light source resulting from optical interference. Since self-mixing interference is not a linear superposition of the electric fields but a non-linear interfering process between the electric field inside the cavity and that from the feedback, the changes of the lasing spectral distribution therefore lead to changes of coherence; the coherence time or length is not fixed as it is in a conventional interferometric system where the light source is carefully arranged to avoid any change from environment, but in self-mixing interference the case is totally different.

The self-mixing interference effect may be monitored by the internal photodetector inside the laser package or by an external photodetector monitoring at either end of the laser cavity. The process of detecting photons generates optical power over the whole band of the frequencies, and the total output power from the laser is then calculated by taking an integral of the equation (4-33) over all frequencies. The output power, P, may thus be given by:

$$P = \int_0^\infty I(\nu)\, d\nu$$

$$= \int_0^\infty p(\nu)[1 + m\cos(2\pi\nu\frac{\Delta L}{c})]\, d\nu \qquad (4\text{-}34)$$

where $p(\nu)$ represents the power spectrum of a diode laser. Without loss of generality, it may be assumed that the power spectrum of a single-mode diode laser is still Lorentzian in shape(otherwise the satellite-peaks occured must be considered, but generally the influence of the side peaks is small (only 1%) and thus may be neglected) , and also that the linewidth of $\delta\nu$ varies inversely with optical intensity, as given by Equ.(2-33) as

$$p(\nu) = \frac{p_o}{(\nu - \nu_o)^2 + (\delta\nu/2)^2}$$

where ν_o is the central frequency of the lasing spectrum and $\delta\nu$ is defined as the FWHM of the spectrum. For a fixed spectral linewidth, the equation (4-34) may be expressed as

$$P = P_o\{1 + m\exp[-\frac{\delta\nu}{2}|\frac{\Delta L}{c}|]\cos(2\pi\nu\frac{\Delta L}{c})\} \qquad (4\text{-}35)$$

where P_o is the optical power of the laser in the absence of feedback. This expression (4-35) is similar to that of Equation(2-34) with a partially coherent light source. Then its visibility function, $V(\Delta L)$, may be calculated as

$$V(\Delta L) = m\exp[-\frac{\delta\nu}{2}|\frac{\Delta L}{c}|] \qquad (4\text{-}36)$$

It is known that the linewidth of the laser in the presence of feedback is not a constant, thus the visibility function, $V(\Delta L)$ will vary with not only the external cavity length, ΔL ($=2n_2d_2$), but also the spectral linewidth, $\delta\nu$, given by the equation (4-26). It should be borne in mind that this expression only holds for a single-mode spectrum under the conditions
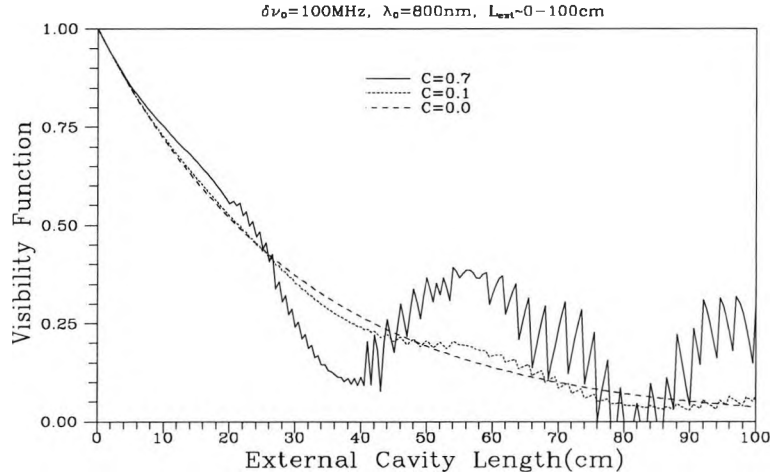
Figure 4.9 Visibility function of the laser with feedback

of the spectrum being Lorentzian in shape and the feedback level being weak($C<1$). Figure 4.9 shows the visibility function, $V(\Delta L)$, with different feedback levels and with dependence on the external cavity length, the values of C are given at external cavity length of 100 cm, corresponding to different feedback levels $R_3=0$, $R_3=10^{-6}$, $R_3=10^{-4}$ repectively). For a very small feedback level,($R_3=10^{-6}$), the visibility function is close to that of the solitary laser, but for the larger feedback level,($R_3=10^{-4}$), the visibility function becomes more complicated as the external cavity length is increased. If $C>1$, the power spectrum of the laser may become a multi-mode distribution as mentioned previously, the visibility function will be much more complicated, and thus it cannot be thus expressed in a simple form shown.

§4.3 Characteristics of self-mixing interference

Characteristics of self-mixing interference in a single-mode diode laser are presented in this section, as they highlight the differences of self-mixing interference and conventional interference.

§4.3.1. Power modulation

Equation (4-33) is the theoretical expression describing the self-mixing interference in a single-mode diode laser with weak optical feedback. Since both the spectral linewidth and the

emission frequency are functions of the external cavity length or time delay, the relationship between the output power and the external cavity length becomes very complicated. To help elucidate its physical meaning, this relationship is depicted in a graphical form in Figure 4.10. This figure shows the dependence of the power, P, on the external phase, $\Delta\phi_2$, corresponding to different feedback coefficients. It is evident that P is clearly a repetitive function with its period corresponding to an optical displacement of $\dfrac{\lambda}{2}$, where λ is the oscillation wavelength. For a small level of C the power modulation is a sinusoidal waveform, but for a larger level of C the output waveform becomes significantly sawtooth-like.
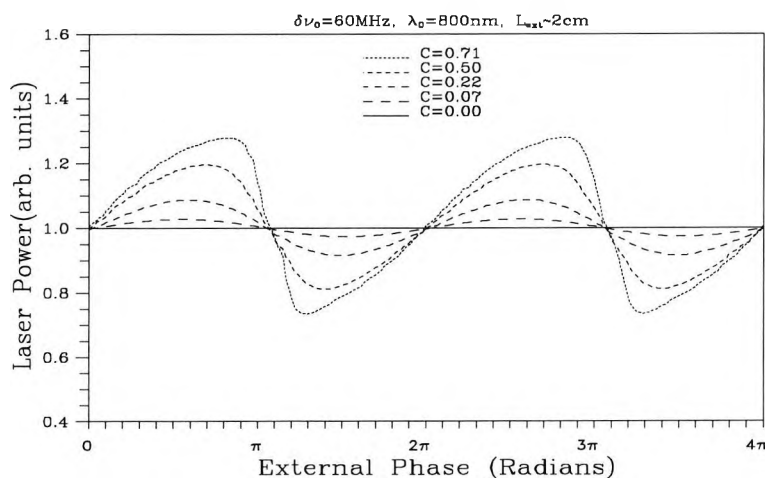
Figure 4.10 Optical power versus external phase change

§4.3.2. Asymmetric fringe patterns and waveform sign inversion

The asymmetry of the sawtooth-like waveform in self-mixing interference has been observed at stronger feedback levels. The simulation of this feature is shown as in Figure 4.11, where the value of $C=0.7$, and the sawtooth-like output waveform is depicted in the upper curve. When the external reflector changes its direction of movement, the sawtooth-like waveform changes its inclination. This feature of fringe inclination has been used for directional discrimination[Simizu 1987 and Wang et al 1992].
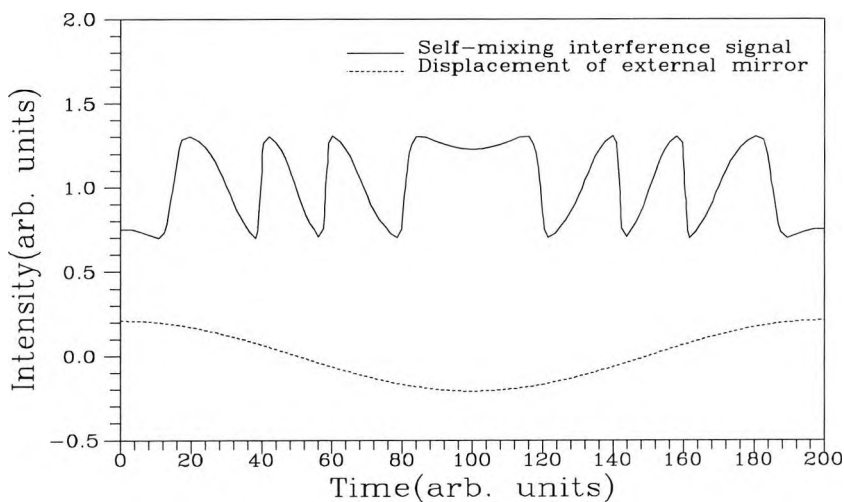
Figure 4.11 A simulation of sawtooth-like waveform

of self-mixing interference

Another feature of the self-mixing interference is the sign inversion between the two laser emission directions. The sign inversion means that the output signals from both directions have a mutual phase difference of π radians. This was originally found by de Groot[1988] in his experiments, but no physical explanation was given in his paper. It has been stated that the self-mixing interference is very complicated process, involving changes of laser threshold and lasing frequency. For a laser oscillation, a standing wave is generated inside the laser cavity. This is further complicated by external refection. By considering this and in comparison with conventional interference, the output intensities, I_+ and I_-, from the two emission directions are thus assumed to be of the form

$$I_+ = I_0[1 + m \cos(2\pi v \frac{\Delta L}{c})]$$ (4-37)

and

$$I_- = I_0[1 - m \cos(2\pi v \frac{\Delta L}{c})]$$ (4-38)
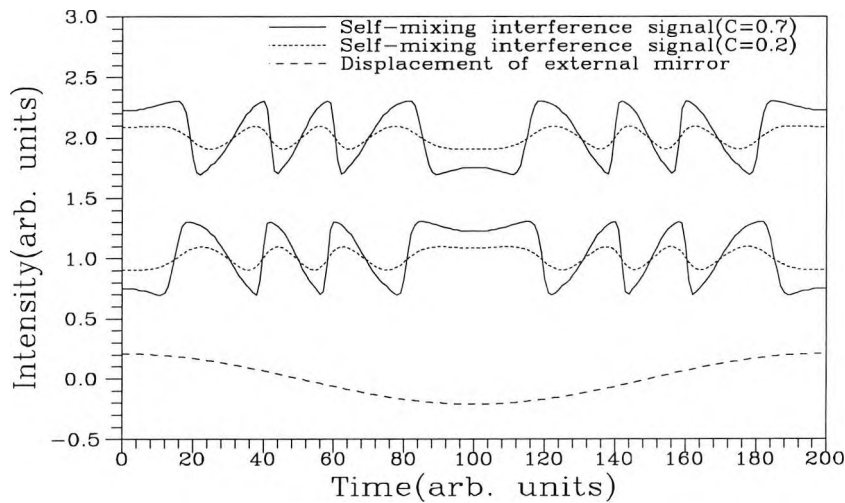
Figure 4.12 Waveform sign inversion of self-mixing

interference between two emission directions

where ΔL is the optical path difference between the laser and the external reflector, and the optical frequency is given by

$$\nu = \nu_{th} - \frac{1}{2\pi\tau_2} \frac{C \sin[\phi(\Delta L)]}{\{1 + C \cos[\phi(\Delta L)]\}} \qquad (4\text{-}39)$$

with

$$\phi(\Delta L) = \arctan(\alpha) + 2\pi\nu_{th}\frac{\Delta L}{c} \qquad (4\text{-}40)$$

Computer generation of both I_+ and I_- are depicted in Figure 4.12, which indicates the sign inversion between the two emission directions of the diode laser and the opposite inclinations of the fringes at a stronger feedback level. This result will be compared with the experimental results obtained in the next chapter.

§4.3.3.Coherence length

The power modulation due to the self-mixing effect has been observed even when the external cavity length is well outside the coherence length of the solitary laser used[Kolink et al 1988, Wang et al 1992]. This discovery is of importance for some applications but

contradicts the existing explanation using the coherence theory. To explain this behaviour requires an extention of the present theory. It is known that the temporal coherence is an important physical parameter related to various interferometric systems and reflects the spectral spread of the light source. According to this theory, if the source used is ideally a single frequency, it will produce an infinite coherence length or coherence time, in contrast to the situation of a white light source when the coherence length drops dramatically.

However, from Figure 4.9, it is shown that the visibility function of a single-mode diode laser in the presence of the feedback is not like that of a conventional laser source in which the visibility decays exponentially with the OPD, ΔL, but it displays a more complicated behaviour when either the feedback level or the external cavity length is increased. For small feedback levels of C, the function, $V(\Delta L)$, can be used approximately to describe the coherent characteristics of the self-mixing interference, but for larger levels of C, the visibility function is dramatically different from that in the absence of the feedback, and this is mainly due to the spectral variations produced by the feedback. In particular, for $C > 1$, corresponding to either strong feedback or a longer external cavity length(greater than the coherence length of the laser) or both, multiple external cavity modes may start lasing(Cohen et al 1990). In this case the lasing spectrum becomes multi-mode which is almost unavoidable with a distant reflector(such as that from the far optical fibre end). For simplicity, it may be assumed that the external cavity laser is operated in a multiple external cavity mode state, as shown in Figure 4-13(a), and the mode spacing of the spectrum is given by

$$\Delta v = \frac{c}{\Delta L} = \frac{c}{2n_2 d_2} \tag{4-41}$$

The corresponding visibility function of this spectrum is depicted in Figure 4-13(b), where the visibility function has several discrete coherence regions, the envelope of the coherence regions being determined by the spectral linewidth of the individual single modes of the spectrum, which are narrowed significantly by the larger feedback coefficient, C. It
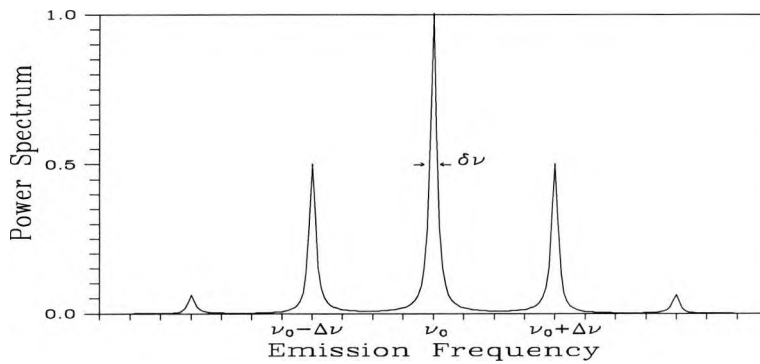
Figure 4.13(a) Schematic of a multi-mode laser spectrum

may be considered that the coherence of the laser is enhanced by the feedback. The central peak represents the zero-order coherence region corresponding to a value of OPD=0 between the two interfering beams. The sub-peaks from the centre represents the 1st-order coherence regions, and the distance of a sub-peak from the centre is just equal to the optical length n_2d_2 of the external cavity. From this point of view, it can be said that no matter how far away the external reflector is, the reflection field is always coherent with the laser field if the 1st-order coherence region is detectable, and therefore the interference fringes produced by self-mixing can be always observed. In contrast, when the spacings beween the multi-mode spectrum are not distingushed, that is the spectrum evolves into a very broad single spectrum due to the
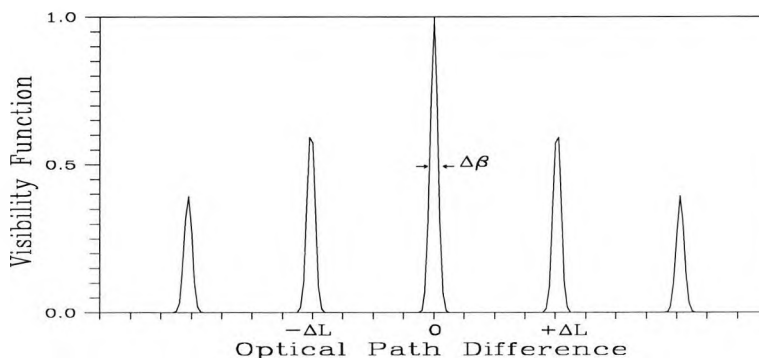
Figure 4.13(b) Visibility function of a multi-mode laser

feedback, the 1st-order and above coherence regions will thus disappear, and only the central coherence region will exist with a very small coherence length compared with that of the solitary laser. This is the "coherence collapse" phenomenon as mentioned in Chapter 1. It is obvious that the coherence of the solitary laser is not a determining factor for observing the self-mixing interference because of the changing spectral distribution of the laser, which is dependent on the feedback level and the phase of external feedback field.

§4.3.4. Modulation coefficient dependence on injection current

The modulation coefficient, m, represents the available signal strength in the laser optical intensity with the self-mixing interference. The larger the modulation coefficient, the higher the signal-to-noise ratio. It is known, from the Eqn.(4-34), that the modulation coefficient in the self-mixing interference is not a constant but varies inversely with the optical intensity, I_o. Above threshold, I_o, or the output power, P_o, is proportional to the injection current, J, which is given by:

$$P_o = \zeta(J - J_{th}) \tag{4-42}$$

where ζ is the incremental quantum efficiency and J_{th} is the threshold current. This relationship implies that m will vary with the injection current. The larger the current, J, the
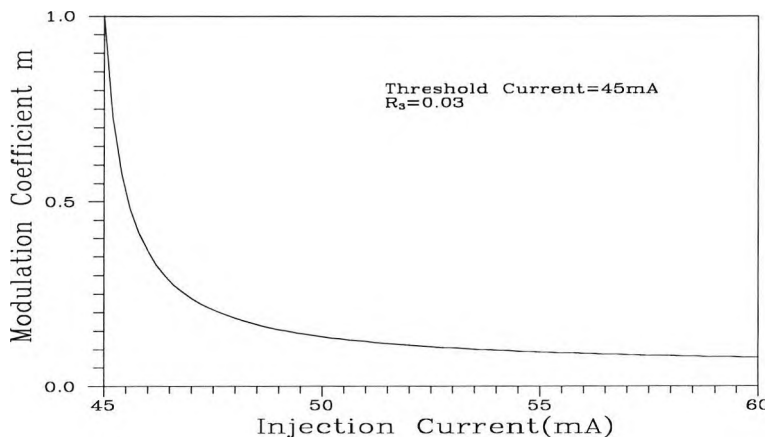
Figure 4.14 Modulation coefficient versus injection current

smaller the coefficient, *m*. Figure 4.14 shows the modulation coefficient variation with the injection current, which is approximately inversely proportional to the laser output power. Near the threshold the coefficient reaches its maximum value. With increasing current, the coefficient is decreased and approaches a stable value.

§4.4 Summary

A theory of self-mixing interference, inside a single-longitudinal-mode diode laser, has been established, for applications to practical optical sensing. Theoretical models, including the variations of the emission frequency, lasing spectral linewidth, threshold gain and output power(intensity), are developed based on the assumptions that the power spectrum of a single-mode diode laser is Lorentzian in shape and the laser structure is a Fabry-Perot resonator.

The characteristics of self-mixing interference have been presented in Section 4.3. In the case of weak feedback($C<1$), the power modulation by self-mixing is similar to that of a conventional two-beam interferometer and the lasing spectrum indicates a single-mode operation. For very weak feedback($C<<1$), the output waveform of the self-mixing interference is sinusoidal, and the increase of the feedback level for a given external cavity length will result in sawtooth-like waveforms and the inclination of the fringe patterns when the reflecting target moves. The larger the value of C, the more sawtooth-like the modulation waveforms become. For longer cavity lengths(e.g. greater than the coherence length of the laser used), the lasing spectrum will become much more complicated and may result in a multiple external cavity mode operation. The changes of the lasing spectral distribution thus produce a number of discrete coherence regions, in which the self-mixing intensity modulation may be always observed. This shows that the occurance of the self-mixing interference is not dependent on the initial coherence length of the laser used.

The asymmetry of the sawtooth-like fringes and the waveform sign inversion have been explained, from the theoretical models, to be due to the emission frequency shifts and the relative direction change of the external reflector movement. The self-mixing modulation depth has also been found to be inversely proportional to the laser output intensity.

The self-mixing interference in a single-mode diode laser results from the variations of the lasing spectral distribution and the threshold gain, which is, in principle, different from that of a conventional interference mechanism. The periodic displacement of the external feedback phase changes the stablized laser oscillation conditions and thus the laser output power. A detailed experimental analysis of self-mixing interference will be presented in the next Chapter, which will give support to the theoretical analysis and show clearly the similarities and the differences of self-mixing interference with conventional interference.

Chapter 5

Experimental study of self-mixing interference in semiconductor lasers

§5.1 Introduction

In order to confirm the theoretical predictions discussed, a number of experiments have been performed. The purpose of these experiments has been twofold: first, to verify the theoretical results in light of the experimental observations, and secondly, to use the self-mixing interference technique for optical sensing applications. In this Chapter, initial experiments for a study of self-mixing interference were carried out in free-space, which may be considered theoretically in terms of a three-mirror Fabry-Perot external cavity laser. A more practical arrangement for sensing applications is then configured by using fibre optics. In this configuration, an optical fibre is used: (i) to transmit the laser output light to a diffused target represented as the external reflector; (ii) to collect the reflected light from the reflector and (iii) to deliver the reflected light back into the laser cavity. The use of fibre optics makes the self-mixing system simple, compact and easy to align.

In this Chapter, a report of the experiments performed is presented and the variations of the laser output power, caused by the feedback light, are monitored by either the use of the internal photodetector accommodated at the rear facet of the laser package used, or by an external photodetector in the front of the laser package. The aim of the work is to observe the power modulation of the laser used subject to the self-mixing effect. The intensity modulation characteristics are found to have some interesting features, which are then compared with the

theoretical simulation presented in the previous Chapter. In addition, the modulation amplitude of the self-mixing interference is examined experimentally by means of changes of the laser injection current. Furthermore, the coherence properties of self-mixing interference is studied, from the conventional point of view, by using a two-beam Michelson interferometer. Finally the characteristics of self-mixing interference are compared with those of a conventional interferometer, which highlights the advantages of the self-mixing interferometer in terms of its simplicity, compactness and robustness.

§5.2 Configurations of self-mixing system

Two types of experimental configuration are presented in this Section. The first one is a basic arrangement in free space for observing self-mixing interference, and the second is more practical, using the fibre optics, and it may easily be used in optical sensing applications.

§5.2.1 Self-mixing interference in free-space

The basic experimental arrangement for self-mixing interference experiment is shown in Figure 5.1. This system basically comprises of a single mode laser(Sharp VSIS-type AlGaAs laser LT024) and an external reflecting surface. The light emitted from the laser, LD, is collimated by a microscope objective lens(x10/NA=0.17), L_1, and propagated through a half-wave length plate, HW, and then it falls onto a polarising beam splitter, PBS. One beam is detected by a photodetector, PD_1, so that the output signals from the front and back facets of the laser diode could be compared, and the other beam is focused by a further microscope objective lens(x10/NA=0.25), L_2, onto a diffused target, M, represented by a vibrating loudspeaker cone. In this arrangement, the light reflected from the laser front facet and from the external target are mixed to produce an intensity modulation in the laser output. The output signal is also detected by the internal photodetector, PD, accommodated in the rear facet of the laser package. It can be seen that the light inside the laser cavity and the light reflected from the external target actually constitute two interfering optical beams of this
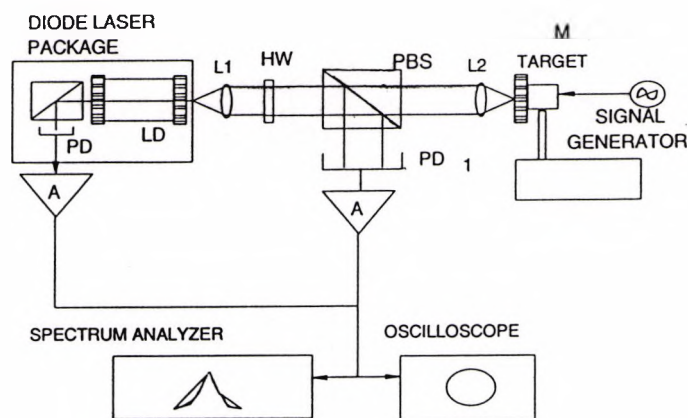
Figure 5.1 Experimental arrangement for self-mixing

interference in free space

PD—internal photodiode, LD—diode laser, A—amplifier,

L_1, L_2—lenses, PM—power meter, HW—half waveplate,

PBS—polarising beam splitter, PD_1—external photodiode.

self-mixing interferometer, which causes an intensity modulation of the laser output when the

target is moved longitudinally.

It should be mentioned here that before performing the self-mixing experiments, the

laser output power and the reflection from the diffused target were measured respectively by

using a power meter via an ordinary beam splitter. The level of the reflection from the

reflecting paper used was measured to be about 4%.

In the experimental arrangment with self-mixing as shown in Figure 5.1, the degree of

reflection level back into the laser cavity could be adjusted by changing the ratio of the two

split beams by rotating the waveplate, HW. The amount of reflected light back onto the laser

front facet was not measured directly, but estimated by knowing the total incident light to the

beam splitter and by measuring the other portion of the output light monitored by the PD_1, via

the beam splitter, PBS. When the self-mixing interference was observed, the reflection level

back onto the laser front surface was estimated to be about 1%. The actual feedback strength depends on the coupling from the external feedback into the laser cavity, so it is difficult to give an absolute value of the feedback level. However, it may be estimated by using the following formula[Lenstra 1985], which gives the feedback coupling coefficient, ξ, as

$$\xi = f(1 - R_2)\sqrt{\frac{R_3}{R_2}} \qquad (5-1)$$

where R_2 and R_3 are the power reflection coefficients of the laser facet($R_2 \approx 0.32$, for diode lasers) and the external target reflector respectively; f is the fraction of the reflected field which couples back into the laser mode due to diffraction limited imaging, for diode lasers with mirror reflection, f was given to be about 0.16[Lenstra 1985], with a diffused target in our experiments, f may be much smaller, but an accuarate value is difficult to estimate. Using $f = 0.02$, ξ can be calculated to be about 2.5×10^{-3} and the feedback strength back into the laser cavity is about 4.6×10^{-5}, If the feedback level is too large, it can lead to an unstable output of the laser.

It has been shown, in Section 4.2.2, that the feedback coefficient, C, is a very important factor describing the feedback strength back into the laser cavity. It can be rewritten as

$$C = \frac{L_{ext}}{L_d}\xi\sqrt{1 + \alpha^2} \qquad (5-2)$$

where L_{ext} and L_d represent respectively the external cavity length and the diode laser cavity length. For $\alpha = 4.6$[Schunk & Petermann 1988], $\xi = 0.02$, and assuming $L_d = 1$ mm, and $L_{ext} = 10$ mm, the value of the feedback coefficient C is then given to be about 1.

In the experiments performed, all optical components were aligned carefully and in particular the waveplate and the beam splitter were tilted so that there was no reflection from their surfaces back into the laser cavity. The only reflection back into the cavity was from the target, M. The use of focusing lens, L2, is to make the feedback less sensitive to misalignment of the self-mixing system, and the lens, L2, together with the target, M, can be moved along

the optical axis so that the distance between the target and the laser could be adjusted. In this system the external reflector can be positioned only between ~40 mm and ~60 mm from the laser front surface, and this distance, of course, corresponds to a larger value of the feedback coefficient C from Equation(5-2). The diode laser was operated at room temperature and above threshold (generally the driving current was ~10% above threshold current).

The intensity modulation signals monitored by both photodetectors, PD, and, PD_1, were amplified separately when the target reflector was vibrated longitudinally, and these two signals were sent to a spectrum analyzer and an oscilloscope, via a Digital Storage Adapter (DSA), for signal analysis.

§5.2.2 Self-mixing arrangement with optical fibres

Optical fibres have been widely used in various optical sensors. The fibres provide flexibility for various optical configurations and ease of alignment. In the configuration for
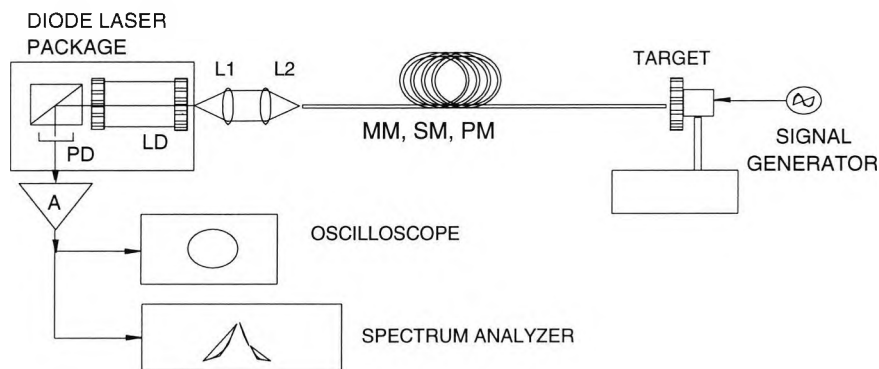
Figure 5.2 Experimental arrangement for self-mixing

interference with fibre optics

PD—photodiode, LD—laser diode, A—amplifier,L_1, L_2—lenses,

MM—multi-mode fibre, SM—single-mode fibre, PM—polarisation maintaining fibre.

self-mixing interference studies, as shown in Figure 5.2, the experiments to investigate the phenomenon were carried out with different lengths and different types of optical fibres. The fibres used were a single-mode fibre (SM -core diameter 5 μm and fibre length of 1.3 m), a polarisation maintaining fibre (PM -core diameter of 4 μm at wavelength of 780 nm and fibre length of 0.9 m) and a multi-mode fibre (MM -core diameter of 50 μm and fibre length of 3.48 m). The light source used was a 780 nm VSIS-type AlGaAs semiconductor laser package (Sharp LT022MC) giving an output power of 3 mW when the driving current was 1.3 times the threshold current. In the arrangement, as illustrated in Figure 5.2, the light from the laser was collimated by a microscope objective lens (x10/NA=0.17), L_1, and then focused by another lens (x10/NA=0.17), L_2, into a length of optical fibre (MM or SM or PM) as appropriate. This light travelled along the fibre and was reflected by an external target reflector. The reflected light was then guided by the same fibre and re-entered the laser cavity, and the resultant laser intensity modulation was detected, in this case, by the internal photodetector, PD. The reflection strength back onto the laser front facet was different, corresponding to different types of fibres used. The levels for all fibres were estimated to be less than 1%(they are given later in Table 5.1). When the fibre used was a multi-mode optical fibre, the self-mixing signal was very easy to observe from the laser output. This is because the multi-mode fibre has a large core diameter so that much of the laser output light could be coupled into the fibre and thus the degree of external reflection is large. However, for the polarization maintaining fibre used, with very small core diameter, it was difficult to obtain the self-mixing signal. It obviously correponded to a small degree of external feedback.

It can be seen that this configuration is different from the free space arrangement described in the previous Section(5.2.1), where there is only one reflection considered to arise from the target, but here the reflections from the fibre entry facet and exit facet($\sim 10^{-3}$ for angle-cut fibre ends)[Ulrich & Rashleigh 1980] are difficult to avoid, and those reflections

and that from the target back into the laser cavity will all cause intensity variations in the laser output.

To simplify the analysis, the feedback effect from the fibre entry facet may be neglected because this reflection level and also the external cavity formed between the laser front facet and this fibre facet were very small. It has been shown, from Equation(5-2), that the value of the feedback coefficient, C, is linearly proportional to the product of the magnitude of the reflection and the length of the cavity. For a given small reflectivity of the fibre end, the shorter the external cavity length, the smaller the reflection coefficient, C, and the less influence on the laser output intensity. In this case the value of C is about 0.1. The cavities of importance therefore are those formed between the laser and the exit fibre facet and between the laser and the target reflector. The equivalent model of this fibre self-mixing system therefore may be represented by a four-mirror Fabry-Perot external cavity laser.

The reflections from the entry facet and the exit facet of the fibre will influence the oscillation conditions of the laser (the output power and the laser spectrum). However, because the fibre facets were in fixed planes, they only change the dc level of the laser ouput intensity. It is only the movement of the target surface which results in the signal modulation of the laser output intensity.

§5.3 Characteristics of self-mixing intensity modulation

In the configurations descibed above, a portion of the emitted laser light was reflected back into the laser cavity from the external reflecting surfaces. If all these reflecting surfaces remain constant, there will be no intensity modulation in the output power of the laser, any change in the longitudinal motion of the surfaces or the refractive index inside the external cavity will result in an intensity variation. For optical sensing applications, the external cavity is used as a measurement "probe" and any changes in the environmental conditions caused by the external target movement or by changing the refractive index of the cavity will cause an

intensity modulation which represents the measurand. Therefore a demodulation, by means of some suitable signal processing method, will need to be used for physical parameter measurements, such as displacement, velocity measurement, refractive index monitoring and ranging, which are important meaurands.

§5.3.1 Sawtooth-like waveform and sinusoidal waveform

A typical self-mixing interference signal is shown in Figure 5.3, where the upper trace represents the voltage signal directly driving the target mirror which is vibrating longitudinally and the resultant intensity modulation of the self-mixing laser diode(lower trace) shows a 2π periodical feature, with respect to the mirror movement. The signals observed in the self-mixing experiments are similar to the interference fringe signals produced by a conventional interferometer, with one fringe corresponding to a half wavelength of the lasing wavelength. Thus most of the methods used for fringe signal processing in conventional interferometers can be adopted for self-mixing interference. However, the signal obtained shows, instead of the sinusoidal output of a conventional interferometer, a
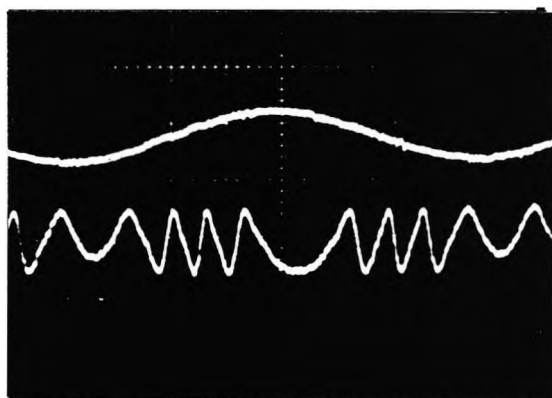
Figure 5.3 A typical self-mixing interference signal

Upper trace—Voltage signal of external target mirror vibration,

Lower trace—intensity modulation detected from laser output.

(vertical axis, arbitrary units; horizontal axis 0.2 ms/division).

sawtooth-like output waveform at strong levels of feedback. Table 5.1 below gives an estimation of the feedback coeffient C based on the Equation(5-2) for both the free space situation and the particular fibres used in the experiments. The corresponding path lengths and the fibre lengths are tabulated and the linewidth enhancement factor,α, is assumed to be 5, R_2 =0.32, and the laser diode cavity length to be ~1 mm.

Table 5.1 Estimation of feedback coefficients			
C	**$L_{ext}(mm)$**	**ξ**	**R_3**
0.45	40	2.3×10^{-3}	1×10^{-2}
0.68	60	2.3×10^{-3}	1×10^{-2}
3.22	900	7.6×10^{-4}	1×10^{-3}
10.4	1300	1.8×10^{-3}	5×10^{-3}
38.9	3480	2.3×10^{-3}	1×10^{-2}

These particular sawtooth-like fringes were obtained using both the free space arrangement and the arrangements employing the fibres. This important feature will be discussed further in the next Section. By decreasing the level of the reflections back into the diode laser, resulting in values of C below those tabulated in Table 5.1, the self-mixing interference fringes become sinusoidal and the sawtooth-like features disappeared, as shown in Figure 5.4. These experimental waveforms observed in the self-mixing interference are in agreement with the results of theoretical simulation previously discussed(Figures 4.11 and 4.12), shown in the previous Chapter. However, it can be seen that, with distant external reflectors, the values of the feedback coefficient, C, calculated in Table 5.1 are much greater than those obtained from the theoretical analysis. This difference indicates two possibilities: (i) these values of C obtained are much greater than those that actually are achieved for the laser cavity, since Eqn.(5.1) is only an esitmation and the fraction of the feedback light actually coupled into the cavity cannot be determined accurately; (ii) the self-mixing
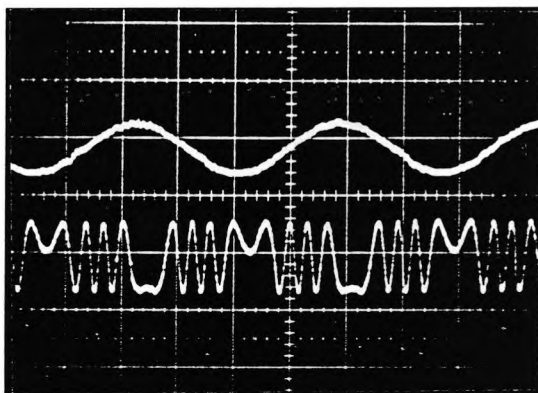
Figure 5.4 Self-mixing interference signal with weak

feedback coefficient(upper trace—displacement of external

mirror, lower trace—self-mixing interference signal)

Vertical axis, arbitrary units; horizontal axis, 0.5 ms/division.

waveforms obtained for larger values of $C(>1)$ display similar characteristics to those obtained when the value of C is less than 1. It may be observed, from the theoretical analysis(Figure 4.5), that the laser oscillation will enter the multiple external cavity mode region if $C>1$. In this case it is impossible to obtain simple descriptions of the intensity variations and the lasing spectrum distribution, but the laser intensity and the spectral distribution of each lasing mode may be considered to undergo the same process as that in a single mode case, described in Chapter 4.

§5.3.2 Asymmetry and waveform sign inversion

The asymmetric feature of self-mixing interference, which has both been observed and predicted, is an important difference from the conventional interference phenomenon. This has been shown, in Section 4.3.2, to be caused by the asymmetric change of the lasing spectrum subjected to the external feedback effect. Figure 5.5 shows an experimental observation of the difference in the output of a two-beam Michelson interferometer and that of a self-mixing interferometer under similar conditions of mirror displacement. It can be seen
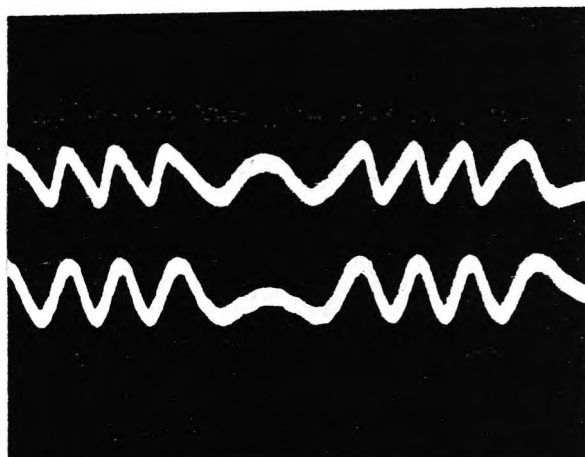
Figure 5.5 Asymmetric feature of Self-mixing interference

Upper trace—self-mixing interference,

Lower trace—two-beam conventional interference,

Vertical axis, arbitrary units, Horizontal axis, 0.2 ms/division

that the two waveforms have the same number of the fringes when the external reflector is

displaced an equal distance but the observed waveforms show a noticable difference in shape,

in which the lower trace(Michelson) is a sinusoidal waveform whilst the upper
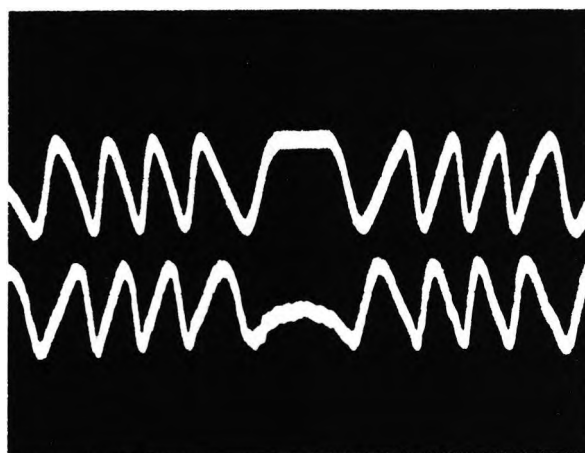
Figure 5.6 Sign inversion of self-mixing interference signal

Upper trace—signla detected in the front of the laser,

Lower trace—signal detected in the rear of the laser.

Vertical axis, arbitrary units, horizontal axis, 0.2 ms/division.

trace(self-mixing) is sawtooth-like and the fringe patterns observed are asymmetric relative to the movement direction of the external reflector. This feature of the fringe inclination, with respect to the movement directions has significant implications for directional discrimination(Simizu 1987 and Wang et al 1992a).

The optical intensity modulation caused by the self-mixing interference is also observed from both emission directions of the laser outputs, the signals obtained having no difference in shape but with a phase difference of π radians between these two signals, which indicates a sign inversion in both directions of the laser output, as shown in Figure 5.6. This feature is in agreement with the prediction of the theory in Section 4.3.2.

§5.3.3 Dependence of intensity modulation on injection current

The modulation depth of the intensity output is an important factor, which relates to the signal-to-noise ratio observed from the interference phenomenon. Since the intensity variation reflects changes of external cavity conditions, the sensitivity of these changes is related to physical parameters to be measured and determines the signal-to-noise ratio of the self-mixing measurement system. In other studies of the self-mixing interference[Shinohana et al 1986, Jentink et al 1988, de Groot et al 1988, and Koelink et al 1992], the modulation coefficient, m, of the self-mixing interference was not measured and considered generally to be constant with the injection current, but in the experiments undertaken in this work it has been found that the modulation coefficient, m, varies with the injection current, J. To investigate the relationship between the modulation coefficient, m, and the injection current, J, the laser current was varied from 0.8 to 1.6 times the threshold current. The experimental arrangement to achieve that was the same as that shown in Figure 5.1, where the external reflector was vibrated and the intensity modulation of the laser output was monitored by a digital storage oscilloscope, via the amplifier, A. The light reflected back onto the front facet of the laser was estimated to be ~1%, as mentioned in Section 5.2.1. When the driving current was gradually increased from threshold, the modulation amplitude of the self-mixing interference was found
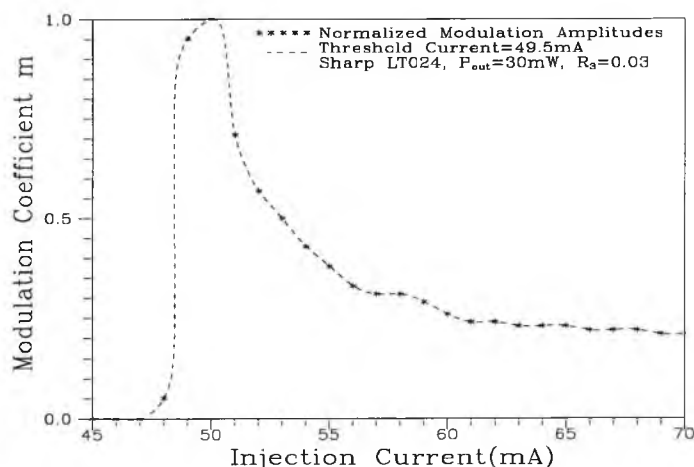
Figure 5.7 Dependence of modulation coefficient

on laser injection current

to decrease and approach a stable value. Close to threshold, the modulation amplitude reached its maximum value; unfortunately, around threshold the intensity modulation was found to be unstable, whilst the modulation amplitude was very small when the laser is operated well above threshold($>1.4J_{th}$). The relationship between the modulation depth and the injection current is depicted as in Figure 5.7, where the modulation coefficient, m, represents a normalised modulation amplitude of the self-mixing signal. When the injection current was under the value of 48 mA, the value of *m* was observed to be very small. Above this value, the modulation signal increased sharply and reached its maximum at the threshold and then the signal amplitude decreased with increasing the current. In the experiments on the self-mixing interference, the laser current was chosen to be 1.1 to 1.2 times the threshold current. At this level the output modulation signal was stable and had a considerable signal-to-noise ratio. This corresponds to the region of the current from 55 mA to 60 mA in Fig.5.7.

The modulation coefficient *m*, defined in Section 4.2.4, represents the modulation signal amplitude in the laser output intensity when the self-mixing interference occurs. The larger the modulation coefficient, the higher the signal-to-noise ratio. Both the experimental result (Fig.5.7) and the theoretical prediction(Fig.4.14) have shown that the modulation coefficients reached their maximum and gradually decreased with increasing injection current and finally approched a stable value. These results show reasonable agreement, although in the theoretical value of the modulation coefficient at the threshold was infinite. In practice the modulation amplitude cannot achieve this value due to the non-linear effect of the self-mixing interference.

§5.4 Coherence properties of self-mixing interference

It has been stated previously that the interference pattern is unobservable if the optical path difference among the interfering beams is greater than the coherence length of the source used. However with the self-mixing interference, the external optical feedback constitutes a part of the laser source, and its presence changes not only the laser intensity but also the laser spectrum. The variations of the spectral distribution produced thus change the coherence length or coherence time of the laser source. The coherence of the radiation in the presence of an external feedback field is therefore determined by the actual lasing spectrum of this external cavity laser.

§5.4.1 Visibility function of the diode laser used

In order to analyze the coherence of self-mixing interference, the coherence length of the diode laser used is measured by using a two-beam Michelson interferometer. The diode laser used is a Sharp type LT022. This laser displays different output modes corresponding to different values of laser injection current. The spectrum of the laser shows characteristics of a multi-mode laser output just above the threshold current and a single-mode spectral distribution above its operating power($\sim 1.25 J_{th}$) of laser output[Sharp 1992]. For the
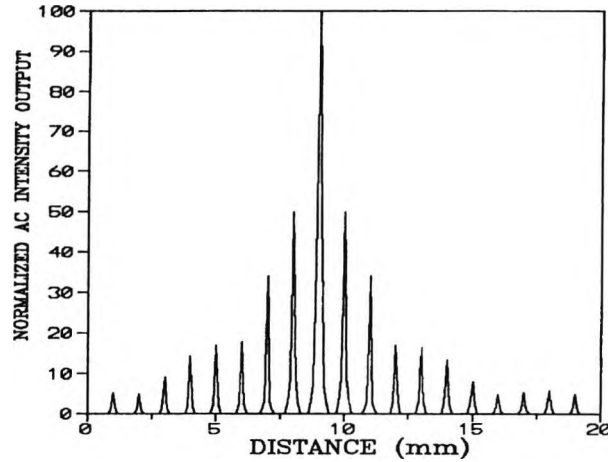
Figure 5.8 Visibility function of the diode laser used

Diode laser—Sharp LT022, Output power—3 mW.

self-mixing interference, the laser driving current is adjusted to be just above the threshold, and the basic coherence characteristics of this laser used are measured at the injection current of $1.2J_{th}$, as shown in Figure 5.8. In summary these are:

1) The optical spacing between the adjacent coherent regions is 1.05 mm, which is equal to the optical length of the laser cavity;

2) The FWHM of each coherent region is 0.11 mm;

3) The FWHM of the envelope of all the coherent regions is ~3 mm and the interference pattern rapidly decreases at the higher orders, over a value of ~10 mm.

It can be seen that the visibility function measured displays a multi-mode feature. It must be noted that for this type of diode laser the coherence length without optical feedback increases as the injection current is increased[Ning et al 1989]. Therefore the coherence measured at a higher injection current is greater than would be if measured at a lower injection current, but the lower current is usually chosen in practice as the self-mixing effect is more easy to observe around the threshold.
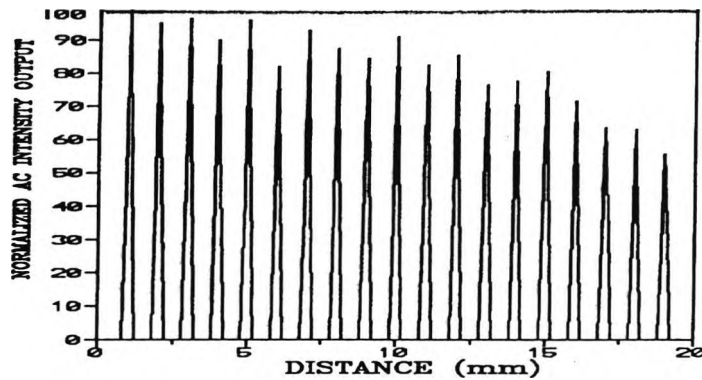
Figure 5.9 The laser undulation dependence on the distance

between laser used and external reflector.

Signals shown represents the amplitude variations of

self-mixing interference corresponding to different distance.

§5.4.2 Coherence of self-mixing interference

To investigate the coherence of self-mixing interference, the experimental arrangement used is the same as that shown in Figure 5.1. In experiments performed, the external target was adjusted from an initial position of about 40 mm in front of the laser to a maximum distance of 60 mm, and this is represented in Figure 5.9 as the X-axis from zero to 20 mm. The output amplitude of the self-mixing signals was monitored against the distance betweem the laser front facet and the target, M. The measured undulation output, P_m, corresponding to a given distance, D_o, is shown in Figure 5.9. Signals are still detected up to a maximum position of about 1500mm from the laser. The modulation amplitude, as Figure 5.9 illustrates, is a function of the target distance, D. The undulation signals display a period of about 1.0 mm. This distance corresponds to the optical length, $n_l d_l$, of the laser cavity, where n_l is the effective refractive index of the laser medium and d_l is the physical length of the laser cavity. Further, when the laser is operated in the multi-mode regime, each lasing mode produces an individual optical intensity, the total of which is the direct superposition of the intensity of

each of the different modes. This, of course, ignores the dispersion in the multi-mode laser cavity. Another feature of the multi-mode self-mixing is that the maximum amplitudes of the self-mixing interference signals do not show significant attenuation with distance.

The experimental results obtained above show that the self-mixing interference phenomenon can be observed even when the external reflector is placed at a distance which is beyond the coherence region of the original diode laser used. For conventional optical interference, there should be no interference signals observed in these places. This means that the interference effect in the self-mixing arrangement is not dependent completely on the coherence length of the laser used, a marked difference from what would be observed with the conventional optical interference.

§5.4.3 Coherence measured using the heterodyne technique

To measure the coherence length of the optical radiation resulting from the self-mixing interference, at a large distance from the diode laser, two long multi-mode fibres, one about 3.48 m, the other about 10.10 m in length, with core diameter 50 μm were used to provide extended values of the OPD, well outside the coherence length of the source. The experimental scheme used is as shown in Figure 5.2. The light emitted from the fibre was reflected back into the cavity by a mirror. When the external mirror was displaced longitudinally, an intensity modulation caused by the self-mixing interference was observed, which was the same type of signal output as shown in Figure 5.3.

Further, to rule out the possibility of these self-mixing signals being caused by interference in the small cavity formed between the end of the fibre and the mirror, pseudo-hetrodyne interferometry[Jackson et al 1982] is employed. In this technique the laser is current-modulated by a triangular wave (500Hz) with a peak-to-peak modulation current amplitude of 0.1mA which produces a 'chirp' frequency modulation of the optical frequency. Interference occurs therefore between two beams, one from the laser front facet and a second
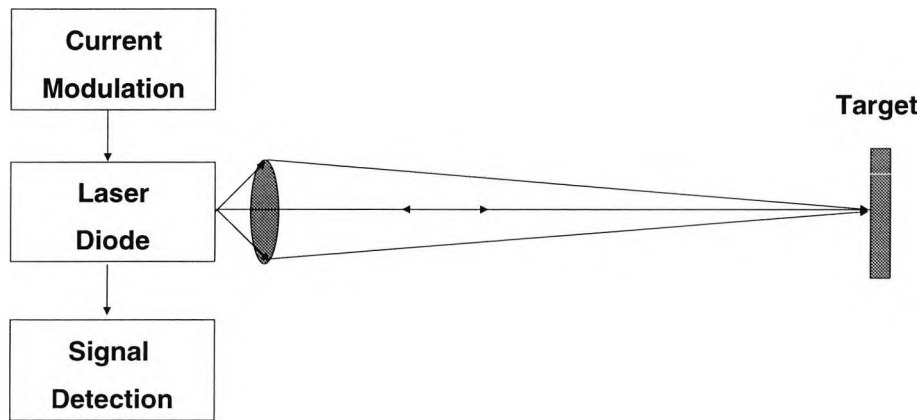
Figure 5.10 Block diagram of self-mixing ranging scheme

The output of diode laser used is current-modulated and focused to external target, the backscattered light re-enters the laser cavity and results in the intensity modulation.

which is time delayed and reflected from the far end of the fibre used or from the mirror at the end of the fibre, at a beat frequency which is proportional to the optical path difference between the beams. With the small value of the modulation current used in this experiment, the optical path difference of the cavity formed by the end of the fibre and the target (typical OPD=1 mm) or even possibly from the feedback of reflections from the end of the fibre nearest the laser (typical OPD=30 mm) are insufficient to produce a beat frequency signal as this frequency is linearly proportional to both the amplitude of the modulation current and the cavity length. This arrangement means that a beat frequency could only result from the feedback from the far end of the fibre, at a frequency proportional to the OPD between the laser and the target mirror.

The block diagram of the experimental setup used is shown in Figure 5.10. The beat frequency produced by the current modulation may be given as

$$f_b = \frac{2D}{c} \, (df/dt) \tag{5-3}$$
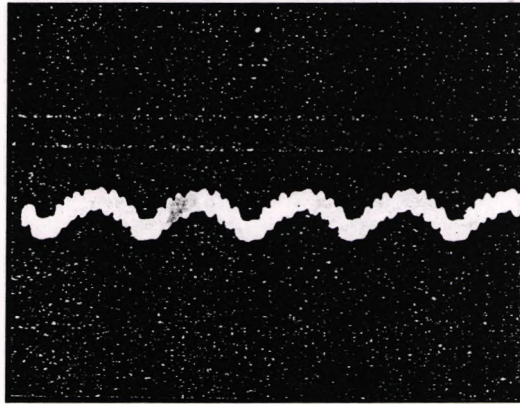
Figure 5.11(a) Beat frequency signal produced by the far end

of fiber surface without incorparating external mirror
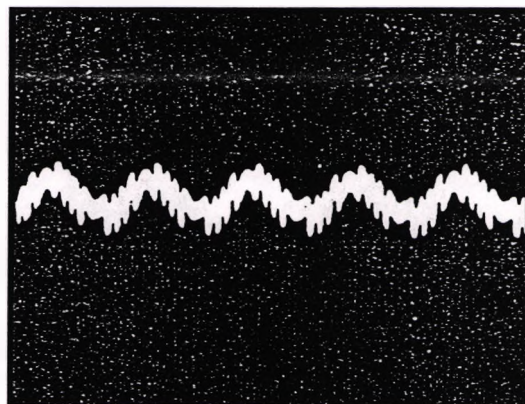
Figure 5.11(b) Beat signal incorporating external reflector

Low frequency signals—current modulation of laser,

Higher frequency signals—beat signals corresponding to distance, D

where D is the distance to be measured between the laser and the target, c is the speed of light, f is the optical frequency of the laser radiation and t is time. If the functional dependence of the optical frequency f with respect to time t is linear, df/dt is a constant. Therefore the beat frequency is linearly proportional to the distance D to be measured.

Figure 5.11 shows the beat frequencies observed in these experiments, when the fibre used is the multi-mode fibre at the length of ~3.48 m. In Figure 5.11(a) the beat signal is produced by reflection from the far end of fibre, incorporating with the reflection from the laser front facet, without an external mirror. In Figure 5.11(b) the beat signal results from reflection from the external mirror, which is buttered against the end of the 3.48 m fibre. In both cases the lower frequency signals displayed in Figures 5.11(a) and (b) are the driving signals of the current modulation, and the beat frequencies of higher frequency are superimposed on this current modulation signals.

It can be seen that the two signals have the same beat frequency but have different amplitudes, which are proportional to the different reflectivities of the fibre end and the mirror. The frequency from the 3.48 m long fibre is measured to be 5.0 kHz and calculated, using Eqn.(5-3), to be 5.14 kHz (with a frequency modulation coefficient 2.6 GHz/mA). The experiment was repeated with a 10.10 m fibre and the beat frequency from this fibre was measured as 15.0 kHz and calculated to be 14.64 kHz. The experimental results are in good agreement with the theoretical calculations and for practical use an improvement of the frequency detecting technique and the more accurate measurement of the frequency modulation coefficient could also be performed. In this work, the frequencies were simply interpreted manually from the oscilloscope trace, to investigate the level of agreement.

In the experiment using the 10.10 m fibre, when the light from the exit facet of the fibre was reflected back into the laser cavity, no beat signal could be detected. This means that the distance between the laser and the external reflector was in the minimum region between the different orders of the self-mixing interference, as shown in Figure 5.9. Alternatively, when an external mirror is used as the reflector, the beat signal can be obtained when the mirror is adjusted away from the fibre end face, it shows the signal amplitude of the self-mixing modulation is away from the minimum region into maximum region. When the mirror is
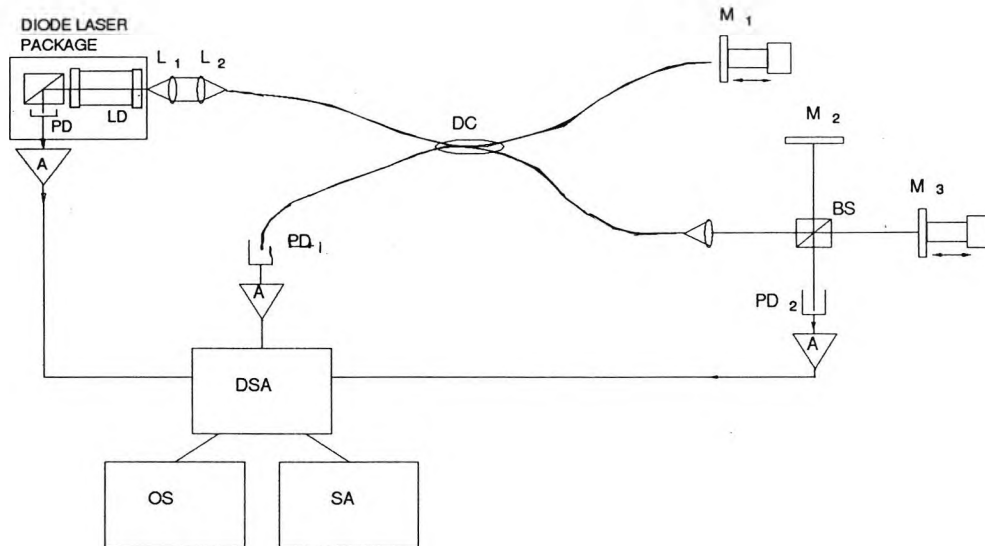
Figure 5.12 experimental arrangement for comparison

between self-mixing interference and conventional interference

L1, L2—lenses, M1, M2, M3—mirrors, PD—photodetector, LD—laser diode, BS—beam splitter,

DSA—digital storage adaptor, OS—oscilloscope, SA—spectrum analyzer

again adjusted to a position further from the end face, the signal returned to a minimum. This indicates the multi-mode property of the diode laser used for the self-mixing interference.

§5.5 Comparison with conventional interferometric method

A experimental comparison of self-mixing interferometry with conventional two-beam Michelson interferometry has been carried out, where a diode laser was coupled to a multi-mode optical fibre coupler, with one output of the coupler used as a source for a two beam Michelson interferometer, the other being used as the sensing probe of the self-mixing interferometer. The experimental arrangement is schematically depicted in Figure 5.12 and the intensity modulation signals from both interferometers are shown in Figure 5.13 with the same frequency of the driven signal simultaneously applied to both mirrors M_1 and M_3. It has
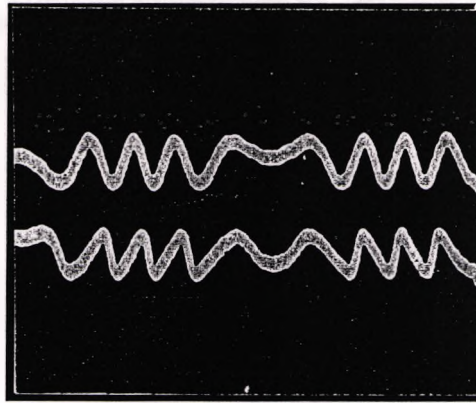
Figure 5.13 Conventional interference pattern(upper trace)

compared with self-mixing interference pattern(lower trace)

Vertical axis, arbitrary units, horizontal axis, 0.2 ms/division.

been stated in Section 5.3.2 that the two signals have a similar intensity modulation with respect to the phase variation at the interferometers, which means that their periodicity is equal to a half of the laser wavelength. However, the self-mixing interference observed shows two significant differences with that of the Michelson interferometer. First, it is sawtooth-like, not sinusoidal, and secondly it is asymmetric relative to the external phase movement, from which the direction of the phase movement can be discriminated.

§5.6. DISCUSSION

The main results obtained may be summarized in that (a) self-mixing interference can occur from targets well outside the coherence length of the laser source, (b) the 'appearance' of this interference signal is an harmonic function of the laser cavity length as shown in Figure 5.9, (c) the effect appears to be independent of whether the source is operating in single-mode or multi-mode manner; (d) the effect appears not to depend on whether the fibre used to couple the source to the target is single-mode or multi-mode. Since these significant differences between the self-mixing interference and conventional interference exist, the

potential applications of using the self-mixing techniques in optical fibre sensing could be very attractive. Thus:

(i) The self-mixing interference has the same phase sensitivity as that of a conventional interferometer, but its significant advantages may lead to some conventional interferometers being replaced by the self-mixing type interferometer, for example, for techniques such as Doppler velocity measurement, and vibration measurement.

(ii) The occurance of self-mixing interference is not dependent on the initial coherence length of the solitary source in the absence of external feedback, which is a great advantage when compared to conventional interference. This makes it very attractive for various applications, such as coherent ranging which is largely limited by the coherence length of the source. Using the self-mixing technique, very large OPDs can be measured provided that sufficient optical feedback is redirected into the laser cavity, in the experiments it was shown that the beat frequency which was proportional to the distance was easily obtained by modulating the diode laser, even over a distance of 10 m, which shows the possibility of the self-mixing ranging in longer distance measurement.

(iii) Self-mixing enables the discrimination of the direction of motion of the target. One of the features of self-mixing interference signal is that it is asymmetric, provided that the reflectivity from the target is sufficiently large. Such an asymmetry is directly related to the direction of the sensing parameter and may be used to discriminate the direction of the target in the laser Doppler velocimeter. This is a very important factor as it minimises the need for alternative, more expensive and complex system.

(iv) A suggested disadvantage of the self-mixing interference is the potential difficulty of coupling the optical feedback into the cavity, but in a fibre coupled system, it was found to be quite easy to reflect the light back into the cavity. This implies that a fibre-coupled self-mixing system will be more attractive for this reason, particularly due to the fact that

multi-mode fibre may be easily used in self-mixing systems, which makes such systems easy to align with a higher signal-to-noise ratio and thus lower costs. In this work, both single mode and multi-mode fibres are used in the above experiments, and the results showing comparatively few differences. The multi-mode fibre is easier to align and has a higher coupling efficiency. However, in the experiments performed it was found that more random noise was generated on the signal with the multi-mode fibre than in the case of the single-mode fibre. It is suggested in the final Chapter that signal analysis is a subject that needs further development and investigation.

(v) Since the self-mixing interference is not dependent on the type of laser used, the inexpensive low coherence solid state type of laser may be used to achieve it in actual sensor systems. For example, the main disadvantage of the conventional fibre optic velocimeter is that the fluid flow is perturbed by the presence of a sensing fibre in the flow itself[Tanaka & Benedek 1975]. Signals from this disturbed region broaden the Doppler spectrum because the fibre lowers the fluid velocity in the "stagnation region" in the close vicinity of the fibre tip. This problem may be overcome by using a multi-mode laser with self-mixing, (as discussed in the experiment with the 10 m fibre) in which an insensitive region (at a distance $<n_1 d_1$) is formed in front of the fibre as the intensity superimposition of each mode, but a thin region of sensitivity may be profiled through and beyond the extent of the "stagnation region". This could of course means that the length of the coupling fibre itself would have to be very carefully defined.

Self-mixing interference in a diode laser results from both a threshold variation and a spectral variation of the laser and this type of interference is not dependent on the conventional coherence length of the laser. The experiments undertaken have shown that the interference by the self-mixing shows some significant differences when compared to conventional optical interference. Applications of these differences have been discussed and the use of the self-mixing technique will be presented in the next chapter.

Chapter 6

Use of self-mixing interferometry for optical sensing applications

§6.1 Introduction

Self-mixing techniques inside lasers have been extensively studied for use in laser Doppler velocimeter and other applications in optical sensors[Dandridge et al 1980, Sinohara et al 1986, de Groot et al 1988, 1989, 1990, Shimizu 1987, Yoshino et al 1987,Jentink et al 1988, and Koelink et al 1992]. In an interferometric configuration, the laser used functions not only as a light source, but also, from the optical point of view as part of an interferometer as well as incorporating a self-aligning detector, which greatly simplifies the system configuration. Particularly, when configured with fibre optics, it makes a dual(or multiple) diode laser self-mixing interferometer very simple and easy to implement. Since the diode laser itself can be considered as a very narrow-band filter, the cross-talk among the different lasers used has been found to be minimal[Wang et al 1992c, 1993b].

For velocity measurement, the optical fibre is used only as the transmission medium by which the interference signals from the fibre end and from the flow particles in such an application are delivered back into the laser cavity, and the fibre length can thus be very long[Wang et al 1992b]. In conventional optical ranging methods, the measurement range cannot exceed the coherence length of the light source. However for a self-mixing system, the interference is not dependent on the coherence length of the laser, it is therefore possible to apply this method for longer distance measurement(greater than the coherence length of the

laser)[Wang et al 1992a]. For vibrational and displacement sensing, one of the problems of using the conventional interferometric method is that the measurement range is usually limited to within half of the oscillation wavelength because of the periodic feature of the interference signals i.e. the 2π unambiguity. To overcome this problem, a two-wavelength interferometer has been configured to achieve two output signals with a phase difference so that a synthetic wavelength could be obtained, which is much greater than that of an individual wavelength. If the two output signals are adjusted to be orthogonal, i.e the phase difference between them is $\frac{\pi}{2}$, direction discrimination from the object movement could be achieved[Wang et al 1993b].

§6.2 Laser Doppler velocity measurement

A fibre-optic Doppler velocimeter that incorporates the effect of self-mixing in a diode laser is described. The results of the experimental research are found to be in good agreement with the theoretical analysis. A Doppler velocity of as much as 3 m/s is measured directly, and a good linear relationship between the Doppler velocity and the Doppler-shifted frequency is obtained, which can be used to determine the velocity of a moving object.

§6.2.1 Introduction

The Doppler effect describes the phenomenon experienced by an observer whereby the frequency of light waves emitted from a source that is travelling away from or toward the observer will be shifted from its original value. This effect was recognised and modelled by Johann Doppler(1803-1853), and so is named the Doppler effect[Watrasiewcz et al 1976, and Figliola et al 1991]. The observed shift in frequency, called the Doppler shift, is directly related to the speed of the emitter relative to the observer. The Doppler effect has been used to measure the velocity of moving objects by monitoring the frequency shift of a laser beam which is monochromatic and remains coherent over a long distance. To measure local velocity in a moving fluid, the emission source and the observer remain stationary. However,

small scattering particles suspended in the moving fluid can be used to generate a Doppler shifted signal from the moving particles.

As a moving particle suspended in the fluid passes through the laser beam it scatters light in all directions. An observer viewing this encounter between the particle and the beam will perceive the scattered light at a frequency, f_s, given by:

$$f_s = f_i + f_d \qquad (6\text{-}1)$$

where f_i is the frequency of the incident laser beam and f_d is the Doppler shift, which is proportional to the velocity of the moving target, V, by:

$$f_d = \frac{2n\cos\theta}{\lambda_o} V \qquad (6\text{-}2)$$

where n is the refractive index of the target medium, θ is an angle between the velocity vector and the optical axis, and λ_o is the wavelength of laser emission.

In this section, self-mixing interferometry is exploited for velocity measurement using Doppler techniques, with the use of a 6 m single-mode optical fibre(core diameter of ~5 μm) and a cheap CD-type diode laser(Sharp LT022MD) operated above its threshold. A Doppler velocity simulation is provided by a rotating disc coated with a white paper and its rotation speed could be adjusted by changing the voltage of a Voltage-Controlled-Motor (VCM). The velocity is varied from 20 mms^{-1} upwards and is measured by using the self- mixing interferometry method. It is compared to that obtained by direct measurement using a opto-electronic pulse counting method. A linear relationship between the velocity of the rotating disc and the Doppler frequency produced is obtained with a minimum resolution of ~3 mms^{-1}. A simple theoretical model is presented together with a description of the experimental arrangement, experimental results and discussion.

§6.2.2 Experimental setup for self-mixing LDV

The self-mixing LDV study reported herein is carried out with a 780 nm diode laser(Sharp LT022MD) and a ~6 m single-mode optical fibre(-core diameter of ~5 μm) as shown in Figure 6.1. The light emerging from the diode laser is collimated, passes via a beam splitter, BS, and then is focused into the fibre. The light emitted from the fibre end is then aimed at a diffused target, which is represented by a white paper attached to a rotating disc, with an angle about 68 degrees to the rotation direction. The disc is driven by the VCM and its velocity could be varied from 20 mms^{-1} to 5000 mms^{-1}. The scattered light from the rotating target re-enters the fibre and is superimposed with the light reflected from the fibre
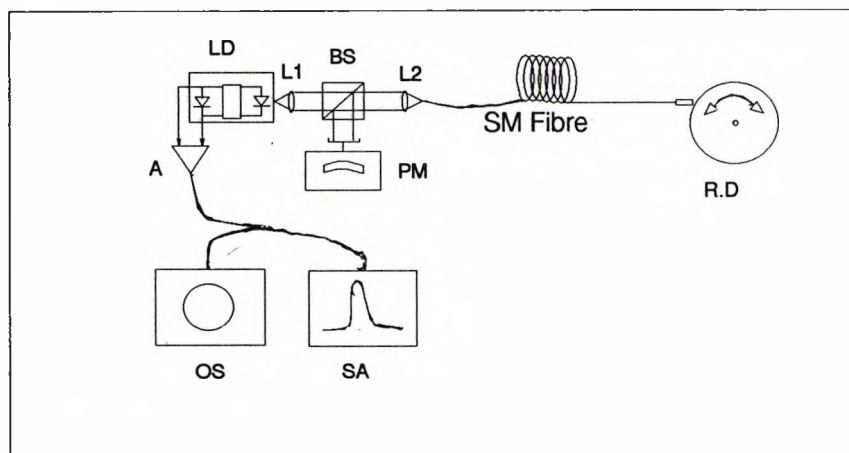
Figure 6.1 Experimental arrangement for self-mixing LDV

LD, laser diode; BS, beam splitter; L$_1$, L$_2$, lenses; OS, oscilloscope; SA, spectrum analyzer; A, amplifier; PM, power meter; SM, single mode; RD, rotating disk.

end. Both beams are guided via the same optical path back into the laser cavity and the amount of optical feedback is monitored through a beam splitter, BS, by a power meter, PM. The diode laser package incorporated a photodiode accommodated in its rear facet, this is employed to monitor the laser intensity variations, which are used in this experiment to observe the self-mixing effect produced by external optical feedback. The laser is operated at

an output power of 2.5 mW(J=1.2J$_{th}$, J$_{th}$ being the threshold current) which has been found to be the optimal output for the Doppler velocity measurement[this is in agreement with the result in Section 5.3.3], whilst the signal-to-noise ratio(SNR) is found to decrease with increasing diode injection current, i.e. increasing the output power of the laser, but there still remains a good SNR at J=2J$_{th}$. The reflected light from the target is measured by the power meter, PM to be 0.01 mW, which is approximately -25 dB of the original output laser power. However, to achieve self-mixing interference, the optical feedback strength can be up to about -10 dB and as small as about -60 dB. The output signal from the laser photodiode is ac-amplified via a wide-band amplifier A and then fed to an oscilloscope and a spectrum analyser for direct Doppler frequency studies.

§6.2.3 Theoretical analysis

The experimental self-mixing LDV scheme using fibre optics(Figure 6.1) may be simplified, in optical terms, to a four-mirror FP cavity structure, as depicted schematically in Figure 6.2[Section 5.2.2]. A portion of light emitted from a diode laser is fed back into the laser cavity after it is reflected from the fibre end and scattered from a diffused target which is
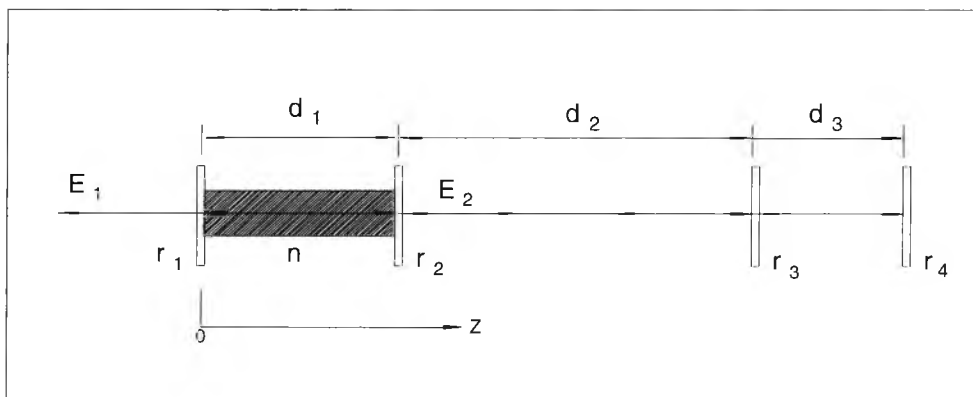
Figure 6.2 Schematic of self-mixing LDV system

r$_1$, r$_2$, laser facet amplitude reflectivities; r$_3$, r$_4$, reflectivities from far fibre end and external target; n, effective index of laser material; d$_1$, d$_2$, d$_3$, respective cavity lengths; E$_1$, E$_2$, laser output waves in two emission directions.

moving, to produce a Doppler shifted frequency superimposed on the original optical frequency of the laser light. According to the theory given in Chapter 4, the effective reflection coefficient r_2' may be expressed as:

$$r_2' = r_2 + (1 - R_2)r_3\exp[-j\phi_3] + (1 - R_2)(1 - R_3)r_4\exp[-j\phi_4] \qquad (6\text{-}3)$$

$$= r_2\{1 + \xi_3\exp[-j\phi_3] + \xi_4\exp[-j\phi_4]\} \qquad (6\text{-}4)$$

where $R_2(=|r_2|^2)$, $R_3(=|r_3|^2)$ are the power reflection coefficients of the fibre end and the target respectively; ξ_3, ξ_4 are the feedback coefficients from external reflection surfaces respectively, and given by

$$\xi_3 = (1 - R_2)\frac{r_3}{r_2}, \ \ \xi_4 = (1 - R_2)(1 - R_3)\frac{r_4}{r_2},$$

and ϕ_3, ϕ_4 represent the corresponding phases from the external reflections respectively, and given by

$$\phi_3 = 4\pi v\frac{d_2}{c} \ \ \phi_4 = 4\pi v\frac{d_2 + d_3}{c} + 2\pi f_d t.$$

Since the reflections from the fibre end and from the target are much less than that from the laser facet, the coupling coefficients ξ_3 and ξ_4 satisfy the following condition:

$$\xi_3 \ll 1 \text{ and } \xi_4 \ 1 \ll 1$$

The excess gain Δg and the additional phase ϕ_2 may be expressed approximately as:

$$\Delta g \approx -\frac{1}{d_1}[\xi_3 \cos(\phi_3) + \xi_4 \cos(\phi_4)] \qquad (6\text{-}4)$$

$$\phi_2 \approx \xi_3 \sin(\phi_3) + \xi_4 \sin(\phi_4) \qquad (6\text{-}5)$$

The resultant optical intensity modulation I is therefore given by:

$$I \approx I_0[1 + m_3 \cos(\phi_3) + m_4 \cos(\phi_4)] \qquad (6\text{-}6)$$

where m_3 and m_4 are the self-mixing modulation coefficients.

The lasing frequency of the self-mixing system must satisfy the lasing phase conditions, and this leads to:

$$2\pi(\nu - \nu_{th})\tau_1 + \xi_3\sqrt{1+\alpha^2}\,\sin[\phi_3 + \arctan(\alpha)] + \xi_4\sqrt{1 + \alpha^2}\,\sin[\phi_4 + \arctan(\alpha)] = 0$$

For very weak feedback level, the lasing frequency may be assumed to be unaltered[Shinohara et al 1986], i.e. $\nu \approx \nu_{th}$, and under this assumption, the intensity modulation produced by self-mixing effect may be expressed as:

$$I_{ac} \propto \cos(\Delta\phi_4 + \omega_d t) \tag{6-7}$$

where I_{ac} accounts for the ac component of the self-mixing intensity modulation; $\Delta\phi_4 = 4\pi\nu_{th}\dfrac{d_2 + d_3}{c}$ is an initial phase determined by the positions of the fibre end and the target and ω_d is the angular frequency produced by the Doppler effect. It is clear that the presence of fibre end reflection does not contribute to the Doppler frequency modulation, but influences the dc component of the output intensity of the laser used.

In this case, the intensity modulation is similar to that seen in conventional LDV, and the Doppler velocity, V, of the target movement may then be expressed directly as

$$V = \frac{\lambda_o}{2n\cos\theta}f_d$$
$$= k\,f_d \tag{6-8}$$

where λ_o is the lasing wavelength of the self-mixing system, n is the refractive index of the scattering medium and θ is an angle between the velocity vector and the optical axis, and k is a proportionality constant. For example, $k=1.04$ when the related parameters are chosen to be $\lambda_o=780\ nm$, $n=1$ and $\theta=68$ degrees and the velocity V is presented in mms^{-1} and f_d in kHz.

§6.2.4 Experimental results

A typical Doppler spectrum produced by the target rotation is shown in Figure 6.3(b). This spectrum may be compared with the output spectrum without the external optical feedback shown in Figure 6.3(a). When the external signal, shifted by the Doppler velocity, is
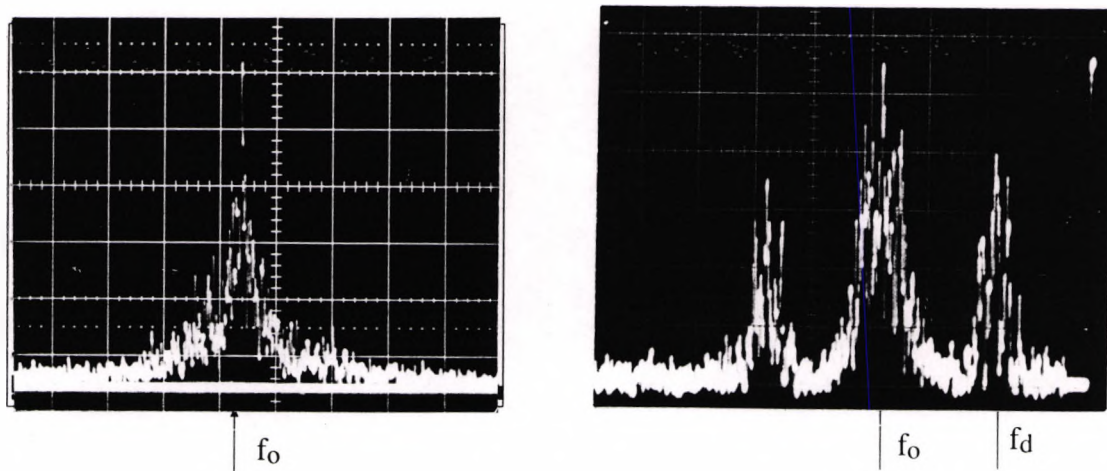
Figure 6.3 Signal spectra of self-mixing LDV system

(a) background spectrum without rotation of the target;

(b) Doppler frequency spectrum produced by rotation of the target.

Vertical logarithmic scale, arbitrary units[same for (a) and (b)]; central

peak, f_o, zero frequency(dc); side peaks, f_d, Doppler shift frequency(b).

fed back into the cavity, two side peaks are seen in the spectrum, and the spacing from the central peak(zero frequency) represents the Doppler-shifted frequency, which is directly proportional to the speed of the rotating disc. The broadening in the Doppler-shifted spectrum represents the low frequency rotation of the disc used, and the equal-spaced peaks around the zero frequency, f_o, and the Doppler frequency, f_d, are separated by the disc rotation frequency.

In the experiments performed, the velocity of the rotation disc could not be given directly so that the Doppler frequency measured from the spectrum analyzer was against the voltage applied to the VCM as shown in Fig.6.4(a). In addition, the Doppler velocity of the rotating disc was also measured against the Motor Voltage applied, as shown in Fig.6.4(b), which shows a linear relationship between the velocity and the motor voltage, i.e. the rotation velocity is proportional directly to the motor voltage. Therefore the Doppler frequency
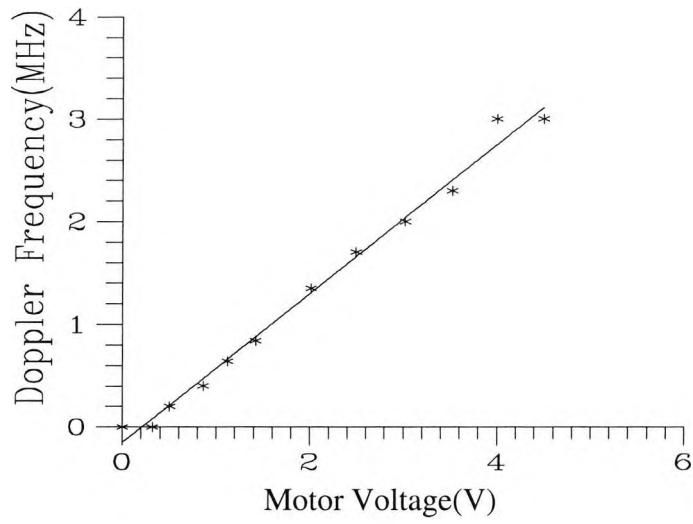
Figure 6.4(a) Doppler frequency dependence on motor voltage

(where the motor voltage is proportional to the rotation speed)
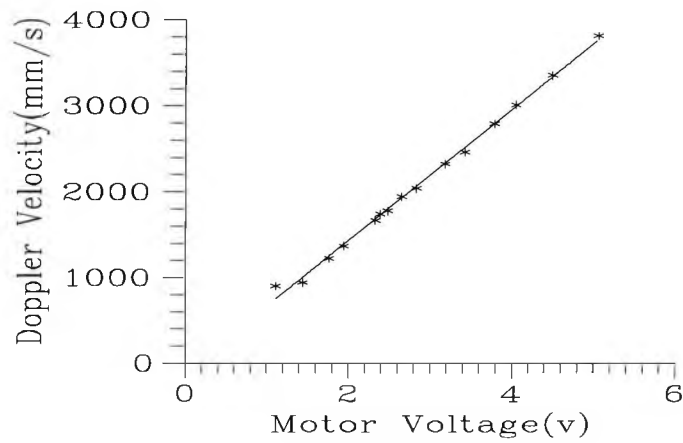
Figure 6.4(b) Doppler velocity vs. Motor voltage

measured could be linked with the rotation velocity. It can be seen that the two curves have a good linear relationship with the voltage applied, the saturation at higher voltage shown in Fig.6.4(a) being due to the bandwidth limitation of the amplifier used. In order to obtain an explicit relationship between the Doppler velocity and the Doppler frequency, adequate data processing has been performed to combine these two curves together and find out a direct relationship between the Doppler velocity, V, and the Doppler-shifted frequency, f_d, which can be expressed as

$$V \, {}^{(mm/_s)} = 1.05 f_d \, (kHz) \pm 7.80 \, {}^{(mm/_s)} \tag{6-9}$$

The offset of 7.8 ${}^{mm/_s}$ is the error limit, which indicates the combined effect of the velocity measurement and the direct frequency measurement against the control voltage, an improvement of the frequency detecting technique and the accurate measurement of the rotation speed would absolutely reduce this limit.

§6.2.5 Discussion

The utility of the self-mixing technique for LDV indicates its significant advantages. These are simplicity, the fact that the self-mixing configuration requires only one optical axis, which simplifies the design and alignment of the optical system; its compactness, and the use of the internal photodiode in the laser package to detect the intensity modulation produced by self- mixing. No external detector is needed, and this detector provides a high detection efficiency for the self-mixing interference. Since the measurement method is not dependent on the coherence length of the laser used, various fibres and low-coherence sources may be exploited in this application.

With strong feedback, the higher harmonics of the measured Doppler-shifted frequency are presented in the output spectrum as shown in Figure 6.5, these higher harmonics indicate the asymmetric feature observed in the self-mixing interference and include the directional

f₀
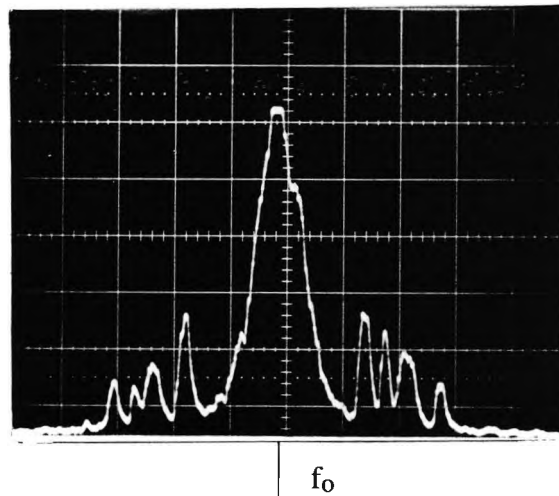
Figure 6.5 Signal spectrum with strong feedback level

Vertical logarithmic scale, arbitrary units; horizontal scale, 0.1 MHz/division

and with video filter of 10 Hz; central peak, zero frequency(dc).

information of the Doppler velocity[Section 5.3.2]. This may be useful for discrimination of the target movement and has been discussed in by Shimizu[1987].

The principle of an optical-fibre laser Doppler velocimeter was demonstrated in this Section, based on self-mixing interference, which is realised with a long optical fibre combining a cheap CD-type diode laser source. The experimental arrangement highlights the simplicity, compactness and suitability of this self-mixing LDV scheme over conventional LDV.

§6.3. Ranging using self-mixing technique

Distance measurement, beyond the coherence length of a diode laser used, is investigated in this section by using the self-mixing interference scheme in a diode laser. Experiments with different length multi-mode optical fibres demonstrate the feasibility and simplicity of the method.

§6.3.1 Introduction

Coherent detection techniques have been exploited in conventional optical interferometers to provide the advantages both of absolute parameter measurement and a large dynamic range[Hymans & lait 1960, Jackson et al 1982]. The coherent detection method is realised by first splitting the light from the source into two beams. One of the beams, termed the reference beam, is maintained at a known optical length to provide a reference for sensing beam. The other beam, termed the signal beam, is subjected to an unknown time delay on reflection from a distant external target. The signal and reference beams are then mixed coherently to produce an intensity variation which can be detected by using a photodetector. When the light source is frequency modulated, a beat frequency occurs from the output of the detector, which is directly proportional to the optical path difference between the signal and reference beams and can be demodulated from the detected optical intensity modulation. This observed beat frequency can represent the target distance from the reference[Dandridge & Goldberg 1982, and Tatsuno &Tsunoda 1987].

Since most coherent detection systems involve some variation of unequal-path interferometry, the measurement range is completely dependent on the coherence length of the source, which limits its application for larger ranges i.e. those beyond the source coherence length. Coherent ranging using the self-mixing effect has been reported by several researchers[Beheim & Fritsch 1986, de Groot et al 1988, 1990], which presents significant advantages in compactness, simplicity and robustness. However, it has been confined only for use within the coherence length of the laser, as the self-mixing interference has been considered to be a form of conventional interference.

In this section, coherent ranging for larger distances(up to 10 m, using fibre optics) is investigated, based on the use of self-mixing interference method, with the measurement range being in excess of the coherence length of the laser used. The experiments performed

demonstrate that self-mixing interference is not dependent on the coherence length of the laser, which provides the possibility of using coherent detection methods for range finding for much longer distances, that provides an advantage over conventional coherent detection method.

§6.3.2. Self-mixing coherent ranging

Self-mixing interference has been observed even with the external reflector well beyond the coherence length of the laser used. The resultant intensity modulation reflects the variations of both threshold gain and spectral distribution of the laser self-mixing effect, which provides two significant differences over conventional interference as mentioned in the previous chapters. i.e. (1) it is non-dependent on the coherence length of the laser; (2) it is asymmetric with respect to the phase change of the target movement. When the external optical feedback is very weak, the intensity modulation for a three-mirror self-mixing system may be expressed approximately[Eqn.(4-33)] as

$$I = I_o[1 + m \cos(2\pi v_{th} \frac{\Delta L}{c})] \qquad (6\text{-}10)$$

where m has been termed as the modulation coefficient, v_{th} is the lasing frequency of the external cavity laser under weak feedback; and ΔL is the optical path difference(OPD) between the laser front facet and the target. It is easy to see that the eqn.(6-10) has the same form as that for a conventional two beam interferometer.

When a direct current modulation is applied to the diode laser, the resultant intensity modulation will include an FM modulation and an AM modulation[Imai & Kawakita 1990]. If the amplitude and the frequency of the current modulation are very small, a beat frequency f_b, produced by the self-mixing can be observed and may be given by

$$f_b = -\frac{2\beta}{\lambda_o^2} D \, (dJ/dt) \qquad (6\text{-}11)$$

where β is the wavelength modulation coefficient(nm/mA), λ_o is the lasing wave length of the diode laser, dJ/dt is the rate of the current change rate, and D is the target distance from the
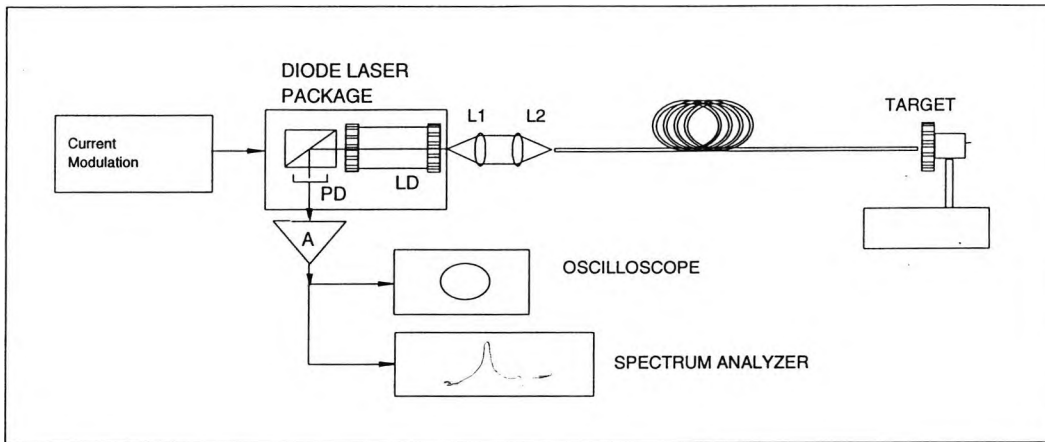
Figure 6.6 Experimental arrangement for self-mixing ranging

PD, photodiode(integral), LD, laser diode; L₁, L₂, lenses; A, amplifier.

laser. It is obvious that if dJ/dt is a constant, a fixed beat frequency f_b can be detected from the intensity modulation of the laser output, and then the distance D to be measured could be calculated directly from the equation (6- 11).

§6.3.3. Ranging experiments

These experiments are performed by using a diode laser package(Sharp LT022MC) and different lengths of multi-mode optical fibres, all with a core diameter of ~50 μm. The experimental arrangement using the self-mixing coherent ranging is shown in Figure 6.6. The light from the laser is collimated by a lens, L₁, and then focused by another lens, L₂, into a multi- mode fibre. The light travelling through the fibre is reflected by the fibre end facet or by a mirror M. The reflected light is guided by the same fibre and re-enters the laser cavity. The light beams from one of the laser facets and from the target are mixed inside the laser cavity, and the resultant intensity modulation is detected by a photodiode accommodated at the rear facet, inside the laser package.

When the laser is current-modulated, the interference due to the self-mixing occurs at a beat frequency which is proportional to the distance between the self-mixing beams. The beat frequency may result from the reflection from the fibre end nearest the laser or from the far

end of the fibre. In the work herein, the laser is dc biased, with a driving current J above its threshold J_{th} (J=1.2J$_{th}$) and in addition current-modulated by a sinusoidal wave at 500 Hz with a peak-to-peak value of 0.1 mA. The small current modulation provides two advantages, which are (1) the feedback from the near end of the fibre is insufficient to produce a significant beat frequency due to the short distance; (2) the mode hopping produced by large current modulation can be avoided. By substituting the experimental data above, the distance D may be expressed as

$$D = 0.69 f_b \qquad\qquad (6\text{-}12)$$

where the wavelength modulation coefficient in the above Equation(6-11) is estimated to be about 5.6×10^{-3} nm/mA for the diode laser used, and the lasing wavelength of the laser used is 780 nm.

The resultant intensity modulation was ac-coupled via an amplifier A(Figure 6.6) to an oscilloscope for waveform analysis. Figure 6.7 shows the observed waveforms in the
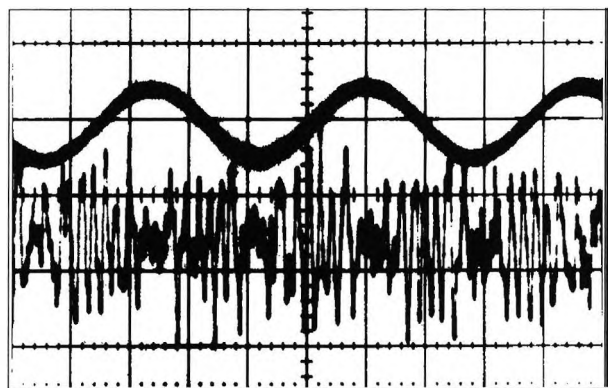
Figure 6.7 Beat frequency(lower trace) produced by current

modulation of diode laser against upper trace(current modulation signal applied to LD).

Vertical axis, arbitrary units; horizontal axis, 0.2 ms/division.

experiment with a 1.51 m long multi-mode fibre, where the upper trace is the ac-current modulation, and the lower waveform is the output modulation signal, produced from the reflection of the external mirror, M, incorporating the reflection from the front facet of the laser. The frequency of the signal represents the beat frequency from the current modulation. It is clear that the self-mixing beat signal(lower trace) has a periodical modulation waveform, the frequency of which is proportional to the distance to be measured. The following, Table 6.1, shows the fibre lengths, L_o, measured against the distance, D_o, calculated using Equation(6-12), from the directly measured beat frequency on the oscilloscope, E represents the error between the fibre lengths and the distances. It is clear that the measured results are in considerable agreement with the theoretical calculations. Improvement in the accuracy of distance measurement requires a more accurate measurement of the beat frequency, which may be improved by using more accurate frequency detection techniques rather than direct measurement from the oscilloscope.

Table 6.1 Estimation of distances measured			
f_b(kHz)	2.0	5.0	15.0
L_o(m)	1.51	3.48	10.10
D_o(m)	1.38	3.45	10.35
E(cm)	13	3	-25

§6.3.4. Discussion

The laser diode used in the ranging studies displays a multi-mode nature, the coherent characteristics of which have been measured using a two beam Michelson interferometer in Chapter 5, as shown in Figure 5.8. The interference was not detectable when the distance difference between the two arms of the interferometer was greater than 11.65 mm, which means that this type of laser cannot be used in a conventional coherent ranging system where

the distance to be measured is greater than 11.65 mm. However, with the self- mixing coherent ranging arrangement, the measurable distance could reach as far as a distance of 10 m, with suitable detector circuitry. This represents a considerable improvement, using a cheap and readily available laser source.

The experiments undertaken have demonstrated that the coherent detection method using the self-mixing interference can incorporate a larger optical path difference than using conventional techniques and the self-mixing arrangement shows the simplicity of operation in terms of self-alignment and self-detection.

§6.4 Vibrational Measurement

Vibration measurement using self-mixing interference is studied in this section, where the vibrational direction of the target movement may be determined if there is enough feedback strength.

§6.4.1.Introduction

Laser interferometry offers a number of desirable features in the measurements of small vibrations[Bruce & Fitzpatick 1975, Nokes et al 1978]. In this work, a self-mixing interferometer with a diode laser is proposed based on "self-mixing interference" where a portion of emitted light from the laser is reflected back into the laser cavity from a vibrating surface, and the resulting intensity modulation is extracted to determine the vibration parameters which are causing the resultant phase change in this interferometer. A simple arrangement with a multi-mode optical fibre is used to measure the vibration with its directional information. Due to the asymmetric nature of the self-mixing interference mentioned in the previous chapters the vibrational direction is discriminated from the resulting intensity output signals which offers an advantage compared to the use of conventional interference techniques.

§6.4.2.Experimental arrangement

The experiment reported was carried out with a 780 nm VSIS-type AlGaAs diode laser and a multi-mode fibre coupler(50 μm core diameter) as shown in Figure 6.8. The light from the diode laser is collimated and then focused into the fibre coupler. The light emitted from one of the fibre arms is pointed at a reflecting surface, which is represented by a small mirror attached to a loudspeaker cone, driven by a signal generator to provide a vibration signal. The reflected light from the mirror is guided by the same path back into the laser cavity and the amount of optical feedback is monitored by a photodetector PD_1. The diode laser package incorporates a photodiode accommodated in its rear facet to monitor the laser power, which is used in this experiment to observe the intensity variations produced by the external optical feedback. The other optical fibre for transmission of light is angle-ended to reduce the reflection from this fibre end. When the mirror M_1 is vibrated, the intensity modulation
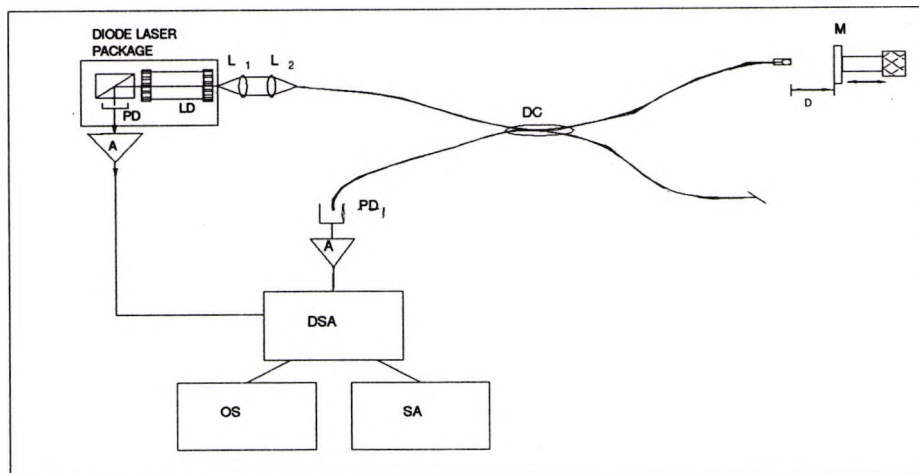
Figure 6.8 Experimental arrangement for vibrational

measurement using self-mixing technique

PD, photodiode; LD, laser diode; L_1, L_2, lenses; A, amplifier;

DC, directional coupler; DSA, digital storage adaptor; OS, oscilloscope;

SA, spectrum analyzer; M, target mirror.
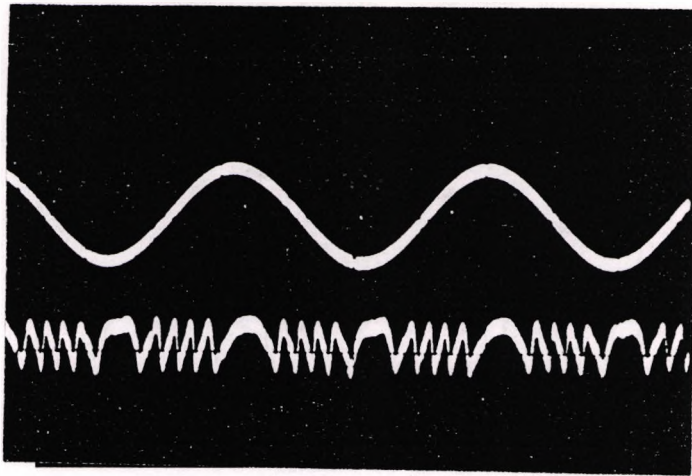
Figure 6.9 Self-mixing signal produced by mirror vibration

Upper trace—electric signal of external vibration applied,

Lower trace—self-mixing interference signal detected from LD.

Vertical axis, arbitrary units; horizontal axis, 0.5 ms/division.

signals are observed from both photodetectors, PD, and PD_1, which represent the self-mixing interference fringes as observed in Section 5.3.

A typical output signal produced by the longitudinal vibration is shown in Figure 6.9. The upper trace is the driving signal applied to vibrating speaker, while the lower trace is the self-mixing interference signal caused by the vibration. As has already been discussed in Chapter 5, the interference signal shows a 2π periodicity with the phase change at the external mirror M1, and the period of the variation is equal to a half of the wavelength of the laser. On the other hand, it is easy to see that the significant differences between them, in that it is sawtooth-like but not sinusoidal, and it is asymmetric relative to the external vibration. From this, it is important to note that the inclination of the signal is dependent on the direction of the "target" movement, and when the target changes its movement direction, the signal changes its inclination. It is from such an asymmetry that the vibration direction can be discriminated, which shows a major advantage over the conventional interferometric method.

To measure the nature of the vibration of a subject under consid eration, two factors must be determined, which are the amplitude and frequency of such a vibration. The

amplitude can be determined by counting the fringe number of the interference in one direction. A good linear relationship between the fringe number and the vibrating amplitude is
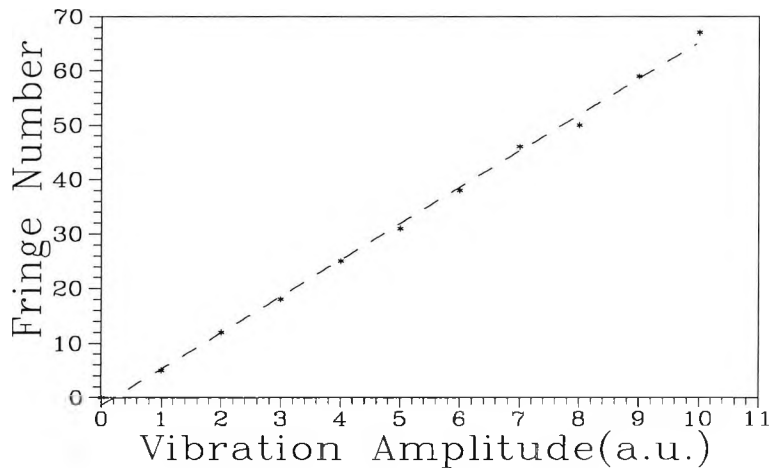
Figure 6.10 Fringe number dependence on vibrational amplitue

shown in Figure 6.10. Thus the amplitude may be expressed as

$$A = N \times \lambda \qquad (6\text{-}13)$$

where N is the fringe number, and λ is the oscillating wavelength of the laser. Again it has been seen that this self-mixing interference signal changes its inclination as the target changes its direction, which implies that the period(the reciprocal of the frequency) can be determined by recording the time between directional change of the target. If the vibration is symmetrical, its frequency may then be given by

$$f = \frac{1}{2\tau} \qquad (6\text{-}14)$$

where τ is the time for one directional change.

§6.4.3. Theoretical analysis

The self-mixing effect may be considered as a kind of optical interference, ("self-mixing interference") and the resulting intensity variation is found to be due to the threshold gain and spectral linewidth change produced by the externally reflected light. Thus the intensity, I, has been expressed as in Eqn.(4-33). The intensity modulation dependence on the external displacement has been shown in Figure 4.8, corresponding to different external reflection coefficients, where the larger the reflectivity, the more sawtooth-like the intensity modulation. For a very small reflection coefficient(C<<1), the modulation becomes sinusoidal, and the intensity may be expressed approximately as:

$$I = I_o[1 + m\cos(2\pi\frac{\Delta L}{\lambda_{th}})] \qquad (6\text{-}13)$$

where I_o is the laser output intensity in absence of external feedback, m is the modulation coefficient or visibility function, and λ_{th} is the lasing frequency at threshold; ΔL is the OPD between the laser front facet and the vibrating mirror. When the target is vibrated with a sinusoidal movement, the OPD, ΔL, may be written as:

$$\Delta L = \Delta L_o + A\sin(2\pi f_d t) \qquad (6\text{-}14)$$

where ΔL_o is an initial position of the vibrator, and the amplitude A and the frequency f_d may be determined from the resulting intensity modulation.

It is worth noting that when the reflected light signal is too weak, i.e. the feedback coefficient C is much less than unity in theory, the useful asymmetry of the intensity output will disappear(as the function approximates closely to a sinusoidal) and it is therefore necessary to keep sufficient light fed back into the laser cavity.

§6.4.4. Discussion

In this Section, a "self-mixing interferometer" with a semiconductor laser was described and preliminary experimental results presented, which show some significant comparative

advantages over the use of a conventional interferometer. For a vibration measurement, the self-mixing method combines simplicity of operation with the ability of discriminating the vibration direction.

§6.5 Displacement measurement with a wide dynamic range

The principles, experimental apparatus and advantages of using the self-mixing technique for extended displacement measurement are described, based on the use of a dual diode laser configuration. This device is capable of creating a synthetic wavelength simultaneously by using the frequency selectivity of the individual laser which responds only to its own wavelength. Theoretical analysis and experimental evidence are presented to show the feasibility of the measurement method, and the simplicity of its operation.

§6.5.1 Introduction

Optical interferometric methods for measurement of displacement and if required, vibration have been widely developed. Such methods are non-contact, are immune to electrical interference and can offer potentially higher resolution than conventional methods in many instrumentational applications.

In recent years, amongst these novel interferometric methods, self-mixing interference in a diode laser has been increasingly of interest because of the inherent simplicity, compactness and robustness of the method. Unfortunately, the measurement range of the self-mixing technique is also limited by the familiar "2π phase ambiguity" in its output due to the periodic nature of the observed transfer function. For displacement measurement, this technique is capable of detecting movements as small as $\sim 9 \times 10^{-5}$nm[Dandridge 1980], but the maximum displacement to be measured is limited to only $\sim 2 \times 10^{-7}$ m for a typical solid-state laser source, operating at a wavelength of ~ 800 nm. This leads to an uncertainty in the observation of the direction of movement and the determination of the true displacement is hence only possible to within $\lambda/4$[Jackson 1987]. Optical methods of measurement can

further be required, with extended range, for machine vision, robotic positioning and automatic inspection. Conventional measurement methods to overcome these limitations of range are based on two or multiple wavelength interferometers[Cheng & Wyant 1984, Kersey & Dandridge 1987, den Boef 1988, and Williams & Wickramasinghe 1986]. Of these, such interferometers that are based on optical fibres enable the optical systems to be simple and insensitive to environmental vibrations[de Groot 1991]. However, to measure the phases of the different wavelengths used, the interferometric systems require some type of temporal, spatial or polarization multiplexing components to separate the individual interferometric phases corresponding to each wavelength. This makes the interferomethric systems complicated and difficult to align. Another technique using "white light" interferometry[Gerges et al 1990, Ning et al 1990] has been also developed for extended displacement measurement, but such schemes require relatively complicated optical configurations and often bulky interferometric components[Smith & Dobson 1989, and Jones 1992].

In this Section, a dual diode laser-based self-mixing interferometer is described for extended displacement measurement with a wide dynamic range. The optical reflection from the target surface is fed back into both diode laser cavities, each laser operating at a distinct wavelength and acting as its own "frequency filter", only responding to the feedback of its own light, and thus allowing the creation of a "synthetic wavelength" by monitoring the two output signals of two diode lasers used. This wavelength is much larger than either of the individual wavelengths corresponding to each laser alone and the method can be used for extended displacement measurement or absolute ranging with a wide dynamic range. Section 6.5.2 presents the theoretical background for the dual diode laser-based self-mixing interferometer, relating to the work undertaken. The experimental apparatus, using fibre optics, is described in Section 6.5.3, and experimental results and conclusions are presented respectively in Sections 6.5.4 and 6.5.5.

§6.5.2 Theoretical background

A free-space version of the dual diode laser-based self-mixing interferometer is illustrated in Figure 6.11. The outputs of the two diode lasers are combined via a mirror, M, and beam splitter, BS, into one light beam. A part of the light is first reflected by the reference mirror, R, and the rest of light propagates to an external target, T, and is then reflected by that target surface. Both of these reflections are fed back, via their original optical paths, into the laser cavities. The self-mixing process inside each laser cavity results in the variation of the laser output power which is monitored by detecting the output light at the rear facet of the laser cavity.

To understand the mechanism of the self-mixing modulation, the dual diode laser self-mixing system may be considered to consist of two Fabry-Perot type external cavity lasers. They have the same structure and may be modelled as a four-mirror Fabry-Perot type cavity laser, as shown in Figure 6.12, where r_1 and r_2 denote the amplitude reflection coefficients of the laser facets respectively, r_3 and r_4 represent the amplitude reflection
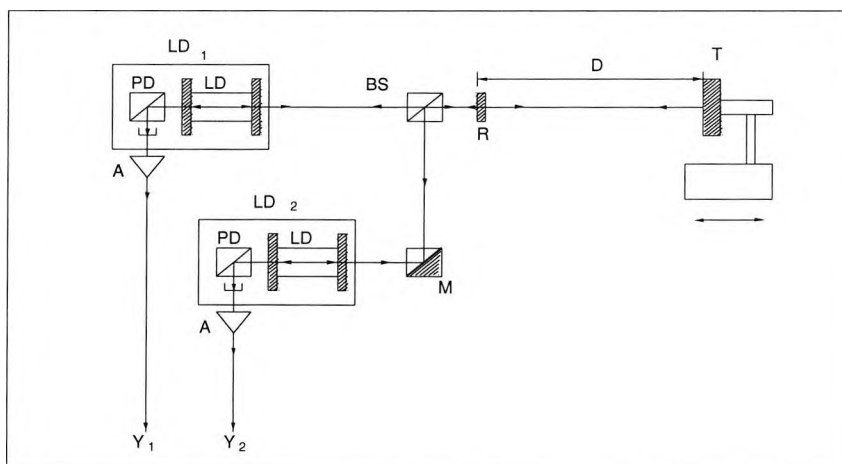
Figure 6.11 Schematic of two diode laser self-mixing system

LD_1, LD_2, diode laser packages; LD, laser diode; PD, photodiode;

BS, beam splitter; M, R, mirrors; D, distance between reference plane

and the target surface; A, amplifier; T, target; Y_1, Y_2, intensity modulations.
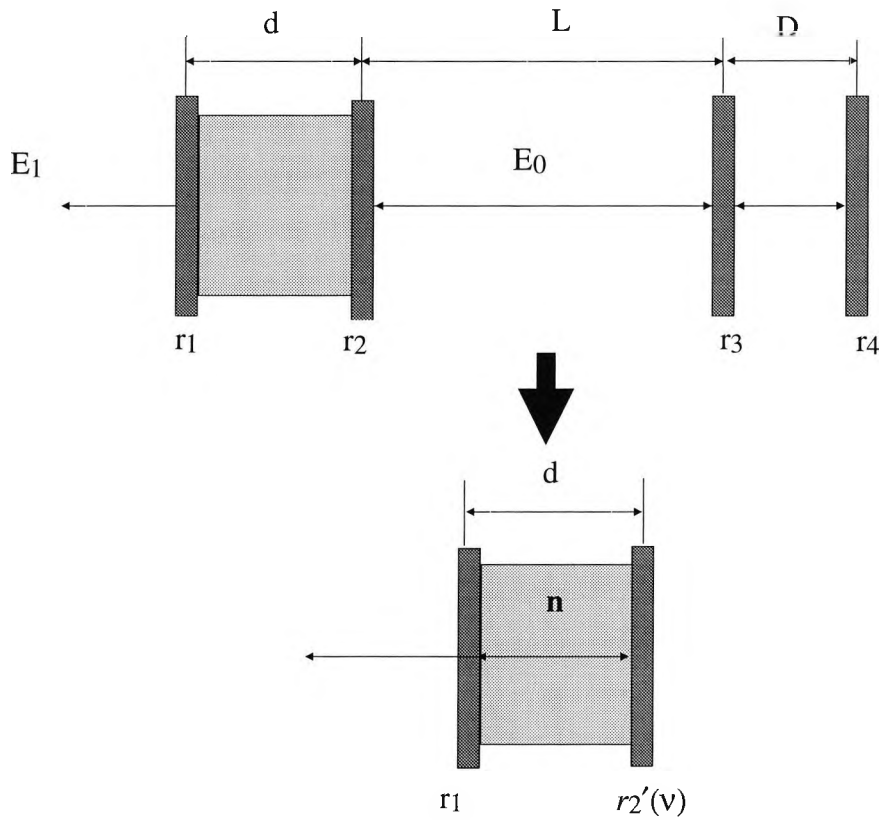
Figure 6.12 Geometry of a four-mirror Fabry-Perot type

cavity laser and its two-mirror Fabry-Perot equivalent

r_1, r_2 — amplitude reflection coefficients of laser facets

r_3, r_4 — amplitude reflection coefficients

of reference mirror and target

d — solitary diode laser cavity length

coefficients of the external reflection surfaces, R and T, and n represents the effective refractive index of the laser cavity material. E_0 and E_1 represent an initial electric field vector and the output electric field vector of the laser respectively, d is the diode laser cavity length, L is the length between the laser front facet and the reference mirror, and D represents the length between the reference plane and the target reflector.

For simplicity, the case of a single-mode laser only is considered in the following theoretical analysis, and the external feedback is assumed to be very weak, thus the multiple reflections within the external cavities may be neglected[Petermann 1991b]. From Figure 6.12, an effective reflection coefficient r_2' accounting for the external optical feedback at frequency, v, may be expressed as

$$r_2'(v) = r_2 + (1 - |r_2|^2)r_3\exp\{-j2\pi v\frac{2L}{c}\} + (1 - |r_2|^2)(1 - |r_3|^2)r_4\exp\{-j2\pi v\frac{2(L+D)}{c}\} \quad (6\text{-}15)$$

The terms $(1 - |r_2|^2)$ and $(1 - |r_3|^2)$ account for the light transmission through the laser front facet and through the mirror, M_r. The above expression is a complex function and may be re-written with respect to amplitude and phase, Φ_2, as

$$r_2'(v) = |r_2'| \exp\{-j\Phi_2\} \quad (6\text{-}16)$$

In the case of the weak feedback with $|r_3|$, $|r_4|<<|r_2|$, the amplitude $|r_2'|$ may be expressed as

$$|r_2'| = r_2\{1 + \xi_3\cos(2\pi v\frac{2L}{c}) + \xi_4\cos[2\pi v\frac{2(L+D)}{c}]\} (6\text{-}17)$$

where the coupling coefficients are

$$\xi_3 = \frac{r_3}{r_2}(1 - |r_2|^2) \quad (6\text{-}18)$$

and

$$\xi_4 = \frac{r_4}{r_2}(1 - |r_2|^2)(1 - |r_3|^2) \quad (6\text{-}19)$$

and c is the speed of light.

In general, for weak feedback, ξ_3, $\xi_4 << 1$ and the phase Φ_2 may be expressed as

$$\Phi_2 = \xi_3 \sin(2\pi v \frac{2L}{c}) + \xi_4 \sin[2\pi v \frac{2(L+D)}{c}] \qquad (6\text{-}20)$$

It is known that for a stationary laser oscillation, the initial electric field vector E_0 inside the laser cavity, which undergoes a complete roundtrip within the cavity, will meet the following laser oscillation condition

$$r_1 r_2'(v) \exp\{(g - \gamma)d - j2\pi v \frac{nd}{c}\} = 1 \qquad (6\text{-}21)$$

where g and γ represent the optical gain and loss per unit length(cm^{-1}) inside the solitary laser cavity respectively, and d is the solitary laser cavity length. This lasing condition requires the threshold gain, g_{th}, for laser oscillation to be

$$g_{th} = g_0 - \frac{\xi_3}{d} \cos(4\pi v \frac{L}{c}) - \frac{\xi_4}{d} \cos(4\pi v \frac{L+D}{c}) \qquad (6\text{-}22)$$

and the lasing frequency, v, to satisfy

$$4\pi(v - v_0) \frac{n_e d}{c} + \xi_3 \sqrt{1 + \alpha^2} \sin(4\pi v \frac{L}{c}) + \xi_4 \sqrt{1 + \alpha^2} \sin(4\pi v \frac{L+D}{c}) = 0 \qquad (6\text{-}23)$$

where g_0 and v_0 are the threshold gain and the lasing frequency in the absence of external feedback, n_e is the effective group refractive index of the laser cavity material, and α is a constant termed the linewidth enhancement factor.

Equations(6-22) and (6-23) may be considered as theoretical models to explain the self-mixing interference inside the laser cavity. Since the laser intensity is proportional to the laser threshold gain, Equation(6-22) accounts for the intensity modulation produced by the change of the external cavity conditions. This expression shows that the intensity modulation of the self-mixing interferometer is similar to that of conventional optical interference. However, Equation(6-23) illustrates the determination of the lasing frequency and only those frequencies satisfying this equation can produce the laser output light. This implies that the laser cavity is acting as a frequency filter which passes the light within the frequency band for amplification and rejects the other light outside the frequency band. Because this frequency

band is usually very narrow for a semiconductor laser, each laser used in this two wavelength self-mixing interferometer can only response to its own feedback light, the light from the other laser being rejected due to its wavelength difference and it has no influence on the laser output signal. This nature greatly simplifies the configuration of the multiple wavelength interferometer as an optical or electronic multiplexing system is not needed.

The principle of the operation of the dual laser diode system is as described below. Firstly, each laser acts as its own "frequency filter", only responding to feedback of its own light. Secondly, the signal obtained from the pin photodetector located in each of the lasers results from the self-mixing interference with the external optical feedback. As the phase of the reflected signal is modulated by the movement of the target, this leads to a modulation of the intensity of the laser output power. Thirdly, as the source lasers are at different wavelengths, a phase difference will arise between the two electrical signals from the internal pin photodiodes. This phase difference will be proportional to the displacement between the reference plane and the target surface and the detection of this phase difference can be used to obtain the relatively large displacement measurement of the target from the reference position, M_r. As the reflection from the reference plane is in a stationary state, it determines the dc level of the laser output signals and the initial phase of the output signals, but has no influence to the ac modulation signals used for phase measurement.

From a theoretical viewpoint, the modulation of the laser output power under weak feedback can be represented by a sinusoidal output signal, Y_i, and described simply as

$$Y_i = A_i[1 + \mu_i\cos(\phi_i) + \rho_i\cos(4\pi\frac{D_o}{\lambda_i} + \phi_i)] \qquad (6\text{-}24)$$

where i=1,2 and the subscript i is used to denote the two individual interference signals, represented by Y_1 and Y_2, obtained at the two pin diode detectors. A_i represents the laser output power without the feedback; μ_i is the proportionality constant related to the reflection coefficient of the reference mirror; ρ_i is the a.c. modulation coefficient induced by the

feedback from the target; λ_i is the corresponding laser wavelength, ϕ_i the initial phase of the two signals which is determined by the optical path difference(OPD) between the laser front facet and the reference mirror, M_r, and Do is the displacement involved. For simplicity, the a.c. amplitudes of the two output signals and the initial phases may be assumed to be the same. This can be achieved practically by using automatic gain control(AGC) in the signal processing circuit and by adjusting the position of one of the lasers to set the initial phase difference.

The phase difference, $\Delta\phi$, between the two signals can then be measured and expressed as

$$\Delta\phi = 4\pi(\frac{1}{\lambda_1} - \frac{1}{\lambda_2})D_o = 4\pi\frac{\lambda_2 - \lambda_1}{\lambda_1\lambda_2}D_o = 4\pi\frac{1}{\lambda_{12}}D_o (6\text{-}25)$$

where $\lambda_{12} = \dfrac{\lambda_1\lambda_2}{\lambda_2 - \lambda_1}$, which is termed the "synthetic wavelength", will be much larger than that of the single lasers(λ_1 and λ_2), depending on the wavelength difference of the lasers used.(e.g. for the extreme case λ_1=783 nm and λ_2=785 nm and thus the synthetic wavelength, λ_{12} can be as large as ~0.3 mm). Hence the maximum range of the displacement
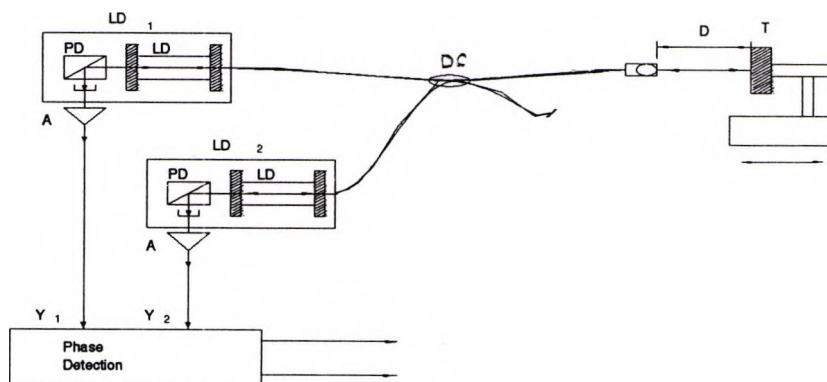
Figure 6.13 Experimental arrangement for the dual diode

laser-based self-mixing interferometer

LD, laser diode; PD, photodiode; A, amplifier; D, displacement;

T, target; DC, directional coupler; Y_1, Y_2, self-mixing signals detected.

measurement involved could be up to ~150 μm(± 75 μm), which is about 550 times the measurement range of a single laser interferometer, with the appropriate choice of diode lasers. The use of two laser wavelengths with a smaller separation would allows a greater range to be examined. If the phase difference $\Delta\phi$ can be accurately measured within the region of $\pm\pi$ rad, a high measurement accuracy can be achieved.

§6.5.3 Experimental apparatus

To demonstrate the measurement of an extended displacement using the self-mixing technique, a practical scheme for the dual-diode laser-based fibre optic self-mixing interferometer was constructed, as shown in Figure 6.13. In this scheme the optical emission from each of these two diode lasers is coupled into an arm of the multi-mode fibre optical coupler(DC) with core diameter of 50 μm which is then used both as a sensing probe and as the reference. This reference reflection surface is achieved by mirror-cleaving the fibre end-face so that a part of the light is directly reflected back from the fibre end. The light emitted from this exit facet of the optical fibre is then positioned to illuminate an external target (a mirror is used here), the reflection from which is collected by the sensing fibre. The two reflected beams, one from the fibre end, and the other from the object are then delivered by the same fibre coupler back into both laser cavities. The other output arm of the coupler is angle-cut to avoid the reflection from this end facet into the lasers.

In the experiments, the external mirror target may be adjusted along the optical axis and is vibrated in a simulation by an electro-mechanical transducer. This results in a modulation of the output of the two lasers which is monitored by the internal pin photodiode detectors. The signal from these detectors is then ac-amplified and displayed on a dual-beam oscilloscope, via a digital storage adaptor, DSA. The output signals displayed represented the last term in Equation(6-24) as the signals are ac coupled. In this work, the phase difference between the two signals is measured by measuring the time difference between the two sample signals frozen by the DSA. In a practical instrument, dedicated circuitry could be
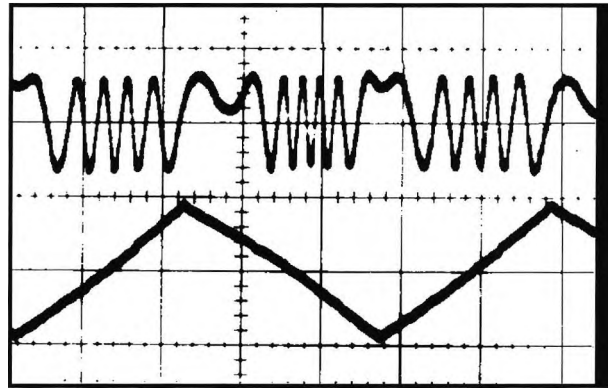
Figure 6.14 Self-mixing signal from one diode laser

Upper trace—self-mixing interference patterns;

Lower trace—displacement of the target mirror.

vertical axis, arbitrary units; horizontal axis, 1 ms/division.

developed to enable this measurement to be made to replace that used in this work. The use of a fibre optical coupler makes this dual diode laser-based self-mixing configuration relatively simple to implement.

Sharp LT022MD AlGaAs index-guided diode lasers were used as sources in the experiments. Their wavelengths(λ_1, λ_2) were respectively 783 nm and 785 nm at a normal output of ~3 mW. With the above arrangement, laser interference signals resulting from the displacement of the external mirror were observed on the oscilloscope.

§6.5.4 Results

A typical self-mixing interference signal from one of diode lasers is shown in Figure 6.14. In this figure each "fringe" corresponds to a half wavelength of the laser light of displacement at the reflector. The upper trace shows the interference signal where the reflector moved through five fringes, representing a displacement of $2.5\lambda_1$, and the lower trace denotes

the displacement at the reflector (proportional to the current through the coil of the electromechanical transducer causing it). If the feedback into the laser cavity is strong enough, the interference signal may become sawtooth-like, but in practice, with a fibre optical system, the reflection from the object is quite weak, and so the interference signal can be considered as a sinusoidal signal.

In the experiment carried out, it was found that the intensity of the modulation in the output of the laser diodes was mainly determined by the strength of the feedback from the target and by the distance between the exit fibre end and the external mirror. The feedback level from the target was estimated to be ~3% and the distance between the fibre end and the target can be adjusted up to ~0.5 mm without using a collimator, and it may be extended, if required, by using a GRIN lens to collimate the output light from the fibre end.

It was also found that there is no significant cross-talk between the two lasers due to the high wavelength selectivity of the laser devices used. To confirm this observation, one of the diode lasers was switched off and no significant change of the output signal from the other laser was observed.

This experimental finding is in agreement with theoretical prediction of the laser wavelength selectivity, presented in Section 6.5.2. Thus, the phase difference between the two intensity modulation signals was determined only by the synthetic wavelength of the two lasers and the displacement D_0 to be measured. By detecting the corresponding phase difference, the value of D_0 can thus be determined. Since the synthetic wavelength can be made much larger than that of the source lasers, for example up to ~0.3 mm here and potentially greater, the dynamic range for displacement measurement or absolute ranging which can be achieved is very large, but at a low accuracy, depending on the phase measurement resolution. This is, in principle, similar to a conventional two-wavelength interferometer.
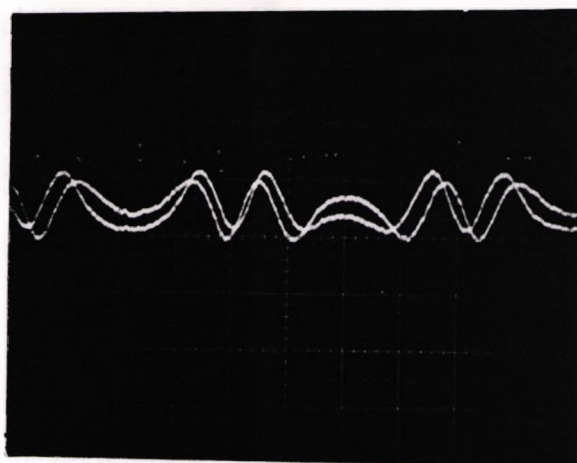
Figure 6.15 Output signals from two diode lasers

The time difference shown between these two output

signals gives the phase difference, Δφ.

Vertical axis, arbitray units; horizontal axis, 1 ms/division.

Figure 6.15 displays the two output signals observed from the diode lasers used, showing a phase difference between them when the reflector was displaced, with one leading the other in phase, and this phase difference is determined by the distance between the target mirror and the fibre exit end. By measuring this phase difference, for example from the separation of corresponding peaks of the two traces, related to the calibrated horizontal axiz, this displacement or distance from the fibre end could then be calculated. It can be seen from this figure that the phase difference is also determined by the direction of the external reflector movement within the synthetic wavelength, showing a relative lead and lag between the two output signals, and when the direction of displacement is reversed the phase relationship is reversed, indicating a direction change.

To measure the phase difference between the output signals in a two wavelength interferometer a phase modulation is required, and it is provided either by an accoustic-optic modulator[Tucker & Christenson 1990] or by a vibrating mirror[de Groot 1991]. In the setup here the phase modulation was achieved simply by vibrating the target mirror with a small
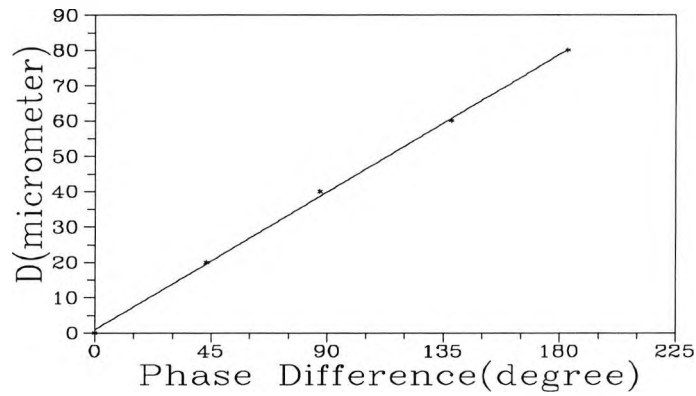
Figure 6.16 Displacement of target mirror dependence on the
phase difference, $\Delta\phi$, of the two output signals of the lasers.

vibration amplitude. In practice, this phase modulation can be introduced by shifting the exit
fibre end longitudinally with a piezo-electric transducer mounted at the end of fibre[Sasaki &
Takahashi 1988]. The two output signals from the lasers were displayed on the oscilloscope
via the DSA when the target mirror was moved. When the two output signals were adjusted in
phase, this position was marked as the initial point. Then the target was moved away from this
point, the signal from the shorter wavength laser leads that of the longer one and the phase
difference was measured by using the DSA. Several displacement measurements were
recorded using a micrometer. When the two signals were seen to be out of phase, the phase
difference between them was measured to be π radians, and the displacement, D_0, from the
initial point was read to be ~78 μm, this value is in agreement with our calculation of 75 μm,
based on the diode lasers used. Further movement of the target changes the sign of the phase
difference, i.e. the signal from the shorter wavelength laser lags that of the longer one. After
experiencing a π radians phase difference, the two signals will be in phase again. Figure 6.16
shows the displacement, D_o, as a function of the phase difference, $\Delta\phi$, up to π radians and a
linear relationship between them is presented.

§6.5.5 Summary

The feasibility of the dual diode laser-based feedback interferometer has been demonstrated and preliminary experimental results are presented. The method used highlights the simplicity of the operation, and this is seen particularly with a fibre optical scheme where the system has a much simpler configuration and a higher signal-to-noise ratio than that of conventional systems. It has been also shown that the system used is capable of achieving extended displacement measurements with a larger relative dynamic range and potential high accuracy, provided that the system can make successive measurements with single wavelength interferometry.

Chapter 7

Overall summary and suggestions for further studies

Self-mixing interferometry with laser sources is a relatively new division of optical interferometric methods. This method is based essentially on the use of optical feedback technique of lasers, and is a very promising research direction for optical sensors. For multiple wavelength interferometry, the self-mixing technique can be used to create synthetic wavelengths simultaneously without using any temporal, spatial or polarisation multiplexing component as needed in conventional multiple wavelength interferometers, this greatly simplifies the configuration of the multiple wavelength interferometer. In this Chapter, the results obtained from the self-mixing interference are listed as an overall summary, and some suggestions for further studies are presented.

§7.1 Summaries

Self-mixing interference based on diode lasers can be considered to be a natural extension of conventional optical interference because of the similarity of the output signals from these two interference methods. However, in this work both theoretical analysis and experimental investigations performed have shown the advantages of using the self-mixing techniques in optical sensing applications(particularly for two wavelength self-mixing interferometry) and also shown the complication of the self-mixing process inside the laser cavity and the differences of the self-mixing interference from conventional optical interference, because of the non-linear effect of self-mixing process. The main features of self-mixing interference can be summarised as the following:

(1) The self-mixing interference is not produced simply by the linear superimposition of two or more light beams as in conventional interference, but is due to the variations of the lasing threshold gain and spectrum, which are produced by the external feedback light.

(2) The change of the laser output power reflects the variation of the lasing threshold gain, which is very similar to that of conventional optical interference under weak feedback conditions. This change can be easily monitored by uses of the internal photodetector or an external photodetector.

(3) The output signal of the self-mixing interference, which shows the sawtooth-like waveform in the case of larger feedback levels, represents the spectral shifts of the lasing spectrum subject to the condition of external optical feedback.

(4) Coherence is an interesting subject in the self-mixing interference as it has been found that the interference signals can be observed even if the external feedback light is from a distant reflector which is placed well beyond the coherence length of the solitary diode laser. From the conventional point of view, if the feedback light from the external reflector is outside the coherence length of the laser used, there should be no interference phenomenon between the light inside the cavity and the light returned. Obviously this assumption is valid under the condition that the light source remains unchanged, but it is not the case in the self-mixing process where both the threshold gain and the spectrum of the diode laser are altered by the feedback light. The variation of the spectrum of the laser source thus changes the coherence properties of the laser source.

From another point of view, it can be seen that the external reflector constitutes actually of an extended part of the laser source used. This part, in combination with the solitary laser, forms an external cavity laser structure. The oscillation condition of the solitary laser is thus changed because of the presence of this external reflector. The new laser oscillation can take place only if the light inside this extended cavity laser satisfy a new lasing condition and only if the lights participating in the lasing process can produce a stable output power. This output power of the laser thus corresponds to the new lasing condition. When the condition in the external cavity is changed, the laser changes its oscillation condition, and therefore the output

power. This implies that the self-mixing interference occured due to the change in the lasing condition; it is not dependent on the coherence of the solitary laser used.

(5) Laser oscillation is a non-linear process and it takes place if the light inside the laser cavity meets the amplitude and phase conditions of the oscillation. The laser output power produced is determined finally by the available photon numbers inside the cavity, while the output spectrum is dependent on the laser cavity structure which functions as a "frequency filter" and determines the oscillation frequency. In this case, the laser can therefore be considered as a very narrow-band amplifier and only the photons within the frequency band can produce output light, while others are rejected. This function has implications for simplifying multiple wavelength interferometric systems.

(6) The self-mixing interference is a very complicated process, especially with multi-mode diode lasers. In this case there is not an appropriate theoretical model to describe it. Thus, in this work only the theory of the single-mode diode laser has been discussed, for the multi-mode laser the output power in the presence of the feedback has been considered to be due to the direct superposition of the individual lasing mode intensity, this leads to the undulation of the interference signals as a function of the external reflector distance(Section 5.4.2).

(7) The theory presented in Chapter 4 can be used to analyze the self-mixing interference in the case of weak feedback levels ($C < 1$), for larger feedback the lasing spectrum becomes multi-mode due to external cavity operation. It is thus impossible to give analytical expressions for this self-mixing process.

(8) It is known that external optical feedback causes a serious problem on conventional optical interferometric systems, and it should be avoided as much as possible. However, in the self-mixing interferometry, the external feedback plays a positive and important part of the self-mixing interference process, and it cannot be excluded from the system. Its use eliminates the need for optical isolators as used in conventional interferometric systems.

§7.2 Suggestions for further studies

As mentioned in the beginning of this chapter, the self-mixing technique based on semiconductor lasers is very promising research direction for optical sensing applications, particularly in applications for machine vision, robotic positioning and automatic inspection. This enables the high precision measurement of optical interferometry widely used in experiments to be extended for practical use in industrial environments.

In this work, due to limitations of time and available equipment, some further interesting work relating to the self-mixing interference has not been able to be performed. Some suggestions for further studies are thus listed below:

(1) Spectrum analysis. As the optical feedback into the laser cavity changes not only the output power of the laser but also the lasing spectrum, it would be better to monitor both the laser spectral changes and the laser output power by using an optical spectrum analyser. This would enable a comparison of the theoretical predictions with the experimental findings in more detail.

(2) Theoretical analysis for the self-mixing interference under the strong feedback level i.e. the value of the feedback coefficient C being greater than unity. The diode laser in this condition will become multi-mode in operation and a numerical method could be used to describe the self-mixing process.

(3) The theory of a single mode diode laser has been developed in this work. The further work should include an extension of this theory covering multi-mode diode lasers.

(4) Multiple wavelength interferometers have been an interesting subject for interferometric measurements with extended range. Although the work undertaken has first demonstrated the feasibility using the dual diode laser self-mixing interferometer, further work should be done to develop a practical system of fibre optical sensor, as this has potential as a simpler configuration at lower cost.

REFERENCES

Acket, G. A., Lenstra, D., den Boef, A. J., and Verbeek, B. H., 1984 **"The influence of feedback intensity on longitudinal mode properties and optical noise in index-guided semiconductor lasers"** IEEE J. Quant. Electron. **QE-20**, pp.1163-1169.

Adams, M. J., 1973 **"Rate equations and transient phenomena in semiconductor lasers"** Opto-electronics, **5**, pp.201-215.

Agrawal, G. P., 1984 **"Line narrowing in a single-mode injection laser due to external optical feedback"** IEEE J. Quant. Electron. **QE-20**, pp.468-471.

Agrawal, G. P., Olsson, N. A., and Dutta, N. K., 1984 **"Effect of fiber-far end reflections on intensity and phase noise in InGaAsP semiconductor lasers"** Appl. Phys. Lett. **45**, pp.597-599.

Ashbire, N. L., Schwiesow, R. L., and Derr, V. E., 1974 **"Doppler Lidar observations of hydrometeors"** J. Appl. Meteorol., **13**, pp.951.

Ashby, D. E. T. F., and Jephcott, D. F., 1963 **"Measurement of plasma density using a gas laser as an infrared interferometer"** Appl. Phys. Lett. Vol. 3, pp.13-16.

Ashby, D. E. T. F., Jephcott, D. F., Malein, A., and Raynor, R. A., 1965 **"Performance of the He-Ne gas laser as an interferometer for measuring plasma density"** J. Appl. Phys., **36**, pp.29-34.

Barwood, G. P., Gill, P., and Rowley, R. C., 1992 **"Longitudinal mode control in laser diodes"** Meas. Sci. Technol., **3**, pp.407-410.

Beheim, G., 1986 **"Fibre-optic interferometry using frequency modulated laser diodes"** Appl. Opt. **23** , pp.3469-3472.

Beheim, G., and Fritsch, K., 1986 **"Range finding using frequency-modulated laser diode"** Appl. Opt. **25**, pp.1439-1442.

Born, Max, and Wolf, Emil, 1975 "**Principles of Optics**" 6th ed, Pergamon. London.

Bracewell, R. N. 1978 "**The Fourier Transform and its Application**" 2nd ed, McGraw-Hill, London.

Bruce, R. A., and Fitzpatrick, G. L., 1975 "**Remote vibration measurement of rough surfaces by laser interferometry**" Appl. Opt., **14**, pp.1621-1626.

Cheng, Y. and Wyant, J. C., 1984 "**Two-wavelength phase shifting interferometry**" Appl. Opt. **23**, pp.4539-4543.

Cheo, Peter K., 1985 "**Fibre Optics-devices and Systems**" Englewood Cliffs, London: Prentice-Hall.

Cho, Y., and Umeda, M., 1984 "**Chaos in laser oscillations with delayed feedback: numerical analysis and observation using semiconductor laser**" J. Opt. Soc. Amer., **B1**, pp.497.

Cho, Y., and Umeda, Y., 1986 "**Observation of chaos in a semiconductor laser with delayed feedback**" Opt. Commun. **59**, pp.131

Chuang, Z. M., Cohen, D. A., and Coldren, L. A., 1990 "**Tuning characteristics of a tunable-single-frequency external-cavity laser**" IEEE J. Quant. Electron. **QE-26**, pp.1200-1205.

Churnside, J. H., 1984 "**Laser Doppler velocimetry by modulating a CO_2 laser with backscattered light**" Appl. Opt. **23**, pp.61-65.

Churnside, J. H., 1984 "**Signal-to-noise in a backscatter-modulated Doppler velocimeter**" Appl. Opt. **23**, 2079-2106.

Cohen, J. S., Drenten, R. R., and Verbeek, B. H., 1988 "**The effect of optical feedback on the relaxation oscillation in semiconductor lasers**" J. Quant. Electron. **QE-24**, pp1989-1995.

Cohen, J. S., and Lenstra, D., 1989 **"Spectral properties of the coherence collapse state of a semiconductor laser with delayed optical feedback"** IEEE J. Quantum Electron. **QE-25**, pp.1143-1151.

Cohen, J. S., Wittgrefe, F., Hoogerland, M. D., and Woerdman, J. P., 1990 **"Optical spectra of a semiconductor laser with incoherent optical feedback"** IEEE J. Quantum Electron. **QE- 26**, pp.982-990.

Dandrige, A., Miles, R. O., and Giallorenzi, T. G., 1980 **"Diode laser sensor"** Electron. Lett. **16**, pp.948-949

Dandridge, A., and Tveten, A. B., 1981 **"Phase noise of single-mode diode lasers in interferomer systems"** Appl. Phys. Lett. **39**, pp.530-532.

Dandridge, A., and Goldberg, L., 1982 **"Current-induced frequency modulation in diode lasers"** Electron. Lett., **18**, pp.302-304.

De Groot, P. J., Gallatin, G. M., and Macomber, S. H., 1988 **"Ranging and velocimetry signal generation in a backscatter-modulated laser diode"** Appl. Opt. **27**, pp.4475-4480.

De Groot, P. J., and Gallatin, G. M., 1989 **"Backscatter-modulation velocimetry with an external cavity laser diode"** Opt. Lett. **14**, pp.165-167.

De Groot, P. J., 1990 **"Range-dependent optical feedback effects on the multimode spectrum of laser diodes"** J. Modern Optics, **37**, pp.1199-1214.

De Groot, P. J., 1991 **"Three-color laser-diode interfeometer"** Appl. Opt. **30**, pp.3612-3616.

De Groot, P. J., and McGarvey, J., 1992 **"Chirped synthetic-wavelength interfeometry"** Opt. Lett. **17**, pp.1626-1628.

Den Boef, A. J., 1988 "**Two-wavelength scanning spot interferometer using single-frequency diode lasers**" Appl. Opt. 27, pp306-311.

Dente, G. C., Durkin, P. S., Wilson K. A., and Moeller, C. E., 1988 "**Chaos in the coherence collapse of semiconductor lasers**" IEEE J. Quantum Electron. Vol.QE-24, pp.2441

Favre, F., Guen, D. L., and Simon, J. S., 1982 "**Optical feedback effects upon laser diode oscillation field spectrum**" IEEE J. Quantum Electron. **QE-18**, pp.1712-1717.

Figliola, Richard S., and Beasley, Donald E., 1991 "**Theory and Design for Machnical Measurements**" New York, NY: Wiley Publisher.

Fleming, M. W., and Mooradian, A., 1981a "**Fundamental line broadening of single-mode(GaAl)As diode lasers**" Appl. Phys. Lett., **38**, pp.511-513.

Fleming, M. W. and Mooradian, A., 1981b "**Spectral characteristics of External Cavity Semiconductor Lasers**" IEEE J. Quant. Electron. **QE-17**, pp.44-59.

Fowles, Grant Robert, 1968 "**Introduction to Modern Optics**" Holt, Rinehart & Winston Publishers.

Fujiwara, M., Kubota, K. and Lang, R., 1981 "**Low frequency intensity fluctuations in laser diodes with external optical feedback**" Appl. Phys. Lett. **38** pp.217-220.

Gerardo, J. B., and Verdeyen, J. T., 1963 "**Plasma refractive index by a laser phase measurement**" Appl. Phys. Lett., **3**, pp.121-123.

Gerges, A. S., Newson, T. P., and Jackson, D. A., 1990 "**Coherence tuned fiber optic sensing system, with self-initialization, based on a multimode laser diode**" Appl. Opt., **29**, pp.4473-4480.

Goldberg, L., Taylor, H. F., Dandrige, A., Weller, J. F., and Miles, R. O., 1982 **"Spectral characteristics of semiconductor lasers with optical feedback"** IEEE J. Quantum Electron. **QE- 18**, pp.555-564.

Grattan, K. T. V., 1987 **"Recent advances in fibre optic sensors"** Measurement, **5**, pp.122-134.

Hamel, W. A., van Exter, M. P., and Woerdman, J. P., 1992 **"Coherence properties of a semiconductor laser with feedback from a distant reflector: experiment and theory"** IEEE J. Quant. Electron., **QE-28**, pp.1459-1469.

Haus, Hermann A., 1984 **"Waves and Fields in Optoelectronics"** Englewood Cliffs, London: Prentice-Hall.

Hecht, Jeff, 1988 **"Understanding Lasers"** Sams Publisher.

Hecht, Jeff, 1989 **"Near-infrared semiconductor diode lasers"** in Chapter 18 of **The Laser Guidebook,** McGraw-Hill Book Company, pp.247-270.

Helms, J., and Petermann, K., 1990 **"A simple analytical expression for the stable operation range of laser diodes with optical feedback"** IEEE J. Quant. Electron., **QE-26**, pp.833-636.

Henry, C. H., 1983 **"Theory of the phase noise and power spectrum of a single-mode injection laser"** J. Quantum Electron. Vol.QE-19, pp.1391

Henry, C. H., 1982 **"Theory of the linewidth of semiconductor lasers"** IEEE J. Quantum Electron. **QE-18**, pp.259-264.

Henry, C. H., 1983 **"Theory of the phase noise and power spectrum of a single mode injection laser"** IEEE J. Quant. Electron. **QE-19**, pp.1391-1397.

Henry, C. H., and Kazarinov, R. F., 1986 **"Instability of semiconductor lasers due to optical feedback from distance reflectors"** IEEE J. Quantum Electron. **QE-22**, pp.294-301.

Henry, C. H., 1986 "**Phase noise in semiconductor lasers**" J. Lightwave Technol. **LT-4**, pp.298-311.

Hirota, O. and Suematsu, Y., 1979 "**Noise properties of injection lasers due to reflected waves**" IEEE J. Quantum Electron. **QE-15**, pp.142-149

Hooper, E. B., and Bekefi, G., 1966 "**Laser interferometer for repetitively pulsed plasma**" J. Appl. Phys., **37**, pp.4083-4094.

Hosokawa, H., Takagi, J., and Yamashita, T., 1988 "**Integrated optic microdisplacement sensor using a Y-junction and a polarization maitaining fiber**" Proc. in **Optical fiber sensor conference-88**, pp.137-140.

Hymans, A. J., and Lait, J., 1960 "**Analysis of a frequency-modulated continous-wave ranging system**" IEE paper No. **3264 E**, pp.365-372.

Imai, M., and Kawakita, K., 1990 "**Measurement of direct frequency modulation characteritics of laser diodes by Michelson interferometry**" Appl. Opt., **29**, pp.348-353.

Jackson, D. A., Kersey, A. D., Corke, M., and Jones, J. D. C., 1982 "**Pseudo Heterodyne Detection scheme for optical interferometers**" Electron. Lett. **18**, pp.1081-1083.

Jackson, D. A., 1987 "**Monomode fibre optic interferometers and their application in sensing systems**" in **Optical Fiber Sensors** edited by A. N. Chester, S. Martellucci and A. M. Verga Scheggi, Martinus Nijhoff Publishers, pp.1-33.

James, J. F. and Sternberg, R. S., 1969 "**The Design of Optical Spectrometers**" Chapman and Hall Publishers.

Jentink, H. W., de Mul, F. F. M., Suichies, H. E., Aarnoudse, J. G., and Greve, J., 1988 "**Small laser Doppler velocimeter based on the self-mixing effect in a diode laser**" Appl. Opt. **27**, pp.379-385.

Jones, R., 1992, "**White light interfeometry-a road to low cost, high performance optical fibre sensors?**" Colloquium on "<u>Fibre Optics Sensor Technology</u>" organised by IEE, UK.

Kersey, A. D., and Dandridge, A., 1987 "**Dual-wavelength approach to interferometric sensing**" SPIE, **798**, pp.176-181.

Kikuchi, K., and Lee, T. P., 1987 "**Spectral stability analysis of weakly coupled external-cavity semiconductor lasers**" J. Lightwave Technol., **LT-5**, pp.1269 -1272.

King, P. G. R., and Steward G. J., 1963 "**Metrology with an optical maser**" New Scientist, **17**, pp.180-181.

Koelink, M. K., Slot, M., de Mul, F. F. M., Greve, J., Graaff, R., Dassel, A. C. M., Aarnoudse, J. G., 1991 "<u>In vivo</u> **blood flow velocity measurement Using the Self-mixing Effect in a Fibre-coupled Semiconductor Laser**" <u>Proc.Fibre Optic Sensors: Engineering and Applications</u>, A. J. Bruinsma and B. Culshaw ed.(SPIE **V-EC04**, The Hague, Netherlands, March, 1991) SPIE, 151, pp120-128.

Koelink, M. K., Slot, M., de Mul, F. F. M., Greve, J., Graaff, R., Dassel, A. C. M., Aarnoudse, J. G., 1992a "**Glass-fibre self-mixing diode laser Doppler velocimeter**" Meas. Sci. Technol. **3**, pp.33-37.

Koelink, M. K., Slot, M., de Mul, F. F. M., Greve, J., Graaff, R., Dassel, A. C. M., Aarnoudse, J. G., 1992b "**Laser Doppler velocimeter based on the self-mixing effect in a fiber-coupled semiconductor laser: Theory**" Appl. Opt., 31, pp.3401-3408.

Lang, R., and Kobayashi, K., 1980 "**External optical feedback effects on semiconductor injection laser properties**" IEEE J. Quantum Electron. **QE-16**, pp.347-355.

Lawrence, T. R., Wilson, D. J., Craven, C. E., Jones, J., Huffaker, R. M., and Thomson, J. A. L., 1972 "**A laser velocimeter for remote wind sensing**" Rev. Sci. Instrum., **43**, pp.512.

Lax, M., 1967 "**Classic noise V: Noise in self-sustained oscillators**" Phys. Rev. **160**, pp.290-307.

Lenstra, D., Verbeek, B. H., and den Boef, A. J., 1985 "**Coherence collapse in single-mode semiconductor lasers due to optical feedback**" IEEE, J. Quantum Electron. **QE-21**, pp.674-679.

Lenstra, D., 1991 "**Statistical theory of the multistable external-feedback laser**" Opt. Comms., **81**, pp.209-214.

Lewin, A. C., Kersey, A. D., and Jackson, D. A., 1985 "**Non-contact surface vibration analysis using a monomode fiber optic interferometer incorporating an open air path**" J. Phys. E: Sci. Instrum., **18**, pp.604-608.

Loudon, Rodney, 1983 "**The Quantum Theory of Light**" 2nd ed, Oxford: Clarendon Press.

Marcuse, D., 1983, "**Classical derivation of the laser rate equation**" IEEE J. Quantum Electron., **QE-19**, pp.1228-1231.

Mark, J., Tromborg, B., and Christiansen, P. L., 1988 "**Bistability and low-frequency fluctuations in semiconductor lasers with optical feedback**" IEEE J. Quantum Electron., **QE-24**, pp.123.

Mark, J., Bodtker, E., and Tromborg, B., 1985 "**Measurement of Rayleigh backscatter-induced linewidth reduction**" Electron. Lett., **21**, pp.1008-1009.

Meggitt, B. T., and Cormier, A. J., 1988 "**Stability requirments for laser diode extended range interferometry**" Electron. Lett., **24**, pp.352-353.

Miles, R. O., Dandrige, A., Tveten, A. B., Taylor, H. F. and Giallorenzi, T. G., 1980 "**Feedback induced line broadening in cw channel substrate planar laser diodes**" Appl. Phys. Lett., **37** pp.990-992.

Mitchell, G. L., 1989 "**A review of Fabry-Perot interferometric sensors**" in <u>**Optical Fiber Sensors.**</u> Springer Proc. in Physics, **44**, Springer-Verlag Berlin, Heidelberg, pp.450-457.

Mitsuhashi, Y., Morikawa, T., Sakurai, K., Seko, A., and Shimada, J., 1976 "**Self-coupled optical pickup**" Opt. Comms., 17, pp.95-97.

Murata, S., Yamazaki, S., Mito, I. and Kobayashi, K., 1986 "**Spectral characteristics for 1.3 mm monolithic external cavity DFB lasers**" Electron. Lett. **22**, pp.1197-1198.

Nillsson, O., and Buus, J., 1990 "**Linewidth and feedback sensitivity of semiconductor diode lasers**" IEEE J. Quantum Electron. **QE-26**, pp.2039-2042.

Ning, Y., Grattan, K. T. V., Meggitt, B. T., and Palmer, A. W., 1989 "**Characteristics of laser diodes for interferometric applications**" Appl. Opt., **28**, pp.3657-3661.

Ning, Y., Grattan, K. T. V., Palmer, A. W., and Meggitt, B. T., 1990 "**Characteristics of a multi-mode laser diode in a dual-interferometer configuration**" J. Lightwave Techn., **8**, pp.1773-1778.

Nokes, M. A., Hill, B. C., and Barelli, A. E., 1978 "**Fiber optic heteodyne interferometer for vibration measurements in biological systems**" Rev. Sci. Instrum., **49**, pp.722-728.

Olsson, A. and Tang, C. L., 1981 "**Coherent optical interference effects in external cavity semiconductor lasers**" IEEE J. Quantum Electron. **QE-17**, pp.1320-1323.

Olessen, H., Osmundsen, J. H., and Tromborg, B., 1986 "**Nonlinear dynamics and spectral behavior for an external cavity laser**" IEEE J. Quantum Electron. **QE-22**, pp.762

Osinski, M., and Buus, J., 1987 "**Linewidth Broadening factor in semiconductor lasers—an overview**" IEEE J. Quant. Electron., **QE-23**, pp.9-29.

Osmundsen, J. H., and Grade, N., 1983 "**Influence of optical feedback on laser frequency spectrum and threshold conditions**" IEEE J. Quantum Electron. **QE-19**, pp.465-469.

Patzak, E., Olessen, H., Sugimura, A., Saito, S., and Muka, T., 1983 "**Spectral linewidth reduction in semiconductor lasers with weak optical feedback**" Electron. Lett. **19**, pp.938-940.

Perina, Jan, 1985 "**Coherence of Light**" 2nd ed, Dordrecht, Lancaster: Reidel.

Petermann, K., and Weidel, E., 1981 "**Semiconductor laser noise in an interferometer system**" IEEE J. Quant. Electron., **QE-17**, pp.1251-1256.

Petermann, K., 1991a "**Laser Diode Modulation and Noise**". Kluwer Academic Publisher.

Petermann, K., 1991b "**Semiconductor lasers with optical feedback**" in **Laser Diode Modulation and Noise**. Kluwer Academic Publisher, Chap. 9, pp.250-290.

Plotter, I. C., 1969 "**Frequency response of the 6328-A Helium-Neon laser interferometer**" J. Appl. Phys., **40**, pp.4770-4776.

Rieck, Heinrich, 1970 "**Semiconductor Lasers**" MacDonald and Co. London.

Rudd, M. J., 1968 "**A laser Doppler velocimeter employing the laser as a mixer-oscillator**" J. Phys. **E1**, pp.723-726.

Saito, S., and Yamamoto, Y., 1983 "**Direct observation of Lorentzian lineshape of semiconductor lasers and linewidth reduction with external grating feedback**" Electron. Lett., **17**, pp.325-327.

Sasaki, O., and Takahishi, T., 1988 "**Sinusoidal phase modulating interferometer using optical fibers dor displacement measurement**" Appl. Opt. **27**, pp.4139-4142.

Schunk, N., and Petermann, K., 1988 "**Numerical analysis of the feedback regimes for a single-mode semiconductor lasers with external feedback**" IEEE J.Quantum Electron. **QE-24**, pp.1242- 1247.

Seippel Robert G., 1981 "<u>**Optoelectronics**</u>" Reston Publisher.

Seo, D. S., Park, J. D., McLnearney, J. G., and Osink, M., 1989 "**Compound-cavity modes in semiconductor lasers with asymmetric optical feedback**" Appl. Phys. Lett. **54**, pp.990-992.

Sharma, B. L., 1974 "<u>**Semiconductor Heterojunctions**</u>" Pergamon, Oxford, England.

Sharp, 1992 "<u>**Technical mannual of Sharp's diode lasers**</u>".

Shimizu, E. T., 1987 "**Directional discrimination in the self-mixing type laser Doppler velocimeter**" Appl. Opt. **26**, pp.4541- 2544.

Shinohara, S., Mochizuki, A., Yoshida, H., and Sumi, M. 1986 "**Laser Doppler velocimeter using the self-mixing effect of a semiconductor laser diode**" Appl. Opt. **25**, pp.1417-1419.

Smith, F. G., 1971 "<u>**Optics**</u>" Wiley, Chichester, England.

Smith, L. M., and Dobson, C. C., 1989 "**Absolute displacement measurement using modulation of the spectrum of white light in a Michelson interferometer**" Appl. Opt. **28**, pp.3339-3342.

Spano, P., Piazolla, S., and Tamburrini, M., 1984 "**Theory of noise in semiconductor lasers in the presence of optical feedback**" IEEE J. Quant. Electron., QE-20, pp.350-357.

Streifer, W., Scifres, D.R., and Burnham, R.D., 1982, "**Analysis of diode laser properties**" IEEE J. Quantum Electron. **QE-19**, pp.1918-1929.

Svelto, Orazio, 1989 "**Principles of Lasers**" 3rd ed, Plenum Publisher(translated from the Italian and edited David C, Hanna).

Tanaka, T., and Bebedek, G. B., 1975 "**Measurement of the velocity of blood flow(in vivo) using a fiber optic catheter and optical mixing spectroscopy**" Appl. Opt. **14**, pp.189-196.

Tatsuno, K., and Tsunoda, Y., 1987 "**Diode laser direct modulation heterodyne interferometer**" Appl. Opt. **26**, pp.37-40.

Temkin, H., Olsson, N. A., Abeles, T. H., Logan, R. A., and Panish, M. B., 1986 "**Reflection noise in index guided InGaP lasers**" IEEE J. Quantum Electron. **QE-22**, pp.286-293 .

Thompson, G. H. B., 1980 "**Physics of Semiconductor Laser Devices**" Chichester: Wiley Publisher.

Tkach, R. W., and Chraplyvy, A. R., 1986 "**Regimes of feedback effects in 1.5 μm distributed feedback lasers**" J. Lightwave Technol., **LT-4**, pp.1655-61.

Tromborg, B., Osmundsen, J. H., and Olesen, O., 1984 "**Stability analysis for a semiconductor laser in an external cavity**" IEEE J. Quantum Electron. **QE-20**, pp.1023.

Tucker, M., and Christenson, E., 1990 "**Absolute interferometer for manufacturing applications**" SPIE, **1369**, pp.289-299.

Uchida, T., 1967 "**Dynamic behavior of gas lasers**" IEEE J. Quant, Electron. QE-3, pp.7-16

Ulrich, R. and Rashleigh, S. C., 1980 "**Beam-to-fiber coupling with low standing wave ratio**" Appl. Opt., **19**, pp.2453-2456.

Vahala, K., Harder, Ch., and Yarin, A., 1983 "**Observation of relaxation resonance effects in the field spectrum of semiconductor lasers**" Appl. Phys. Lett. **42**, pp.211-213.

Vahala, K., and Yariv, A., 1983 "Semiclassical theory of laser noise: part one & two" IEEE J. Quant. Electron., **QE-19**, pp.1096-1101 & pp.1102-1109.

Verdeyen, J. T., 1981 "<u>**Laser Electronics**</u>" Prentice-Hall, Inc. Englewood Cliffs. New Jersey

Wang, W. M., Boyle, W. J. O., Grattan, K. T. V., and Palmer, A. W., 1992a "**An interferometer incorporating active optical feedback from a diode laser with application to vibrational measurement**" Proc. in <u>8th Optical Fiber Sensors Conference,</u> Jan. 29-31, IEEE Catalog #92CH3107-0, pp.358-361.

Wang, W. M., Boyle, W. J. O., Grattan, K. T. V., and Palmer, A. W., 1992b "**Fiber-optic Doppler velocimeter that incorporates active optical feedback from a diode laser**" Opt. Lett. **17**, pp.819-821.

Wang, W. M., Boyle, W. J. O., Grattan, K. T. V., and Palmer, A. W., 1992c "**Characteristics of a dual diode laser-based feedback interferometer with applications for extended ranging and directional discrimination**" Techni. Digest of <u>XVIII International Quantum Electron. Conf.,</u> June 14-19, 1992, Vienna, Austria, pp.66-68.

Wang, W. M., Boyle, W. J. O., Grattan, K. T. V., and Palmer, A. W., 1992d "**Characteristics of a diode laser-based self-mixing interferometer**" Proc. of <u>Conf. on Appl. Opt. and Opto-electron.</u> 14-17 Sept. 1992, Leeds, pp.207-210.

Wang, W. M., Boyle, W. J. O., Grattan, K. T. V., and Palmer, A. W., 1993a "**Self-mixing interference in a diode laser: Experimental observations and theoretical analysis**" Appl. Opt. **32**, pp.1551-1558.

Wang, W. M., Grattan, K. T. V., Boyle, W. J. O., and Palmer, A. W., 1993b "**Active optical feedback in a dual diode laser configuration applied to displacement measurement with wide dynamic range**" Accepted by Appl. Opt.(In press).

Wang, W. M., Grattan, K. T. V., Boyle, W. J. O., and Palmer, A. W., 1993c "**Theory of self-mixing interference in a diode laser**" Submitted to J. Lightwave Technol.

Watrasiewcz, Bohdan Maciej, and Rudd, M. J., 1976 "**Laser Doppler measurements**" London: Butterworth Publisher.

Wheeler, C. B., and Fielding, S. J., 1972 "**Interferometry using a laser as radiation source, amplifier and detector**" J. Phys. E: Sci. Instru., **5**, pp.101-103.

Williams, C. C., and Wickramasinghe, H. K., 1986 "**Optical ranging by wavelength multiplexed interferometry**" J. Appl. Phys. **60**, pp.1900-1903.

Wilson, J. and Hawkes, J. F. B., 1987 "**Lasers**—Principles and Applications" Prentice Hall, London.

Woodward, S. L., and Thompson, E. J., 1992 "**The onset of coherence collapse in DFB lasers**" IEEE Photon. Technol. Lett. **4**, pp.221-223.

Wosinski, L., and Breidne, M., 1990 "**An in-situ fibre interfeometer for measuring quasi-conical diamond-turned surfaces**" SPIE, **1266**, pp.138-141.

Yasaka, H., Yoshikuni, Y., and Kawaguchi, H., 1991 "**FM noise and spectral linewidth reduction by incoherent optical negative feedback**" IEEE J. Quantum Electron. **QE-27**, pp.193-204.

Yoshino, T., Kurosawa, K, Itoh, K., and Ose, T., 1982 "**Fiber-optic Fabry-Perot interferometer and its sensor applications**" IEEE J. Quant. Electron. **QE-18**, pp.1642-1633.

Yoshino, T., Nara, M., Mnatzakanian, S., Lee, B. S., and Strand, T. C., 1987 "**Laser diode feedback interferometer for stabilization and displacement measurement**" Appl. Opt., **26**, pp.892-897.

A systematic classification and identification of optical fibre sensors

Y. N. Ning, K. T. V. Grattan, W. M. Wang and **A. W. Palmer**

Measurement and Instrumentation Centre, Department of Electrical, Electronic and Information Engineering, City University, Northampton Square, London, EC1V 0HB (U.K.)

Abstract

In this work, a new kind of classification for optical fibre sensors is introduced. Optical fibre sensors are classified according to the type of fibre, the light source and the modulation scheme on which they are based. Each of these categories is further subdivided and illustrations from systems developed and reported in the literature are given, with various sensor designs represented according to these criteria.

1. Introduction

Various optical fibre sensor techniques have been discussed and reviewed by a number of authors [1–5] over the last ten years, during which an explosive growth in the number of papers published in the field has been observed. A general framework for the classification and categorization of such sensor techniques can be seen from a number of different points of view. However, the classification rules used to frame the various optical fibre sensor techniques differ substantially from one author to another. This is largely due to their different fields of interest, the nature of the grouping of sensors that they use, and indeed the intended readership of the paper. For instance, Jackson *et al.* [1] and Jones [2] have classified sensors according to whether a coherent or incoherent optical measurement technique is used. Other reviews have been made on the basis of different measurands [3] or the use of modulation techniques, such as the use of the optical fibre sensor (OFS) for temperature measurement by Glenn [4], for chemical measurement by Harmer [5], for biomedical applications by Katzir [6] and on the basis of intensity modulation by Medlock [7]; in addition, for example, one of the authors has focused upon new developments and trends [8].

Although a basic classification of optical fibre sensors, as being merely 'intrinsic' or 'extrinsic', has been introduced in a number of publications [1–3], this is somewhat oversimplified for OFS techniques, because such a classification neither gives an overview of the sensor itself nor detailed information about the range of activity in the OFS techniques area.

In order to develop a fuller overview of the variety of OFS devices under study today, it is worthwhile to introduce a new classification of these techniques. By examining the structure of a typical OFS, it may be seen as logical to classify the techniques according to three basic and separate criteria:

(a) source of illumination used;

(b) type of fibre employed;

(c) optical modulation/sensor techniques.

Such a classification springs almost instinctively from the nature of the term optical fibre sensor: the *optical* source, coupled to a transmitting *fibre* to allow the light to undergo transduction or modulation in the *sensor* process.

2. Classification in Cartesian geometry representation

If a Cartesian coordinate representation is used to group these three 'variables', a spatial

framework for the classification process can be employed and different types of sensor can then be fitted into such a representation to illustrate their comparative features.

Such a classification for generalized sensors, whether electrical, mechanical or otherwise, has been discussed by Middelhoek [9] and Finkelstein [10], but here it is applied in a rather different way to one specific class of sensor rather than to the general family of all sensors.

2.1. Source of illumination used

The x-axis of the geometrical space is used to represent light sources which may then be characterized by their spectral distribution, as shown in Fig. 1. There are at least five common and convenient classifications of light sources that have been reported for use in various types of OFS:

(i) single-mode laser source (e.g., single-mode He–Ne laser, single-mode laser diode);

(ii) two-mode or 'few-mode' light sources (e.g., lasers with various cavity configurations);

(iii) N-mode light source ($N > 2$) (e.g., multimode laser, such as an Ar ion laser/laser diode);

(iv) narrow-band continuous spectrum light source (e.g., light-emitting diode (LED) or superluminescent LED);

(v) broad-band continuous spectrum light source (e.g., tungsten lamp, mercury lamp, continuous output xenon lamp).

2.2. Type of fibre employed

On the y-axis of the geometrical space, the various fibres that may be employed are classified by their mode-propagation characteristics. The number of modes transmitted and the polarization-related characteristics can be used on the basis of a division of fibre types into at least five groups, as shown in Fig. 1:

(i) mono-mode fibre;

(ii) polarization-maintaining fibre;

(iii) two-mode fibre;

(iv) multi-mode fibre;

(v) specialized fibres, e.g.. doped fibres, liquid-core fibres etc.

2.3. Optical modulation/sensor techniques

On the z-axis of the space, as shown in Fig. 1, is a characteristic of the OFS based on the parameters of the interaction electric field, E, given by $E = E_0 \exp(j(\omega t + 2\pi n L/\lambda))$, where E_0 is the amplitude, ω the optical frequency, n the refractive index of the medium, L is the optical path, λ the wavelength and σ the wave number $(1/\lambda)$. The modulation of the field can be categorized into at least seven groups:

(i) intensity modulation $(I–E.E)$;

(ii) polarization modulation $(I–E)$;

(iii) wavelength/frequency modulation $(I–\lambda/\omega)$;

(iv) path modulation $(I–L)$;

(v) refractive index modulation $(I–n)$;

(vi) time modulation $(I–t)$;

(vii) coherence length modulation $(I–k)$, where k is the fringe visibility.

The modulation types (iii) to (vi) are termed 'phase modulations' because their variation will cause a change of the phase of the light propagating in the optical fibre. It should be pointed out that the phase of an optical wave is defined with respect to a particular reference and thus a useful phase modulation for sensing can only be achieved, in practice, for a light source with fixed and known initial phase conditions. The random variation in the initial phase over a period of time (the detector response time) will result in a degradation of, for example, the fringe visibility, k (as discussed later) in an interferometer
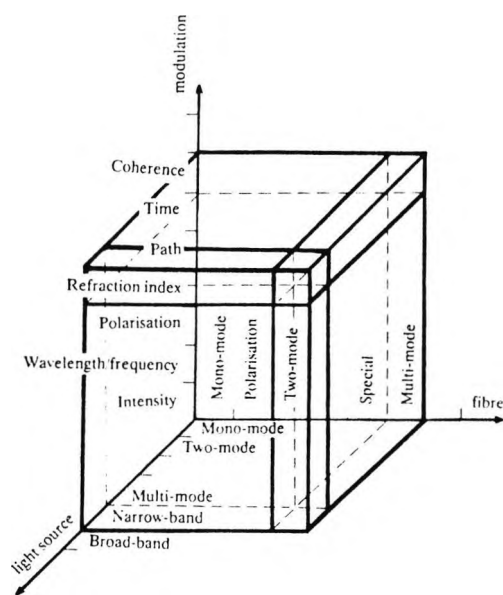
Fig. 1. The systematic classification in a 3-D Cartesian coordinate scheme.

used to detect the phase condition or its change, and will make the detection of the phase modulation particularly difficult. In other words, a phase-modulation sensor can only effectively be operated with the two optical path differences inside the coherence length of the optical source.

By using this classification system, as illustrated in Fig. 1, the many OFS techniques described can more readily be surveyed and examined, and their relationship to one another be seen. What is more, such a representation can more clearly indicate those areas where sensor schemes have already been proposed and/or exploited and its examination may show both areas of inactivity or those that are underdeveloped and point to new techniques which could be further exploited as the technology to achieve them matures.

It should be noticed that an OFS can employ more than one type of light source, modulation technique or fibre at any one time. Such types of OFS can then be represented by more than one 'cubic unit' in the geometrical space in Fig. 1. If an OFS 'family' is represented by a number of different 'cubic units', such a family may be of a multiplexed type [11], while if the same cubic unit represents a number of types of OFS, this may be a distributed type of OFS [12].

3. Light sources: optical characteristics of the OFS family

Light sources can be classified, for example, according to their spectral or coherence characteristics into at least five groups. Table 1 shows the spectral distribution, coherence length and intensity/wavelength relationship for a number of such sources. The coherence characteristic of a light source is a measure of the extent to which a phase relationship is maintained both across the beam (spatial coherence) and along the beam (temporal coherence). In an OFS, the spatial coherence of the light wave is often not particularly important because of the small cross-sectional area of the fibre core, but in contrast, the temporal coherence of the optical radiation is often extensively considered in selecting the appropriate light source for a particular sensor. In a multi-mode fibre, the spatial

coherence of the modes is lost, whilst in a single-mode fibre it is, by definition, preserved. A useful indicator of the temporal coherence is the coherence length of the source or the resulting fringe visibility of the interference fringe in a detection interferometer, the relationship between the coherence length and the spectral width of the light source being written as [13]

$$L_c = 1/\Delta\omega = \lambda^2/\Delta\lambda$$

where L_c is the coherence length, λ is the wavelength of light and $\Delta\lambda$ (or $\Delta\omega$) is the spectral width of the light source.

3.1. Mono-mode light sources

Many types of single-mode laser or laser diode belong to this group of sources. Because their bandwidth is very narrow, their coherence lengths are usually very long compared to the optical path inside the OFS itself. For a suitably chosen He–Ne gas laser, the coherence length is of the order of a few hundred meters, for example, and a typical spectral width for a single longitudinal mode in such a laser is about 1 MHz, which corresponds to a coherence length of the order of 300 m [13]. For a typical laser diode such as that used in a compact disc player, a very short coherence length is desired and used, to avoid phase-sensitive effects in the reading of data from the optical disc. The spectral width can be adjusted to ≈ 100 MHz, resulting in L_c having a value up to a few metres [14].

3.2. Two-mode light sources

Such light sources can be produced relatively easily for use in an OFS by, for example, 'ramping' a single-mode laser diode at two different values of drive current [15], by combining two or more single-mode lasers which have different wavelengths [16] or by the use of band-pass filters to obtain several wavelengths from an LED [17]. The coherence length obtained in each of these cases is, in general, much less than that of a single-mode laser. Obviously, in the latter two cases, the coherence lengths of the wavelengths generated will be independent of each other, and may be equivalent to those obtained from separate sources. However, when observing fringes in a detection interferometer, the fringe visibility changes periodically with the

TABLE 1. The spectral distribution $(I(\lambda))$, coherence length representation $(K \sim L_c)$ and intensity expression for five groups of light sources (I: intensity, λ: wavelength, k: fringe visibility, ΔL: optical path difference)

Mono-mode light source	$I = I[\delta(\lambda)]$	
Two-mode light source	$I = I[\delta(\lambda_1) + \delta(\lambda_2)]$	
Multi-mode light source	$I = \sum_{j=-\frac{M}{2}}^{j=\frac{M}{2}} I[\delta(\lambda_j)]$	
Narrow-band light source	$I = \int_{\lambda_o - \Delta\lambda/2}^{\lambda_o + \Delta\lambda/2} I[\lambda]\,d\lambda$	
Broad-band light source	$I = \int_{\lambda_1}^{\lambda_2} I[\lambda]\,d\lambda$	
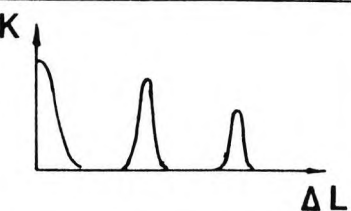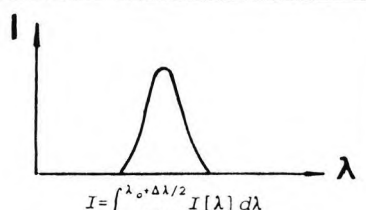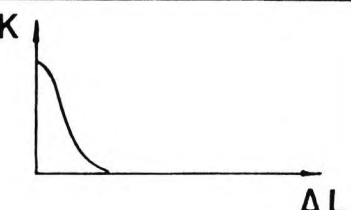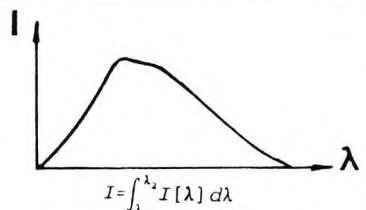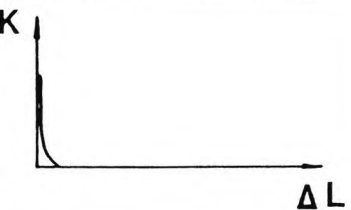
change of the optical path difference, as shown in Table 1.

3.3. N-mode (multi-mode) light sources

This group of light sources covers a wide range of multi-mode solid-state (doped insulator), liquid or gas lasers or the semiconductor laser diode. For instance, the He–Ne gas laser with a cavity length of 0.5 m has a mode separation of 300 MHz and the width of the lasing mode at 633 nm is typically about 1.5 GHz, with the number of longitudinal modes in the laser output being of the order of four or five [13].

By operating a single-mode laser diode with a drive current under the threshold for laser action, it may conveniently be used as an N-mode light source as well [18], as the coherence characteristics deteriorate severely under these circumstances. The coherence characteristics of this type of light source are not easily described because the interference

effects of multi-mode light are much more complex than those of light from a mono-mode laser. Thus interference fringes will appear in some spatial regions but not in others. This is due to the superposition of the fringes which are generated by each longitudinal mode of the device [19]. As a result of this superposition, those interference regions will occur periodically along the optical path difference. The concept of a 'coherence region' has been introduced in some papers to explain this and the coherence characteristics of these sources have been discussed in greater detail [19, 20].

The laser diode is revolutionizing the potential for OFS devices and in summary the devices range from low coherence length, simple structures with a wavelength FWHM of 2-5 nm, available at prices from a few tens of dollars (depending upon the power delivered), through distributed feedback lasers with sub-nanometer linewidths and at a price that rules them out for most OFS applications, to quantum-well devices with the linewidth performance of a He–Ne laser. The convenience of this semiconductor laser package is mitigated by the high cost (in the region of thousands of dollars per item).

Other laser devices may be employed for OFS use, e.g., the Ar ion laser or the He–Cd laser. Both these devices are expensive, physically quite large and require power supplies that use a considerable level of electrical input, but they do provide a continuous (and thus capable of modulation) output in the blue or ultraviolet part of the spectrum. This is a region where LEDs or laser diodes are very weak and for sensors such as those employing luminescence, where excitation at short wavelengths is preferable, they are a useful source. In addition, early work on distributed sensors employed these sources, due to their high power (several watts being routinely available) and favourable non-linear scattering characteristics. The coherence length of a typical Ar ion laser may be quite long, comparable to that of the He–Ne laser.

3.4. Narrow-band continuous spectrum light source

This is another type of light source widely used for many different kinds of OFS. The ordinary LED or SRD (super-radiant diode) are examples of this group with importance for OFS use. Illustrated schematically in Table 1, the width of their output spectrum is about 20-80 nm [21]. and as a consequence their coherence length is of the order of 50 μm or less [22]. In addition, discharge lamps can produce a series of spectral lines of varying widths, distributed across the spectrum according to the energy levels present within the gas itself. The low-pressure mercury lamp, for example, gives a series of lines from UV into the visible spectrum, but there is some difficulty in coupling the divergent output from such a device into an optical fibre. This is a significant problem for all lamp sources, although output optical powers may be such that efficient coupling, whilst preferable, is not essential. A range of low-pressure gas discharge lamps yields specific lines over a wide range of the spectrum. However, there are often problems with the bulk of the lamp and power supply in OFS applications, and the need for lamp cooling. Invariably, in cases where the lamp is inefficient or delivering low optical power at the wavelength of interest, good optical coupling via a carefully chosen lens combination is required. This will usually increase the physical bulk of the source and may limit the application to OFS devices.

3.5. Broad-band continuous spectrum light sources

This group of light sources is well suited to a number of OFS applications, particularly those requiring excitation at wavelengths of less than ≈ 550 nm, and especially in the ultraviolet part of the spectrum ($\lambda < 350$ nm) where solid-state sources are largely unavailable and the use of lasers is uneconomic. Additionally, these sources can offer a wide wavelength spread which is useful for sensors using wavelength-encoding techniques. Modulation of the light can be achieved using simple 'chopper' techniques (limited to about a few kHz) or using an electro-optic approach, but these are usually very inefficient with such sources. As an example, a millimetre-sized tungsten–halogen incandescent lamp is available [23], the optical output being in the spectral range from wavelengths in the near UV and in the visible from about 400 nm upwards, into the IR part of the spectrum, where substantial power can be obtained.

Discharge lamps such as the xenon lamp or mercury lamp (at low or high pressure) are widely employed for emission on either discrete spectral lines or as a broad band over the region from the vacuum UV to longer wavelengths.

The coherence characteristics of this group of light sources are usually very poor, e.g., the coherence length of a typical white light source is only three of four wavelengths. Details of such sources are discussed in a number of familiar reference texts [14], as their use in conventional analytical instrumentation has been familiar for many years. However, their mechanical instability and physical bulk makes them unsuitable for many OFS applications, in addition to which such lamps are often inexpensive but yield a substantial percentage of their power output as heat.

4. Fibre-structure characteristics of the OFS

Current OFS technology has arisen largely on the basis of optical components and especially optical fibres made available as a result of the explosive growth in their use for communications purposes. Whilst the technology for producing ultra-low-loss mono-mode fibres has been developed in recent years to a highly sophisticated level, this same technology is also applicable to the production of fibres for sensor purposes, where, however, other fibre characteristics are needed. Thus the OFS development market is fortunate in being able to call upon relatively cheap and readily available technology to produce fibres with specific characteristics to suit sensing purposes. Whilst fibres produced for communications purposes are preferred to have as low a sensitivity as possible to external effects, even ordinary silica fibres are used in many distributed sensor applications, due to their sensitivity to temperature, for example, through changes in non-linear scattering processes. As these OFS techniques have developed rapidly, different types of fibre have been manufactured and the number of these types will continue to increase to meet new and special applications. The fibres considered here are characterized by the nature
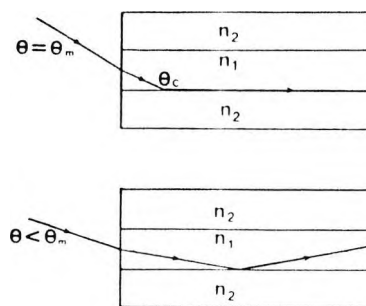
Fig. 2. Propagation of light beams in fibre.

of their structure (such as the core radius, numerical aperture (NA), polarization performance), and other considerations.

The NA is given by

$$NA = \sin \theta_m = (n_1^2 - n_2^2)^{1/2}$$

where n_1, n_2 are the refractive indices of the core and cladding respectively, and θ_m is the maximum angle of incidence to retain guiding of light, as shown in Fig. 2.

4.1. Mono-mode fibre

Mono-mode optical fibre with a Vebert (V) number <2.405 (defined as $V = (2\pi a/\lambda)\cdot(n_1^2 - n_2^2)^{1/2}$ where a is the fibre core diameter, λ is the wavelength of light guided in the fibre and n_1 and n_2 are the refractive indices of fibre core and the outer cladding respectively) is widely used in optical fibre sensors based on phase modulation, to encode the measurand. The main characteristic of this is the maintenance of the optical phase relationship along the guided beam in the fibre. A typical mono-mode fibre designed to operate at a wavelength of 633 nm has an NA value of about 0.25 [24], a core radius of a few micrometers, with a cladding radius of between 40 and 50 μm [21]. In an ideal fibre which is perfectly circular, two orthogonal polarization states are generated and the state of polarization of the guided wave (the HE_{11} mode) propagates along the fibre unchanged. Unfortunately, in the practical fibre, such ideal conditions do not exist. As a result of its dominant intrinsic and any additional extrinsic birefringence, the two guided waves at two orthogonal polarization states will develop a phase difference between them after propagating a certain distance along the fibre. The distance over which a phase difference of 2π occurs is called the beat length (L_b), which can be written as

$$L_b = \frac{\lambda}{n_x - n_y}$$

where n_x, n_y are the effective refractive indices with x and y being the axes of a non-circularly symmetric fibre core, and λ is the free-space wavelength. Typical single-mode fibres have L_b in the centimetre region, dependent upon their physical characteristics [13]. Thus this kind of fibre can only be used where the polarization state can be neglected in the sensing operation.

4.2. Polarization-maintaining fibre

Many optical fibre sensors rely upon the use of polarization effects, and the maintenance of the state of polarization of light propagating in fibre is important. In order to overcome the problem of a variable state of polarization in a mono-mode fibre, considerable effort has been expended to develop polarization-maintaining fibre. This characteristic is achieved during the manufacturing process by inducing stresses in the material itself.

There are two categories of polarization-maintaining fibre (PMF) available, linear polarization-maintaining fibre (LPMF) and circular polarization-maintaining fibre (CPMF). In the former category, only one of two orthogonal polarizations states (HE_x or HE_y) can be maintained at the output of the fibre, whilst in the CPMF a round fibre is twisted to produce a difference between the propagation constants of the clockwise and counter-clockwise circularly polarized HE_{11} modes. Table 2 shows in more detail the classification of PMF and the subject is discussed in greater detail by, for example, Okoshi [25].

4.3. Two-mode fibre

Fibre allowing the propagation of only a few modes represents a new type, recently developed, which can provide a number of independent transmission channels in a single-strand fibre. A number of investigations have been carried out to understand better the modal and polarization characteristics of these fibres [26, 27]. Although the multichannel capacity of few-mode fibre has not yet been fully exploited due to mode-control problems, two-mode fibre has been used in several types of OFS [28, 29]. It is usual to derive the two excited modes from a single source to ensure a known coherence relationship between

them. It is very difficult to excite and maintain two modes independently. A two-mode fibre with a V number between 2.4 and 3.8 can guide two spatial modes, the LP_{10} and LP_{11} modes [30]. The polarization and intensity distribution for a highly elliptical core, two-mode fibre (operated with LP_{10} and LP_{11}) can be kept unchanged for wavelengths between 488 and 633 nm [31].

4.4. Multi-mode fibre

Multi-mode optical fibre, with a V number significantly greater than 2.4, has a much larger core size and sometimes also much larger refractive index differences between core and cladding. The number of modes (M) guided by the fibre is determined from the V number and is given by $4V^2/\pi$. The core diameter of a multi-mode fibre is usually larger than 50 μm, which means it has more than 100 times the core cross-sectional area of a mono-mode fibre. This factor is also reflected in the material costs and thus in the price of the fibre itself. This is essentially significant for long lengths or specialized fibres. A large index difference between core and cladding yields a large numerical aperture, but may be difficult to fabricate. As a result of the larger core area and a large value of NA, multi-mode fibre presents a greater launching efficiency from an optical source.

Multi-mode fibres are often used in an OFS in applications where high light intensities are required, particularly in those that employ intensity-modulation techniques. There is flexibility to use a wide variety of optical sources, with suitable coupling optics. In many cases, light signals can be launched into fibres with reasonable efficiency and often incoherent sources show a high degree of optical power over a usable spectral band, so inefficient coupling still results in adequate light levels in the optical fibre for many sensor purposes. Multi-mode optical fibre sensors based on coherence modulation have been produced [22, 32].

4.5. Specialized fibres

A number of types of special fibres have been made for particular use in the field of optical fibre sensors, and are designed with only limited applicability in optical fibre communications systems. However, the use of fibre lasers as optical sources and subsequent

TABLE 2. Classification of various polarization-maintaining optical fibres [25]

	(Truly) single polarization fibres (differential attenuation fibres)	Geometry type	(1) Side-pit (2) Side-tunnel
		Stress type	(1) Bow-tie (2) Flattened depressed cladding (3) Stress-guiding
Linear polarization maintaining (LPM) fibres	Linearly birefringent fibres	Geometry	(1) Elliptical core (2) Dumb-bell (3) Side-pit (4) Side-tunnel
		Stress type	(1) Elliptical cladding (2) Elliptical jacket (3) PANDA (4) Four-section (5) Bow-tie
Circular polarization-maintaining (CPM) fibres	Circularly birefringent fibres	Stress type	Twisted round fibre fibre

laser amplifiers as part of an optical communications system may bring some specialist fibres into the communications field. The difference between these and other kinds of fibre lies mainly in the modified shape of the fibre core or the material from which it is made. As the varied techniques used in OFS are developing steadily, the number of special fibres in use continues to increase. However, only a few of the wide variety of specialist fibres are considered below to illustrate the broad nature of the field.

4.5.1. D-shaped fibre

When light is guided along a fibre with D-shaped core, the result is the exposure of the evanescent field near the core of fibre. As most of the cladding on one side of the fibre is removed, the thickness of the material that is left is very small (as shown in Fig. 3), and light modulation can be achieved in the evanescent field near the core. The techniques for manufacturing D-shaped fibre are described by Millar *et al.* [33] and Dyott *et al.* [34]. One of the main potential uses of single-mode D-shaped fibre is for polarization-holding directional couplers, where the process of coupling the guiding region, either through etching or by fusion, should be greatly simplified [35].
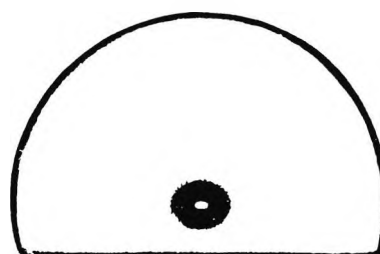
Fig. 3. The cross section of a D-shaped fibre.
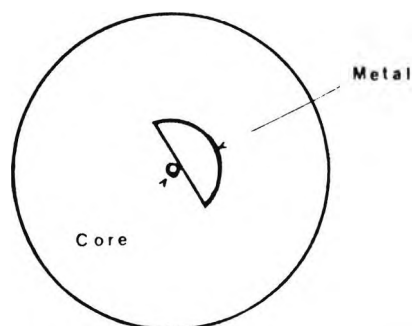
Fig. 4. Schematic diagram of a composite metal–glass polarizer.

4.5.2. Hollow-section fibre

Hollow-section fibres are a further development of the D-shaped fibre. They may be produced by having a single longitudinal aperture at a fixed distance from the fibre core. Figure 4 shows such an acrylate-coated metal–glass fibre, with a numerical aperture

of about 0.16, a cut-off wavelength for transmission of about 1.25 μm and a distance between the core and hollow section of about 3 μm. It can give a high performance in optical polarization, e.g., for a 5 cm length of such polarizing fibre, the extinction ratio is about 40 dB over the spectral region 1300 to 1600 nm [36], which is useful in sensor applications.

4.5.3. Fibre doped with rare earths

As an alternative to modifying the shape of the optical fibre, new kinds of specialized fibre have been developed by modifying the materials from which the fibre is normally fabricated (pure silica) or by adding additional materials. Fibres doped with rare earths have a number of special properties, due to the introduction of ions such as Nd, Eu or Dy into the light-guiding regions of the fibre. Those properties are exploited to construct different 'in-fibre' sensor devices, to improve the measurement region of the OFS, or even to form new kinds of devices such as fibre lasers, fibre amplifiers, a fibre with an increased Verdet number or a fibre showing an increased Kerr effect and non-linear optical coefficients [37]. An important application has been the distributed temperature sensor with a rare-earth-doped fibre which has been developed recently. The sensitivity reported for it is better than 1 °C over the temperature region −200 to +100 °C and higher, with a spatial resolution of 3.5 m [38].

4.5.4. Liquid-core fibre

Liquids have been used as core materials for fibres where the special characteristics of the liquid have been required for a specific sensor purpose. Thus the refractive index or scattering properties of the core material may be tailored to a particular application through the use of a specially chosen liquid. An important early example is in the work of Hartog [39], where a fibre filled with an organic liquid with significant scattering properties was used as the basis of an early distributed temperature sensor. However, problems exist in the fabrication of long lengths of such fibre and the possible hazards from spillage of the core material. Additionally, such fibres are expensive to fabricate, and are not widely acceptable in industrial installations.

5. Sensor modulation techniques

The modulation techniques employed in optical fibre sensors vary widely in their measurand function, performance and position in the sensor system itself. The basic techniques considered here, however, are those in which the light itself is modulated. This process may be categorized into several groups, according to the parameters of the electric field or the optical radiation varied. More than one type of modulation technique may be employed in one sensor; for example, path-length modulation is often associated with refractive-index modulation, and this is still a dominant mechanism in many optical fibre sensors.

5.1. Intensity modulation

Intensity-modulation techniques, employed widely in the earliest types of OFS, show the virtues of simplicity, reliability and achievability at low cost. The variation of the light intensity at the probe itself indicates the encoded change of an applied measurand, such as temperature, pressure [40], acceleration [41], or 'on/off' state in a simple switch [42]. Various schemes to produce this type of intensity modulation have been produced, for example [7] fibre displacement, shutter modulation, reflective schemes, fibre loss, intensity of coupling via the evanescent field, absorption, light scattering, digital encoding and electro-optic modulation, amongst others. However, a basic drawback is the lack of an accurate reference signal in many cases, although several internal referencing schemes [43, 44] have been proposed. This intensity-based approach is not widely used in modern types of OFS, except for simple switches, although such devices tend to be comparatively inexpensive.

5.2. Polarization modulation

Polarization modulation is another interesting and very valuable technique for measurand encoding and signal recovery in many types of OFS. The basic principle of operation is that the relevant physical quantity to be measured is transduced into a polarization change through an appropriate interactive effect, e.g., the electro- or elasto-optic effect. The measured field can be *inside* the fibre

(intrinsic sensor) or *outside* the fibre (extrinsic sensor), or even both situations may apply in one system. Historically, these were some of the first modulation schemes to be developed and many new sensors based on polarization modulation have been developed in the last few years. These are, in particular, sensors for measuring temperature, stress, current and magnetic field, amongst others, which have been reported in detail in the literature [45].

5.3. Wavelength modulation/encoding

Wavelength modulation/encoding techniques are very valuable as a means by which a non-intensity-dependent measurement may be made using optical fibres. Wavelength division multiplexing (WDM) has been discussed by a number of authors [46, 47] and relies on the encoding of the measured information in terms of a specific wavelength of light received from the transducer. This frequently means, in a real sensor, the use of a wide-band optical source with the transducer acting as a wavelength-encoder, depending on its perturbation by an external parameter. Several displacement/rotation transducers have recently been developed [48, 49], primarily for testing in the aerospace environment, using gratings or filters which are mechanically rotated or moved in a linear fashion to yield the appropriate output.

There are two further kinds of wavelength modulation in common use in interferometric sensors. The first is the so-called 'frequency modulated continuous wave' (FMCW) technique [50–52]. In this case a mono-mode laser diode is driven by a linear current ramp, and the wavelength (frequency) of the output is varied as the change of the drive current in an unbalanced interferometer. The variation of wavelength of the diode output causes a phase change, and therefore the intensity received from the interferometer will change and yield information on the optical path difference in the interferometer and thus information on the measurand. A second example is modulation either by the Doppler shift from a moving body or a frequency modulator such as a Bragg cell in the experimental optical arrangement [53]. A considerable amount of effort has been expended in recent years in the development of such

systems, using fibres where appropriate [54–56], and it has become established as an important technique for the measurement of fluid flow and surface velocity [57, 58], often with medical measurement applications, e.g., blood flow [59].

5.4. Optical-path-difference modulation

This modulation is one of the most commonly used modulation schemes in optical fibre sensors, usually of the interferometric type. The change of optical path difference is caused by a physical displacement in an interferometer, operated in a 'zero path length difference' mode, and the linear displacement range is less than $\lambda/4$, corresponding to a value of < 200 nm for a typical laser light source. However, when the displacement is greater than $\lambda/2$, the fringes will appear periodically, each fringe representing a $\lambda/2$ change in optical path difference, corresponding to a change of $2N$ rad. By counting the number of the fringes, the displacement change can be calculated from the simple equation

$$\Delta L = N\lambda/2$$

where ΔL is the change of optical path difference, N is the number of fringes counted and λ is the wavelength of the light source. A very wide range of sensors based on optical path modulation has been developed. The measurands vary from distance [60], to vibration [61], to those associated with a change of displacement, such as pressure [62]. A number of parameters can be configured so as to produce a displacement and thus be amenable to measurement by this sensitive technique.

5.5. Index modulation

Modulation of the material refractive index and its use for measurement purposes can be achieved both inside and outside the optical fibre in sensor use. In the first case, measurands such as temperature or pressure may be used to vary the index difference between the core and the cladding of a fibre, and thus the amount of light 'leaking' from core to cladding causes a change in the output light intensity observed. In the second case, an external sensor element may be employed, for instance, by using a lithium niobate

(LiNbO$_3$) crystal as a temperature sensor. The refractive index of such a sensor element is modulated by the measurand, and therefore the optical path within the material is changed. When an interferometer with a mono-mode light source is employed to determine this in an optical fibre sensor, the change of optical path difference can be used to vary the phase difference of the radiation in the interferometer and thus the output intensity observed. The fractional change in optical length in a silica fibre is given by $dn/dT = 10^{-5}$ K^{-1} [4] and the phase shift by $2\pi nl/\lambda$, which is approximately 1 rad K^{-2} cm^{-1} for a wavelength of 633 nm, the wavelength of the He–Ne laser. Other glasses less commonly used for optical fibres will show different characteristics. An approach using index modulation outside an optical fibre has been reported by Scheggi et al. [63] in a sensor application.

5.6. Time modulation

With the use of coherent light sources, a temporal modulation can be transduced into a path-length modulation through the use of the relationship

$$\Delta L = c\, \Delta t$$

where ΔL is the optical path length traversed by light during a period of time Δt and c is the speed of light. Therefore time modulation can be considered to be equivalent to path-length modulation under these circumstances. With the use of an incoherent light source, time modulation, also known as rate modulation, is the form of modulation achieved using a low frequency applied to the light intensity or to produce pulses of known temporal duration. Information conveyed in the time domain can be highly dependent on the measurand using the correct sensor encoding. For example, the rate information from a rotating object such as a turbine, in a vortex-shedding flow meter or from a rotating shaft, can be delivered to an optical detector by optical fibre links to detect the optical radiation containing the information signal. The detected signal can then be converted into a digital signal.

A number of OFS techniques based on time modulation have been developed, such as a quartz resonator hybrid OFS for displacement measurement [64] and pressure

[65] and temperature sensors [66] based on fluorescent time decay. By the use of correlation techniques, the rotation of a shaft can be monitored directly from the light scattered by the shaft [61]. In such an application the signal received due to the reflection from the shaft is subjected to auto-correlation, and the rotation rate can be then calculated. Agreement to within the few percent accuracy of a mechanical device was observed in recent work [61].

5.7. Coherence-length modulation

'Coherence length' is a term used as a measure of the temporal coherence of a light source. The 'coherence region' of an interferometer output is the region where phase modulation can be achieved, e.g., in a Michelson interferometer, this being less than twice the 'coherence length'. When the optical path difference (OPD) in an interferometer is less than the coherence length of the light source employed, the fringe visibility [1] of the output obtained is in the region between 1 and 0, and phase modulation can be achieved. However, when the OPD is greater than the coherence length, the fringe visibility is zero and the phase modulation becomes undetectable. In this latter case, a coherence-length-modulation technique can be used to 'shift' an unbalanced interferometer into a 'balanced' or a 'near balanced' region. The basic function of this modulation is to compensate the large OPD which is observed in order to shift the coherence region from its original position to where phase modulation can be achieved.

When coherence-length modulation is introduced, it is necessary that a second detector interferometer is employed. The OPDs of the two interferometers are set to be larger than the coherence length of the light source, with the difference between them being less than the coherence length. Under this condition, two interferometers give out an interference intensity distribution which shows the so-called 'fringes of superposition' [67]. The scheme used in this modulation is sometimes called 'path-matched differential-interferometry' or 'white-light interferometry' and has recently been exploited in interferometric fibre optic sensors.

32

TABLE 3

Examples of different 'cubic units' of the OFS space

Light source	Intensity modulation	Length modulation	Wavelength/frequency modulation	Polarization modulation	Refraction index modulation	Time modulation	Coherence modulation
Mono-mode fibre							
Mono-mode	86	71	92	79	96	103	88
Two-mode			105	81			
Multi-mode		89	102				58
Narrow band		85			95		
Broad band				82			
Polarization maintaining fibre							
Mono-mode	87	101	84		83		
Two-mode							
Multi-mode		90					
Narrow band							
Broad band							
Two-mode fibre							
Mono-mode		78		100			106
Two-mode							
Multi-mode							
Narrow band							
Broad band							107
Multi-mode fibre							
Mono-mode	91	97					
Two-mode	40						
Multi-mode	76						
Narrow band	72	99				77	
Broad band	98		94		93		
Special fibre							
Mono-mode	104						
Two-mode							74
Multi-mode	75						
Narrow band	73						
Broad band							

The most commonly used low-coherence light sources for such arrangements are the LED, superluminescent diode or multimode laser diode, in addition to broad-band sources, and significant work has been done recently to develop optical fibre sensors operating by means of coherence-length modulation. As an example, sensors for pressure measurement [22], remote displacement [60, 68], acceleration [69] and flow speed [70] have been reported recently.

6. Conclusions

In this paper a new kind of classification for optical fibre sensors has been introduced and discussed. The details of each 'division' of the classification have been reviewed and corresponding examples given. Several points worthy of note emerge, and examples of the different schemes which have been discussed in the literature are seen in the reference matrix, Table 3.

Most work done in past years, in interferometric-based sensors, for example, has concentrated on two major areas. The first is the 'mono-mode light source, mono-mode fibre and phase modulation' category, which is represented using all types of interferometers. The second is the 'broad-band, continuous spectrum light source, multi-mode fibre, with intensity modulation' type, which covers many of the incoherent types of OFS employed.

A number of examples have been shown to reveal other applications, including the use of low-coherence light sources such as the

LED or the multimode laser diode. Such work emphasizes the recent tendency towards the exploitation of these new light sources, which are both convenient and inexpensive, and operate at low voltages.

Few-mode optical fibres and specialized fibres show significant possibilities for the development of novel types of OFS. However, their full applications have not yet been seen due to their lack of availability at low cost; this is likely to remain a problem.

Light-modulation techniques have been investigated in different fields. The tendency for the development of sensing techniques is towards a combination of different modulation schemes together with the mixing of, for example, optical modulation with electronic modulation, where appropriate.

It is clear that a considerable body of work has been undertaken to develop OFS techniques; however, there are still many 'blank cubes' which may be filled inside the OFS 'techniques space', in other words, this OFS techniques space has not yet been fully exploited. It is not expected that this space will be filled immediately, if ever, but this may gradually change as new kinds of light source, optical fibre or sensor approach emerge. However, it is likely that due to the basic physical mechanism and for sound commercial reasons, many cubes will remain 'blank' and perhaps in only a few areas will there be real commercial success with OFS techniques, where their unique advantages are seen. However, the field is very much alive and an increasing number of commercial products are appearing. This categorization draws attention to those areas where devices do not exist and may be a stimulus to new developments with the emergence of new technology.

References

1 D. A. Jackson and J. D. C. Jones, Extrinsic fibre optic sensors for remote measurement: part one, *Optics Laser Technol., 18* (1986) 243.
2 B. E. Jones, Optical fibre sensors and systems for industry, *J. Phys. E: Sci. Instrum., 18* (1985) 770.
3 K. T. V. Grattan, Fibre optic sensors — the way forward, measurement, *J. Int. Meas. Confed., 5* (1987) 122.
4 W. H. Glenn, Fibre optic temperature sensors, *OFS NATO ASI Series, Series E: Applied Sciences,* No. 132, 1987, pp. 185-200.
5 A. L. Harmer, Guided wave chemical sensors, *OFS NATO ASI Series, Series E: Applied Sciences,* No. 132, 1987, pp. 210-216.
6 A. Katzir, Biomedical fiberoptic sensors, *Proc. Int. Conf. Optical Fibre Sensors, New Orleans, LA, U.S.A., 1988,* pp. 4-5.
7 R. S. Medlock, Fibre optic intensity modulation sensors, *OFS NATO ASI Series, Series E: Applied Sciences,* No. 132, 1987, pp. 123-124.
8 K. T. V. Grattan, New developments in sensor technology — fibre and electro-optics, *Meas. Control, 22* (1989) 165-175.
9 S. Middelhoek and D. C. Van Duyn, Classification of solid-state transducers, *Australasian Instrumentation and Measurement Conf., Adelaide, Australia, Nov. 14-17, 1989,* pp. 1-4.
10 L. Finkelstein, The formation of engineers and scientists in measurement and instrumentation, *Australasian Instrumentation Measurement Conf., Adelaide, Australia, Nov. 14-17, 1989,* pp. 56-58.
11 H. Ishio, J. Minowa and J. Nosu, Review and status of wavelength-division multiplexing technology, *IEEE J. Lightwave Technol., LT-2* (1984) 448-463.
12 A. R. Mickelson, O. Klevhus and M. Eriksrud, Backscatter readout from serial microbending sensors, *IEEE J. Lightwave Technol., LT-2* (1984) 700-709.
13 *Proc. Workshop on Single Fibre Sensor Technology, University of Kent, Canterbury,* p. 42 (unpublished).
14 J. Dakin and B. Culshaw, *Optical Fiber Sensors: Principles and Components,* Artec House, 1989, pp. 151, 198.
15 K. Ho Tate and D. Kamatani, Reflectometry with high spatial resolution and no moving parts by means of source-coherence modulation, *Proc. OFS '89 Paris, 1989,* p. 64.
16 B. T. Meggitt, A. W. Palmer and K. T. V. Grattan, Fibre optic sensor using coherence properties — signal processing aspects, *Int. J. Optoelectron., 3* (1988) 451.
17 D. J. Webb, J. D. C. Jones and D. A. Jackson, Extended-range interferometry using a coherence-tuned synthesized dual-wavelength technique with multimode fibre link, *Electron. Lett., 24* (1988) 1173-1174.
18 C. H. F. Velzfl and R. P. Brouwer, Output power and coherence length of stripe geometry double-heterostructure semiconductor laser in incoherent feedback, *IEEE J. Quantum Electron., QE-15* (1979) 782-786.
19 Y. N. Ning, K. T. V. Grattan, B. T. Meggitt and A. W. Palmer, Characteristics of laser diodes for interferometric use, *Appl. Opt., 28* (1989) 3657-3661.
20 K. T. V. Grattan, A. W. Palmer, Y. N. Ning and B. T. Meggitt, Interferometric sensors — extension of range using low coherence light from laser diode, *Proc. EFOC/LAN, Amsterdam, The Netherlands, June 1989,* p. 375.
21 R. Kist, Source and detectors for fibre optic sensors, *OFS NATO ASI Series, Series E: Applied Sciences,* No. 132, 1987, p. 267.
22 G. Beheim, K. Fritsch and R. N. Poorman, Fibre-linked interferometric pressure sensor, *Rev. Sci. Instrum., 58* (1987) 1655-1659.

34

23 *Manufacturer's data,* Micro-Gluhlampen-Gesellschaft, Hamburg, Lanster, 1, D-2057.

24 D. A. Jackson, Monomode fibre optic interferometers and their application in sensing systems, *OFS NATO ASI Series, Series E: Applied Sciences,* No. 132, 1987, pp. 1–33.

25 T. Okoshi, Polarization phenomena in optical fibres, *OFS NATO ASI Series, Series E: Applied Sciences,* No. 132, 1987, pp. 227–242.

26 B. Y. Kim, Few mode fibre devices, *Proc. Int. Conf. Optical Fiber Sensors, New Orleans, LA, U.S.A., 1988, Tech. Digest Series,* Vol. 2, Part 1, 1988, pp. 146–149.

27 S. Y. Huang, J. N. Blake and B. Y. Kim, Mode characteristics of highly elliptical core two-mode fibre perturbations, *Proc. Int. Conf. Optical Fiber Sensors, New Orleans, LA, U.S.A., 1988, Tech. Digest Series,* Vol. 2, Part 1, 1988, pp. 14–17.

28 J. N. Blake, B. Y. Kim, H. E. Engan and H. J. Shaw, Analysis of inter-modal coupling in a two-mode fibre with periodic microbends, *Opt. Lett., 12* (1987) 281.

29 G. Meltz, J. R. Dunphy, W. W. Morey and E. Snitzer, Cross-talk fiber-optic temperature sensor, *Appl. Opt., 22* (1983) 464.

30 W. V. Sorin, B. Y. Kim and H. J. Shaw, Phase-velocity measurements using prism output coupling for single- and few-mode optical fibers, *Opt. Lett., 11* (1986) 106.

31 B. Y. Kim, J. M. Blake, S. Y. Huang and H. J. Shaw, Use of highly elliptical core fibers for two-mode fiber devices, *Opt. Lett., 12* (1987) 729.

32 T. Bosselmenn, Multimode fibre coupled white light interferometer position sensor, *OFS NATO ASI Series, Series E: Applied Sciences,* No. 132, 1988, p. 429.

33 C. A. Millar, B. J. Ainslie, M. C. Brierley and S. P. Craig, Fabrication and characterisation of D-fibres with an accurately controlled core/flat distance, *Electron. Lett., 22* (1986) 322–324.

34 R. B Dyott, J. Bello and V. A. Henderek, Indium-coated D-shaped fiber polarizer, *Opt. Lett., 12* (1987) 287–289.

35 R. B. Dyott and P. F. Shrank, Self-locating elliptically cored fiber with an accessible guiding region, *Electron. Lett., 18* (1982) 980.

36 L. Li, G. Wylandgowski, D. N. Payne and R. D. Birch, Broadband metal/glass single-mode fibre polarisers, *Electron. Lett., 22* (1986) 1020–1022.

37 J. Dakin and B. Culshaw, *Optical Fibre Sensors: Principles and Components,* Artec House, 1989, p. 249.

38 M. C. Farries, M. E. Fermann, R. I. Laming, S. B. Poole, D. N. Payne and A. P. Leach, Distributed temperature sensor using Nd^{3+} doped fibre, *Electron. Lett., 22* (1986) 418–419.

39 A. H. Hartog, A distributed temperature sensor based on liquid core fibers, *IEEE J. Lightwave Technol., LT-1* (1983) 498–501.

40 G. Martens, J. Kordts and G. Weidinger, A photo-elastic pressure sensor with loss-compensated fibre link, *Proc. OFS '89, Springer Proc. in Physics,* Vol. 44, 1989, p. 458.

41 L. Jonsson and B. Hok, Multimode fibre-optic accelerometers, *Proc. 2nd Int. Conf. Optical Fibre Sensors, Stuttgart, F.R.G., 5–7 Sept. 1984, SPIE,* Vol. 514, pp. 191–194.

42 J. D. Place, Optical control and alarm switch for the process industries, *Proc. Conf. Promecon, London, June 19–22, 1984,* pp. 157–163.

43 R. C. Spooner, Fibre optics in physics and chemical sensors, *Institute of Measurement and Control Conf., Harrogate, U.K., Nov. 1985,* Institute of Measurement and Control, London, 1985.

44 B. Culshaw, Optical system and sensors for measurement and control, *J. Phys. E: Sci. Instrum., 16* (1983) 987–986.

45 D. A. Jackson, Monomode optical fibre interferometers for precision measurements, *J. Phys. E: Sci. Instrum., 18* (1985) 981.

46 H. Ishio, J. Minowa and J. Nosu, Review and status of wavelength-division multiplexing technology, *IEEE J. Lightwave Technol., LT-2* (1984) 448–463.

47 G. Winzer, Wavelength multiplexing components — a review of single-mode devices and their applications, *IEEE J. Lightwave Technol., LT-2* (1984) 369–378.

48 M. C. Hutley, Wavelength encoded optical fibre sensors, *Proc. 2nd Int. Conf. OFS, Stuttgart, F.R.G., 1984, SPIE,* Vol. 514, pp. 111–116.

49 B. E. Jones and S. J. Collier, Optical fibre sensors using wavelength modulation and simplified spectral analysis, *J. Phys. E: Sci. Instrum., 17* (1984) 1240–1241.

50 H. Ghafoori-Shiraz and T. Okoshi, Fault location in optical fibers using optical frequency domain reflectometry, *IEEE J. Lightwave Technol., LT-4* (1986) 316.

51 S. A. Al-Chalabi, B. Culshaw, D. B. N. Davies, I. P. Giles and D. Uttam, Multiplexed optical fibre interferometers: an analysis based on a radar system, *Proc. IEE, 132A* (1985) 150–156.

52 D. Uttam and B. Culshaw, Precision time domain reflectometry in optical fibre systems using a frequency modulated continuous wave ranging technique, *IEEE J. Lightwave Technol., LT-3* (1985) 971.

53 R. B. Dyott, Fibre-optic Doppler anemometer, *IEEE J. Microwaves Opt. Acoust., 20* (1978) 13–18.

54 T. T. Nguyen and L. N. Birch, A fiber-optic laser-Doppler anemometer, *Appl. Phys. Lett., 45* (1984) 1163.

55 D. A. Jackson, J. D. C. Jones and R. K. Y. Chan, A high-power fibre optic laser Doppler velocimeter, *J. Phys. E: Sci. Instrum., 17* (1984) 977–980.

56 T. Nakayama, Fibre LDA system, *NATO ASI Series E: Applied Sciences,* No. 132, 1987, p. 217.

57 K. Kyuma *et al.,* Laser Doppler velocimeter with a novel optical fibre probe, *Appl. Opt., 20* (1981) 2424–2427.

58 Y. N. Ning, K. T. V. Grattan, A. W. Palmer and A. E. Baruch, A heterodyne vibration sensor using coherence length modulation technique, *IEEE Proc. J.,* to be published.

59 M. D. Stern, Laser Doppler velocimetry in blood and multiply scattering fluids: theory, *Appl. Opt., 24* (1985) 1968.

60 G. Ulbers, A sensor for dimensional metrology with an interferometer in integrated optics technology, *Proc. OFS '89, Springer Proceedings in Phys.,* Vol. 44, 1989, p. 240.

61 K. T. V. Grattan, A. W. Palmer, B. T. Meggitt and Y. N. Ning, Use of laser diode source in low coherence operation in fibre optic sensors, *Australasian Instrumentation and Measurement Conf., Adelaide, Australia, Nov. 14–17, 1989,* pp. 305–308.

62 D. Trouchet, B. Laloux and P. Graindorge, Prototype industrial multi-parameter F.O.S. using white light interferometry, *Proc. OFS '89, Springer Proc. in Phys.,* Vol. 44, 1989, pp. 227–233.

63 A. M. Scheggi, M. Brenci, G. Conforti, R. Faliai and G. P. Preti, Optical fibre thermometer for medical use, *1st Int. Conf. Optical Fibre Sensors, IEE Conf. Publication,* Vol. 221, 1983, pp. 13–16.

64 S. M. McGlade and G. R. Jones, Optical sensors for displacement measurement, *Colloq. Digest, Proc. Control, London, Jan. 1984,* IEE, 1984/7.

65 B. Hok and L. Jonsson, Pressure sensor with fluorescence decay as information carrier, *Proc. 2nd Int. Conf. OFS, Stuttgart, F.R.G., Sept. 5–7, 1984, SPIE,* Vol. 514, 1984, pp. 391–394.

66 K. T. V. Grattan, R. K. Selli and A. W. Palmer, Ruby decay-time fluorescence thermometer in a fiber-optic configuration, *Rev. Sci. Instrum., 59* (1988) 1328–1335.

67 M. Born and E. Wolf, *Principles of Optics,* Oxford University Press, Oxford, 1980, pp. 360–367.

68 G. Behiem, Remote displacement measurement using a passive sensor with a fiber-optic link, *Appl. Opt., 24* (1985) 2335–2340.

69 C. J. Zarobila, J. B. Freal, R. L. Lampman and C. M. Davies, Two fibre-optic accelerometers, *Tech. Digest, Proc. OFS Conf., New Orleans, LA, U.S.A., 1988,* Vol. 2, Part 1, p. 296.

70 B. T. Meggitt, Y. N. Ning, K. T. V. Grattan, A. W. Palmer and W. Boyle, Fibre optic anemometer using an optical delay cavity technique, *Eighth Int. Conf. Fibre Optics and Opto-electronics, London, Apr. 1990, SPIE,* Vol. 1314, pp. 321–329.

71 F. Farahi *et al.,* Optical-fibre flammable gas sensor, *J. Phys. E: Sci. Instrum., 20* (1987) 435–436.

72 F. P. Milanovich *et al.,* Remote detection of organo-chlorides with a fibre optic based sensor, *Anal. Instrum. (U.S.A.), 15* (1986) 542–558.

73 I. Aeby, Non-destructive measurement in advanced composite materials and structures using a fibre optic sensing system, *Proc. SPIE,* Vol. 986, 1989, pp. 140–147.

74 A. Safaai-Jazi and R. O. Clau, Synthesis of interference patterns in few-mode optic fibers, *Proc. SPIE,* Vol. 986, 1989, pp. 180–185.

75 P. B. Macedo *et al.,* Development of porous glass fibre optic sensors, *Proc. SPIE,* Vol. 986, 1989, pp. 200–205.

76 J. K. Zienkiewicz, Self-reference fibre optic methane detection system, *Proc. SPIE,* Vol. 992, 1989, pp. 192–197.

77 G. W. Fehrenbach, Fibre optic temperature measurement system based on luminescence decay time, *Tech. Mess., 56* (1989) 85–88.

78 F. Gonthier *et al.,* Circular symmetry modal interferometers in optical fibres, *Ann. Telecommun. (France), 44* (1989) 159–166.

79 T. G. Giallorenzi *et al.,* Optical fibre sensor technology, *IEEE J. Quantum Electron., QE-18* (1982) 626.

80 M. Corke *et al.,* All fibre Michelson thermometer, *Electron. Lett., 19* (1983) 471.

81 P. Akhavanleilabady, A dual intermometer implemented in parallel on a single birefringent monomode optic fibre, *J. Phys. E: Sci. Instrum., 19* (1986) 143.

82 S. A. Al-Chalabi *et al.,* Partially coherent sources in interferometric sensor, *Proc. 1st Int. Conf. Optic Fibre Sensors, London, 1988,* pp. 132–135.

83 H. L. W. Chan *et al.,* Polarimetric optical fiber sensor for ultrasonic power measurement, *IEEE 1988 Ultrasonic Symp. Proc.,* Vol. 1, 1988, pp. 599–602.

84 H. Tsuchida *et al.,* Polarimetric optical fibre sensor using a frequency stabilized semiconductor laser, *IEEE J. Lightwave Technol., LT-7* (1989) 799–803.

85 A. V. Belov *et al.,* The measurement of chromatic dispersion in single-mode fibre by interferometric loop, *IEEE J. Lightwave Technol., LT-7* (1989) 863–868.

86 E. Wittendorp-Rechenmann, *Radiat. Prot. Dosim. (U.K.), 23* (1988) 199–202.

87 H. Takahara, F. Togashi and T. Aragaki, Ultrasonic sensor using polarization-maintaining optical fiber, *Can. J. Phys., 66* (1988) 844–846.

88 F. Farahi, N. Takahashi, J. D. C. Jones and D. A. Jackson, Multiplexed fibre-optic sensors using ring interferometers, *J. Mod. Opt., 36* (1988) 337–348.

89 A. S. Georges, High sensitivity fiber-optic accelerometer, *Opt. Lett., 15* (1989) 251–253.

90 H. Takahashi *et al.,* Laser diode interferometer for small displacement and sound pressure measurements, *Conf. Precision Electromagnetic Measurements, Tsukuba, Japan, June 1988,* pp. 135–136.

91 E. Theocharous, Differential absorption distributed thermometer, *1st Int. Conf. Optical Fibre Sensors, Apr. 1983,* IEE, London, pp. 10–12.

92 M. L. Henning *et al.,* Optical fibre hydrophones with down lead insensitivity, *1st Int. Conf. Optical Fibre Sensors, Apr. 1983,* IEE, London, pp. 25–27.

93 K. Spenner *et al.,* Experimental investigations on fibre optic liquid level sensors and refractometer, *1st Int. Conf. Optical Fibre Sensors, Apr. 1983,* IEE, London, pp. 75–78.

94 E. R. Cox and B. E. Jones, Fibre optic colour sensors based on Fabry–Perot interferometry, *1st Int. Conf. Optical Fibre Sensors, Apr. 1983,* IEE, London, pp. 122–126.

95 K. Shibata, A fibre optic electric field sensor using the electrooptic effect of bismuth germinate, *1st Int. Conf. Optical Fibre Sensors, Apr. 1983,* IEE, London, pp. 164–166.

96 S. C. Rashleigh, Polarimetric sensors: exploiting the axial stress in high birefringement fibres, *1st Int. Conf. Optical Fibre Sensors, Apr. 1983,* IEE, London, pp. 210–213.

97 A. J. A. Brunsma and J. A. Vogel, Ultrasonic non-contact inspection system with optical fibre methods, *Appl. Opt., 27* (1988) 4690–4695.

98 K. Iwamoto and I. Kamato, Pressure sensors using optical fibres, *Appl. Opt., 29* (1989) 375–377.

99 T. Okamoto and I. Y. Yamaguchi, Multimode fibre optic Mach–Zehnder interferometer and its use in temperature measurement, *Appl. Opt., 27* (1988) 3085–3087.

100 S. Y. Huang *et al.,* Mode characteristics of highly elliptical core two-mode fibres under perturbation, *Tech. Digest, Proc. Int. Conf. Optical Fiber Sensors (OFS-88),* (IEEE/OSA) 1988, p. 14.

101 E. Sakaoka *et al.,* Polarisation maintaining fibers for fibcroptic gyroscopes, *Tech. Digest, Proc. Int. Conf. Optical Fiber Sensors (OFS-88),* (IEEE/OSA) 1988, p. 18.

36

102 D. T. Dong and K. Hotate, Frequency division multiplication of optical fibre sensors using an optical delay line with a frequency shifter, *Tech. Digest, Proc. Int. Conf. Optical Fiber Sensors (OFS-88),* (IEEE/OSA) 1988, p. 76.

103 A. D. Kersey and A. Dandridge, Tapped serial interferometric fibre sensor array with time division multiplexing, *Tech. Digest, Proc. Int. Conf. Optical Fiber Sensors (OFS-88),* (IEEE/OSA) 1988, p. 80.

104 H. Hosokawa *et al.,* Integrated optical microdisplacement sensor using a Y junction and a polarization maintaining fibre, *Tech. Digest, Proc. Int. Conf. Optical Fiber Sensors (OFS-88),* (IEEE/OSA) 1988, p. 137.

105 H. Koseki *et al.,* Optical heterodyne gyroscope using two reversed fibre coils, *Tech. Digest, Proc. Int. Conf. Optical Fiber Sensors (OFS-88),* (IEEE/OSA) 1988, p. 168.

106 G. Kotrotsios and D. Pariaux, White light interferometry for distributed sensing on dual mode fibres, *Proc. OFS '89, Springer Proceedings in Physics,* Vol. 44, 1989.

107 S. Y. Huang, H. G. Park and B. Y. Kim, Passive quadrature phase detector for coherence fibre optic system, *Proc. OFS '89, Springer Proceedings in Physics,* Vol. 44, 1989, p. 38.

Biographies

Kenneth T. V. Grattan was born in County Armagh, Northern Ireland on December 9th, 1953. He received the B.Sc. degree with first class honours in physics and the Ph.D. degree from the Queen's University of Belfast, Northern Ireland, in 1974 and 1978, respectively. His doctoral research involved the development of ultraviolet gas discharge lasers and their application to the study of the photophysics of vapour phase organic scintillators. From 1978–83 he was a research assistant at Imperial College, University of London, working in the field of ultraviolet and vacuum ultraviolet lasers and their application to the measurement on excited states of atoms and molecules. In 1983 he was appointed a 'New Blood' lecturer in measurement and instrumentation at City University, London, in 1987 senior lecturer, in 1988 reader and in 1991 professor of measurement and instrumentation, where his research interests are currently in the field of optical sensing with industrial, environmental and bioengineering applications. He has authored or co-authored over 100 journal and conference papers in the field of optical measurement and sensing. Professor Grattan is a member of the Institute of Physics, Chairman of their Instrument Science and Technology Group, and a member of the Institution of Electrical Engineers and the Institute of Measurement and Control.

Yanong Ning was born in Shaanxi Province, China, on September 24th, 1957. He received the B.Sc. degree in physics from the Xi'an Jiaotong University, Shaanxi, China in 1982. From 1982 to 1986, he was an assistant professor of modern optics at the Chongqing University, Chongqing, China, where he had lectured on physical optics for two years.

He is currently a research student in the Department of Electrical, Electronic and Information Engineering, City University, where he is completing his Ph.D. degree. His research interests are currently in the field of theory and application of optical fibre sensing techniques.

Andrew W. Palmer was born in New Zealand on March 15th, 1938. He received the B.Eng. degree in electrical engineering with first class honours from Canterbury University, New Zealand and subsequently became a member of the New Zealand Institute of Electrical Engineers. He has lectured at City University, London, in the Department of Electrical, Electronic and Information Engineering, where he obtained the degrees M.Phil. and Ph.D., for a number of years, and is currently senior lecturer. His research interests have been laser control and more recently in the field of fibre-optic sensing for measurement purposes. Dr Palmer is a member of the Institution of Electrical Engineers.

Wen Ming Wang was born in Sichuan, China, on January 19, 1963. He received his B.Sc. degree in electrical engineering from Wuhan Iron and Steel University and M.Sc. degree from the Institute of Optics and Electronics, Academia Sinica, in 1982 and 1985 respectively.

In 1987, he was appointed as a lecturer in the department of Optical Instrumentation, Wuhan Technical University of Surveying and Mapping. He is currently studying at the City University of London for a Ph.D. degree, sponsored by the British Council. His research interests have been in optical and electronic measurement and control, adaptive optics and more recently in the field of fibre-optic sensors and their applications.

CONFERENCE PROCEEDINGS

8th Optical Fiber Sensors Conference

January 29 - 31, 1992

Monterey Marriott
Monterey, CA

IEEE

An interferometer incorporating active optical feedback from a diode laser with applications to coherent ranging and vibrational measurement

W.M.Wang, W.J.O.Boyle, K.T.V.Grattan and A.W.Palmer
Measurement and Instrumentation Centre,
Department of Electrical, Electronic and
Information Engineering, City University,
Northampton Square, London EC1V 0HB, England.
Tel: +44 71 477 8000
Fax: +44 71 477 8568

Abstract

A novel application of an interferometer is proposed based on the effect of "self-mixing interference" in a diode laser. Coherent ranging, beyond the coherence length of the laser used, and directional vibration measurement have been demonstrated with optical fibre schemes.

An interferometer incorporating active optical feedback from a diode laser with applications to coherent ranging and vibrational measurement

W.M.Wang, W.J.O.Boyle, K.T.V.Grattan and A.W.Palmer
Measurement and Instrumentation Centre,
Department of Electrical, Electronic and
Information Engineering, City University,
Northampton Square, London EC1V 0HB, England.

I. Introduction

Optical self-mixing effects or backscattered intensity modulation in different lasers have been considerably exploited for various applications, such as Laser Doppler Velocimetry(LDV)[1-4], coherent ranging[5-6] and acoustic sensing[7]. The modulation mechanism inside a laser cavity caused by external optical feedback, however, is not well understood, which confines its applications to limited areas. Recently a theory of the external optical feedback in a single-mode semiconductor laser has been developed and proposed, indicating that the intensity modulation by the external feedback results from the spectral linewidth variation of the laser used, which is due to a "phase interference" between the light from an external reflector and the light from one of laser mirror facets. A detailed study of self-mixing interference will be reported elsewhere[9].

In this work, a self-mixing interferometer incorporating a diode laser is proposed based on the effect of "self-mixing interference", where a portion of emitted light from the laser is reflected back into the laser cavity from a reflecting surface, and the resulting intensity modulation may be extracted to determine the parameter to be measured which is causing the phase change in the interferometer. A simple arrangement with different length multi-mode optical fibres is exploited for coherent ranging and vibration measurement. The experiments performed have demonstrated that self-mixing coherent ranging is not dependent on the coherence length of the laser used, which provides the possibility of using coherent detection methods for range finding for much longer distances. In addition, for small vibrational measurements, the self-mixing interference method shows that the directional information of the vibration can be discriminated from the asymmetric nature of the resulting intensity output signal, which offers an advantage compared to use of conventional optical interference techniques.

II. Self-mixing interferometer

The experiments reported were carried out with a 780 nm VSIS-type AlGaAs diode laser(Sharp LT022MC) and different length multi-mode optical fibres with core diameter of 50 μm, as shown in Figure 1. The light from the laser was collimated by a lens, L_1, and then focused by another lens, L_2, into a multi-mode fibre. This light travelled through the fibre and was reflected by an external mirror M. The reflected light was guided by the same fibre and re-entered the laser cavity, where the light from the laser front facet and from the target mirror, M, was mixed coherently inside the cavity, and the resultant laser intensity modulation was detected by a photodetector accommodated at the rear facet inside laser package. When the mirror M was vibrated periodically, an intensity modulation was observed from the laser photodiode,PD, which is very similar to conventional optical interference and termed "self-mixing interference"[9]. The light inside the laser cavity and the light from the mirror M constitutes two interfering beams of the self-mixing
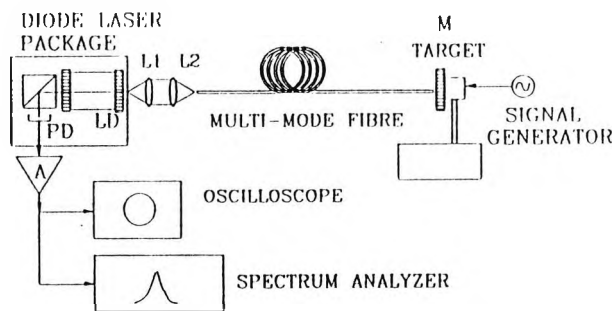
Fig.1 Experimental arrangement
for self-mixing interferometer

interferometer with self-aligning and self-detecting features and only one optical axis.

A typical self-mixing interference signal is shown in Figure 2(upper trace) with a comparison to that of a Michelson interferometer(lower trace). The interference shows a 2π periodicity, with respect to the phase change at the external mirror M, which is equal to a half of the wavelength of the laser.
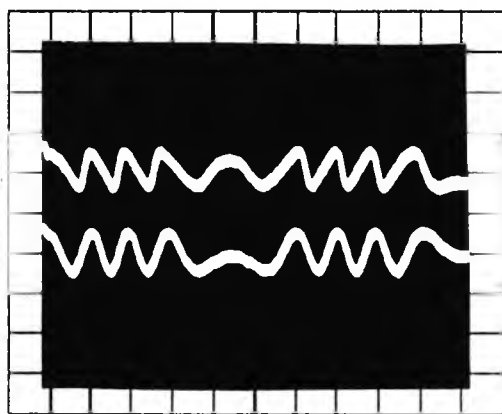
Fig.2 Self-mixing interference(upper trace) with
comparison to conventional interference(lower trace).
Time axis-0.2 ms/Div, Intensity-arb. units.

However, the upper signal shows two significant differences with that of the Michelson interferometer. First, it is sawtoothlike but not sinusoidal, and secondly it is asymmetric relative to the external vibrational direction, from which it is important to note that the inclination of the signal is dependent on the direction of the "target" movement, and when the target changes its movement direction, the signal changes its

inclination. It is from such an asymmetry that the vibrational direction can be discriminated, which shows a major advantage over conventional interferometric methods[8]. In experiments with different length optical fibres it was found that the interference pattern is not dependent on the coherence length of the laser used. These differences present some interesting features which could be utilised in various applications as discussed.

III. Self-mixing coherent ranging

The intensity modulation in self-mixing interference, with weak external optical feedback, may be expressed approximately as:

$$I = Io[1 + m(\xi,\chi)cos(2\pi\frac{1}{\lambda_0}\Delta L + \phi_o)] \qquad (1)$$

where $m(\xi,\chi)$ is defined as the modulation coefficient which is determined by the linewidth factor χ of the source laser and the feedback factor ξ(the ratio of the external amplitude reflectivity to the laser facet reflectivity). λ_o is the central wavelength of the laser, ΔL is the optical path difference(OPD) between the laser and the target, and ϕ_0 an initial phase condition. When a direct current modulation is applied to the diode laser, the resultant intensity modulation will include an FM modulation and an AM modulation[10]. If the amplitude and the frequency of the current modulation are very small, a beat frequency F_b, produced by the coherent mixing, can be easily observed and is given by:

$$F_b = (2\beta/\lambda_o)(dJ/dt)D \qquad (2)$$

where β is the wavelength modulation coefficient (nm/mA), dJ/dt is the rate of the current change with time, and D is the target distance from the laser. If dJ/dt remains a constant, a fixed beat frequency F_b can be detected from the laser intensity modulation, and the distance D, then, can be calculated directly from Equation(2).

In the work herein, the laser was dc-biased, with an output power of 3 mW, and current-modulated by a triangular wave at 500 Hz with a peak-to-peak modulation current of 0.1 mA. The small current modulation provides two advantages, which are: (1) the feedback from the near end of the fibre is insufficient to produce a significant beat frequency due to the short OPD; and(2) the mode hopping

produced by a large current modulation can be avoided. By substituting the experimental data above, the required target distance may be expressed as:

$$D=0.69F_b \qquad (3)$$

where β is given to be 5.6×10^{-3} nm/mA, and λ_o is 780 nm.

The intensity modulation of the laser was ac-coupled via an amplifier A(Figure 1) to an oscilloscope for waveform analysis and to a spectrum analyser for frequency measurement. Figure 3 shows the observed waveform in the experiment performed with a long multi-mode fibre of 3.48 m, where the upper trace was produced due to reflection from the far end of fibre without the mirror M, whilst the lower waveform was produced incorporating the reflection from the mirror M. It is clear that the two
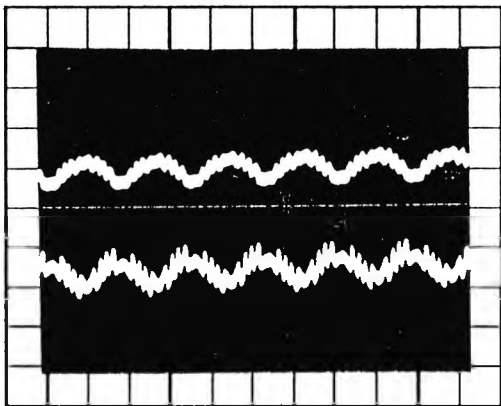
Fig.3 Waveform observed with 3.48 m multi-mode
fibre, (a) reflection from fibre end(upper trace)
(b) reflection from an external mirror(lower trace)
Time axis-1.0 ms/Div, Intensity-arb. units

signals have the same beat frequency but different amplitudes, which is due to the different reflectivities of the fibre end and the mirror. In the experiments carried out, three different length multi-mode optical fibres were used. Table 1 gives the measured fibre length, L_o, the calculated distance, D_o, using Equation(3), and the corresponding beat frequency, F_b. It is evident that the measured results are in good agreement with the theoretical calculations.

Table 1			
F_b(kHz)	2.0	5.0	15.0
L_o(m)	1.51	3.48	10.10
D_o(m)	1.38	3.45	10.35

IV. Vibrational Measurement

To measure the nature of the vibration of an object under consideration, two factors must be determined, these being the amplitude and the frequency of such a vibration. The amplitude can be determined by counting the fringe number of the interference in one direction. A linear relationship between the fringe number, N, and the vibrating amplitude, A, was obtained, as depicted in Figure 4. Thus the amplitude may be expressed as:
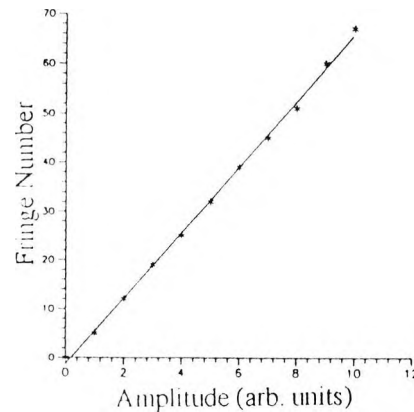
Fig.4 Fringe number dependence on
vibration amplitude

$$A = N \lambda_o \qquad (4)$$

where λ_o is the central wavelength of the laser used.

It has been seen, from Figure 2, the interference signal changes its inclination as the target changes its direction, which implies that the period can be determined by measuring the time of one directional change of the target. If the vibration is symmetrical, the vibration frequency may be given by:

$$f = 1/2\tau \qquad (5)$$

where τ is the time for one direction change.

V. Discussion

In the present study, a "self-mixing interferometer" incorporating a semiconductor laser is described and

361

preliminary experimental results presented, which show some significant comparative advantages over the use of a conventional interferometer.

For coherent ranging, the laser diode used displayed a multi-mode nature with a low output power, the coherence characteristics of which were measured using a two beam Michelson interferometer at an output of 3 mW, as shown in Figure 5. In summary these features are: (1) the full width at half maximum(FWHM) of each coherent region was 0.11 mm; (2) the separation between the adjacent coherent regions was 1.05 mm; (3) the FWHM of the envelope of all the coherent regions was 3.07 mm and the interference was not detectable when the OPD was greater than 11.65 mm. These data mean that this type of laser cannot be used in a conventional coherent ranging system where the distance to be measured is greater than 11.65 mm. However, in a self-mixing ranging scheme, the measurable distance could reach as far as a distance of 10 m, with the use of suitable circuitry. This
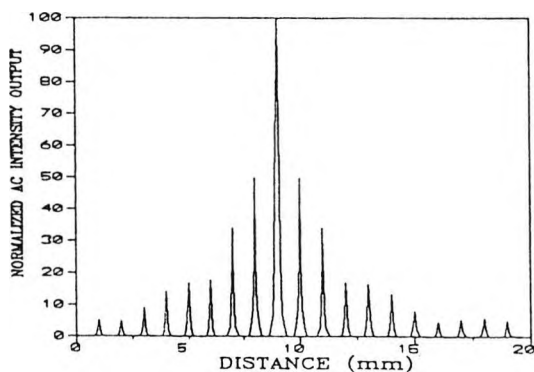
Fig.5 Visibility function of laser used
for ranging experiments obtained from a
two beam Michelson interferometer

represents a considerable improvement, using a cheap and readily available laser source.

For a vibration measurement, the self-mixing method combines simplicity of operation with ability of discriminating the vibration direction, as demonstrated.

VI. Acknowledgements

VII. References

[1]. M. J. Rudd "A laser Doppler velocimeter employing the laser as a mixer-oscillator" J. Phys. **E1**, pp.723-726, 1968

[2]. J. H. Churnside "Laser Doppler velocimetry by modulating a CO_2 laser with backscattered light" Appl. Opt. **23**, pp.61-65, 1984

[3]. S. Shinohara, A. Mochizuki, H. Yoshida and M. Sumi "Laser Doppler velocimeter using the self-mixing effect of a semiconductor laser diode" Appl. Opt. **25**, pp.1417-1419, 1986

[4]. H. W. Jentink, F. F. M. de Mul, H. E. Suichies, J. G. Aarnoudse and J.Greve "Small laser Doppler velocimeter based on the self-mixing effect in a diode Laser" Appl. Opt. **27**, pp.379- 385, 1988

[5]. P. J. de Groot, G. M. Gallatin and S. H. Macomber "Ranging and velocimetry signal generation in a backscatter-modulated laser diode" Appl. Opt. **27**, pp.4475-4480, 1988

[6]. G. Beheim and K. Fritsch "Range finding using frequency-modulated laser diode" Appl. Opt. **25**, pp.1439-1441, 1986

[7]. A. Dandrige, R. O. Miles and T. G. Giallorenzi "Diode laser sensor" Electron. Lett. **16**, pp.948-949, 1980

[8]. E. T. Shimizu "Directional discrimination in the self-mixing type laser Doppler velocimeter" Appl. Opt. **26**, pp.4541-4544, 1987

[9]. W. M. Wang, W .J .O. Boyle, K. T. V. Grattan and A. W. Palmer "Optical sensor applications of self-mixing interference in a diode laser" submitted to Applied Optics, 1991.

[10]. M. Imai and K. Kawakita "Measurement of direct frequency modulation characteristics of laser diode by Michelson interferometry" Appl. Opt. **29**, pp.348-353, 1990

Fiber-optic Doppler velocimeter that incorporates active optical feedback from a diode laser

W. M. Wang, W. J. O. Boyle, K. T. V. Grattan, and A. W. Palmer

Measurement and Instrumentation Centre, Department of Electrical, Electronic and Information Engineering, City University, Northampton Square, London EC1V OHB, UK

A fiber-optic Doppler velocimeter that incorporates the effect of self-mixing in a diode laser is described. A theoretical model, based on self-mixing interference theory, is presented, and a simple experimental arrangement is constructed. The results of the experimental research are found to be in good agreement with the theoretical analysis. A Doppler velocity of as much as 3 m/s was measured directly, and a good linear relationship between the Doppler velocity and the Doppler-shifted frequency was obtained, which can be used to determine the speed of a moving object.

The self-mixing or optical feedback technique was first used by Rudd[1] to measure the Doppler velocity with a He–Ne laser. This approach has been of growing interest in recent years for laser Doppler velocimetry (LDV) with semiconductor lasers[2-5] owing to its significant advantages in simplicity, compactness, and robustness over conventional LDV methods. A fiber-coupled LDV for *in vivo* blood flow measurement, which provided a simple optical arrangement with easily alignable components and a comparatively large signal-to-noise ratio, has been also reported by Koelink *et al.*[6]

It is well known that the output characteristics of semiconductor lasers are affected greatly by external optical feedback, which has been commonly used to alter the spectral characteristics, such as the spectral linewidth,[7] and the mode patterns[8] of conventional lasers. A common feature of external optical feedback theories is the assumption that the external optical feedback is coherent with the light inside the laser cavity owing to the similarity of the dynamic features of the optical feedback effects to features in conventional interference. However, recent investigations have found that the output characteristics could be altered by incoherent optical feedback,[9,10] that the intensity modulation inside a laser cavity by the self-mixing is due to the spectral mode modulation produced by the periodical modulation of the external optical feedback, and that the modulation depth achieved is directly proportional to the strength of optical feedback.[11,12] Because the power modulation by self-mixing has been assumed to result from the spectral variation rather than from a conventional interference effect, the modulation signal is not dependent on the coherence length of the laser used. These features result in some distinct peculiarities of the self-mixing interference when compared with conventional interference, e.g., the asymmetrical nature of the intensity output and its independence of the coherence length of the laser used.

In this research, self-mixing interferometry is exploited for velocity measurement by using Doppler techniques along with a 6-m single-mode optical fiber (~5-μm core diameter) and a compact-disc-type diode laser (Sharp LT022MD) operated with a multilongitudinal-mode output. A Doppler velocity simulation was provided by a rotating disk coated with a white paper, and its rotation speed could be adjusted by changing the voltage of a voltage-controlled-motor. The velocity was varied from 20 mm/s upward and was measured by using the self-mixing interferometry method. It was compared with that obtained by direct measurement with the use of an optoelectronic pulse-counting method. A linear relationship between the velocity of the rotating disk and the Doppler frequency produced was obtained with a minimum resolution of ~3 mm/s. A simple theoretical model, the experimental arrangement with a presentation of experimental results, and a discussion are presented below.

In a self-mixing LDV scheme, as depicted in Fig. 1, a portion of light emitted from a diode laser is fed back into the laser cavity after it is scattered from a diffused target that is moving to produce a Doppler-shifted frequency superimposed on the original optical frequency of the laser light. The resultant optical intensity variation with time, $I(t)$, owing to the weak optical feedback, thus may be expressed as

$$I(t) \approx \frac{I_o}{[1 + (D\xi/nl)\cos \phi(t)]^2}, \qquad (1)$$

where $\phi(t) = \phi_o + 2\pi f_d t$, I_o is the laser output intensity without the external optical feedback, D is the distance between the laser and the target, ξ is the ratio of the external amplitude reflectivity r_3 (including geometric effects and coupling losses at laser facet) to the amplitude reflectivity r_2 of the laser facet, f_d is the Doppler frequency induced by the target movement, ϕ_o is an arbitrary initial phase, t is the time, n is the effective refractive index of the laser medium, and l is the laser cavity length. Relation (1) only holds under the condition of $\beta(=D\xi/nl) < 1$. IF $\beta \geq 1$, then the variation
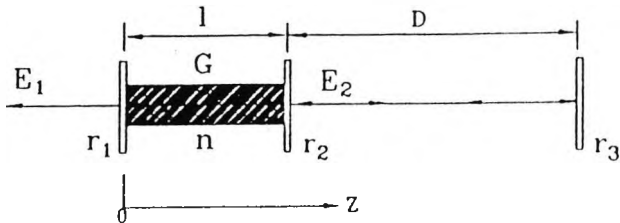
Fig. 1. Schematic of a diode laser with external optical feedback. r_1, r_2, laser facet amplitude reflectivities; r_3, target amplitude reflectivity; G, single-pass gain transfer function; and n, effective refractive index of gain medium.
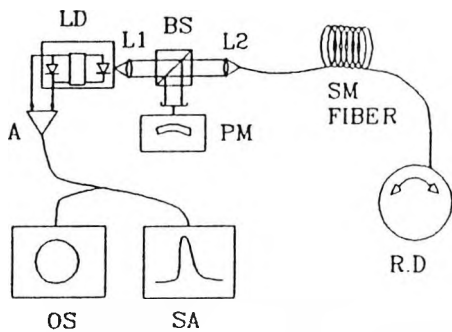
Fig. 2. Experimental arrangement for self-mixing LDV. LD, laser diode; BS, beam splitter; L_1, L_2, lenses; OS, oscilloscope; SA, spectrum analyzer; A, amplifier; PM, power meter; SM, single mode; RD, rotating disk.

of the phase $\phi(t)$ may lead to the occurrence of multimode lasing operation, the output power will increase sharply and become asymmetric with respect to the phase variation, and hence the larger the feedback coefficient ξ, the more sawtoothlike the intensity variation.[6] When the external feedback is weak, i.e., $\xi \ll 1$, relation (1) may be simplified to

$$I(t) \approx I_o[1 + v \cos(2\pi f_d t + \phi_o)], \qquad (2)$$

where $v[= -(2D/nl)\xi]$ is termed the visibility function in optical interference. In this case, the intensity modulation is similar to that seen in conventional interference, and the Doppler velocity V of the target movement may then be expressed directly as

$$V = (\lambda_o/2n \cos \theta)f_d = k f_d, \qquad (3)$$

where λ_o is the central wavelength of the laser, n is the refractive index of the target medium, and θ is an angle between the velocity vector and the optical axis. k is a proportionality constant. For example, $k = 1.041$ when the related parameters are chosen to be $\lambda_o = 780$ nm, $n = 1$, and $\theta = 68$ degrees, and the velocity V is given in millimeters per second and f_d is given in kilohertz.

The proof-of-principle study reported was carried out with a 780-nm compact-disc-type diode laser (Sharp LT022MD) and an ~6-m single-mode optical fiber (~5-μm core diameter) as shown in Fig. 2. The light emerging from the diode laser was collimated by a beam splitter BS and then focused into the fiber. The light emitting from the fiber end was then aimed at a diffused target, which was represented by a white paper attached to a rotating

disk, with an angle of ~68° to the rotation direction. The disk was driven by the voltage-controlled motor, and its velocity could be varied from 20 to 5000 mm/s. The scattered light from the target was guided through the same path back into the laser cavity, and the amount of optical feedback was monitored by the beam splitter by a photodetector D1. The diode-laser package incorporated a photodiode accommodated in its rear facet to monitor the laser power, which was used in this experiment to observe the intensity variation produced by the external optical feedback. The laser was operated at an output power of 2.5 mW ($I = 1.2I_{th}$, where I_{th} is the threshold current), which was found to be the optimal output for the Doppler velocity measurement, whereas the signal-to-noise ratio was found to be decreased when increasing the injection current, i.e., increasing the output power of the laser, but there is still a good signal-to-noise ratio at $I = 2I_{th}$. The reflected light from the target was measured by the power meter PM to be 0.01 mW, which was approximately -25 dB or the original output power at the experiment. However, for self-mixing interference, the feedback strength can be as large as approximately -10 dB and as small as approximately -60 dB. The output signal from the laser photodiode was amplified by a wideband amplifier A and then fed to an oscilloscope and a spectrum analyzer for direct Doppler frequency studies. A typical Doppler spectrum produced by the target rotation is shown in Fig. 3(a) with a comparison to the noise
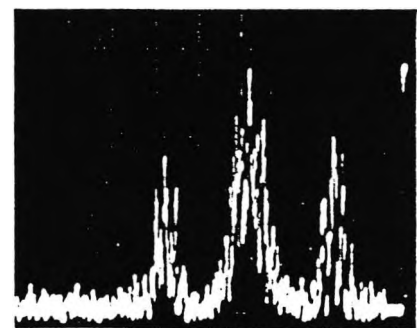
(a)
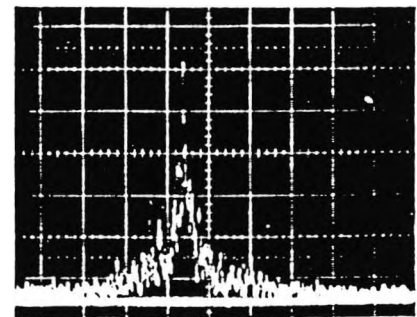
(b)

Fig. 3. Output spectra: (a) Doppler spectrum produced by Doppler-shifted frequency, (b) noise spectrum without rotation of the target. Vertical logarithmic scale, arbitrary units [same for (a) and (b)]; horizontal scale, 0.5 MHz per division [same for (a) and (b)]; central peak, zero frequency (dc) [same for (a) and (b)].
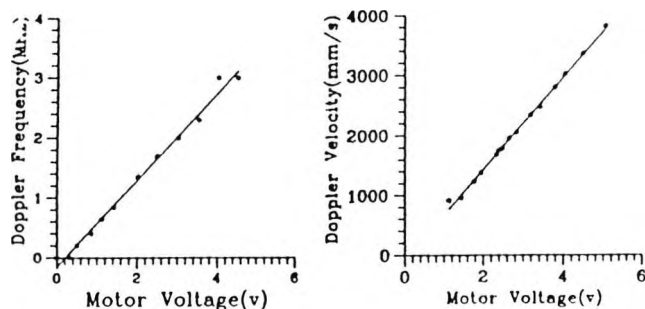
Fig. 4. Measured velocity of rotation disk dependence on the Doppler-shifted frequency.
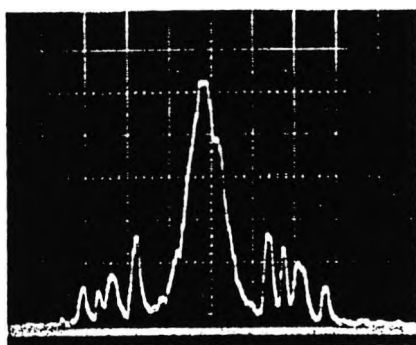
Fig. 5. Higher harmonics of Doppler-shifted frequency in self-mixing spectrum. Vertical logarithmic scale, arbitrary units; horizontal scale, 0.1 MHz per division and with video filter of 10 Hz; central peak, zero frequency (dc).

spectrum without the external optical feedback in Fig. 3(b). When the external signal, shifted by the Doppler velocity, is fed back into the cavity, two side peaks are seen in the spectrum, and the spacing from the central peak (zero frequency) represents the Doppler-shifted frequency, which is directly proportional to the speed of the rotating disk. The broadening in the Doppler-shifted spectrum is assumed to be due to the multimode operating property of the laser used.

To obtain an explicit relationship between the Doppler velocity and the Doppler frequency, these two variables were measured independently against the control voltage. By adequate data processing, the rotation speed dependence on the Doppler-shifted frequency is depicted in Fig. 4. It can be seen that there is a good linear relationship between these two variables, the saturation at higher velocity being due to the bandwidth limitation of the amplifer used, and the relationship can be expressed as

$$V\text{(mm/s)} = 1.05 fd\text{(kHz)} \pm 7.80 \text{ (mm/s)}. \quad (4)$$

The offset of 7.8 mm/s indicates the combined accuracy from the velocity measurement and the direct frequency measurement against the control voltage, for practical use an improvement of the frequency-detecting technique, and the accurate measurement of the rotation speed could be performed.

The utility of the self-mixing technique for LDV indicates its significant advantages. These are its simplicity (the fact that the self-mixing configuration requires only one optical axis, which simplifies the design and alignment of optical systems), its compactness, and the use of the internal photodiode in the laser package to detect the intensity modulation produced by self-mixing. No external detector is needed, and this provides a high detection efficiency for the self-mixing interference. Because the self-mixing interference is not dependent on the coherence length of the laser used, various fibers and low-coherence sources may be exploited in the velocity measurement. However, the presentation of higher harmonics of the measured Doppler-shifted frequency in the output spectrum with strong feedback, as shown in Fig. 5, makes it difficult to use heterodyne techniques in LDV. The directional information of the target movement may be obtained by making use of the asymmetry of the self-mixing interference,[13] but it is not easy to obtain clear directional information for a diffused target.

Thus an optical-fiber laser Doppler velocimeter has been demonstrated based on the self-mixing interference that is realized with a long optical fiber greater than the coherence length of the laser used) combining a cheap low-coherence source. The experimental arrangement highlights the simplicity, compactness, and suitability of a self-mixing LDV scheme over a conventional LDV scheme.

References

1. M. J. Rudd, J. Phys. E 1, 723 (1968).
2. S. Shinohara, A. Mochizuki, H. Yoshida, and M. Sumi, Appl. Opt. 25, 1417 (1986).
3. H. W. Jentink, F. F. M. de Mul, H. E. Suichies, J. G. Aarnoudse, and J. Greve, Appl. Opt. 27, 379 (1988).
4. P. J. de Groot, G. M. Gallatin, and S. H. Macomber, Appl. Opt. 27, 4475 (1988).
5. P. J. de Groot and G. M. Gallatin, Opt. Lett. 14, 165 (1989).
6. M. K. Koelink, M. Slot, F. F. M. de Mul, J. Greve, R. Graaff, A. C. M. Dassel, J. G. Aarnoudse, Proc. Soc. Photo-Opt. Instrum. Eng. 1511, 120 (1991).
7. Z. M. Chuang, D. A. Cohen, and L. A. Coldren, IEEE J. Quantum Electron. 26, 1200 (1990).
8. M. W. Fleming and A. Mooradian, IEEE J. Quantum Electron. QE-17, 44 (1981).
9. J. S. Cohen, F. Wittgrefe, M. D. Hoogerland, and J. P. Woerdman, IEEE J. Quantum Electron. 26, 982 (1990).
10. H. Yasaka, Y. Yoshikuni, and H. Kawaguchi, IEEE J. Quantum Electron. 27, 193 (1991).
11. G. P. Agrawal, N. A. Olsson, and N. K. Dutta, Appl. Phys. Lett. 45, 597 (1984).
12. P. J. de Groot, J. Mod. Opt. 37, 1199 (1990).
13. W. M. Wang, W. J. O. Boyle, K. T. V. Grattan, and A. W. Palmer, paper title, submitted to Appl. Opt.

IQEC '92

XVIII INTERNATIONAL
QUANTUM ELECTRONICS CONFERENCE

JUNE 14–19, 1992 • VIENNA • AUSTRIA

In cooperation with

American Physical Society
European Physical Society
International Union of Pure and Applied Physics
Lasers and Electro-Optics Society of IEEE
Optical Society of America

TECHNICAL DIGEST

Austria. The modified QUANTEL laser as transmitter delivers 10 mJ/30 ps pulses in green. To collect the echo photons, we used the Contraves 0.5 m diameter laser tracking telescope. To detect the satellite laser echoes we used the UNITED OPTO Modular Streak Camera.[1] The reflected signal passing the receiver telescope is focused on the Streak tube S25 photocathode, the output image is intensified by a gateable microchannel plate intensifier and is read out by the SIT TV camera interfaced to the IBM PC image processing system. The modular Streak Camera system provides either linear or trigger free two-dimensional sweep, both with picosecond resolution.

From the analysis we estimated the echo energy to be 1,000 up to 10,000 photons, well corresponding to the energy balancy calculation. The temporal analysis of a typical echo from the satellite STARLETTE is on Fig. 1. The first peak corresponds to a strong return already saturating the photocathode of the streak camera. The second peak is within the linear range of the streak camera system. Considering 8 ps/pixel sweep velocity, the temporal response coincides well to the 30 ps transmitted pulse and the satellite retroreflector geometry.

On the other hand, the analysis of the AJISAI echoes (Fig. 2) shows pronouced irregularities in time, due to the random contributions of several retro-reflectors. The simulations confirm this behavior with respect to the shape of this satellite, which is a sphere of 2.2 m in diameter, covered by retro cubes.

1. I. Prochazka, K. Hamal, M. Schelev, V. Postovalov, V. Lozovoi: Modular Streak Camera for Laser Ranging; published in SPIE 1385, 55.

16:45 PM
MoQ3   Non-Mechanical Laser Beam Steering with an Experimental Optical Array Antenna

W. M. NEUBERT, W. R. LEEB, and A. L. SCHOLTZ, Institut für Nachrichtentechnik und Hochfrequenztechnik, Technische Universität Wien, Gusshausstrasse 25/389, A-1040 Wien, Austria

Transferring the principle of phased array antennas from the microwave regime into optics is not straightforward due to the small wavelengths involved.[1] Path differences between the wavefronts leaving the individual subantennas of an array have to be actively controlled to within a fraction of the wavelength.[2] To this end we developed a phasing concept using a common reference wavefront of a so called pilot beam, which is slightly offset in frequency. By heterodyning the pilot beam with representative samples of the individual subwavefronts, the optical phases are transformed into electrical phases at intermediate frequency signals. They permit phasing via heterodyne phase-locked loops.

To verify our concept we designed an optical antenna group consisting of three subapertures fed by a single diode-pumped Nd:YAG ring laser operating at $\lambda = 1.06$ μm. The pilot beam was generated by acousto-optically frequency shifting a small portion of the array feeding laser beam.

The phasing quality experimentally obtained was excellent. Figure 1(a) depicts the measured far-field intensity pattern. The corresponding calculated pattern assuming ideal phasing (see Fig. 1(b)) shows near-perfect agreement both qualitatively and quantitatively. By electronically setting the phase differences between the subantenna fields we demonstrated the expected beam steering effect. Figure 2 shows the measured far-field intensity pattern for the case that one subfield is phase shifted by 1 rad. For a steering angle of 10% of the diffraction limited divergence of a single subaperture, the antenna gain inherently decreases by 0.12 dB. The measured settling time of a commanded steering angle amounts to about 0.7 ms. It is mainly determined by the response of the phase actuators employed, i.e. by piezo-electric fiber stretchers.

Optical array antennas may be applied, e. g., for optical space radar and communication systems. By coherently combining the power of several lasers, each feeding a subantenna, high optical transmit power can be achieved. Besides the advantageous inertia-free and hence fast beam steering capability, optical array antennas have reduced size, mass, and cost as compared to a single large antenna.

1.   J. S. Fender, Proc. SPIE **643**, 122 (1986).

2.   W. M. Neubert, Proc. SPIE **1417**, 122 (1991).

17:00 PM
MoQ4   A Metrology System for the Active Control of a Large Radio Telescope

J. M. PAYNE, National Radio Astronomy Observatory, 949 N. Cherry Ave., Campus Bldg. 65, Tucson, Arizona 85721-0655, USA

The National Radio Astronomy Observatory (NRAO) is constructing a radio telescope of 100-meter diameter clear aperture designed to operate at wavelengths as short as 3 mm.

The precision which may be maintained in a steel structure of this size in the open air is determined by environmental changes, the most significant being wind and temperature. In fact it may be shown that, even in the absence of wind, unavoidable temperature differences result in an abort wavelength limit of approximately 8 mm for a steel structure of this size. The solution adopted is to construct the reflecting parabolic surface from two thousand individual panels mounted to the back-up structure with adjustable linear actuators. A metrology system monitors the shape of the reflecting surface continuously and the necessary corrections to the surface are applied through the linear actuators.

The metrology system described in this paper uses three laser range measurement systems to measure 2,000 points on the reflector surface by trilateration. Consideration of the precision required together with the dynamics of the structure lead to the basic requirements of the rangefinder. The performance required is to measure five ranges per second to an accuracy of better than 50 microns. These ranges may be from 20 meters to 120 meters.

The paper describes an instrument that satisfies these requirements. A series of tests over ranges up to 120 meters is described that demonstrates that neither atmospheric turbulence

nor bulk refractive index changes will impose unacceptable limits on the performance of the instrument. Tests made with three such instruments used in the trilateration configuration demonstrate that the required precision in three dimensions may be achieved.

17:15 PM
MoQ5   Characteristics of a Dual Diode Laser-Based Feedback Interferometer with Appliactions for Extended Ranging and Directional Discrimination

W. M. WANG, W. J. O. BOYLE, K. T. V. GRATTAN, and A. W. PALMER, Measurement and Instrumentation Centre, Department of Electrical, Electronic and Information Engineering, City University, Northampton Square, London EC1V 0HB, England

Self-mixing interference in a diode laser has been extensively studied for various applications including velocity measurement, ranging, acoustic sensing and displacement measurement.[1-4] The self-mixing technique, based on the use of a diode laser shows some advantages in simplicity, compactness and robustness compared with conventional interferometric methods, and it also shows the ability to achieve directional discrimination of the phase movement, but, however, the useful directional information will disappear if the feedback strength from external reflector is weak. In addition, there is an increasing requirement for extended ranging with high accuracy. This can be achieved by using a multi-wavelength interferometer,[5] but the systems based on this are quite bulky and complicated.

In this work, the characteristics of a dual diode laser-based feedback interferometer are described, based on the self-mixing interference in diode lasers. The lasers used were Sharp LT022MD AlGaAs index-guided diode lasers with wavelengths of 783 nm and 784 nm at a normal output of 3 mW. The optical emissions from these two lasers were coupled with a single-mode fibre optical coupler, with one output arm of the coupler used as a sensing probe. The light reflected from the fibre end and from the external reflector interfered and was fed back via the original optical path into both laser cavities. The signal ouputs from the laser internal photo detectors were monitored with an oscilloscope. It has been found that the resultant intensity modulation of each laser is dependent on the feedback strength and the distance of external reflector, and the cross-interference between the two lasers has little influence on each signal output due to the wavelength selectivity of laser itself. Nevertheless, the phase of the intensity modulation is determined by its own lasing wavelength and the Common Optical Path Difference (COPD) between the fibre end and the external reflector. The phase difference between these two outputs is, therefore, determined by the COPD and the synthetic wavelength of two lasers. By measuring this phase difference, the distance D between the fibre end and the reflector can be determined. Since the synthetic wavelength can be made much larger than those of the source lasers, for example 0.6 mm here, the unambiguous distance to be measured can be

made very large. This is similar to a conventional multi-wavelength interferometer. Furthermore, if D is adjusted to make the phase difference be $\pi/2$ radians, the two output signals can readily be used for directional discrimination in optical sensing, for example, laser Doppler velocimetry or small vibrational measurement.

In summary, the feasibility of the dual diode laser-based feedback interferometer has been demonstrated and the preliminary experimental results are presented. The method used highlights the simplicity of the operation with the ability of extended ranging and directional discrimination, particularly, with a fibre optical scheme where the system has simpler configuration and higher signal-to-noise ratio than that of conventional systems.

1. S. Shinohara, A. Mochizuki, H. Yoshida, and M. Sumi "Laser Doppler velocimeter using the self-mixing effect of a semiconductor laser diode" Appl. Opt. **25**, pp. 1417–1419, 1986.

2. P. J. de Groot, G. M. Gallatin, and S. H. Macomber "Ranging and velocimetry signal generation in a backscatter-modulated laser diode" Appl. Opt. **27**, pp. 4475–4480, 1988

3. A. Dandrige, R. O. Miles, and T. G. Giallorenzi "Diode laser sensor" Electron. Lett. **16**, pp. 948–949, 1980.

4. W. M. Wang, W. J. O. Boyle, K. T. V. Grattan, and A. W. Palmer "An interferometer incorporating active optical feedback from a diode laser with applications to coherent ranging and vibrational measurement" Paper presented at the 8th Optical Fiber Sensors conference, Monterey, CA, USA, 29–31, Jan. 1992.

5. P. de Groot "Three-color laser-diode interferometer" Appl. Opt. **30**, pp. 3612–3616, 1991.

17:30 PM   Invited paper

MoQ6   Application of High-Average-Power, Visible Lasers at Lawrence Livermore National Laboratory to Commercial and Scientific Problems

B. E. WARNER, R. P. HACKEL, S. R. HARGROVE, H. W. FRIEDMAN, and J. A. PAISNER, University of California, Lawrence Livermore National Laboratory, P. O. Box 5508, L-464 Livermore, California 94550, USA

The Lawrence Livermore National Laboratory's (LLNL) Atomic Vapor Laser Isotope Separation (AVLIS) Program has developed a high-average-power, pulsed, tunable, visible laser system. Testing of this hardware is in progress at industrial scales. The laser demonstration facility (LDF) system consists of copper vapor lasers arranged in oscillator-amplifier chains providing optical pump power to dye-laser master-oscillator-power-amplifier chains. This system is capable of thousands of watts (average) tunable between 550 and 650 nm. In the last several years, a number of other applications of AVLIS laser technology have been recognized and pursued at LLNL. Two of these to be dicussed in this presentation are laser material processing and atmospheric correction of astronomical telescopes. This presentation is divided into three parts: laser system

summary, laser material processing with high brightness lasers, and sodium beacon generation for atmospheric correction.

The copper laser system at LLNL consists of 12 chains operating continuously. The copper lasers operate at nominally 4.5 kHz, with 50 ns pulse widths and produce 20 W at near the diffraction limit from oscillators and > 250 W from each amplifier. Chains consist of an oscillator and three amplifiers and produce > 750 W average, with availablities > 90% (i. e., > 7900 h/y). The total copper laser system power averages ~ 9000 W and has operated at over 10,000 W for extended intervals. The 12 copper laser beams are multiplexed and delivered to the dye laser system where they pump multiple dye laser chains. Each dye laser chain consists of a master oscillator and three or four power amplifiers. The master oscillator operates at nominally 100 mW with a 50 MHz single mode bandwidth. Amplifiers are designed to efficiently amplify the dye beam with low ASE content and high optical quality. Sustained dye chain powers are > 1000 W average with dye conversion efficiencies > 50%, ASE content < 5%, and wave front qualities correctable to < $\lambda/10$ RMS, using deformable mirrors. Since the timing of the copper laser chains can be offset, the dye laser system is capable of repetition rates which are 4.4 kHz, up to 26.4 kHz, limited by the dye pumping system.

Key laser material processing applications in industry include cutting, welding, drilling, surface heat treatment, and marking of metals and nonmetals. At the present CO_2 lasers and solid-state (Nd: YAG) lasers dominate these applications in industry. Excimer lasers are finding a growing number of lower applications in microlithography, micromachining, and marking. Our copper and dye laser system are high radiance laser sources because of their visible wavelength, near diffraction limited beam quality, and high-average power. They show promise in improving material throughput and in increasing precision, particularly with fine-hole drilling and cutting. We are currently using both high-power dye and copper laser beams to map out precision cutting and hole drilling operating regimes. In addition, we are developing diagnostics to better understand the high-radiance-laser/material interactions.

Over the last two years LLNL has started a research initiative into development of laser guide stars and adaptive optics to correct atmospheric distortion for large astronomical telescopes. The principles are well known: a laser creates a point source in the upper atmosphere and by observing the aberrated wave front from this "star," a deformable mirror can be adjusted to cancel out the effects of atmospheric turbulence. The unique capability that LLNL brings to this research is a reliable, high-power, near diffraction limited, tunable laser system. We plan in 1992 to propagate nominally 1 kW of 590 nm light into the atmosphere, creating a bright sodium-layer guide star. The first phase of this research investigates properties of sodium guide stars and identifies issues in adaptive optics. Our goal over the next several years, in cooperation with a broad research community, is to develop an integrated laser/adaptive optics capability for large astronomical telescopes, including the Keck 10 meter telescope.
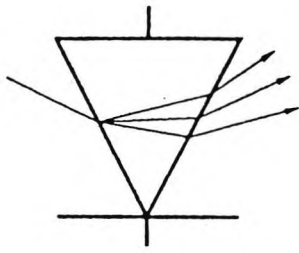
Applied Optics and Opto-Electronics

14-17 September 1992
Leeds

Organised by:
The Applied Optics Division
of
The Institute of Physics

IOP

CHARACTERISTICS OF A DIODE LASER-BASED SELF MIXING INTERFEROMETER

W M Wang, W J O Boyle, K T V Grattan, A W Palmer
City University, London

A diode laser-based interferometer, utilizing the self-mixing effect, has been described and a theoretical model, discussing intensity modulation by external optical feedback, is presented. The sensitivity of this intensity modulation to the laser injection current was measured, indicating that a relatively optimal operating current condition is about 1.2Ith for self-mixing interference.

The behaviour of a continuously operating semiconductor laser can be significantly affected by external optical feedback. For practical use, it has exploited for laser Doppler velocimetry (LDV) [1], ranging [2] and displacement measurement [3]. Recently there is a growing interest in the applications in the interferometry of the self-mixing effect in diode lasers because of some significant advantages of such techniques, such as simplicity, compactness, and ease of alignment. In the self-mixing configuration a portion of the emitting light from a diode laser is intentionally reflected by an external reflecting surface, back into the laser cavity the reflected light then mixing coherently with the light inside the cavity and this modulates the laser output intensity, which may be monitored by photodetectors at either end of the laser or simply by the internal photodetector accommodated at the rear facet of a commercially available diode package. In the latter case the laser is used not only as a light source but also, from the optical point of view, as part of an interferometer as well as incorporating a self-aligning detector, which greatly simplifies the system configuration.

The self-mixing interferometer can be generally considered as equivalent to an external cavity laser. The output intensity, I, of the laser in the presence of weak external feedback may thus be expressed as [4]:

$$I = I_0[1 + m cos p(L)] \qquad (1)$$

With

$$p(L) = 4\pi v_0 \frac{L}{C} - \frac{C \sin\left(4\pi v_0 \frac{L}{C} + \varphi_0\right)}{1 + C\cos\left(4\pi v_0 \frac{L}{C} + \varphi_0\right)} \qquad (2)$$

$$C = \frac{L}{nl}\xi\sqrt{1+\alpha^2} \qquad (3)$$

where I_0 is the laser output intensity in the absence of feedback; m is termed the modulation coefficient related to the internal parameters of the diode laser and the feedback stregth; n is the effective refractive index of the laser cavity; l is the laser cavity length; $\varphi_0 = \tan^{-1}(\alpha)$ with α the linewidth enhancement factor; ζ is the ratio of the amplitudes between the laser facet reflection and

the feedback inluding coupling loss and geometry effect; C is termed the feedback coefficient. The condition of external feedback changes not only the lasing threshold but also the lasing spectral distribution. The threshold gain variation thus results in optical intensity modulation, while the actual lasing spectrum variations lead to a saw tooth-like modulation waveform and change the coherent properties of the feedback. When the external reflector is modulated periodically, the output, I, also shows a periodical characteristic with one period corresponding to an optical displacement of $\lambda/2$ of the oscillation wavelength. For a small value of the feedback coefficient C, the intensity modulation is sinusoidal, but for the larger value of C the output waveform becomes saw tooth-like. This relationship between I and the external phase is depicted in graphical form, as shown in Figure 1.
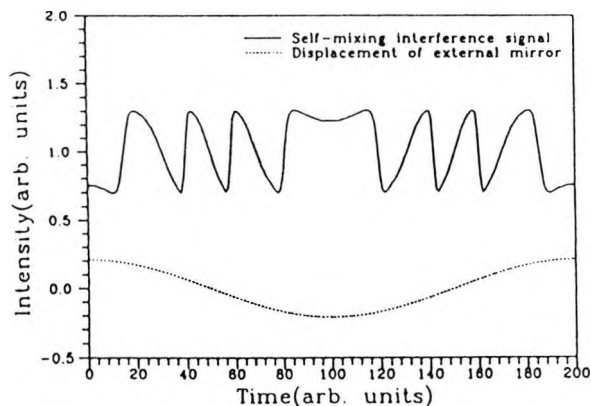
Figure 1 Intensity modulation by self-mixing interference
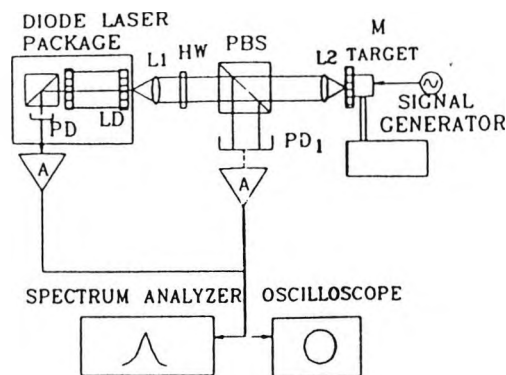
Figure 2 Experimental arrangement for self-mixing interference

A schematic diagram of the "self-mixing interferometer" is shown in Figure 2, which consists basically of a single mode laser (Sharp LT024) and an external reflector, R_3. The light emitted from the laser, LD, was collimated by a lens L_1, and propogated through a half wave-length plate, HW, and then onto a polarizing beam splitter. PBS. One beam was detected by a photodetector, PD_1, for comparison; the other focused by a further lens,L_2, onto a focused target M, represented by a white vibrating loud speaker cone. The light reflected from the laser front facet and from the external target mixed coherently to produce an intensity modulation in the laser output, which was detected by the internal photodiode,PD, accommodated in the rear facet of the laser. The light inside the laser cavity and that reflected from the taget actually constitute two interfering optical beams of the self-mixing interferometer with self-aligning, aelf-detecting features and only one optical axis.

The feedback strength could be adjusted by changing the ratio of two split beams by means of a rotation of the waveplate. The experiments were carried out under the condition of the feedback strength measured by PD_1 being less than 4% (the feedback strength depends on the coupling from the external feedback into the laser cavity, so it is difficult to give as absolute value). If the feedback is too large, it may lead to an unstable output of the

laser.
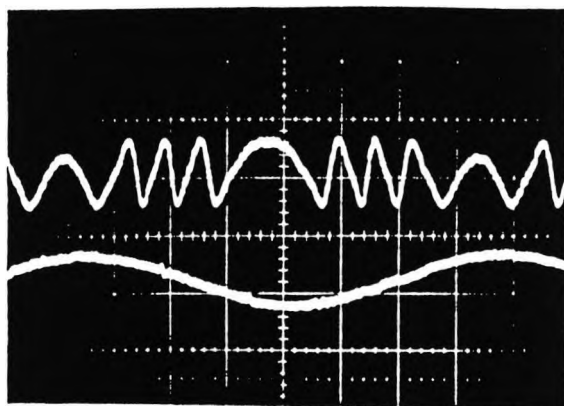
Figure 3: Experimental observation of self-mixing interference

A typical self-mixing interference signal is shown in Figure 3, where the lower trace is the signal with which the external mirror vibration is driven and the resultant intensity modulation (upper trace) shows a 2π periodicity, with respect to the phase change at the mirror. One fringe change corresponds to a half-wavelength displacement of the mirror, which is the same as that of a conventional interferometer. However, the signal obtained shows two significant differences from that of a conventional interferometer. First, it is saw tooth-like but not sinusoidal, and secondly it is asymmetric relative to the direction of the phase variation, from which it is important to note that the inclination of the signal is dependent on the direction of the mirror movement, and when the mirror changes its movement direction, the signal changes its inclination. The intensity modulation was also observed from two emission directions of the laser output, which indicates a sign inversion in both directions.

To investigate the relationship between the self-mixing interference and the injection current of the laser, the current was varied from $0.8I_{th}$ to $1.6I_{th}$, where I_{th} is the threshold current. The modulation amplitude was found to decrease with an increase in the injection current. Close to threshold, the modulation sensitivity reached its maximum value; unfortunately, the intensity modulation around threshold was unstable, whilst the sensitivity was very small when the laser was operated well above the threshold. In the experiments reported the laser current was chosen to be $1.2I_{th}$ where the output modulation signal was stable and had a good sensitivity related to variation of the external feedback strength.

In summary, a self-mixing interferometer using a single mode diode laser has been described. The device shows significant advantages in simplicity, compactness and robustness over conventional interferometric methods. It has been shown that simple theoretical analysis is in good agreement with the experimental results.

References

[1] S Shinohara, A Mochizuki, H Yoshida, M Sumi, Appl.Opt.25,1417 (1986).

[2] P J Groot, G M Gallatin, S H Macomber, Appl.Opt 27, 4475 (1988)

[3] T Yoshino, M Nara, S Mnatzakenian, B Lee, T Strand, Appl.Opt.26 892 (1987)

[4] W M Wang, W J O Boyle, K T V Grattan, A W Palmer, "Theory of self-mixing interference in a sinlge-mode diode laser" to be published on Applied Optics

Self-mixing interference in a diode laser: experimental observations and theoretical analysis

W. M. Wang, W. J. O. Boyle, K. T. V. Grattan, and A. W. Palmer

The experimental results of an investigation of self-mixing effects or backscatter modulation in diode lasers coupled with a simple theoretical analysis are presented. The laser is used to send light, either in free space or through an optical fiber, to a movable target from which the optical backscatter is detected and fed back into the laser. In the experiment three significant conclusions are drawn: (1) self-mixing interference is not dependent on the coherence length of the laser, (2) the interference is not dependent on the use of a single-mode or multimode laser as the source, and (3) the interference is independent of the type of fiber employed, i.e., whether it is single mode or multimode. A comparison of this kind of interference with that in a conventional interferometer shows that self-mixing interference has the same phase sensitivity as that of the conventional arrangement, the modulation depth of the interference is comparable with that of a conventional interferometer, and the direction of the phase movement can be obtained from the interference signal. The above factors have implications for the optical sensing of a wide range of physical parameters. Several applications of the method are discussed that highlight the significant advantages of simplicity, compactness, and robustness as well as the self-aligning and self-detecting abilities of fiber-based self-mixing interferometry when compared with the use of conventional interference methods.

1. Introduction

The output characteristics of a single-mode semiconductor laser are greatly affected by external optical feedback, as is discussed in the research of a number or authors.[1-15] In practical applications, the effects of external optical feedback lie in the following two areas: (1) spectral linewidth reduction,[7-9] whereby the spectral purity of a laser is enhanced by optical feedback from an external cavity and which is of relevance to coherent optical communications, high-density frequency-division multiplexing systems, and interferometric sensors; and (2) self-mixing interferometry,[10,16-26] where external feedback is used to carry information from which data may be extracted.

External optical feedback is also of interest because of the deleterious effects in many applications caused by reflections from various optical components into

The authors are with the Department of Electrical, Electronic, and Information Engineering, Measurement and Instrumentation Centre, City University, Northampton Square, London, EC1V 0HB, England.

the laser cavity,[11-13] e.g., from fiber ends or in a major application from the surfaces in compact discs, which can increase intensity noise and modify the coherence properties of laser diodes.[14] A dramatic effect of this nature has been described by Lenstra et al.,[15] who termed it "coherence collapse." Here feedback increases the spectral linewidth of the laser to many times that of the solitary laser linewidth, with a consequential collapse in the coherent length of the laser from several meters to a few millimeters.

Since the approach of self-mixing was first reported by Rudd[16] by using the He–Ne laser to measure the Doppler velocity of scattering particles, the phenomenon of self-mixing or backscatter modulation has been investigated by several researchers. A simple diode laser sensor was reported by Dandridge et al.[17] for acoustic sensing. Churnside[18,19] studied laser Doppler velocimetry by using a modulated CO_2 laser in 1984. Later, a small laser Doppler velocimeter was reported by Shinohara et al.,[20] who used the self-mixing effect in a semiconductor laser. Based on their experimental results Shimizu[21] found that the direction of the Doppler velocity could be determined from the inclination of the sawtoothlike waveforms observed in the self-mixing signal, which reverses when the direction of movement of the target

is reversed. Jentink et al.[22] simply explained self-mixing in terms of the interference between the light inside the laser cavity and the light re-entering the laser cavity. This is an oversimplified assumption that leads to the misinterpretation that the spectral linewidth of the laser mode of the multimode laser diode used in the experiments was less than 2×10^{-3} nm. This linewidth corresponds to an unusually long coherence length (160 mm) for a multimode laser, which conflicts with their own measurements for the linewidth, using conventional interferometry, of 4.6 nm.

A theory of self-mixing has been developed by de Groot et al.[23] that is based on the mode structure of a three-mirror Fabry–Perot cavity. They applied this approach to the analysis of coherent ranging and velocimetry measurement with self-mixing.[23,24] With the use of the multimode laser diode, de Groot[25] explained the self-mixing effect as a spectral mode modulation that was dependent on the phase of the returned light. Koelink et al.[26] used the self-mixing effect in a fiber-coupled semiconductor laser for in vivo blood-flow measurement.[26] They presented a theoretical model that was based on a series of internal laser-parameter variations produced by external optical feedback to explain and thus calculate the nature of the modulation signals in the self-mixing laser cavity.

To date, various theoretical models have been used to explain the observed phenomena in the self-mixing process, but the modulation mechanism of external optical feedback on the laser output is not well understood. For example, the main observed phenomena lie in the production of direction-dependent sawtoothlike signals,[21] the waveform-sign inversion between the two emission directions,[23] the independence of the coherence length of the laser used, and particularly in self-mixing phenomena in a multimode laser.[10] It is obvious that some phenomena observed with external optical feedback are dramatically different from those of conventional interferometry, and they cannot be explained simply by using existing coherent interference theory.

It is well known that any laser oscillation is based on the principle of positive feedback and that the establishment of a stable laser oscillation must meet the amplitude and the phase conditions of the oscillation, which means that the amount of amplified light in a complete round trip inside the laser cavity becomes equal to the total light lost through the side of the cavity, by the mirror facets and by absorption in the active medium.[27] The presence of external optical feedback affects not only the laser threshold but also its spectral distribution.[28] The intensity modulation produced by external feedback has consequences in the variation of the threshold and the optical spectrum and is a fruitful area for study.

Here we present experimental results obtained on the use of optical feedback in optical sensing applications; we use a simple theoretical model to explain the experimental results observed. The aim has not

been to provide a full theoretical description but to give a simple and adequate analysis. Because self-mixing interference requires the consideration of only one optical axis, in addition to the use of fewer optical components (and is self-aligning as well as self-detecting), it presents significant advantages in compactness, simplicity, robustness, and ease of alignment in comparison with the conventional interferometer. In particular, in fiber-coupled systems this method provides a simpler optical arrangement with easily alignable components and a comparatively large signal-to-noise ratio.

2. Experimental

The experimental scheme used to investigate the effects of external feedback and self-mixing interference is shown in Fig. 1. In this scheme light from a V-channel substrate inner-stripe-type AlGaAs laser diode (Sharp Model LT022MC) with a wavelength of 780 nm was collimated by a lens L1 and focused by a further lens L2 on the target T, which is represented by a white reflective surface attached to a loudspeaker cone driven by a signal generator, to provide a phase variation of external optical feedback. The diode laser incorporates a photodiode accommodated in the rear facet for monitoring for the laser power. This characteristic of the device is particularly well suited to observing the self-mixing interference and provides a convenient internal detector. A typical output obtained from this photodiode is shown in Fig. 2. The feedback strength measured from the laser front facet was ~4%, and the maximum feedback strength observed was estimated to be less than ~10% in all experiments. The upper trace in Fig. 2 is the signal applied to achieve the periodic target movement, and the resultant intensity modulation (lower trace) is the self-mixing interference signal observed. To observe the self-mixing interference at different positions from the laser, we mount the lens L2 and the target T on a movable table that is controlled by a stepper motor, which makes it possible for the distance from the laser to the target to be adjusted by the motor.

Fig. 1. Schematic experimental arrangement: PD, photodiode (integral); LD, laser diode, A, amplifier; D, distance; L1, L2, lenses.

is reversed. Jentink et al.[22] simply explained self-mixing in terms of the interference between the light inside the laser cavity and the light re-entering the laser cavity. This is an oversimplified assumption that leads to the misinterpretation that the spectral linewidth of the laser mode of the multimode laser diode used in the experiments was less than 2×10^{-3} nm. This linewidth corresponds to an unusually long coherence length (160 mm) for a multimode laser, which conflicts with their own measurements for the linewidth, using conventional interferometry, of 4.6 nm.

A theory of self-mixing has been developed by de Groot et al.[23] that is based on the mode structure of a three-mirror Fabry–Perot cavity. They applied this approach to the analysis of coherent ranging and velocimetry measurement with self-mixing.[23,24] With the use of the multimode laser diode, de Groot[25] explained the self-mixing effect as a spectral mode modulation that was dependent on the phase of the returned light. Koelink et al.[26] used the self-mixing effect in a fiber-coupled semiconductor laser for in vivo blood-flow measurement.[26] They presented a theoretical model that was based on a series of internal laser-parameter variations produced by external optical feedback to explain and thus calculate the nature of the modulation signals in the self-mixing laser cavity.

To date, various theoretical models have been used to explain the observed phenomena in the self-mixing process, but the modulation mechanism of external optical feedback on the laser output is not well understood. For example, the main observed phenomena lie in the production of direction-dependent sawtoothlike signals,[21] the waveform-sign inversion between the two emission directions,[23] the independence of the coherence length of the laser used, and particularly in self-mixing phenomena in a multimode laser.[10] It is obvious that some phenomena observed with external optical feedback are dramatically different from those of conventional interferometry, and they cannot be explained simply by using existing coherent interference theory.

It is well known that any laser oscillation is based on the principle of positive feedback and that the establishment of a stable laser oscillation must meet the amplitude and the phase conditions of the oscillation, which means that the amount of amplified light in a complete round trip inside the laser cavity becomes equal to the total light lost through the side of the cavity, by the mirror facets and by absorption in the active medium.[27] The presence of external optical feedback affects not only the laser threshold but also its spectral distribution.[28] The intensity modulation produced by external feedback has consequences in the variation of the threshold and the optical spectrum and is a fruitful area for study.

Here we present experimental results obtained on the use of optical feedback in optical sensing applications; we use a simple theoretical model to explain the experimental results observed. The aim has not

been to provide a full theoretical description but to give a simple and adequate analysis. Because self-mixing interference requires the consideration of only one optical axis, in addition to the use of fewer optical components (and is self-aligning as well as self-detecting), it presents significant advantages in compactness, simplicity, robustness, and ease of alignment in comparison with the conventional interferometer. In particular, in fiber-coupled systems this method provides a simpler optical arrangement with easily alignable components and a comparatively large signal-to-noise ratio.

2. Experimental

The experimental scheme used to investigate the effects of external feedback and self-mixing interference is shown in Fig. 1. In this scheme light from a V-channel substrate inner-stripe-type AlGaAs laser diode (Sharp Model LT022MC) with a wavelength of 780 nm was collimated by a lens L1 and focused by a further lens L2 on the target T, which is represented by a white reflective surface attached to a loudspeaker cone driven by a signal generator, to provide a phase variation of external optical feedback. The diode laser incorporates a photodiode accommodated in the rear facet for monitoring for the laser power. This characteristic of the device is particularly well suited to observing the self-mixing interference and provides a convenient internal detector. A typical output obtained from this photodiode is shown in Fig. 2. The feedback strength measured from the laser front facet was ~ 4%, and the maximum feedback strength observed was estimated to be less than ~ 10% in all experiments. The upper trace in Fig. 2 is the signal applied to achieve the periodic target movement, and the resultant intensity modulation (lower trace) is the self-mixing interference signal observed. To observe the self-mixing interference at different positions from the laser, we mount the lens L2 and the target T on a movable table that is controlled by a stepper motor, which makes it possible for the distance from the laser to the target to be adjusted by the motor.

Fig. 1 Schematic experimental arrangement: PD, photodiode (integral); LD, laser diode; A, amplifier; D, distance; L1, L2, lenses.

Fig. 2. Typical interference signals observed from self-mixing (vertical axis, arbitrary units; horizontal axis, 0.2 ms/division).

One of the useful characteristics of the laser we used is that different output modes correspond to different values of diode forward current, giving a multimode laser output at ~ 1 mW and a single-mode output above ~ 3 mW of optical power. This output permits an investigation of the self-mixing interference by using different laser modes but with no change of the experimental arrangement. The basic coherence characteristics of the laser used in the experiments were measured with a two-beam Michelson interferometer at ~ 2.5 mW output power, as shown in Fig. 3. In summary these characteristics were: (1) the optical spacing between the adjacent coherent regions was 2.10 mm, which is equal to twice the optical length of the cavity; (2) FWHM of each coherent region was 0.22 mm; and (3) the FWHM of the envelope of all of the coherent regions was 6.15 mm, and the interference was not detectable when the optical path difference (OPD) was greater than 9.30 mm.
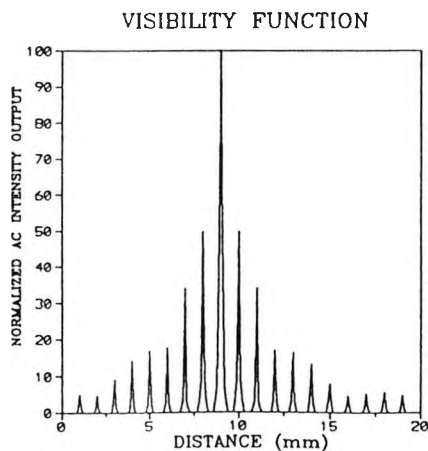
In the self-mixing experiments carried out the target was adjusted from a initial position of ~ 40 mm in front of the laser to a maximum distance of 60 mm. The measured undulation output, P_m, corresponding to a given distance, D_0, is shown in Fig. 4. Signals were detected up to a maximum position of ~ 1000 mm from the laser. The modulation amplitude shown in Fig. 4 is a function of the target distance D. The periodicity of the signals corresponds to a distance of ~ 1.0 mm, which corresponds to the optical length nl of the laser cavity, where n is the effective-refractive index of the laser medium and l is the physical length of the laser cavity. Further, when the laser is operated in the multimode regime each lasing mode produces an optical intensity, the total of which is the direct superposition of the intensity of each of the different modes without taking dispersion into account in the multimode laser cavity. Another feature of the multimode self-mixing is that the maximum amplitudes do not show significant attenuation with distance. This lack of significant attenuation shows that the interference effect in the self-mixing arrangement is independent of the OPD between the laser and the target.

To investigate this phenomenon further, we used two long multimode fibers, one ~ 3.48 m and the other ~ 10.10 m in length, with core diameters of 50 μm to provide extended values of the OPD well outside the coherence length of the source. In the experimental scheme to analyze this phenomenon as shown in Fig. 5, the light emitted from the fiber is reflected back into the cavity by a mirror. The result of this experiment was that the same type of signal output as shown in Fig. 2 was observed.

To rule out the possibility of these signals being caused by interference in the small cavity formed between the end of the fiber and the mirror, we employed pseudohetrodyne interferometry.[29] In this technique the laser is current modulated by a triangular wave (500 Hz) with a peak-to-peak modulation current amplitude of 0.1 mA, which produces a chirp frequency modulation of the optical frequency. Interference therefore occurs between two beams,

VISIBILITY FUNCTION

Fig. 3. Visibility function obtained from the multimode laser diode (with output power of 2.5 mW) and determined with a Michelson interferometer.

SELF—MIXING MODULATION FUNCTION
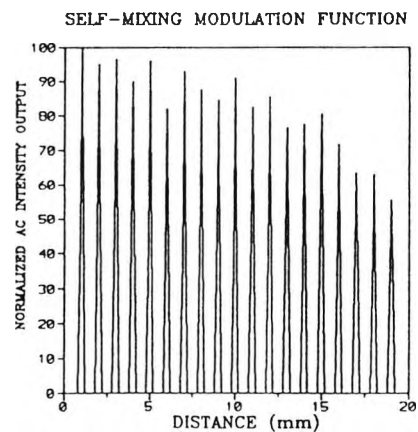
Fig. 4. Dependence of a self-mixing interference profile (for a multimode laser diode) on the distance of the external reflector from the laser.
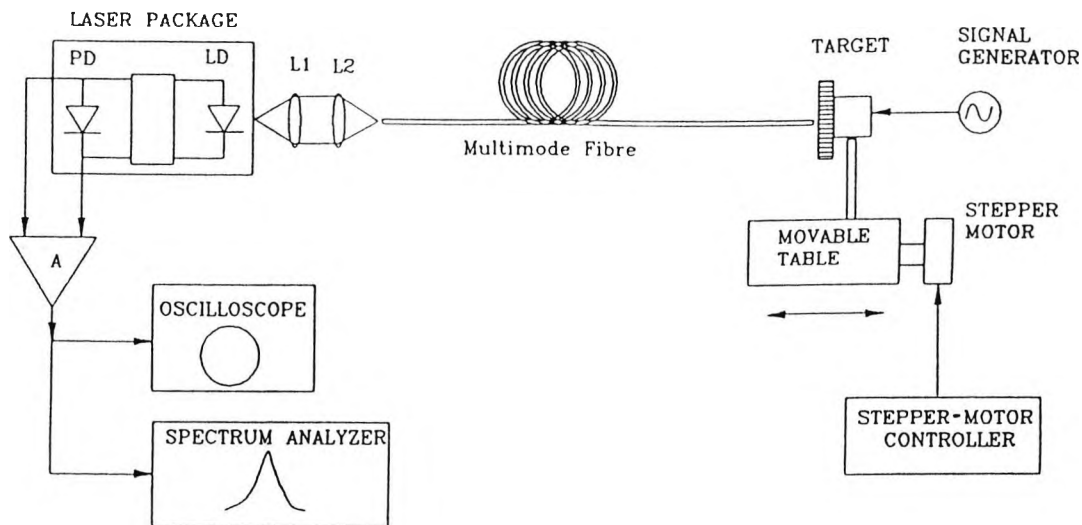
Fig. 5. Schematic experimental arrangement with a long multimode fiber between a laser and target. PD, photodiode; LD, laser diode; L1, L2, lenses; A, amplifier.

one from the laser and a second that is time delayed and reflected from the mirror at the end of the fiber, at a beat frequency that is proportional to the OPD between the beams. With the small value of the modulation current used in this experiment, the OPD of the cavity formed by the end of the fiber and the target (typical OPD = 1 mm), or even possibly from the feedback of the reflections from the end of the fiber nearest the laser (typical OPD = 30 mm), is insufficient to produce a beat-frequency signal. A beat frequency could only result from the feedback from the far end of the fiber, at a frequency proportional to the OPD between the laser and the mirror. Figure 6 shows the beat frequencies observed in these experiments. In Fig. 6(a) the beat signal is produced by the reflection from the far end of the fiber without the mirror, whereas in Fig. 6(b) the beat signal results from the reflection from the mirror itself.

It is easy to see that the two signals have the same frequency (but a different amplitude), which is proportional to the different reflectivities of the fiber end and the mirror. The frequency from the 3.48-m-long fiber is measured to be 5.0 kHz and is calculated to be 5.14 kHz (with a frequency-modulation coefficient of 2.6 GHz/mA). The frequency from the 10.10-m-long fiber is measured at 15.0 kHz and is calculated to be 14.64 kHz. The experimental results are in good agreement with the theoretical calculations (as we discuss later), and for practical use an improvement of the frequency-detecting technique and the accurate measurement of the frequency-modulation coefficient could be performed. In this research the frequencies were simply interpreted from the oscilloscope trace.

In the experiment with the 10.10-m-long fiber the signal obtained from the reflections from the mirror was observed to increase when it was adjusted away from the fiber end face, as there was no signal from the reflection from the end face of the fiber. When

(a)

(b)
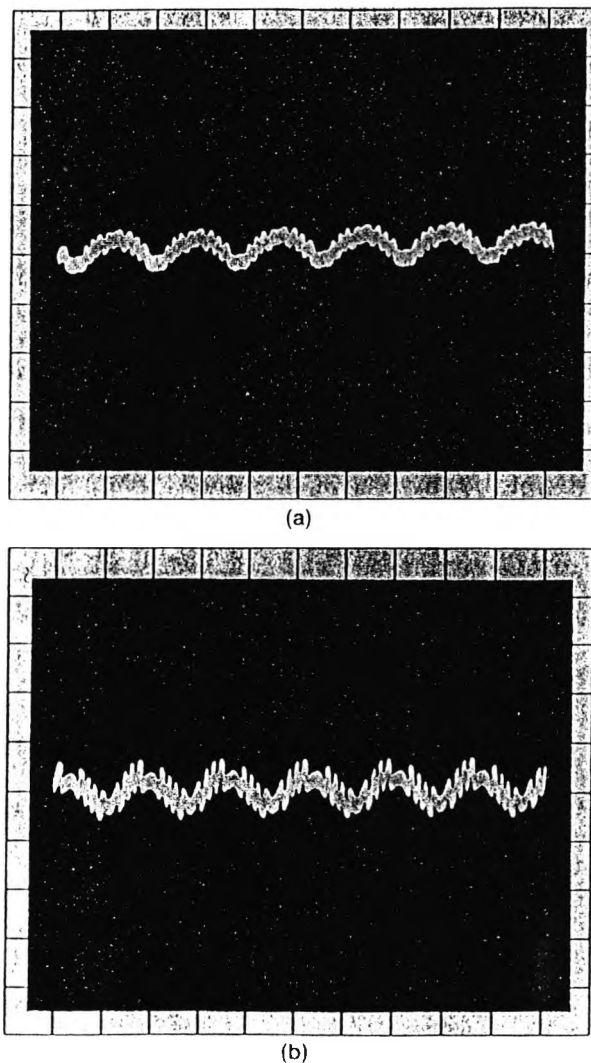
Fig. 6. Current modulation and beat signals (a) without and (b) with mirror reflection (Vertical scale, arbitrary units; horizontal axis, 1.0 ms/division).

the mirror was adjusted to a position further from the end face the signal returned to a minimum. This phenomenon indicates that the OPD between the fiber end and the laser probably resulted in the signal having its minimum amplitude at this distance and that the signal was restored by an adjustment of the path difference with the mirror to an integer multiple of the laser cavity length.

Figure 7 shows the sawtoothlike signal output and its dependence on the direction. To achieve this signal-output dependence we drove the mirror by a sinusoidal wave generator, and it can be seen that while the wave changes its direction the signal changes its inclination. The laser was operated in both the single-mode and multimode cases; in both instances the self-mixing interference is easily observed, with the results showing no significant differences. A experimental comparison of self-mixing interferometry with conventional two-beam Michelson interferometry has been carried out. In this comparison a diode laser was coupled to a multimode optical fiber coupler, with one output of the coupler used as a source for a two-beam Michelson interferometer and the other used as the sensing probe of the self-mixing interferometer. The experimental arrangement is depicted schematically in Fig. 8, and the intensity-modulation signals from both interferometers are shown in Fig. 9 with the same driven signal simultaneously applied to both mirrors M1 and M3. It can be seen that the two signals have a similar intensity modulation with respect to the phase variation at the interferometers, which means that their periodicity is equal to half of the laser wavelength. However, the self-mixing interference shows two significant differences from that of the Michelson interferometer. First, the self-mixing interference is sawtoothlike but not sinusoidal; second, it is asymmetric relative to the external phase movement from which the direction of the phase movement can be discriminated.

We also observed the self-mixing interference pat-

Fig. 8. Schematic experimental arrangement for a comparison between self-mixing interference and conventional two-beam interference: LD, laser diode; D1, D2, photodiodes, L1–L3, lenses; A, A1, A2, amplifiers; M1–M3, mirrors; BS, beam splitter.

terns from two emission directions of the laser, using photodetectors D1 and D2 as shown in Fig. 8, and at this time we blocked one beam of the interferometer to eliminate the conventional interference effect. The result observed is shown in Fig. 10, where the two signals have a phase difference of π rad.

3. Supporting Theoretical Analysis

Various theories based on the Lang and Kobayashi equations[1] have been developed and used, primarily for explaining the spectral properties of a single-mode semiconductor laser with external optical feedback.[30–33] The power-modulation mechanism in self-mixing has been assumed to be caused by the modulation of the threshold gain of the laser.[25]

In our study here a simple theory is developed to relate to the experimental results given in Section 2. The self-mixing interferometer can generally be considered to be a simplifed external cavity laser as shown schematically in Fig. 11, where the surface of

Fig. 7. Sawtoothlike signal-output dependence on direction of phase variation.
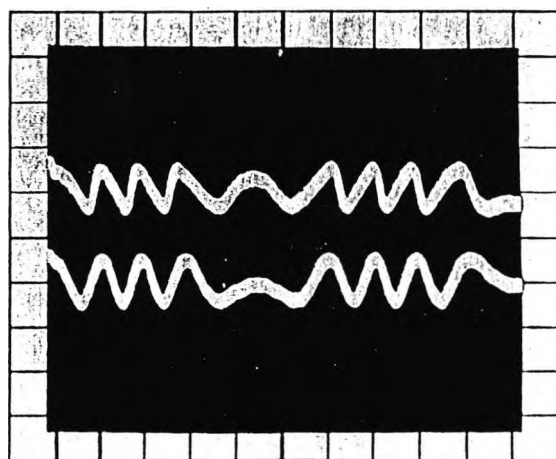
Fig. 9. Self-mixing interference patterns (upper trace) compared with conventional interference patterns lower trace) (vertical axis, arbitrary units; horizontal axis, 0.2 ms/division).
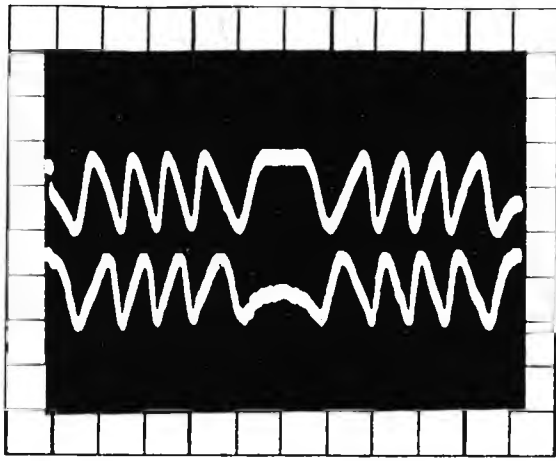
Fig. 10. Self-mixing interference signals observed in two emission directions of a laser.

the external reflector, $r3$, and one of the laser facets, $r2$, constitutes an effective laser mirror, $r2'$, the power reflectivity of which may be expressed as

$$R2' = R2[1 + \xi^2 + 2\xi \cos(2\pi\Delta L/\lambda)], \qquad (1)$$

where $R2$ is the power reflectivity of the laser facet; $\xi(= r3/r2)$ is the ratio of the amplitude reflectivity of the external reflector (including the geometric loss and the feedback-coupling efficiency) to the laser-facet amplitude reflectivity, here termed the feedback coefficient; ΔL is the OPD between the laser and the external reflector; and λ is the lasing wavelength of the laser. When a single-mode laser is operated above its threshold, without considering the external feedback, the total emitted power P_0 from the laser facets caused by stimulated emission may be given by[32]

$$P_0 = (h\upsilon)(c/n)(S/2l)\ln(1/R1R2), \qquad (2)$$

where h is Planck's constant, υ is the optical frequency of the laser, c is the velocity of light, n is the effective-refractive index of the laser cavity, S represents the photon number in the laser cavity caused by stimulated emission, l is the cavity length, and $R1$ and $R2$ are the power reflectivities of the laser facets, respectively. The presence of the external cavity changes the effective reflectivity of the laser mirror
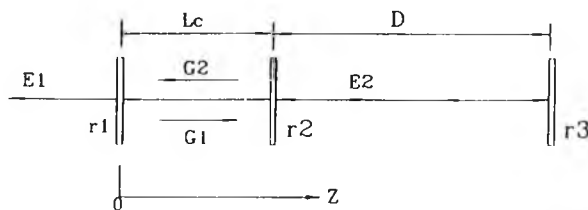
Fig. 11. Schematic of a simple laser with external optical feedback: Lc, laser-cavity length; D, distance from laser-cavity front face to target; E1, electric field from back face; E2, combined electric field from front face and reflected from target; G1, G2, forward and backward gain coefficients in the laser cavity; r1–r3, reflectivities of the laser-cavity ends and the target; Z, direction.

through Eq. (1) and therefore changes the emitting power of the laser.

The substitution of Eq. (1) into Eq. (2) under the assumption of weak optical feedback results in an emitting power from the laser of

$$P \approx P_0[1 + \zeta \cos(2\pi\Delta L/\lambda)], \qquad (3)$$

where $\zeta[= 2\xi/\ln(R1R2)]$ is related to the feedback coefficient ξ and the power reflectivity of the laser facets, which is referred to here as the modulation coefficient. Figure 12 shows the dependence of the output power on the phase $\phi(= 2\pi\Delta L/\lambda)$, which corresponds to different values of reflectivities of the external reflector. It is clear that the modulation term in relation (3) is dependent on the feedback strength and the distance of the external reflector; it is a repetitive function with a period of 2π rad (corresponding to a variation of the $\lambda/2$ displacement at the external reflector). This simple model, based on the threshold modulation, can be used to explain most of the experimental results reported earlier.

A common feature in the existing theories has been an assumption that the light fed back into the laser cavity is coherent with the light inside the laser cavity because of a similarity in the dynamic features of optical feedback to features in conventional interference.[1,33] However, similar behavior in the output was recently observed with incoherent optical feedback in semiconductor lasers,[9,34] and the use of optical fibers with a reflector distance as long as 7 km has been seen to produce similar results.[12] In the experiments reported here, the laser-power modulation by the feedback could be observed even when the external reflector was well beyond the coherence length of the laser used. It is evident from the above investigations that the output characteristics of a semiconductor laser are altered by external feedback, whether the feedback is fully coherent or incoherent with the cavity radiation. This result can be understood in the following way. The conventional coherence concept is based on a stabilized spectral output from the source used. The spectral linewidth determines the coherence length of the laser, but the
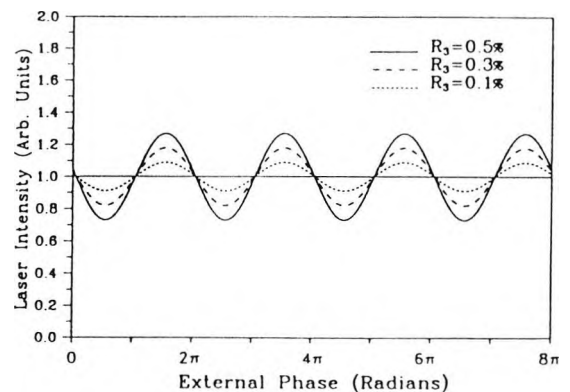
Fig. 12. Power-modulation dependence on external phase and reflectivity in self-mixing interference obtained from a theoretical model.

power modulation with the feedback was assumed to result from the spectral modulation rather than from a conventional interference effect.[25] This assumption means that the laser's modulation mechanism is dependent on the variations of the laser spectrum and its threshold and not on the coherence length itself.

The theoretical model illustrated by relation (3) describes self-mixing interference in diode lasers that is mainly due to the threshold variation produced by external optical feedback; however, the external optical feedback effect changes not only the threshold but also the laser spectrum. Therefore, a detailed theoretical analysis should consider both the variations of the threshold and the spectrum of the laser oscillation. In addition, because the laser used was operated in the multimode regime, its multimode output characteristics should be also considered. All of these factors make the theoretical analysis complicated and difficult to express in simple analytical expressions. However, the theory employed has been sufficient to provide justification of the experimental results.

4. Discussion

The main result may be summarized as follows: (1) self-mixing interference can occur from targets well outside the coherence length of the laser source; (2) the appearance of this interference signal is a harmonic function of the laser-cavity length; (3) the effect is independent of the operation of the source, whether single mode or multimode; and (4) the effect does not appear to depend on whether the fiber used to couple the source to the target is single mode or multimode. Because these significant differences between the self-mixing interference and conventional interference exist, the potential applications that use the self-mixing techniques in optical fiber sensing could be attractive. Thus we may reach the following conclusions:

First, self-mixing interference has the same phase sensitivity as that of a conventional interferometer, but its significant advantages may lead to the conventional interferometer being replaced by the self-mixing interferometer for several applications, e.g., for techniques such as Doppler velocity measurement, vibration measurement, coherent detection, or the use of heterodyne methods.

Second, self-mixing interference is not dependent on the coherence length of the source, which is a great advantage when compared with conventional interference. This makes self-mixing interference attractive for various applications such as coherent ranging, which is largely limited by the coherence length of the source. Using the self-mixing technique one can measure large OPD's, provided that sufficient optical feedback is redirected into the laser cavity. In our experiments it was shown that the beat frequency that is proportional to the distance was easily obtained by modulating the diode laser, even over a distance of 10 m, which shows the possibility of the self-mixing ranging in longer-distance measurements.

Third, self-mixing permits the discrimination of the direction of the target. Figure 7 has shown how the self-mixing interference signal is asymmetric provided that the reflectivity from the target is sufficiently large. Such an asymmetry is directly related to the direction of the sensing parameter and was used by Shimizu[21] to discriminate the direction of the target in the laser Doppler velocimeter.

Fourth, a possible disadvantage of the self-mixing interference is the potential difficulty of coupling the optical feedback into the cavity, but in a fiber-coupled system it was found to be quite easy to reflect the light back into the cavity. This finding implies that a fiber-coupled self-mixing system will be more attractive, particularly because the multimode fiber may be easily used in self-mixing systems, which makes such systems easy to align with a higher signal-to-noise ratio and implies lower costs. In this study both single-mode and multimode fibers were used. The results of our experiments showed comparatively few differences between the fibers; the multimode fiber was easier to align and easier to obtain a higher coupling efficiency from. However, it was more sensitive to the environmental change to be measured. The single-mode fiber showed the opposite characteristics.

Fifth, because the self-mixing interference is not dependent on the type of laser used, the inexpensive low-coherence solid-state laser may be used to achieve it in the sensor systems. For example, the main disadvantage of the conventional fiber-optic velocimeter is that the fluid flow is perturbed by the presence of a sensing fiber in the flow itself. Signals from this disturbed region broaden the Doppler spectrum because the fiber lowers the fluid velocity in the stagnation region in the close vicinity of the fiber tip. This problem may be overcome by using a multimode laser with self-mixing, as discussed in the experiment with the 10-m fiber. In this method an insensitive region (at a distance $< nl$) is formed in front of the fiber as the intensity superimposition of each mode, but a thin region of sensitivity may be profiled through and beyond the extent of the stagnation region.

Self-mixing interference in a diode laser results from both a threshold variation and a spectral variation of the laser. This type of interference is not dependent on the conventional coherence length of the laser. The experiments explained herein have shown that the interference by self-mixing has some significant differences compared with conventional optical interference. Applications of these differences have been discussed and a further theoretical study is being undertaken.

References

1 R. Lang and K. Kobayashi, "External optical feedback effects on semiconductor injection laser properties," IEEE J Quantum Electron **QE-16**, 347–355 (1980).

2. M. Fujiwara, K. Kubota, and R. Lang, "Low frequency inten-

sity fluctuations in laser diodes with external optical feedback," Appl. Phys. Lett. **38**, 217–220 (1981).

3. F. Favre, D. L. Guen, and J. S. Simon, "Optical feedback effects upon laser diode oscillation field spectrum," IEEE J. Quantum Electron. **QE-18**, 1712–1717 (1982).

4. G. A. Acket, D. Lenstra, A. J. den Boef, and B. H. Verbeek, "The influence of feedback intensity on longitudinal mode properties and optical noise in index-guided semiconductor lasers," IEEE J. Quantum Electron. **QE-20**, 1163–1169 (1984).

5. J. S. Cohen and D. Lenstra, "Spectral properties of the coherence collapse state of a semiconductor laser with delayed optical feedback," IEEE J. Quantum Electron. **25**, 114–115 (1989).

6. S. Murata, S. Yamazaki, I. Mito, and K. Kobayashi, "Spectral characteristics for 1.3 fm monolithic external cavity DFB lasers," Electron. Lett. **22**, 1197–1198 (1986).

7. E. Patzak, H. Olessen, A. Sugimura, S. Saito, and T. Muka, "Spectral linewidth reduction in semiconductor lasers with weak optical feedback," Electron. Lett. **19**, 938–940 (1983).

8. G. P. Agrawal, "Line narrowing in a single-mode injection laser due to external optical feedback," IEEE J. Quantum Electron. **QE-20**, 468–471 (1984).

9. H. Yasaka, Y. Yoshikuni, and H. Kawaguchi, "FM noise and spectral linewidth reduction by incoherent optical negative feedback," IEEE J. Quantum Electron. **27**, 193–204 (1991).

10. W. M. Wang, W. J. O. Boyle, K. T. V. Grattan, and A. W. Palmer, "An interferometer incorporating active optical feedback from a diode laser with applications to coherent ranging and vibrational measurement," presented at the Eighth Optical Fiber Sensors Conference, Monterey, Calif., 29–31 January 1992.

11. O. Hirota and Y. Suematsu, "Noise properties of injection lasers due to reflected waves," IEEE J. Quantum Electron. **QE-15**, 142–149 (1979).

12. G. P. Agrawal, N. A. Olsson, and N. K. Dutta, "Effect of fiber-far end reflections on intensity and phase noise in InGaAsP semiconductor lasers," Appl. Phys. Lett. **45**, 959–957 (1984).

13. H. Temkin, N. A. Olsson, T. H. Abeles, R. A. Logan, and M. B. Panish, "Reflection noise index guided InGaP lasers," IEEE J. Quantum Electron. **QE-22**, 286–293 (1986).

14. R. O. Miles, A. Dandrige, A. B. Tveten, H. F. Taylor, and T. G. Giallorenzi, "Feedback induced line broadening in cw channel substrate planar laser diodes," Appl. Phys. Lett. **37**, 990–992 (1980).

15. D. Lenstra, B. H. Verbeek, and A. J. den Boef, "Coherence collapse in single-mode semiconductor lasers due to optical feedback," IEEE J. Quantum Electron. **QE-21**, 674–679 (1985).

16. M. J. Rudd, "A laser Doppler velocimeter employing the laser as a mixer-oscillator," J. Phys. E **1**, 723–726 (1968).

17. A. Dandridge, R. O. Miles, and T. G. Giallorenz, "Diode laser sensors," Electron. Lett. **16**, 948–949 (1980).

18. J. H. Churnside, "Laser Doppler velocimetry by modulating a CO_2 laser with backscattered light," Appl. Opt. **23**, 61–65 (1984).

19. J. H. Churnside, "Signal-to-noise in a backscatter-modulated Doppler velocimeter," Appl. Opt. **23**, 2079–2106 (1984).

20. S. Shinohara, A. Mochizuki, H. Yoshida, and M. Sumi, "Laser Doppler velocimeter using the self-mixing effect of a semiconductor laser diode," Appl. Opt. **25**, 1417–1419 (1986).

21. E. T. Shimizu, "Directional discrimination in the self-mixing type laser Doppler velocimeter," Appl. Opt. **26**, 4541–4544 (1987).

22. H. W. Jentink, F. F. M. de Mul, H. E. Suichies, J. G. Aarnoudse, and J. Greve, "Small laser Doppler velocimeter based on the self-mixing effect in a diode laser," Appl. Opt. **27**, 379–385 (1988).

23. P. J. de Groot, G. M. Gallatin, and S. H. Macomber, "Ranging and velocimetry signal generation in a backscatter-modulated laser diode," Appl. Opt. **27**, 4475–4480 (1988).

24. P. J. de Groot and G. M. Gallatin, "Backscatter-modulation velocimetry with an external cavity laser diode," Opt. Lett. **14**, 165–167 (1989).

25. P. J. de Groot, "Range-dependent optical feedback effects on the multimode spectrum of laser diodes," J. Mod. Opt. **37**, 1199–1214 (1990).

26. M. K. Koelink, M. Slot, F. F. M. de Mul, J. Greve, R. Graaff, A. C. M. Dassel, and J. G. Aarnoudse, "*In vivo* blood flow velocity measurement using the self-mixing effect in a fibre-coupled semiconductor laser," in *Fiber-Optic Sensors: Engineering and Applications*, A. J. Bruinsma and B. Culshaw eds., Proc. Soc. Photo-Opt. Instrum. Eng. **1511**, 120–128 (1991).

27. J. T. Verdeyen, "Laser oscillation and amplification," in *Laser Electronics* (Prentice-Hall, Englewood Cliffs, N.J., 1981), Chap. 8, p. 159.

28. J. H. Osmundsen and N. Grade, "Influence of optical feedback on laser frequency spectrum and threshold conditions," IEEE J. Quantum Electron. **QE-19**, 465–469 (1983).

29. D. A. Jackson, A. D. Kersey, M. Corke, and J. D. C. Jones, "Pseudo heterodyne detection scheme for optical interferometers," Electron. Lett. **18**, 1081–1083 (1982).

30. R. W. Tkach and A. R. Chraplyvy, "Regimes of feedback effects in 1.5 fm distributed feedback lasers," IEEE J. Lightwave Technol. **LT-4**, 1655–1661 (1986).

31. L. Goldberg, H. F. Taylor, A. Dandrige, J. F. Weller, and R. O. Miles, "Spectral characteristics of semiconductor lasers with optical feedback," IEEE J. Quantum Electron. **QE-18**, 555–564 (1982).

32. N. Schunk and K. Petermann, "Numerical analysis of the feedback regimes for a single-mode semiconductor lasers with external feedback," IEEE J. Quantum Electron. **24**, 1242–1247 (1988).

33. A. Olsson and C. L. Tang, "Coherent optical interference effects in external cavity semiconductor lasers," IEEE J. Quantum Electron. **QE-17**, 1320–1323 (1981).

34. J. S. Cohen, F. Wittgrefe, M. D. Hoogerland, and J. P. Woerdman, "Optical spectra of a semiconductor laser with incoherent optical feedback," IEEE J. Quantum Electron. **26**, 982–990 (1990).

35. K. Petermann, *Laser Diode Modulation and Noise* (Kluwer, Dordrecht, The Netherlands, 1991), Chap. 1, p. 25.